Targeting Heart Rate as a Novel Therapeutic Approach in Acute Heart failure

By Aqeela Imamdin

Presented for the degree of DOCTOR OF PHILOSOPHY

Department of Medicine

UNIVERSITY OF CAPE TOWN

October 2018

Supervisors: Professor Sandrine Lecour, Dr Feriel Azibani, Professor Karen Sliwa & Dr Joy McCarthy

“The whole of life is just like watching a film. Only it’s as though you always get in ten minutes after the big picture has started, and no-one will tell you the plot, so you have to work it out all yourself from the clues.”

~ Terry Pratchett, Moving pictures

Acknowledgements:

I would like to acknowledge and thank the following parties for their contributions to my PhD:

- The National Research Foundation (NRF) for financial support through the course of my PhD (2014-2017)
- The German Academic Exchange Service (DAAD) for financial support (2014-2016), for their assistance and for including me in their development programs
- Servier, the National Research Foundation, the Medical Research Council, the Maurice Hatter Foundation and the University of Cape Town for support in the form of grants contributing to this project
- Emeritus Professor Lionel Opie for his faith in the ideas I had presented to him in the infancy of my project
- Professor Karen Sliwa, my co-supervisor, for allowing me to join as a sub-study to her ongoing research in cardiac maternal health to obtain the clinical data reported here
- Professor Sandrine Lecour, my supervisor, for guiding and supporting me through this project, for troubleshooting, motivating, advising, funding, planning and helping tie together the separate aspects of the project – in short, for helping me to make this project possible and successful
- Dr Feriel Azibani, my co-supervisor, particularly for her assistance and guidance with the PPCM aspects of this project – both clinical and experimental – for her insight in shaping the research conducted here, for compiling results, and for all of her contributions which helped me to make this project possible and successful
- Dr Nkanyiso Hadebe for his assistance, in-depth knowledge and guidance with the animal work relating to echocardiogram acquisition and analysis
- Dr Wentzel Dowling and Dr Johann Baard for collection and collation of the data from the Cardiac Maternity Clinic at Groote Schuur Hospital
- Jakobus Visser, Trevor Adams, the late Raymond Abdol, Suraya Basterman and all other members of the University of Cape Town Animal Unit who coordinated the special animal breeding program for this project

- Associate Professor Neil Davies and Senior Histologist Helen Ilsley for their assistance with histological aspects of this project

- Mr Victor Klaasen for advice and construction of the Langendorff perfusion rig used in this project

- Dr Emilene Breedt, at the University of Stellenbosch, for her invaluable assistance in constructing the pressure-sensing balloons for mouse heart perfusions

- All students and staff at the Hatter Institute for Cardiovascular Research in Africa for their support and assistance every step of the way along my PhD

- Jeremy Jarman for help with sourcing pieces for my perfusion rig, help with installing and running statistical programs, correcting my perfusion pressure system, and for being reliable, patient, and pleasant.

- Sajjad Karamsi for his support and patience, for helping me to shape ideas and arguments, and for his advice in strategic approaches to elements related to my research

- Patricia van der Walt, and her husband Gert, for ongoing moral support, assistance and advice in and around the lab, and for tea and snacks whenever I grew peckish

- Dr Joy McCarthy, for absolutely everything she has done to motivate me, for her continual support, for her guidance, for breakfast, tea and treats, and for the most enjoyable, cheerful company I could ask for

- The late Yusuf Omarjee, and A'ishah Hartmann for all of their contributions which have helped ease my way through my PhD

- My brother Mohammed Irfaan Imamdin for proof-reading the initial drafts of my thesis, for his unerring support, for listening to my complaints, for taking care of me and for everything he has done to help me through the duration of my PhD

- My parents, Dr Shamsuddin Imamdin and Zubeida Imamdin for doing everything that was possible to ease my way, for absolutely everything they have done for me to get me to and through my PhD, and their support in all aspects of life

Plagiarism Declaration

I declare that this thesis is my own unaided work. It is submitted for the degree of Doctor of Philosophy to the, University of Cape Town. It has not been submitted before for any degree or examination at the University of Cape Town or any other university.

Name: Aqeela Imamdin

Student number: IMMAQE00 1

Signature: Signed by candidate

Date: 14.06.2018

Table of contents:

Acronyms

ACE	Angiotensin-converting enzyme
ACEi	Angiotensin-converting enzyme inhibitor
ACS	Acute coronary syndromes
AF	Atrial fibrillation
AHF	Acute heart failure
AKT	Protein kinase B
Ang II	Angiotensin II
ANP	Atrial natriuretic peptide
ANS	Autonomic nervous system
ANT	Adenine nucleotide translocator
APO-1	Apoptosis antigen 1
ARVC	Arrhythmogenic right ventricular cardiomyopathy
ATP	Adenosine triphosphate
AV	Atrio-ventricular
BMP	Bone morphogenic protein
BNP	B-type natriuretic peptide
CAD	Coronary artery disease
cAMP	Cyclic adenosine monophosphate
cDNA	Complimentary DNA
Col 1	Collagen 1
Col 3	Collagen 3
CPT1	Carnitine palmitoyltransferase 1
CT	Cycle threshold
CVD	Cardiovascular disease
DBP	Diastolic blood pressure
DCM	Dilated cardiomyopathy
dNTP	Deoxyribo Nucleotide Tri-Phosphate
ECG	Electrocardiogram
ECL	Enhanced chemiluminescence
EDV	End diastolic volume
EF	Ejection fraction
eNOS	Endothelial nitric oxide synthase
ERK	Extracellular signal–regulated kinase
ESV	End systolic volume
Fas	First apoptosis signalling receptor
FFA	Free fatty-acid
FS	Fractional shortening
Gαq	G-protein alpha subunit, group Q

GAPDH	Glyceraldehyde 3-phosphate dehydrogenase
GLUT 1	Glucose transporter 1
GLUT 4	Glucose transporter 4
GMP	Guanosine monophosphate
H&E	Haematoxylin & Eosin
HCM	Hypertrophic cardiomyopathy
HCN	Hyperpolarization-activated cyclic nucleotide–gated
HF	Heart failure
HFmrEF	Heart failure with mid-range ejection fraction
HFpEF	Heart failure with preserved ejection fraction
HFrEF	Heart rate with reduced ejection fraction
HRV	Heart rate variability
If	Funny channel
IGF	Insulin-like growth factor
IQR	Inter-quartile range
JKN	Janus kinase receptor
KHB	Krebs-Henseleit buffer
KO	Knockout
LDL	Low-density lipoproteins
LV	Left ventricle
LVAW	Left ventricular anterior wall thickness
LVAWd	Left ventricular anterior wall thickness in diastole
LVAWs	Left ventricular anterior wall thickness in systole
LVDP	Left ventricular developed pressure
LVEDP	Left ventricular end diastolic pressure
LVEF	Left ventricular ejection fraction
LVID	Left ventricular internal diameter
LVIDd	Left ventricular internal diameter in diastole
LVIDs	Left ventricular internal diameter in systole
LVPW	Left ventricular posterior wall thickness
LVPWd	Left ventricular posterior wall thickness in diastole
LVPWs	Left ventricular posterior wall thickness in systole
MAPK	Mitogen-activated protein kinase
MHC	Myosin heavy chain
α-MHC	alpha Myosin heavy chain
β-MHC	Beta Myosin heavy chain
Min	Minutes
MLC2V	Myosin Light Chain 2V
MMP	Matrix metalloproteinase
MnSOD	Manganese superoxide dismutase

MRA	Mineralocorticoid receptor antagonist
mRNA	Messenger RNA
mTORC	Mammalian target of rapamycin complex
NADH	Acidified nicotinamide adenine dinucleotide
NADPH	Acidified nicotinamide adenine dinucleotide phosphate
NFκβ	Nuclear factor kappa-light-chain-enhancer of activated B cells
NO	Nitrous oxide
NYHA	New York heart association
PBS	Phosphate-buffered saline
PCR	Polymerase chain reaction
PD-1	Programmed cell-death protein 1
PGC-1α	Peroxisome proliferator-activated receptor gamma coactivator 1-alpha
PI3K	Phospho-inositol 3 kinase
PPCM	Peripartum cardiomyopathy
pro-BNP	N-terminal pro b-type natriuretic peptide
PVDF	Polyvinylidene difluoride
qPCR	Quantitative PCR
RAAS	Renin angiotensin aldosterone system
RNA	Ribonucleic acid
ROS	Reactive oxygen species
RSA	Respiratory sinus arrhythmia
RT	Reverse transcription
SA	Sino-atrial
SBP	Systolic blood pressure
SEM	Standard error of the mean
sFLT1	Soluble fms-like tyrosine kinase-1
STAT3	Signal transducer and activator of transcription 3
STAT3 KO	STAT3-deficient mice
TBS	Tris-buffered saline
TBS-T	Tris-buffered saline with tween
TC	Takotsubo cardiomyopathy
TGF-β	Transcription growth factor beta
TIMP1	Tissue inhibitors of metalloproteinases-1
TNFα	Tumour necrosis factor alpha
TTE	Transthoracic echocardiography
USA	United States of America
USD	United States dollars
VEGF	Vascular endothelial growth factor
WHO	World Health Organisation
WT	Wildtype

Abstract

Background and hypothesis: Standard pharmacological treatment for heart failure improves cardiac remodelling and survival in the setting of chronic heart failure, but is suboptimal in cases of acute heart failure (AHF). Peripartum cardiomyopathy (PPCM), de-novo hypotension (often due to haemorrhagic shock), and Takotsubo cardiomyopathy (TC) are conditions which have acute onset of heart failure, and often present with high mortality rates. In patients treated for these pathologies, a variation in the heart rate is observed and could potentially be used as a target to improve the treatment of AHF. We therefore questioned whether the use of a sinoatrial node inhibitor (ivabradine) to modulate heart rate may improve outcomes in AHF.

Objectives and methods: Our objectives were 3-fold: (1) to explore the effect of a standard treatment strategy on heart rate in a South African cohort of PPCM patients after 6 and 12 months follow-up. (2) To explore the effect of ivabradine, a sinoatrial node inhibitor in an established signal transducer and activator of transcription 3 (STAT3) knockout mouse model of PPCM (with 3 consecutive pregnancies). Mice were fed ivabradine for 30 days (10mg/kg/day in drinking water), following the 3rd weaning. Trans-thoracic echocardiograms (TTE) were done at the end of the 3rd weaning, and after 30 days of treatment with ivabradine. Hearts were harvested after the second TTE for histology staining and messenger ribonucleic acid (mRNA) quantitation of transcripts involved in heart failure. (3) To explore the role of the sinoatrial node inhibitor in an ex-vivo model of de-novo AHF due to hypotension, and a newly developed ex-vivo model of TC. In the AHF model, hearts were stabilised before administering Ivabradine (3μM) in a buffer containing high free fatty-acids at a low pressure (to mimic hypotension/ haemorrhage shock conditions). A pressure-sensing balloon in the left ventricle measured heart rate, diastolic and systolic pressure, left ventricular developed pressure, rate pressure products and functional recovery. In the TC model, hearts were stabilised, then given a buffer with high free fatty-acid content and 10 times a

physiological dose of adrenaline to mimic the adrenergic response seen in TC. Thereafter, hearts were restored to stabilisation pressure and substrate for recovery.

Results: (1) Clinical outcomes indicated that patients on maximum standard therapy improved symptomatically and on the New York Heart Association scale. However, heart rates of PPCM patients remained elevated after 6 months of treatment. (2) In PPCM mice, a treatment with ivabradine was associated with reduced fibrotic infiltration in cardiac tissue and with a decrease in levels of atrial natriuretic peptide and Fibronectin mRNAs. (3) Both hypotensive AHF and TC models showed a tendency toward better cardiac function with ivabradine at the end of the acute phases. This advantage was lost after withdrawal of ivabradine during recovery.

Conclusion: In South African women with PPCM treated with standard therapy, heart rate remains elevated, therefore suggesting that these women may benefit from the use of ivabradine as an additional therapy, particularly in patients who may be intolerant to β-blockers. The long-term use of ivabradine in the setting of cardiac dysfunction appears to have beneficial effects on remodelling, as treatment with ivabradine in our mouse PPCM model showed reduced cardiac fibrosis. The ex-vivo models of hypotensive AHF and TC both showed benefit in reducing heart rate during the acute phases, and hold the potential of being an intervention therapy to improve the outcome in patients who are brought to hospital while still in the acute phase.

Chapter 1

Introduction

1. An introduction to heart failure

Our understanding of the structure, purpose and mechanics of the heart has evolved gradually over millennia. The heart has paramount importance in many ancient cultures, and the spiritual aspects lent it to greatly influenced how humankind has perceived its role in the physical form. Our knowledge of how the heart functions, and our understanding of how it fails to function properly has grown over the last 50 years. In recent decades, surgical and pharmaceutical interventions have improved the outcome and prognosis of heart failure (HF). Presently, we are trying to improve and refine the symptoms of HF, to increase quality and length of life. Over time, our understanding of the process and development of HF has influenced how we have approached treatment. This understanding is closely linked to the circulatory system, and it is our knowledge of the circulatory system that has helped us piece together how we categorise the pathophysiology of heart failure.

1.1 A brief history of cardiac dysfunction

The first historical step in understanding HF had been in recognising the function of the circulatory system in distributing blood through the body. At first, the outward display of HF sufferers was not linked to the heart, but attributed instead to lung problems, and even magic (see review by Katz) [1]. In more recent centuries, the heart has been identified as a muscular pump, and as the source of symptoms of HF rather than the previously believed respiratory problems [2]. Time has refined the medical practices used to diagnose and treat HF – from lung taps, to cauterisation, to bleeding, and in the1700's, the discovery of digitalis in a herbal remedy containing the foxglove plant [3,4]. This discovery sparked interest in a new scientific approach and inspired pharmaceutical investigations giving rise to the modern therapies used to alleviate cardiac congestion and related troubles.

The distribution of cardiovascular diseases has varied in different regions over time- from atherosclerosis, to rheumatic heart diseases, to heart attacks, to heart failure (HF), with many others in between. The early 20th century saw poor prognosis for those with heart disease. Later, in the 1940's, the Framingham study [5–11] was initiated – This was the first major study to investigate cardiac and circulatory diseases, and led to the formal recognition of atherosclerosis, with increased incidences attributed to the condition [10]. The study also led to the identification of cholesterol by John Gofmann and his team at the University of California, as well as the original finding of increased levels of low density lipoproteins (LDL) and decreased levels of high density lipoproteins (HDL) with arterial blockage. This was followed by Ancel Keys's observation in the 1950's that those in the Mediterranean with a low-fat diet experienced lower incidences of heart disease. This started the movement recognising diet as a contributor to heart disease [12].

Perhaps it had been such that other maladies had always been at the forefront – environmental diseases involving access to resources, bacterial and viral infections. In the late 19th century, cardiovascular diseases came to attention, even though they have been around for millennia. From recognising HF symptoms in early Egypt, significant strides were made to expand knowledge of cardiac physiology, and as of the 15th century led to identification of (i) the structure of the heart as a 4-chambered vessel [13], (ii) the function of the heart as a muscular pump [13], (iii) the mechanics and contributions of systolic and diastolic contraction [13,14], (iv) the double circulatory system loop carrying venous and arterial blood between the heart, lungs and peripheries [14], (v) the initial stages of heart diseases such as angina and CAD [15], which, together with other conditions can further lead to (vi) HF, often underlying oedema and dyspnoea [16].

Hence, in research, our objectives should lead us to dissect with finesse the molecular problems underlying the different forms of cardiac dysfunction in HF so that we can offer personalised and optimised approaches which will help to shape the future direction of cardiac medicine.

1.2 What is heart failure?

1.2.1 Definition, signs and symptoms

Cohn defines Hart failure (HF) as "the inability of the heart to fill with or eject blood" [17]. The guideline of the European Society of Cardiology considers HF as a clinical syndrome with specific combinations of signs and symptoms [18]. These signs include tachycardia, pulmonary rales, tachypnoea, pleural effusion, raised jugular venous pressure, and hepatomegaly [19]. Symptoms include breathlessness when at rest or with exertion, dyspnoea, orthopnoea, fatigue, swelling of the ankles, and coughing. These signs and symptoms are caused by structural or functional abnormalities which reduce cardiac output or elevate intra-cardiac pressures at rest or with exertion.

1.2.2 Acute and chronic heart failure

1.2.2.1 Chronic heart failure

The onset of HF can occur at different paces (see table 1.1). Chronic HF develops with a gradual onset of symptoms, and it is said to be stable if these symptoms remain unchanged for at least one month [18]. Chronic HF can occur as a result of a number of conditions and cardiomyopathies, such as dilated cardiomyopathy, peripartum cardiomyopathy (PPCM), rheumatic heart disease, ischaemic heart disease, pericardial disease, human immunodeficiency virus (HIV)-associated cardiomyopathy. endomyocardial fibrosis, pulmonary hypertension, or valvular diseases [20,21]. Deterioration of symptoms in chronic cases is known as 'decompensation' and can occur gradually or suddenly [18].

The severity of HF (both acute and chronic) is classified using the New York Heart Association (NYHA) scale.

Table 1.1: A comparison of acute and chronic heart failure. Abbreviations: ACE – angiotensin-converting enzyme; DCM – dilated cardiomyopathy; HIV – human immunodeficiency virus; PPCM – peripartum cardiomyopathy

	Chronic Heart Failure	Acute Heart Failure
Timing	Gradual worsening of cardiac function	Rapid worsening of cardiac function requiring urgent therapy
Symptoms	Shortness of breath, fatigue, swelling of lower limbs, palpitations, reduced exercise capacity	Similar to chronic, but more rapid and severe development
Causes	DCM, PPCM, hypertension, ischaemic cardiomyopathy, HIV cardiomyopathy, rheumatic heart disease, previous cardiac damage	Can occur de novo, or due to acutely onset cardiac events such as hypotensive/ haemorrhagic shock, Takotsubo cardiomyopathy, PPCM
Management	B-blockers, ACE inhibitors, diuretics, mineralocorticoid receptor blockers	Symptom-based, to improve perfusion and remove precipitating agent

1.2.2.2 Acute heart failure

Acute heart failure (AHF) develops with a sudden onset of symptoms which require urgent treatment tailored to address these symptoms [22]. Symptoms presented in AHF are the same as those presented in chronic HF but are more sudden and severe in presentation. It can occur as first presentation (de novo), as a consequence of acute decompensation of chronic HF, or as a result of cardiac conditions [22]. These conditions include tachyarrhythmia, infection, bradyarrhythmia, toxic shock, pulmonary embolism, surgical and perioperative complications, metabolic and hormonal derangement – conditions which culminate in hypotensive /haemorrhagic shock, Takotsubo cardiomyopathy, PPCM, acute viral myocarditis, or tachycardiomyopathy, which may lead to AHF [22–24]. Some of these conditions may resolve completely in certain cases such as PPCM and Takotsubo cardiomyopathy. However, when it occurs in addition to other cardiac conditions, such

as acute myocardial infarction, dilated cardiomyopathy, or in addition to chronic heart failure, the prognosis is poor [24].

The outcome of AHF is often grave, with patients frequently needing re-hospitalization, and a mortality rate of 30% within a year of an initial AHF incident [18,25,26]. A study investigating AHF was conducted across 30 European countries and found equal gender frequency, with coronary artery disease, hypertension, and atrial fibrillation as the most common preceding factors. Arrhythmias, valvular dysfunction, and acute coronary syndrome (ACS) were also found to contribute as auxiliary factors [25]. A third of all cases had pre-existing heart failure with a preserved left ventricular ejection fraction (>45%) [27].

AHF can present clinically in different ways; (i) acute pulmonary oedema resulting from cardiac dysfunction, (ii) acute worsening (decompensation) of chronic heart failure or (iii) cardiogenic shock, often in the setting of an ACS, characterised by hypotension, peripheral vasoconstriction, or oliguria [28,29]. Patients who present with hypotensive AHF are characterised by having low systolic blood pressure (<90mmHg), and make up 5-8% of reported AHF cases, but these cases are associated with high mortality rates, particularly with loss in circulatory power typical of cardiogenic / haemorrhagic shock [18,30,31].

1.2.3 New York Heart Association classification

The New York Heart Association (NYHA) scale is used to describe and grade the severity of HF signs and symptoms as previously described (see section 1.2.1). NYHA classification is determined as follows [18,32]:

- Class I: Patients with cardiac disease who experience no limitations with physical activity. No breathlessness, fatigue or palpitations with physical activity.

- Class II: Patients with cardiac disease who experience slight limitations with physical activity. Comfortable at rest, but slightly increased breathlessness, fatigue or palpitations with ordinary physical activity.
- Class III: Patients with cardiac disease who experience marked limitations with physical activity. Comfortable at rest, but increased breathlessness, fatigue or palpitations with less than ordinary physical activity.
- Class IV: Patients with cardiac disease who experience severe limitations with and/ or without physical activity. Not comfortable at rest. Increased breathlessness, fatigue or palpitations with less than ordinary physical activity. Discomfort with all physical activity, with possible symptoms at rest too. Increased discomfort with any physical activity undertaken.

1.2.4 Left ventricular dysfunction in heart failure

LV ejection fraction (EF), which measures the capacity of the heart to fill and eject blood, varies with HF. The outcome of the EF with HF can fall into 1 of 3 categories; (i) EF below 40%, classified as HF with a reduced EF (HFrEF), (ii) EF between 40% and 49% is classified as HF with mid-range EF (HFmrEF), and (iii) EF above or equal to 50%, classified as HF with preserved EF (HFpEF) [28]. These 3 categories based on EF are due to different underlying conditions (see figure 1.1), and responses to treatment. The outcomes in patients with HFrEF and HFpEF varies in terms of response to treatment and reduction in morbidity and mortality [33,34].

Diagnosing HFpEF is more challenging as patients do not have dilated LV, but rather thickened LV walls or an increased left atrial size which coincides with an increased filling pressure [24]. Many patients display impaired LV filling capacity, diastolic dysfunction, thus it is sometimes referred to as 'diastolic HF' [35,36]. Patients who have reduced EF display signs of predominantly systolic dysfunction, but sometimes diastolic dysfunction too[35]. HFmrEF is a grey area that exists between

preserved and reduced ejection fraction, with patients displaying mild systolic dysfunction with features of diastolic dysfunction [24].

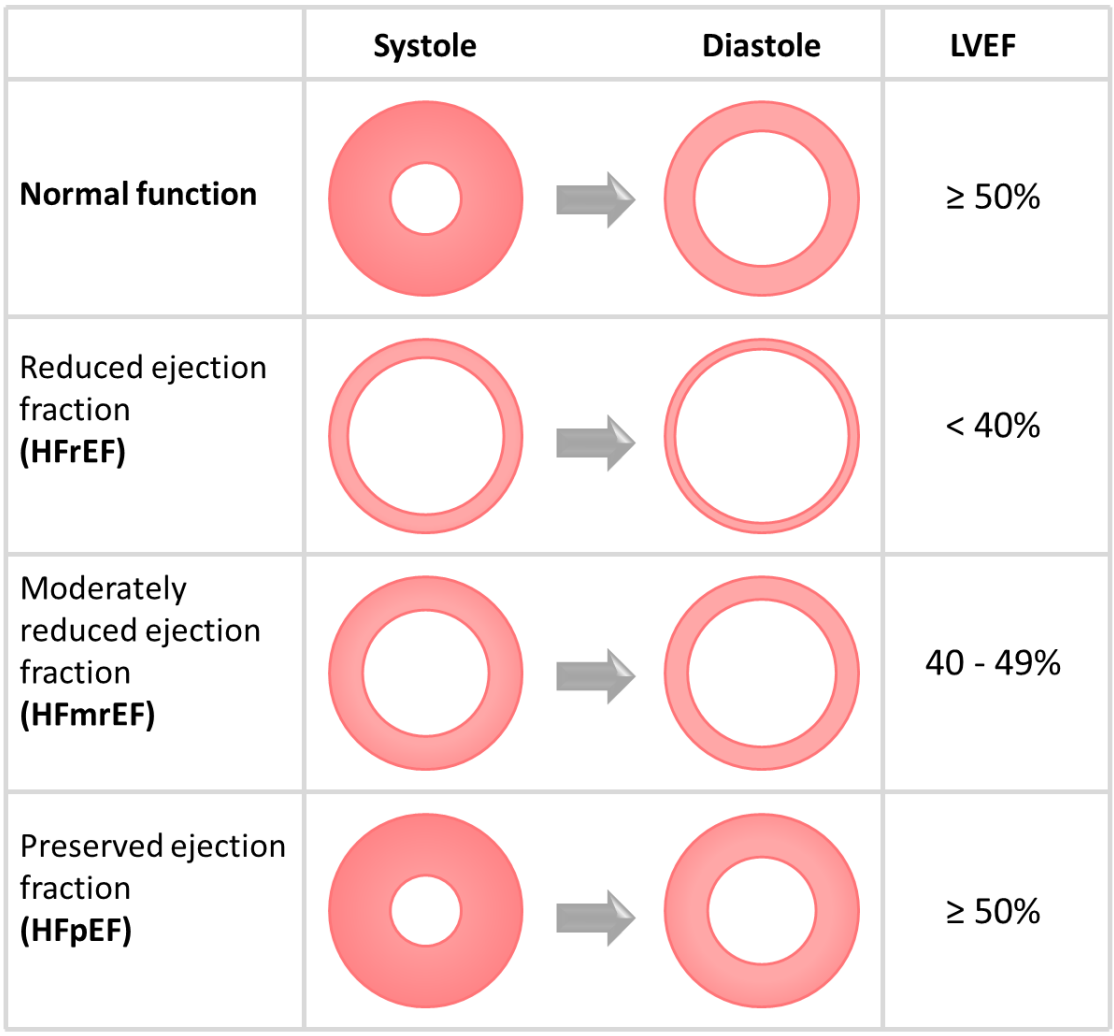

Figure 1.1: Cross-sectional view of the left ventricle showing changes in ventricular wall thickness and contraction underlying heart failure. LV cavity is dilated in HFrEF and unable to contract properly during systole, thereby reducing ejection fraction. HFmrEF has similar dysfunction to HFrEF, but to a lesser degree. HFpEF displays diastolic dysfunction with preserved ejection capacity. Abbreviations: LV – left ventricle; LVEF – left ventricular ejection fraction; HFmrEF – heart failure with mid-range ejection fraction; HFpEF – heart failure with preserved ejection fraction; HFrEF – heart failure with reduced ejection fraction

HFpEF is found with various underlying conditions, but it is more typically found in the elderly without evidence of fluid overload and with the presence of comorbidities [37]. Clinical signs and symptoms are similar for HFpEF, HFmrEF and HFrEF, but may vary in severity.

1.2.5 Diagnostic tests

1.2.5.1 Clinical examination

The first step in diagnosing HF is recognition and evaluation of HF symptoms and signs (see section 1.2.1) by medical history and physical examination. Identifying the underlying cause of each case of HF is central to the treatment strategy. Once signs and symptoms have been clinically confirmed, electrocardiogram (ECG) analysis is performed to examine function and evaluate irregularities. This also helps to categorise patients into NYHA classes (see section 1.2.3). Blood tests are also performed to detect levels of biomarkers such as brain natriuretic peptide (BNP), N-terminal pro-BNP, normal levels of which will rule out the HF state (see section 1.2.5.4).

1.2.5.2 Electrocardiogram

There are several tools which can be used for diagnosis, the choices of which will depend on what resources are available. The electrocardiogram (ECG) is the first line tool used to diagnose cardiac dysfunction. ECG traces of the heartbeat on its own cannot be used for diagnosis, but rather it assists in the diagnosis of HF by providing information related to the underlying causes and can be used to direct the therapeutic approach [18,37–40].

There is no gold standard for the identification of HFpEF (see section 1.2.4) – clinical diagnosis needs support with measures, such as ECG, taken at rest or during exercise, as well as plasma levels of biomarkers. Atrial fibrillation (AF) can compound the complexity of identifying HFpEF, as patients with AF present with similar levels of natriuretic peptides [24,41]. Conversely, patients with HFpEF may resultantly present with AF, which may also be more severe than cases where patients have stable sinus rhythms [24].

1.2.5.3 Imaging tools for diagnosis

Many different imaging tools can be used to assist in confirming the diagnosis HF and cardiac anomalies. Diagnosis of HF is largely clinical, and these imaging tools help to support the diagnosis. Transthoracic echocardiography (TTE) is an ultrasound-based technique which is widely used in the assessment of cardiac function in the clinical setting. It is a relatively low-cost technique used to measure chamber dimensions and contractile function of atria and ventricles, but is not always readily available, and requires skilled handling to obtain an image. Other methods, such as chest x-rays, tomography, coronary angiography and cardiac magnetic resonance are used for various purposes to identify origins of dysfunction.

1.2.5.4 Blood-borne biomarkers

Natriuretic peptides such as brain natriuretic peptide (BNP), N-terminal pro-BNP, and mid-regional pro atrial natriuretic peptide (ANP) found in plasma can be helpful in the initial diagnosis of HF, as high levels of these peptides can assist in the diagnosis of patients who may be asymptomatic and warrant further investigation [42–46]. ST2 and troponin are both useful as biomarkers of cardiomyocyte stretch, higher levels of which indicate hypertensive cardiac dysfunction [47–49]. However, several non-cardiovascular factors may also affect the levels of these peptides, such as ethnicity, age, gender, obesity, hypertension, non-cardiac dyspnoea, non-HF hypertrophy, and renal failure, so it is best to consider these peptides with caution [43,50–53]. The use of biomarkers to identify heart failure holds the potential to be of great benefit in developing countries, as the skills and equipment that are required for imaging and other diagnostic tools are not readily available.

1.3 The prevalence and economic burden of heart failure

In 2010, an estimated 41 million individuals suffered from HF internationally, the preceding causes of which varied by region [54]. In developed countries, 1 – 2% of the adult population suffer

from HF, and analysis by age shows that this rose to approximately 10% of the population over the age of 70 [35,55,56]. The risk of HF at age 55 is 28% for women and 33% for men [55]. The proportion of patients with HFrEF and HFpEF vary greatly, depending on age, sex, and location [57,58].

HF has a high mortality rate varying from 39% to 67% across regions of Europe and Africa within 5 years of diagnosis [59–61]. Individuals may have several different pathologies (both cardiovascular and non-cardiovascular) underlying and sometimes exacerbating HF. In Sub-Saharan Africa in particular, heart failure has proven to be the dominant form of cardiovascular disease [62]. This has significant social and economic impact, as it has a high prevalence, impact, and mortality on young individuals who would otherwise be economic contributors [20]. Non-endemic cardiomyopathies include arrhythmogenic right ventricular cardiomyopathy and hypertrophic cardiomyopathy. Endemic cardiomyopathies include endomyocardial fibrosis, dilated cardiomyopathy and peripartum cardiomyopathy [63]. Hypertensive heart disease, cardiomyopathies and myocarditis accounted for 40 – 45% of recorded cases of HF in Sub-Saharan Africa [64].

1.4 Aetiology

1.4.1 Aetiology of chronic heart failure

The causes behind the development of HF vary by region. There have been noted general tendencies in high income countries for HF to be the outcome of hypertension, coronary heart disease, and occasionally cardiomyopathy and valvular disease [54,65]. These are largely attributed to the high prevalence of cardiovascular risk factors such as obesity, diabetes, physical inactivity, smoking, and excess alcohol consumption [65,66]. HF in Africa is largely non-ischemic in origin. It stems mainly from cardiomyopathies, hypertension, chronic lung disease, pericardial and rheumatic heart diseases [63]. Low to middle-income countries, such as those in sub-Saharan Africa, have very different causes of HF, though urbanisation may be a contributor to the shift toward tendencies seen in high income regions [67]. Previous persistence of disease such as endomyocardial

fibrosis, rheumatic heart disease, tuberculous pericardial disease and anaemia have in the past been significant contributors to HF in Southern Africa [65,68].

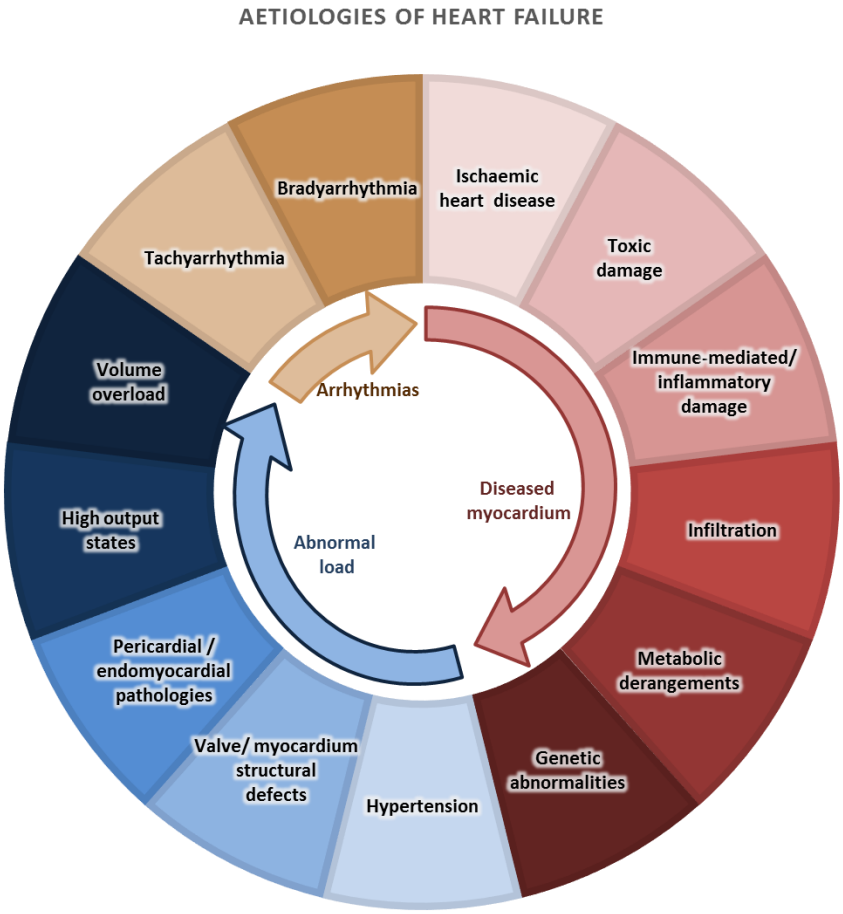

Figure 1.2: Aetiologies of heart failure. There are varying causes of HF which can be divided into 3 categories: diseased myocardium, abnormal load, and arrhythmias. Adapted from Ponikowski et al [18].

There are a number of additional factors which could affect LV function and lead to the development of HF. These include acute myocardial infarction and revascularisation [69]. There are also a number of other causes of HF including viral infection, pulmonary hypertension and valvular heart disease [22]. Development of HF is non-specific and can relate to circulatory insufficiency and load irregularities, inadequate tissue perfusion, as well as decreased muscle contraction and other mechanistic abnormalities. The figure above, adapted from Ponikowski et al

(see figure 1.2), summarises possible causes of HF separating them into categories due to myocardial disease, abnormal loading conditions, and arrhythmias [18,70].

1.4.2 Aetiology of acute heart failure

Chronic HF decompensated into AHF as a result of a multitude of precipitant factors – rapid hypertensive changes, ACS, bradycardia and other conduction anomalies together with sudden onset of arrhythmias, and acute mechanical dysfunction [18]. Independent predictors of AHF include low LV ejection fraction at presentation, advanced age, higher troponin levels at peak and admission, and physical stressors preceding the acute event (see table 1.2) [24].

AHF in Africa is commonly due to hypertension and rheumatic heart disease [20,71]. The THESUS-HF study examined 12 different centres across Sub-Saharan Africa, and found mortality rates for AHF of 4.2% in-hospital, and 17.8% after 6 months [20]. It mainly affected middle-aged men and women, in equal proportion. These findings mirror non-African AHF registries, suggesting that AHF has a dire prognosis globally, regardless of cause [59].

Table 1.2: Major and minor risk factors in acute heart failure as described by the Heart failure association, 2010.. Most notable risk factors for AHF include older age with lower systolic blood pressure, pulmonary oedema, unexplained syncope, ventricular fibrillation or tachycardia, and / or low ejection fraction.

Risk factor	Higher risk	Lower risk
Major risk factors		
Age	≥75 years	See minor risk factors
Systolic BP	<110mmHg	>110mmHg
Clinical pulmonary oedema	Present	Absent
Unexplained syncope, ventricular fibrillation or tachycardia	Present	Abset
LVEF	<35%	See minor risk factors
LV outflow tract obstruction	≥40mmHg	<40mmHg
Mitral regurgitation	Moderate – severe	Absent – mild
Apical thrombus	Present	Absent
New ventricular-septel defect or contrained LV wall rupture	Present	Absent
Minor risk factors		
Age	70 – 75 years	<70 years
ECG		
QTc	≥500ms	<500ms
Pathological Q waves	Present	Absent
Persistent ST elevation	Present	Absent
LVEF	35 – 45%	≥45%
Physical stressor	Present	Absent
Natriuretic peptides		
BNP	≥600pg/mL	<600pg/mL
NT-proBNP	≥2000pg/mL	<2000pg/mL
Bystander obstructive CAD	Present	Absent
Biventricular involvement	Present	Absent

Adapted from Carita et al [29]. Abbreviations: AHF – acute heart failure; BNP – brain natriuretic peptide; BP – blood pressure; CAD – coronary artery disease; LV – left ventricle; LVEF – left ventricular ejection fraction; ml – millilitre; mmHg – millimetres of mercury; ms – milliseconds; NT – N-terminal; pg – picograms.

1.5 Pathophysiology of heart failure

Pathophysiology in chronic HF occurs when physiological adaptations meant for short-term become aberrantly expressed in the long-term. Physiological adaptations occur in response to transient overload scenarios such as those which occur with exercise and pregnancy. Pathophysiology engages mechanisms involved in persistent inflammation, followed by those in matrix remodelling, resulting in fibrosis and myocardial stiffening associated with HF. It can also occur following tissue damage, as occurs with myocardial infarction, after which adaptation occurs, leading to failure.

1.5.1 Metabolic changes in heart failure

Metabolic changes associated with heart failure can occur instantaneously. The setting of HF in some ways resembles that of the foetal heart. One such instance is oxygen availability – due to poor circulation in HF, there is limited oxygen availability. Similarly, in the foetus, where there is a shared circulatory system, oxygen pressure is relatively low. Hypoxia conditions found in the foetal setting favours the use of glucose as a fuel, as opposed to the adult heart which favours the use of fatty acids as a fuel. Glucose availability influences the myosin heavy chain isoform expression – MHC-B is predominantly expressed in the adult heart and provides greater contractile power as is required in an oxygen rich environment with the need to react to physical stresses. MHC-α is predominantly expressed in the foetal heart [72–74]. Pressure/volume overload sees a shift from MHC-α to MHC-β – a switch hypothesised to be triggered by forced glucose uptake [72–75].

Transcription of glucose regulatory elements, such as the GLUT1 and GLUT 4 receptors which coordinate cellular uptake of blood glucose, as well as pyruvate dehydrogenase kinase 2, muscle-glycogen synthase, mitochondrial Carnitine palmitoyltransferase I, medium chain acyl-CoA dehydrogenase and acetyl-CoA carboxylase, are all higher in the healthy adult human heart than in the foetal and failing heart [72,76–78].

In the stressed myocardium, the switch from highly aerobic metabolism of fatty acids to the oxygen-sparing metabolism of glucose is necessary for short-term tissue survival. Glycolysis is thought to provide the fuel for ion pumps cycling calcium. Without this transient switch in metabolism, the energy deficit which may occur could exacerbate contractile dysfunction, leading to apoptosis or necrosis [79]. A similar switch from fat to glycogen is seen in animals exhibiting the phenomenon of hibernation, as a strategy for programmed cell survival [80].

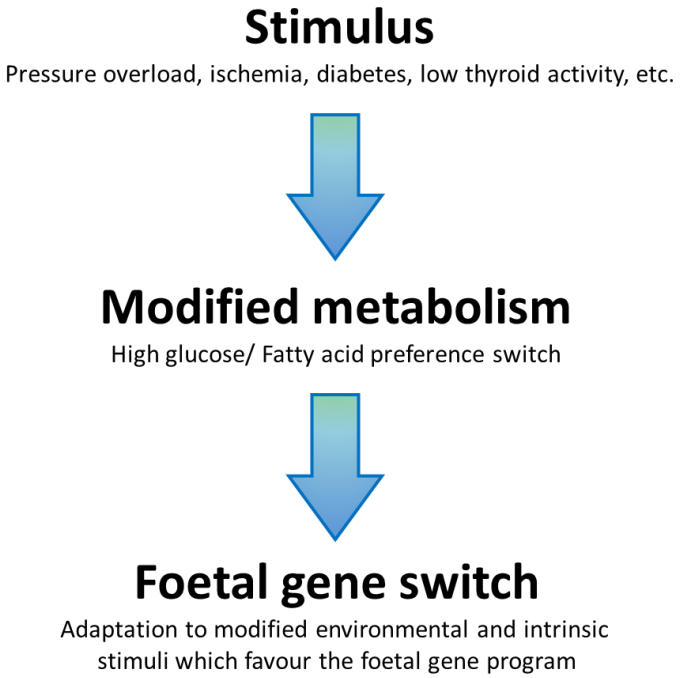

Figure 1.3: Modification of metabolism in the heart due to various stimuli. These stimuli cause a switch from glucose to fatty acids as a fuel, as this is less oxygen expensive. This favours activation of the foetal gene program which is designed to favour low blood oxygen levels, as would be present in the womb. In the short-term, this switch is beneficial, but long-term activation is strongly linked to chronic heart failure. Figure adapted from Taegtmeyer et al [72]

The switch to the foetal gene program activates cardioprotective anti-apoptotic pathways involving signalling cascades with PI3 kinase and protein kinase B (akt) activation [81–83]. Akt regulates metabolic substrate use, phosphorylating GLUT4, and promotes glucose uptake independently of insulin while simultaneously inhibiting fatty acid oxidation [84–86].

In some cases – in cases such as pressure overload, hemodynamic unloading, hypoxia, low-flow ischemia -remodelling as a result of changes in load causes transcriptional reversion to the foetal gene program (see figure 1.3). This is cardioprotective and adaptative, and does not necessarily dictate irreversible tissue damage [72].

1.5.2 Endothelial dysfunction

Endothelial dysfunction occurs when there is an impaired release of nitric oxide (NO) in the endothelial layer lining blood vessels. This causes impaired balance between vascular constriction and relaxation which inhibits blood flow [87]. Reactive oxygen species (ROS) which are released in response to injury, stress, and with impaired cellular function accelerate the degradation of NO species [88–90]. Targeting ROS by means of xanthine oxidase, Acidified nicotinamide adenine dinucleotide/ Acidified nicotinamide adenine dinucleotide phosphate (NADH/NADPH) oxidase, and uncoupled endothelial nitric oxide synthase could potentially help to prevent endothelial dysfunction, as it would prevent the loss of NO (see figure 1.4) [89,90]. The shift in the vascular oxidative balance to an increase in levels of ROS, and depletion of NO is a contributing factor to endothelial dysfunction seen in cases of HF [90]. Poor endothelial response to vasodilatory agents like acetylcholine, adenosine, nitro-glycerine and sodium nitroprusside has been noted in patients who experience cardiovascular events [88,91]. Endothelial dysfunction can be a predictor of cardiovascular disease, and is an indicator of high mortality risk in HF patients [87,92].

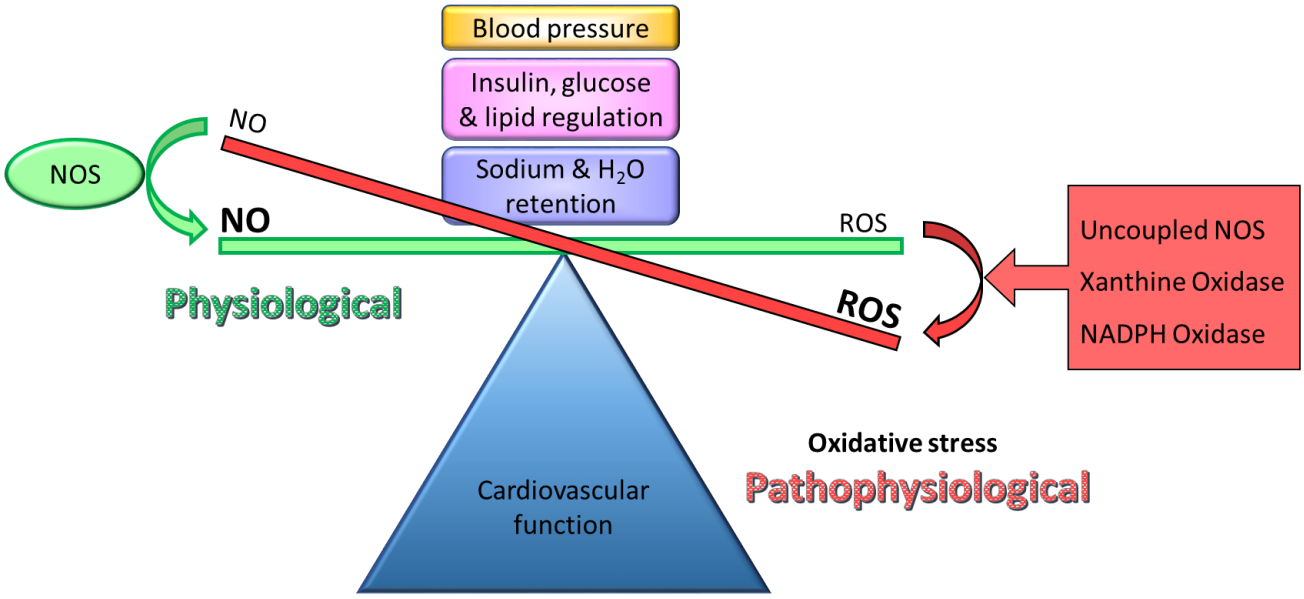

Figure 1.4: Balance in oxygen species underlie the pathophysiology of endothelial dysfunction. Uncoupled NOS, xanthine oxidase and NADPH oxidase increase cellular levels of ROS. Poor regulation of blood pressure, metabolic substrate levels and blood volume skew the balance for oxidative stress, resulting in pathophysiological endothelial function. Image adapted from Cai et al [89]. Abbreviations: NADPH – nicotinamide adenine dinucleotide phosphate; NO – nitric oxide; NOS – nitric oxide synthase; ROS – reactive oxygen species.

1.5.3 Physiological adaptation of the heart

1.5.3.1 Hypertrophy

Physiological hypertrophy is defined by the changes in the cellular and macroscopic structures of the heart as a result of a natural physiological increase in volume overload. This physiological adaptation occurs over extended periods of time (weeks), and can be reversible [93,94]. Adaptive hypertrophy happens in response to signalling cascades and the activation of certain biochemical factors such as extracellular-signal-regulated kinase (ERK) and insulin-like growth factor (IGF), which stimulates pathways involving protein kinase B (AKT) [95,96]. These are pro-survival pathways which inhibit apoptosis and promote growth, thus offering protection to the heart [97]. Another path offering protection is initiated by natriuretic peptides (ANP and BNP) which leads to the formation of cyclic guanosine monophosphate (GMP), the end result of which is the restriction of hypertrophy by repression of remodelling transcription factors [98,99].

1.5.3.2 Angiogenesis

Angiogenesis forms part of the remodelling process in the long-term. It aims to supply oxygen and nutrients to damaged tissue, and to newly formed or densified tissue, through the formation of new blood vessels from pre-existing vasculature. This is a complex process regulated by a number of signalling pathways. Signal transducer and activator of transcription 3 (STAT3) plays a role in angiogenesis under both physiological and pathological conditions by regulating the expression of multiple pro-angiogenic molecules [100]. Expression of vascular endothelial growth factor (VEGF) correlates with STAT3 activity, as STAT3 regulates transcription of VEGF [101]. Constitutive activation of STAT3 has been linked to angiogenesis involved in the progression of cancer [102]. Transient activation of STAT3 can be beneficial in the cardiovascular setting where tissue may be at risk of necrosis, due to cell damage and limited oxygen access. Loss of STAT3 in cardiomyocytes decreases capillary density, thus implicating STAT3 in the homeostatic regulation of vessel formation in the heart [103]. STAT3 deficient animal models have surprisingly not shown physiological changes in VEGF expression, but these animals show upregulation of anti-angiogenic and pro-fibrotic genes [104–106]. Many of the anti-angiogenic factors linked to inactivity of STAT3 are involved in the structural integrity of the extracellular matrix [107–109]. These findings support the idea of STAT3 playing a central role in the fundamental mechanisms regulating not just vasculature, but also the extracellular matrix in the heart.

Physiological hypertrophy differs from pathological hypertrophy in many ways; normal gene programming is maintained, fibrosis does not develop, and normal cellular function continues in physiological hypertrophy [98].

1.5.4 Pathological hypertrophy

Progressing from a normal, healthy heart structure to the structures present in pathologically affected hearts can occur either as a result of mechanical or neurohormonal stimulus. There are 2

mechanical triggers; an increased circulatory load due to (i) increased pressure or, (ii) increased volume (see review by Opie et al, 2006) [110]. These affect the contractile apparatus in muscle fibres.

Alpha-actin elements play a role in contractility of the heart, with α-skeletal actin and α-cardiac actin serving as the sarcomeric forms in adult hearts [111]. Messenger RNA expression of α-skeletal actin correlates with a greater increase in cardiac contractility compared to that of α-cardiac actin [112]. A-skeletal actin plays a role in pressure overload response, initially its mRNA transcription increases, and within a few days of the incident, declines [113]. These sarcomeric α-actins are paired and equally co-expressed (but independently regulated) in the foetal heart and in regenerating skeletal muscle [114–116]. Relative levels of expression of these 2 isoforms provides information as to the state of the tissue, as mRNA expression levels of α-skeletal actin are elevated transiently during hypertrophy, and fall to an intermediate level in overt HF [116,117].

Endocrine stimulation of the progressive HF state can be the end product of the release of noradrenaline [118], or with binding of natriuretic peptides to natriuretic receptors at the cell surface, activating signalling cascades modifying rate of function and effectivity of the target tissue [119].

1.5.4.1 Concentric LV hypertrophy

An increase in the circulatory pressure load causes the contractile tissue comprised of myocytes to thicken, which better opposes the pressure and continues to pump [98,110]. This leads to thickening of the chamber wall (see figure 1.5) reducing the internal volume capacity. This process is known as concentric LV hypertrophy. It is deemed beneficial, but when cardiomyocytes respond by apoptosis, the remodelling leads to LV dilatation (see figure 1.5).

Concentric hypertrophy is a pathological state which causes a metabolic and transcriptional reversion to the foetal gene program in rodent models [72,78,120]. It is the most fibrotic of the hypertrophic states, and in some instances, is characterised by myocardial cellular dysfunction.

The reaction of the heart to haemodynamic and metabolic stress causes the suppression of the post-natal gene program, and reversion to the foetal gene program [121]. The foetal heart is geared toward surviving the stress of hypoxia, favouring oxygen-sparing mechanisms in metabolism, thus preferring glucose and carbohydrates as metabolic substrates over fatty acids [72].

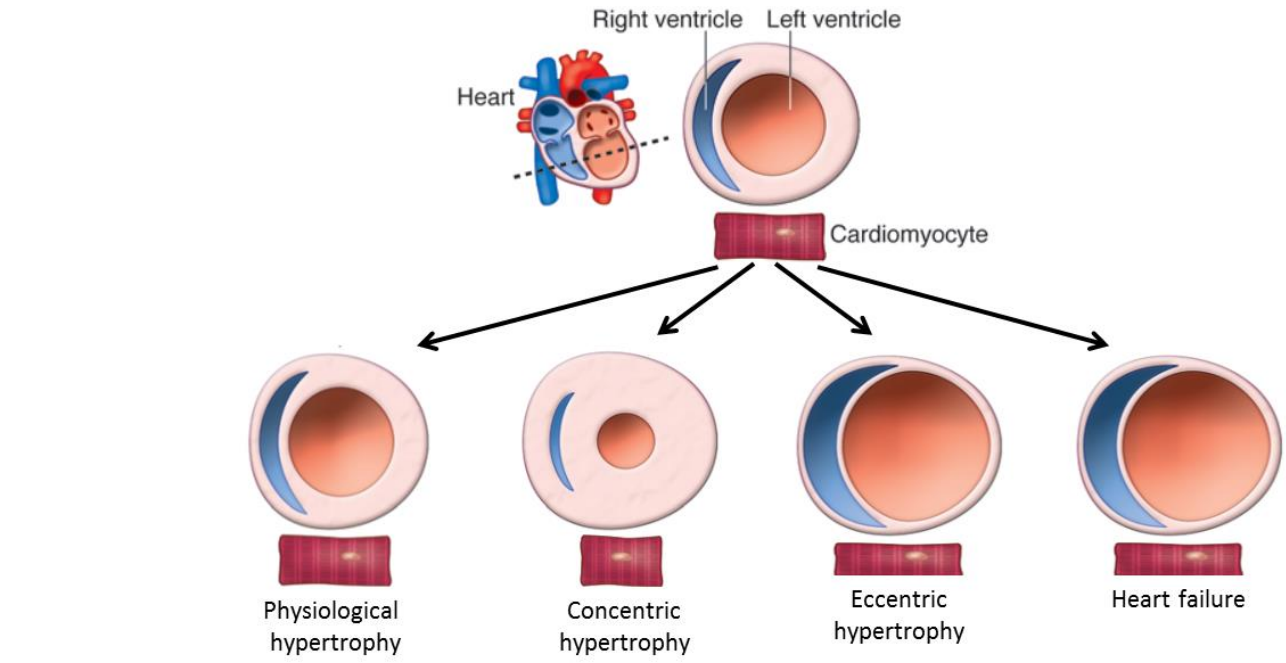

Foetal genes	-	+	+	+
Fibrosis	-	+++	-/+	++
Cellular dysfunction	-	-/+	-/+	++

Figure 1.5: Cardiovascular remodelling occurring in the left ventricle as a result of pathological stimulus. Physiological hypertrophy may be reversed and does not activate the foetal gene program, fibrosis, or cellular dysfunction. Concentric hypertrophy due to an increased pressure load, and eccentric hypertrophy which occurs as a compensatory measure, activate the foetal gene program and may cause cellular dysfunction. Image adapted from van Berlo et al & Opie et al [110,122]

Metabolism and HF form a negative feedback loop: aberrant metabolism leads to HF leading to further altered metabolism, etc. [123]. The defunct energy dynamics result from adrenergic activation, together with increased deleterious free fatty acid metabolism, decreased beneficial glucose metabolism, and compounded by insulin resistance in some instances [121,124]. The cellular fuel ATP becomes depleted in the myocardium and the efficiency of mechanical potential decreases [72]. Postnatally, energy substrate metabolism switches rapidly to fatty acid oxidation [72]. This metabolic switch is accompanied by the switch in expression of metabolic enzymes as well as other proteins [72,78].

Under hypoxic and hypertrophic conditions, such as may be present in pathological maladaptive conditions and HF, the adult heart reverts to the foetal gene program.

Reversion to the foetal gene program favours the re-expression of atrial natriuretic peptide (ANP), transforming growth factor β (TGF-β), and switches to foetal expression isoforms of metabolic enzymes and sarcomeric proteins such as myosin heavy chains and α-actins [72]. Certain factors, such as Periostin, which are re-expressed in HF and hypertrophy have altered fibroblast function, affecting the structural integrity of the muscle [125].

The isoform expression of many sarcomeric proteins switches at birth. The myosin heavy chain (MHC) isoform switch appears to be directly related to the required mechanical performance and efficiency of function required after birth. In mice, MHC-β is the predominant isoform in the ventricle of the developing heart, but is replaced by MHC-α isoform postnatally [126]. Humans, however, express the MHC-β isoform regardless of whether they are in developmental or adult stage [74,127], although skeletal α-actin and titin isoforms are developmentally regulated. In the foetal and neonatal heart α-skeletal actin is the dominantly expressed isoform. This switches to α-cardiac actin in the adult heart [72,127]. With time, the foetal expression program is insufficient to support mechanical function and structure of the heart [72].

Increased pressure activates the release of angiotensin II enzyme and aldosterone (which promote reabsorption of water), further increasing volume load, and TGF-β, which in turn activate the mitogen-activated protein kinase (MAPK)/ JNK pathway promoting fibrosis and cell death [110,128]. The renin-angiotensin-aldosterone system (RAAS) can also directly activate hypertrophy, inflammation, or fibrosis independently of load changes, as demonstrated in animal models [129–132].

1.5.4.2 Eccentric LV hypertrophy

An increase in the circulatory volume load causes the contractile tissue comprised of myocytes to lengthen. This leads to enlargement of the chamber (see figure 1.5), often thinning the muscle walls - a process known as eccentric LV hypertrophy[98,110]. This often occurs in a pathological setting as a compensatory measure after the formation of infarct scars. Transient eccentric LV hypertrophy is deemed beneficial, but when cardiomyocytes respond by apoptosis, the remodelling leads to LV dilatation (see figure 1.5). Dilatation can also occur in certain cardiomyopathies as a result of dysfunctional sarcomeric proteins which facilitate binding of adjacent cardiomyocytes, such as B-myosin heavy chain (β-MHC), myosin-binding protein C, myosin light chains, cardiac troponin T and cardiac actin [133–136].

Eccentric hypertrophy is a pathological state which causes a metabolic and transcriptional reversion to the foetal gene program [72,78,120]. There may be some instances when fibrosis or cellular dysfunction occurs. In the event that it progresses to HF, hearts will revert to the foetal gene program, have moderate fibrosis, and will have cellular dysfunction.

1.5.5 Mixed remodelling

Concentric left ventricular hypertrophy occurs in response to increased pressure load. This causes thickening of myocytes and LV chamber wall. Eccentric hypertrophy occurs in response to an increased volume load, which causes lengthening of the myocytes (see figure 1.6). Presence of scar

tissue together with a mixed volume and pressure load increases LV volume and has mixed concentric and eccentric remodelling [98,110,122]. This can occur after formation of an infarct in the progression to HF (see figure 1.6).

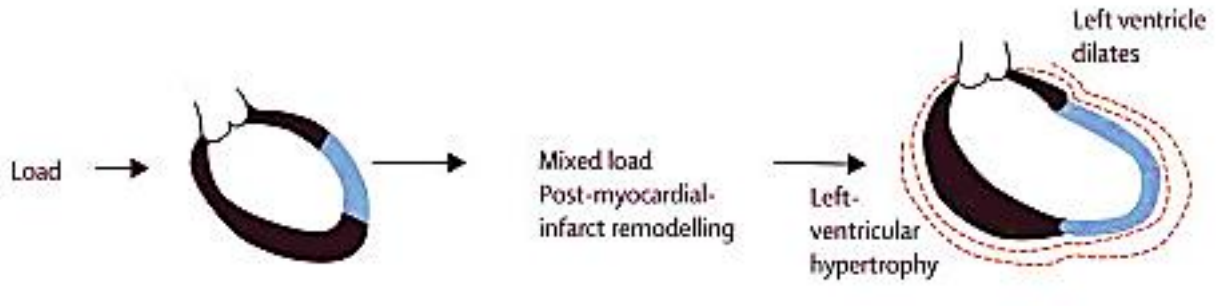

Figure 1.6: Mixed remodelling is can occur in the presence of myocardial scarring (indicated in blue). An increased load in this instance causes dilation of the scarred regions, and hypertrophy in healthy regions. Image adapted from Opie et al [110]

1.5.6 Inflammation and Fibrosis

The medley of factors involved in the development of fibrosis is complex. Initial inflammation facilitated by the immune system, in response to stimulus by the likes of Angiotensin I & Angiotensin II (Ang II). This causes the release of intrinsic inflammatory response cells including neutrophils, monocytes and macrophages to sites of tissue damage. Ang II induces expression of collagen 1 (col1) & collagen 3 (col 3), TGFβ1, and tumour necrosis factor (TNF) mRNA – cytokine and chemokine compounds - which precede fibrosis [137]. Monocytes circulate in the blood and are recruited to hypertrophic tissue in response to chemokines [138]. Once there, they may differentiate into macrophages [139]. Macrophages serve various functions including immune defence and tissue remodelling, particularly with hypertrophy induced by mechanical overload [140].

These processes of hypertrophy are influenced by cardiomyocyte-fibroblast balance. The above process is known as reaction fibrosis and occurs due to pressure or volume overload, prior to cardiomyocyte death. Replacement fibrosis occurs due to scar formation, after cardiomyocyte

death. Chronic HF is characterised by systemic inflammation with raised circulating levels of cytokines and chemokines, such as TNFα and interleukin 1β, in proportion to the degree of severity [140]. This inflammation can be infectious (e.g. endotoxins), or non-infectious (e.g. haemodynamic overload or oxidative stress), and can originate in a multitude of tissues and cells outside of the myocardium [141]. These include endothelial cells, leukocytes, platelets and tissue macrophages among others and are sometimes as a result of neurohormonal activation [142].

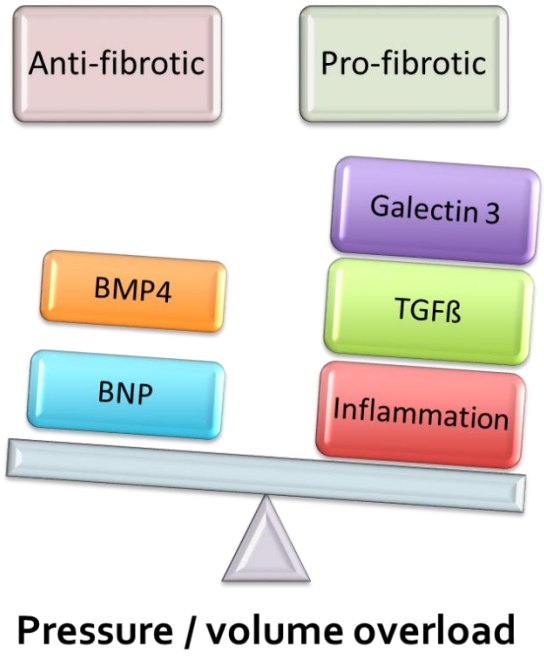

Figure 1.7: Regulation of fibrosis. Fibrosis is regulated by a balance between pro-fibrotic compounds pro-fibrotic and anti-fibrotic compounds and processes. Abbreviations: BMP4 – bone morphogenic protein 4; BNP – brain natriuretic peptide; TGFB – transcription growth factor β.

Fibrosis associated with cardiac dysfunction is a factor which is a result of cardiac remodelling – a series of events involving imbalances of structural elements of the extracellular matrix, as well as agents which degrade it. It is a slow process which starts with long-terms inflammation [143,144]. TGFβ is one of the factors released in response to injury, playing a role in tissue repair and as an agent facilitating fibrosis. Its activity is function to the cytokine profile (and thus the inflammatory nature) of the surrounding tissue [145,146]. An imbalance of anti-inflammatory factors such as tumour necrosis factor α (TNFα) weigh against the activity of pro-inflammatory factors such as

angiotensin II, and aldosterone in early stages, and can be part of the initial profile of individuals who go on to develop cardiac fibrosis and pathological hypertrophy (see figure 1.7) [110,147,148].One such factor is galectin-3, a soluble β-galactoside-binding protein secreted by activated macrophages which mediates aldosterone-induced cardiovascular inflammation and fibrosis [149]. It promotes collagen deposition and cardiac fibroblast proliferation [150]. It can be used as a prognostic tool for heart failure (particularly with HFpEF) as plasma levels correlate with heart failure outcomes [151]

Bone morphogenic protein 4 (BMP4) is a factor produced in endothelial cells in response to oscillatory shear stress (i.e. factors which apply great pressure and cause cell-slippage) [152,153]. Persistent elevation of BMP4 is associated with endothelial dysfunction, increased oxidative stress, and activation of inflammatory pathways which facilitate cell apoptosis and fibrosis in the long-term [154]. BMP4 plays a regulatory role in inflammation, by producing ROS and NADPH, leading to the adhesion of monocyte cells to endothelial cells [152]. Down-regulation of bone morphogenic protein receptor type II is noted for its role in pulmonary hypertension – an effect prevented by the activity of IL-6, and STAT3 [155]

Expression of TGF-β1 in the heart induces the expression of collagen – this is the backbone of scaffolding for the structure of the cardiac chambers [156]. Collagen 1 is known for re-enforcing scar tissue and is a good indicator of the density of chamber wall thickness [157]. Activation of collagen 1 in the LV leads to hypertrophy, and further, fibrosis [147]. Collagen 3 plays a role in the elasticity of the chamber wall [158]. The long-term expression of collagens 1 & 3 leads to fibrosis of the cardiac tissue and is associated with apoptosis of cardiomyocytes, which hampers the contractile ability of the wall.

Fibronectin also contributes to the structural integrity of the chamber wall. It is an extracellular matrix protein regulated by Ang II which binds extracellular matrix components including

collagen [159]. Overexpression of fibronectin coincides with that of collagen 1 and is associated with the development of fibrosis [160].

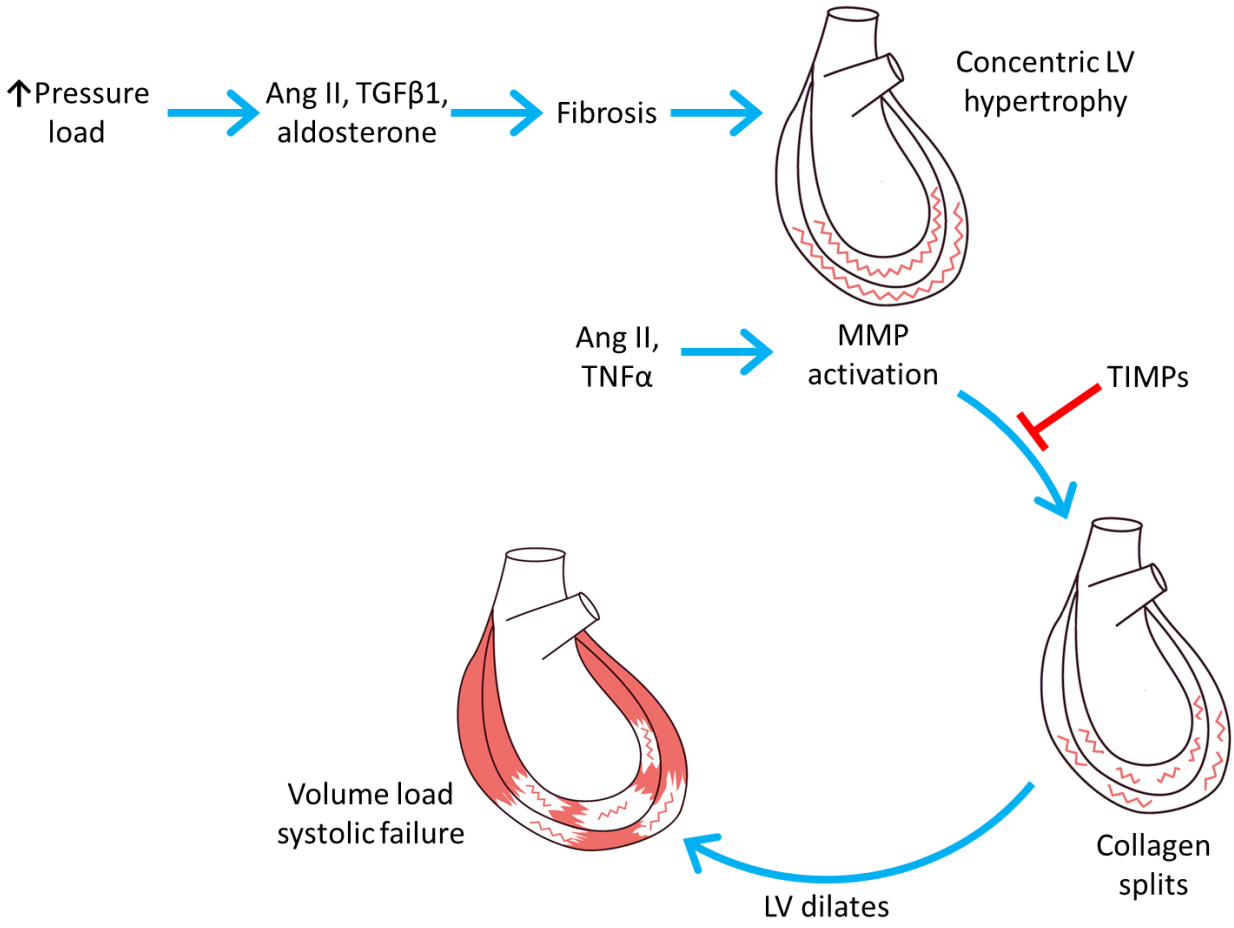

Figure 1.8: Increased pressure load causes the release of key factors Ang II, TGFβ1, and aldosterone which over time cause fibrosis. MMP activation over extended time causes collagen crosslinks to split, leading to LV dilation, later evolving to systolic failure. Ang II, TNFα and reactive oxygen species can also directly activate MMPs without the development of hypertrophy. Collagen crosslinks are saved from splitting by the activity of TIMPs, which oppose the activity of MMPs. Figure adapted from Opie et al [110]. Abbreviations: Ang II – angiotensin II; LV – left ventricle; MMP – Matrix metalloproteinase; TGFβ1 – transcription growth factor β1; TIMPs – tissue inhibitor of metalloproteinases; TNFα - tumour necrosis factor α

With time, matrix metalloproteinases (MMPs) in the hypertrophied heart degrade the collagen crosslink structure, with their activity opposed by tissue inhibitors of metalloproteinases (TIMP1). MMPs can be induced by stress responses and the release of stress response factors such as TGFB1, tumour necrosis factor α (TNFα), reactive oxygen species (ROS) and angiotensin II (AngII). This

leads to splitting of the crosslinked collagen network, weakening the integrity of the scaffolding, causing dilation of the LV and ultimately systolic failure (see figure 1.8). In instances of HF, TIMP 1 mRNA expression is increased, correlated with levels of pro-inflammatory cytokines [161]. MMPs and TIMPs appear to be regulated independently of each other, and an imbalance in expression determines the progression of fibrosis [162]. On progression to heart failure, selective upregulation of MMPs together with downregulation of TIMPs favours extracellular matrix degradation, leading to dilatation [163].

2. Pregnancy and heart failure

The maternal body must adapt during pregnancy to supply both foetal and maternal needs. There are systemic physiological changes, most notably affecting the cardiovascular system, which fulfil the needs of the foetus. These physiological changes may appear to be pathological, but they are temporary changes which resolve after delivery with minimal residual effects. Under certain circumstances the maternal circulatory system takes strain, and pathologically modifies without resolution. It is the case, for example, in the heart failure-like symptoms seen in peripartum cardiomyopathy (PPCM).

2.1 Physiological changes during pregnancy

The physiological changes observed in pregnant women are fulfilling the oxygen, metabolic fuel, and nutrient needs of both the mother and the growing foetus, while also eliminating metabolic waste products (see figure 1.9). Thus as the foetus grows in a normal pregnancy, the circulating volume steadily increases in proportion to the growth[164]. This increase in volume is due to an increase in plasma, and not necessarily all of the components comprising whole blood [165]. Pregnancy is itself a state of heightened coagulability, proposed to be in preparation for haemostasis following delivery [166].

Cardiac remodelling in pregnancy is homeostatically regulated. Non-fibrotic remodelling develops with an extended capillary network to accommodate the increased volumetric load – this is reversible and does not carry the classical markers of pathological hypertrophy (see section 1.5) [93,167]. Pregnancy is a natural physiological instance of volume overload, the outcome of which is an increase in the heart muscle mass. This is a reversible process and the heart reverts shortly after delivery.

2.1.1 Stroke volume, heart rate and blood pressure

The increased volumetric load during pregnancy results in cardiovascular changes where the heart and blood vessels adapt to accommodate the new circulatory needs of the body. These changes begin during early pregnancy, with a graded increase in cardiac output and peripheral vasodilation (see review by Soma-Pillay et al)[165]. With vasodilation, there is a fall in vascular resistance, and a compensatory increase in cardiac output – primarily by increased stroke volume, and to a lesser extent, a higher heart rate [168]. An increase in stroke volume is accompanied by the development of physiological hypertrophy as the ventricular wall mass and the end-diastolic volume both increase, and there is greater myocardial contractility [168]. As the pregnancy reaches term, cardiac output is maintained even though stroke volume begins to return to normal, while the maternal heart remains 10 to 20 beats per minute (BPM) higher than normal [168].

2.1.2 Cardiac output during labour and delivery

Cardiac output increases by up to 50% during the late stages of labour, with increases between and during contractions [168]. Uterine contractions auto-transfuse blood back into circulation which increases the pre-load. Pain and anxiety felt during labour activate the sympathetic nervous response [165]. Immediately after delivery, there is an increase in cardiac output, which rapidly declines to pre-labour levels within an hour. Recovery to non-pregnant levels happens 4 – 8 weeks after delivery [169,170].

Normal pregnancies have increased cardiac output as a result of relieved pressure on the inferior vena cava, and contraction of the uterus. Thus, women with cardiovascular conditions are most at risk for pulmonary oedema during late labour and immediately post-partum.

The changes in the cellular and macroscopic structures of the heart due to increased load (hypertrophy) are reversible physiological adaptations which are often seen in pregnancy in both humans and other animals [93,94].

2.1.3 Water and haemodynamic regulation

Relaxin is a peptide hormone released by the corpus luteum and placenta, which plays a role in water regulation [171]. Serum concentrations of this hormone are increased during pregnancy, rising until the end of the first trimester, and decreasing slightly thereafter to above-normal levels for the remained of the pregnancy [171,172]. It stimulates the release of endothelin, releasing nitric oxide which causes renal vasodilation [172].

The Renin-Angiotensin-Aldosterone system (RAAS) is also differentially regulated during pregnancy. Arterial under-filling due to reduced vascular filling and blood pressure stimulates the sympathetic nervous system, thus activating RAAS [173–175]. This increases renin released by the kidneys and aldosterone levels in the plasma, causing the sodium and water retention typically found in pregnancy [173,176]. During RAAS activation in early pregnancy, women develop relative resistance to Ang II, facilitating vasodilation without a marked increase in blood pressure [177]. The same relative resistance may occur with other vasoconstrictive receptors such as adrenergic agonists [171].

2.1.4 Release of natriuretic peptides

During the mid- to late- stages of pregnancy the expression of the aminopeptidase and vasopressinase by the placenta is dramatically increased, and in cases such as twin pregnancies or pre-eclampsia it may result in the development of transient diabetes [178]. Vasopressinase has a downstream effect of volume expansion, activating atrial stretch receptors, which is associated with the release of atrial natriuretic peptides (ANP) during the last trimester and post-partum.

These are notably higher in pregnancy with hypertension or pre-eclampsia [179]. BNP increases at the onset of pregnancy, but remains steady during all 3 trimesters in healthy women [180,181].

2.1.5 Changes in cellular respiration

The circulatory system has to adapt to provide oxygen for both the mother and the foetus. A growing foetus increases the maternal metabolic rate, and demand and consumption of oxygen. It may be accompanied by a sensation of breathlessness at rest without actual hypoxia – a physiological adaptation commonly presented during the last trimester which may paradoxically improve with mild exercise [165].

2.1.6 Release of prolactin

During pregnancy, the nursing hormone, prolactin, is released by the pituitary gland. It is primarily responsible for lactogenesis in pregnant and nursing women – a process which enlarges mammary glands to produce milk when infants are suckled. The prolactin peptide is produced as a 30kD protein which can be differentially cleaved. Prolactin levels increase right from the start of pregnancy, and are up to ten-fold higher at the time of delivery [182,183]. It continues to be produced in the post-partum period in response to suckling.

2.1.7 Glucose metabolism

Glucose is the primary source of fuel for the developing foetus as it grows in its hypoxic environment. Glucose and amino acids are diverted to the foetus, and the mother primarily uses lipids as fuel during pregnancy [165]. The maternal body enters a diabetogenic state which alters metabolism to allow the foetus to harness the glucose in the shared blood supply [184]. There is an over-production of insulin by pancreatic β cells, together with an increase in insulin resistance that starts in the second trimester and peaks in the third trimester [185]. This is caused by the release of diabetogenic factors such as prolactin, placental lactogen, growth hormone, progesterone and

cortisol which impair insulin activity [186,187]. This resistance ceases after delivery and insulin sensitivity is restored [188].

2.1.8 Oestrogen and progesterone

In the late phase of pregnancy, the release of oestrogen induces PI3K-Akt signalling in the heart via c-Src-kinase. It has been proposed that oestrogen is cardioprotective in pregnancy [93,189,190]. At the onset of pregnancy, plasma levels of progesterone increase to maintain the placenta and uterine wall for the growing foetus, as well as to develop breast tissue for milk production [191]. Progesterone levels start to drop 5 weeks before the onset of labour [192]. They restore to levels in the luteal phase of a normal menstrual cycle within 24 hours of delivery [193].

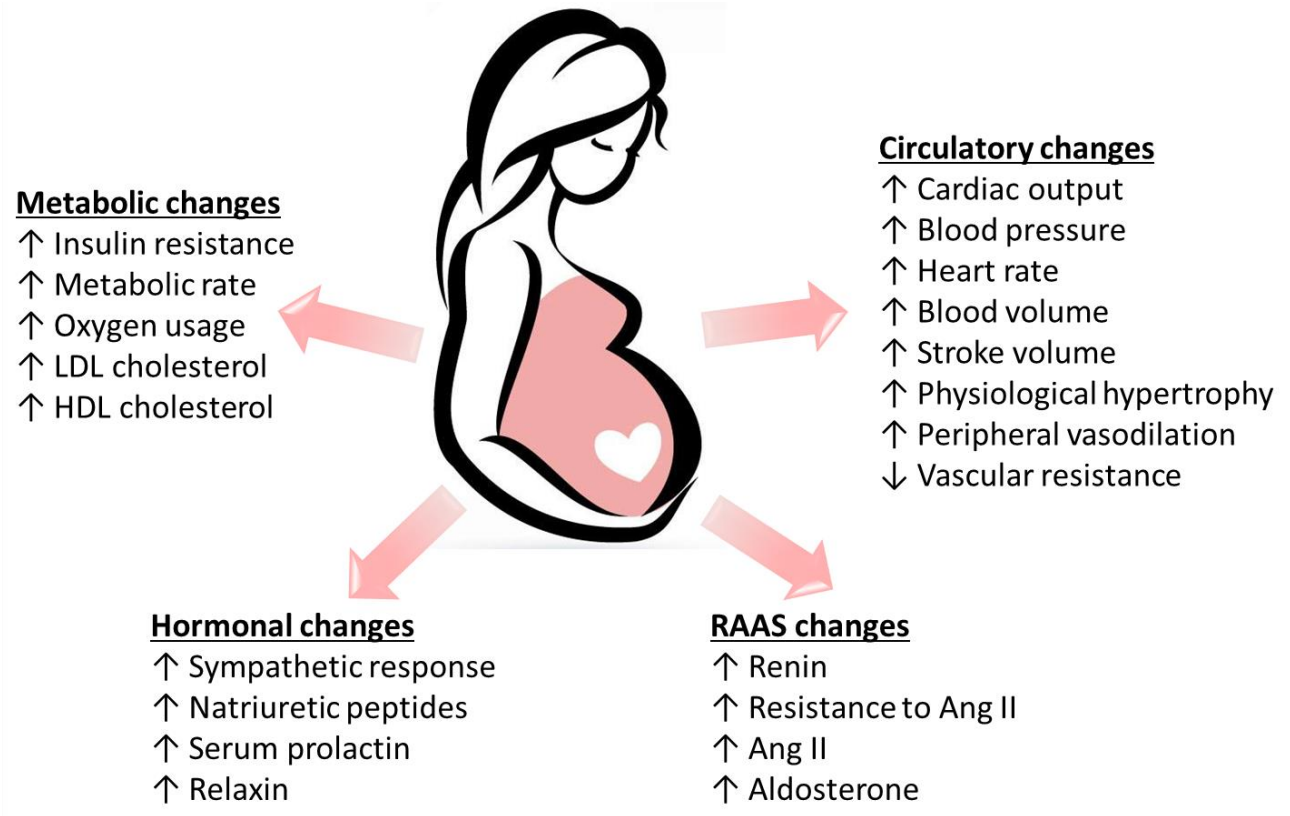

Figure 1.9: Biochemical changes which occur during normal pregnancy. Abbreviations: Ang II – angiotensin II; HDL – high density lipoprotein; LDL – low-density lipoproteins; RAAS – renin-angiotensin aldosterone system.

2.2 Peripartum cardiomyopathy

2.2.1 Definition, prevalence & outcome

Peripartum cardiomyopathy (PPCM) is defined as an idiopathic cardiomyopathy presenting with HF secondary to LV systolic dysfunction towards the end of pregnancy or in the months following delivery, where no other cause of HF is found [194]. The LV may not be dilated but the EF is always reduced below 45% [195].

PPCM patients present with typical symptoms of heart failure such as dyspnoea, exercise intolerance, coughing and orthopnoea. The most common presentation in these patients is either sinus rhythm or sinus tachycardia [19,196].

PPCM is not exclusive to ethnicity, and the prevalence is geographically diverse, with higher incidences in some regions. It has a prevalence of approximately 1 in 300 births in Haiti, 1 in 1000 births in South Africa, and 1 in 1150–4000 births in the USA [197–200]. Incidences in the rest of the world are not well studied. Prevalence and overall outcome of PPCM in certain regions appears to correlate with low socio-economic status and ethnicity [194,200–203].

Pregnancy is a physiological stress on the cardiac system and can prematurely precipitate genetic cardiomyopathies. Individuals with deleterious truncations can develop the related cardiomyopathies which can be (mis)diagnosed as PPCM for lack of family history or other underlying cardiac factors. Screening for genes known to play a role in dilated cardiomyopathy in patients diagnosed with PPCM have revealed that some of the PPCM patients (3 of 5) carried familial mutations associated with DCM [204]. Distinction between genetic and non-genetic predisposition to PPCM may be particularly significant, as early epidemiological studies have indicated that the outcomes for women who have a family history of cardiac dysfunction have poor prognosis [205].

2.2.2 Aetiology

The precise mechanisms leading to the development of PPCM are not clearly defined, but might be exacerbated by factors such as hypertension, diabetes, gravidity and parity [206].

PPCM appears to be an acute cardiomyopathy which may have an autoimmune basis. Certain studies have found prevalence of unique antibodies and cardiac specific autoantigens, as well as foetal michrochimerisms in the maternal circulation [207]. Antibodies to cardiac-specific antigens include adenine nucleotide translocator (ANT), cardiac myosin, and β-2-adrenergic receptor protein antibodies [208–213]. These have been identified in blood samples in patients with idiopathic cardiomyopathies (i.e. the category under which PPCM falls), supporting the idea of an auto-immune basis for cardiomyopathies [208–213]. There have also been antibodies found in sera of human patients with PPCM which are not present in other idiopathic cardiomyopathy profiles [214,215]. The PPCM phenotype is an interplay between the adaptative changes associated with pregnancy, such as aberrant activation of vasoactive hormones, as well as other factors in the altered immune environment [207].

The development of PPCM has also been linked to the differential cleavage of the nursing hormone prolactin, the mechanism of which is detailed in section 2.2.3.

2.2.3 Pathophysiology

The time course and evolution of PPCM is highly variable by patient phenotype and thus not well understood. PPCM is an acute-onset heart failure condition. One main pathophysiological feature is left ventricular systolic dysfunction with reduced ejection fraction and fractional shortening. Not all patients present with left ventricular dilatation, rather it is generally observed in the more severe and irreversible cases [195,199,216].

The precise mechanism leading to left ventricular dysfunction in PPCM remains elusive, but many clinical and experimental studies lend support to the idea that increased oxidative stress may play an important role in the initiation of the disease. This hypothesis is supported by observed increased levels of pro-oxidative factors in circulation – a critical feature which initiates angiogenic imbalance and inflammatory processes [196,217–219].

2.2.3.1 Proteolytic cleavage of prolactin

Recently, prolactin has been implicated in the pathogenesis of PPCM. Proteolytic cleavage of the full-length nursing hormone by Cathepsin D to its anti-angiogenic 16kD fragment under the influence of unbalanced oxidative stress, which is responsible for pro-inflammatory, apoptotic and anti-angiogenic effects [203,220–222]. It promotes adhesion of inflammatory cells to the endothelium and further vasoconstriction [223,224]. Levels of progenitor dendritic cells (which play a role in innate and adaptive immunity) are reduced in PPCM patients which accounts in part for the dysregulation of cardiac remodelling in pregnancy which contributes to pathogenesis of PPCM [225].

Cleavage of prolactin in this manner by Cathepsin D has been identified as a factor initiating and driving PPCM [196] - a hypothesis fits well with the observation that bromocriptine, a blocker of prolactin formation, improved the outcome of PPCM patients in clinical trials [226,227].

Increase in levels of 16kD prolactin has been attributed to the low activation of two cardioprotective signalling pathways – signal transducer and activator of transcription 3 (STAT3), and peroxisome proliferator-activated receptor-γ coactivator 1α (PGC-1α) [196,228–230]. The 16kD isoform is also linked to the activation of STAT3 in several cell types including cardiomyocytes [196,231]. Cardiomyocyte deletion of STAT3 or PGC-1α in mice induces PPCM-like phenotypes (see section 2.2.2) with a decrease of cardiac antioxidant activity. Increase in reactive oxygen species together with a decrease in manganese superoxide dismutase (MnSOD) levels activates cathepsin D. An increase in cathepsin D activity has been observed in human patients with PPCM with

amplified levels of oxidised low density lipoproteins as well as diminished levels of PGC-1α and STAT3 [196,217,228]. The mechanisms by which these factors are decreased in PPCM patients is still unknown.

2.2.3.2 Inflammatory cytokines

Present efforts in expanding the knowledge-base for PPCM highlight the role of inflammation and autoimmune reactions as pathological causes [206,232]. Animal models show higher circulating levels of pro-inflammatory cytokines (Interleukin-6, TNFα, Interferon γ and C-Reactive Protein), where levels of these cytokines correlate with reduced LV function [219,233,234]. In addition to these factors, cardiac fibrosis has been demonstrated in PPCM animal models, but has not been well studied in humans.

2.2.3.3 Matrix metalloproteinase activity

Cleavage of prolactin into its 16kD isoform may also be related to the activity of matrix metalloproteinases (MMP1, 2, 3, 8 & 13) [221]. MMP2 has been implicated in PPCM, as patients have higher circulating levels of this protein, while MMP3 expression levels were found to be higher in the hearts of PPCM mice [196,217]. Pro- and anti-oxidative processes must be balanced for maintenance of good maternal health [203]. An increase in oxidative stress with PPCM activates cathepsin D which promotes MMP activation, exacerbating cardiac dilatation (see section 1.5) and the PPCM phenotype [189,235–237].

2.2.3.4 Endothelial dysfunction and apoptosis

Endothelial dysfunction and angiogenic imbalance appear to promote metabolic shortages in the heart which cause cardiomyocytes apoptosis and dysfunction of cardiac contractility in PPCM [229,230,233,238].The rapid cardiac decompensation observed may be explained by maladaptive remodelling and poor cardiac compensation.

There are two distinct pathways which involve 16kD prolactin: Nuclear factor kappa-light-chain-enhancer of activated B cells microRNA-146a (NFκB–miR-146a), and soluble fms-like tyrosine kinase-1 (sFlt1)/VEGF which mainly trigger the vascular impairment preceding HF. The NFκB pathway, activated by 16kD prolactin, up-regulates endothelial expression of miR-146a, inhibiting endothelial cell proliferation and migration. Exosome release of miR-146a into the circulation affects cardiomyocytes metabolism and adaptability [238]. Downregulation of PGC-1α inhibits the activity of VEGF which results in an imbalance with sFlt1 observed in the peripartum phase [228]. An increase in levels of circulating miR-146a, sFlt1 and apoptosis signalling molecules (Fas/Apo1) have been observed in PPCM patients [218,219,228,238].

In addition to endothelial cell death and capillary constriction, an increase in cardiomyocyte apoptosis has been reported in PPCM, proposed to be facilitated by caspase 3 [229]. An improvement of cardiac function was observed with inhibition of apoptosis, reducing mortality, which supports the idea of apoptosis as an underlying factor of PPCM pathogenesis [230].

One marker which links to poor outcomes is the first apoptosis signalling receptor / apoptosis antigen 1 (Fas/APO-1), a receptor involved in apoptotic signalling [218]. In clinical studies, significantly higher levels of soluble Fas/APO-1 were found in PPCM patients when compared to healthy controls [218]. It was further found that levels of Fas/APO-1 can be a predictor of mortality in PPCM patients, as patients who die have significantly higher levels compared to those who survive [218,219].

2.2.4 Animal models used to study peripartum cardiomyopathy

Animal models have been developed to investigate the patho-mechanisms of PPCM. These different mouse models develop the PPCM phenotype at different rates. Multiple pregnancies appear to proportionally increase the severity of the PPCM phenotype – this also links to the genetic background of the mice with the gene knockout [239,240].

There are various genetic knockout mouse models used to study PPCM:

1) Mice with cardiac-specific deletion in the STAT3 gene go on to develop a PPCM, proving lethal after 3 to 4 pregnancies in females with heterozygous deletions, and after 2 pregnancies in homozygous females [196]. These mice also showed upregulation of the pro-apoptotic factor, Bcl-2/adenovirus EIB 19kD-interacting protein 3 (BNIP3), associated with greater myocardial apoptosis [196,241]. They developed severe fibrosis and dilatation of the chambers in the post-partum period, highlighting the significant role of STAT3 in pregnancy-related cardioprotection. These mice have been used to identify the significance of the 16kD isoform of prolactin (which links to STAT3) and the beneficial role of bromocriptine as a treatment strategy in the setting of PPCM [196].
2) Mice with cardiac-specific overexpression of the α-subunit of Gq (Gαq) go on to develop severe and lethal PPCM as a result of excessive cardiomyocyte apoptosis after just a single pregnancy [230]. This model highlights the role of apoptosis as a causative factor in the development of PPCM. They showed that inhibition of the pro-apoptotic factor Nix in this model reduced mortality and LV remodelling [242].
3) Mice with knockout of the programmed death 1 (PD-1) gene, encoding a negative immunoregulatoy receptor [240]. This autoimmune model is used to study dilated cardiomyopathies and can develop a PPCM-like phenotype with pregnancy. These mice develop severe contractile abnormalities and sudden death by congestive heart failure.
4) Mice with cardiac-specific knockout of PGC1α, which limits mitochondrial biogenesis, and disturbs cardiac metabolic programming and angiogenic balance. These mice develop PPCM-like symptoms of cardiac dilatation and extensive fibrosis with spontaneous death after the first or second pregnancy [228–230].

5) Mice with a dual knockout of dystrophin and cardiac β1 integrin show high mortality in peripartum settings, with severe fibrosis, myocardial necrosis, and extensive dystrophic calcification [243,244].

2.3 Current treatment strategies

2.3.1 Beta-blockers

B blockers competitively inhibit the β-adrenergic receptors in the heart by binding and blocking the sites which respond to sympathetic activation hormones released by the adrenal glands. This method of competitive inhibition prevents the excessive increase in HR and contractility – it prevents worsening of the condition, but has limited ability to improve existing contractility and HR problems which are not caused by sympathetic nervous activation [245].

2.3.2 Angiotensin-converting enzyme inhibitors

ACEi treatments target enzymes that originate in the lungs and prevent the conversion of angiotensinogen to angiotensin I and further to angiotensin II (see figure 1.10). The final version, angiotensin II, (a) increases sympathetic activity, causing the heart to beat faster, (b) promotes water retention by reabsorption of sodium and chlorine in renal tubules, (c) increases aldosterone excretion from the adrenal glands, causing further water retention, (d) causes arterial vasoconstriction, thereby increasing blood pressure, and (e) promotes the release of anti-diuretic hormone by the pituitary gland, also increasing water retention. ACEi treatments decrease the levels of angiotensin, reducing the hormone aldosterone which contributes to the control of sodium and water retention. These actions also contribute to the excretion of water and the outcome is similar to that of diuretics – better oxygenation of tissues, lower blood pressure, and reduced circulating water volume, which indirectly improve breathing and contractility of the heart

[18,36,246,247]. ACEi treatment is contra-indicated during pregnancy, as it is linked to an increased risk of foetal renal damage, but is recommended for treatment post-partum, [248].

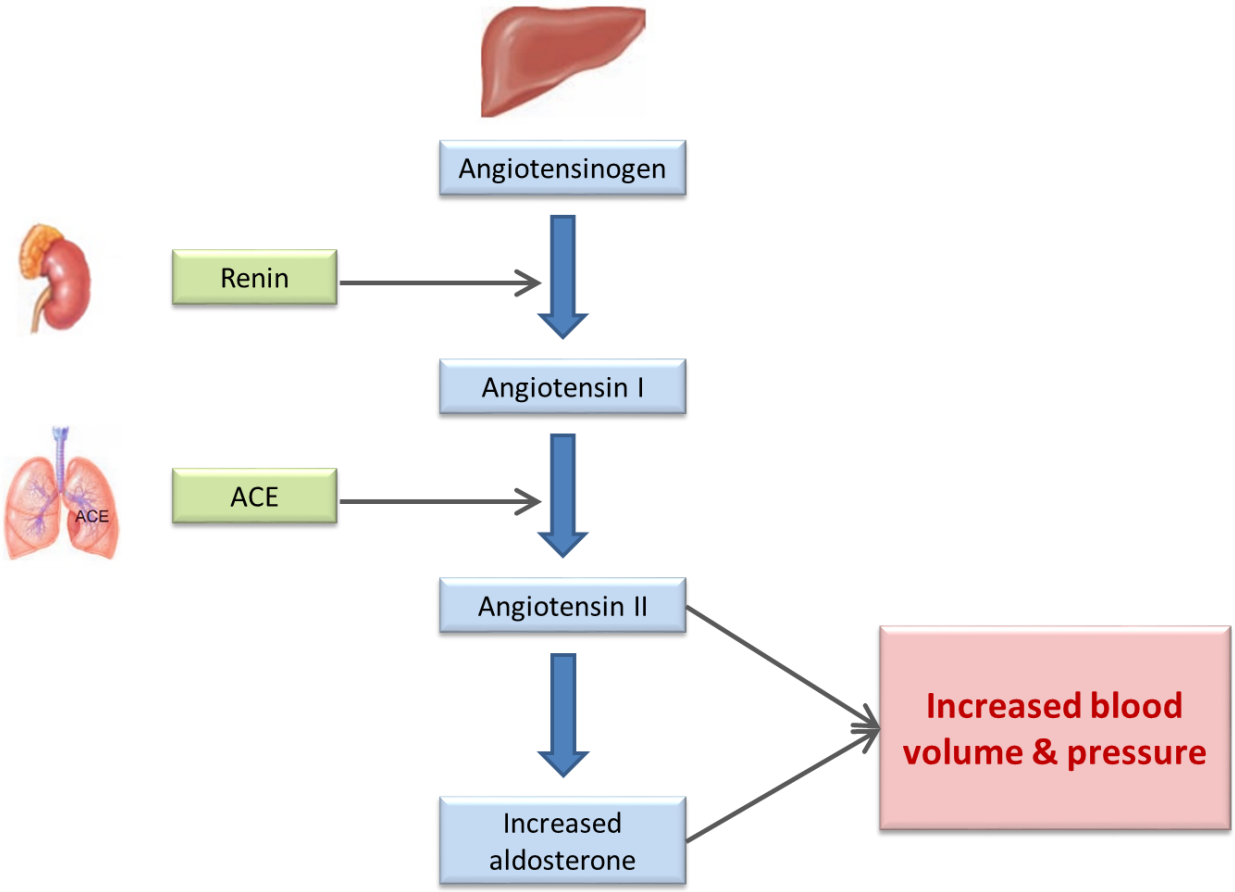

Figure 1.10: The renin-angiotensin-aldosterone system. ACE released from the lung facilitated the conversion of Angiotensin I to the vasoactive form, Ang II. Ang II directly increases blood pressure by its effects on the renal tubules. It also stimulates the release of aldosterone by the adrenal cortex, which further increases blood volume, and pressure. ACE inhibitors prevent the conversion of angiotensinogen to angiotensin by targeting enzymes in the liver. Adapted from Antranik.org [249]. Abbreviations: ACE – angiotensin-converting enzyme; Ang II – angiotensin II.

2.3.3 Mineralocorticoid receptor antagonist compounds

Mineralocorticoid receptor antagonist (MRA) compounds have diuretic effects which target the kidneys, increasing the rate of excretion of water from the circulatory system, thereby decreasing blood pressure and the load on the heart. The outcome of this is better oxygenation of tissues, lower

blood pressure, and reduced water retention. This improves breathing and contractility of the heart as secondary outcomes [18,246,247].

MRA compounds antagonise the action of aldosterone in the kidneys, increasing the rate at which water is excreted. Aldosterone is secreted by the adrenal cortex and stimulates Na+/K+–ATP pumps in the distal convoluted tubule portions of the nephrons, thus retaining water. MRAs inhibit this activity, acting as a diuretic, thus sodium and water are not reabsorbed in the kidneys [18,246,247]. The overall outcome is better oxygenation of tissues, lower blood pressure, and reduced water retention, improving breathing and contractility of the heart as secondary outcomes.

MRAs serve not only as diuretics, but also oppose the pro-fibrotic activity of aldosterone, thus helping to prevent remodelling [250,251]. Use of MRAs improve the outcomes both in terms of morbidity and mortality in patients with chronic HF [252,253].

2.3.4 Digoxin

Digoxin, derived from the foxglove plant, has been used to treat HF for many decades but has been largely replaced in recent times by different treatment strategies. It has inotropic effects, modulates arrhythmias and the autonomic nervous system [254]. It is the drug of choice for treatment of an abnormal ejection fraction during pregnancy, in PPCM [255,256], and can be used in patients who remain symptomatic, despite treatment with ACEi and diuretics.

2.3.5 Hydralazine and nitrates

Hydralazine and nitrates are used to decrease preload and afterload [257]. Hydralazine is safe for use during pregnancy as well as with breastfeeding post-partum [258,259]. Hydralazine, used in combination with nitrates, is used to reduce afterload and improve vasodilation, thus reducing blood pressure [257]. The combination of hydralazine and nitrates are the preferred regimen during pregnancy [259], but patients are switched to ACEi after delivery.

2.3.6 Bromocriptine

Bromocriptine (2 brom-x-ergocryptine, CB 154), a long-acting dopamine receptor agonist has been used previously to treat type 2 diabetes [260]. It improves glucose tolerance, decreases plasma insulin and fasting glucose levels, and is also associated with a reduction in cardiac morbidity [239], It has also been used to treat infertility in women, eliciting its effect by reducing levels of prolactin [261,262]. Although treatment with bromocriptine in both mice and humans has been beneficial, it blocks the release of prolactin, thus preventing its cleavage to the 16kD isoform [196,226,239]. Bromocriptine has an anti-coagulation effect, opposing the coagulatory effect of prolactin and as such, it cannot be prescribed to patients with certain circulatory problems [263,264]. Bromocriptine plays a great role in the treatment of PPCM, but its use in treatment is not without challenges – use of bromocriptine prevents lactation, and in the setting of Africa, this may not be a feasible option from an economic stand point. Physicians would have to consider the cost-benefit balance of prescribing bromocriptine in the lives of the PPCM patients they treat.

2.4 Outcomes of peripartum cardiomyopathy

Over the past few decades, refinement of treatments and implementation has improved survival in PPCM and other heart failure patients. The outcomes however often remain unsatisfactory. After 6 months, recovery of LV function varies by location – with 46 – 63% of patients regaining function in the USA, Germany, Turkey, China and Japan, while regions such as South Africa, Nigeria, Pakistan, and the Philippines only report 21 – 36% of patients regaining normal function (see position paper by Sliwa et al) [194]. Similar patterns of variability in LV functional recovery after 12 months [194]. Studies reporting adverse events recorded for PPCM patients, in 12 months following an initial diagnosis and commencement of treatment, included rehospitalisation of approximately 8% and cardiac mortality of approximately 5% of total PPCM patients [265].

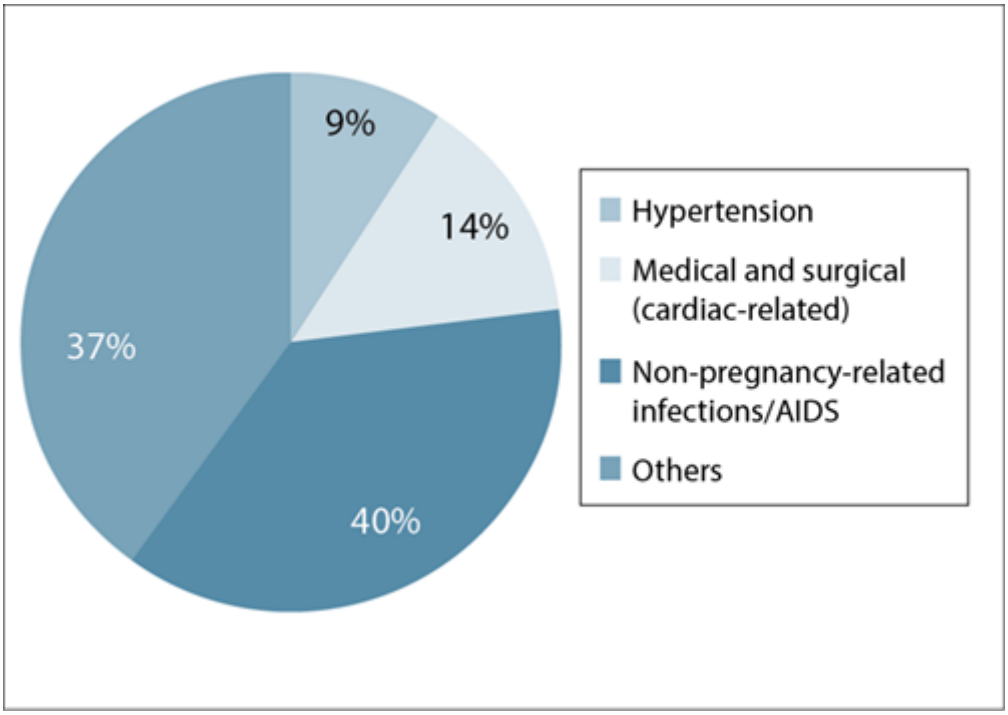

Figure 1.11: Maternal deaths in South Africa by cause. Cardiac-related deaths account for 14% of all maternal deaths. Taken from Elliot et al [266]. Abbreviations: AIDS – acquired immune-deficiency syndrome

This, however, is not necessarily representative on a large-scale, as Africa bears a great load of PPCM burden and there is great vulnerability with peripartum diseases. Cardiac disease in the peripartum period is one of the leading indirect causes of maternal death in South Africa [266]. The proportion of maternal deaths in this region is due to cardiovascular events (excluding hypertension) is 14% of total maternal deaths (see figure 1.11). The outcome in terms of mortality for PPCM in South Africa (and Africa at large) is far worse than that of the developed world, not only for a greater phenotypic severity observed in African patients, but also for lack of access to healthcare and treatments [267]. Presently, the treatment strategies documented here are those available on offer to patients who can access healthcare, but additional therapies are still needed, particularly for the more severe cases of PPCM.

3. Takotsubo Cardiomyopathy-induced acute heart failure

Acute heart failure (AHF) refers to rapid onset or worsening of signs and symptoms of HF together with a drastic drop in pressure. It has high morbidity and requires rapid intervention, typically leading to urgent hospital admission (Ponikowski et al. 2016). AHF may present as a consequence of acute decompensation of chronic HF, and may be caused by primary cardiac dysfunction or precipitated by extrinsic factors – often in patients with chronic HF. It may occur as a result of rapid decompensation, as will be discussed in this chapter. In certain cases, it presents as a first occurrence (de novo) without preceding cardiac complications.

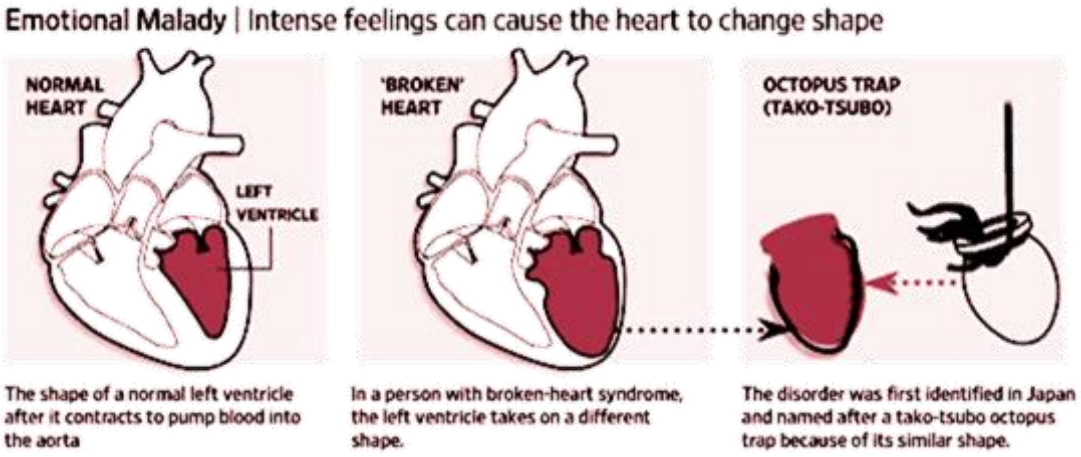

Figure 1.12: Takotsubo cardiomyopathy. Apical ballooning due to stress causes the left ventricle to extend and take the shape of a Japanese 'Takotsubo' octopus trap, thereby obtaining the name 'Takotsubo Cardiomyopathy'. Image taken from Akashi et al [268].

Takotsubo cardiomyopathy (TC) is a rare and specific instance of acute-onset HF. It was first described by a Japanese team in the 90's when they observed changes in the shape of the left ventricle with acute stress [268]. The ventricle during this cardiac event typically resembles that of an apical balloon – constricted at the base and dilated at the apex of the heart (see figure 1.12). This resembles the Japanese 'Takotsubo' fishing contraption used to catch octopuses, giving rise to the name of the cardiomyopathy. It is also used interchangeable with names such as apical ballooning syndrome, ampulla cardiomyopathy and broken heart syndrome [29]. This condition appears to

mainly affect post-menopausal women, but men and younger women can also develop this condition [24] .

3.1 Definition

Takotsubo cardiomyopathy (TC) is a form of acute, usually reversible heart failure – a critical feature which differentiates it from other forms of AHF [24]. It has been regarded as relatively benign, but there is growing evidence that it is a more serious cardiac disorder than previously thought, and its prevalence may be underestimated [269]. The symptomatic features of TC closely resemble those of an acute myocardial infarction –patients present with chest pain, dyspnoea or syncope [269,270]. In order to distinguish TC, it is necessary to use coronary angiography with left ventriculography as a diagnostic tool to confirm or exclude TC [269].

Table 1.3: Variants of TC with regard to ventricular shape, and their estimated prevalence as clinically observed. Taken from Ponikowski et al [18]. Abbreviations: LV – left ventricle; MRI – magnetic resonance imaging; TC – Takotsubo cardiomyopathy.

Variant	Estimated prevalence
Apical with or without mid-LV variant	75 – 80%
Mid-LV	10 – 15%
Inverted or basal	5%
Biventricular	Clinical <0.5%, Cardiac MRI 33%
Right ventricular	Unknown
Apical tip-sparing	Unknown
Possible Atypical variants	
Global	Unknown
Focal	Unknown

The classical pattern of TC follows certain developmental characteristics: LV contractile abnormalities including reduced EF, with apical and circumferential mid-ventricular hypo-kinesia and basal hyper-contractility [271,272]. The LV narrows at the neck while remaining globular closer to the apex, giving it an appearance of apical ballooning – a phenotype present in 50 – 80% of recorded cases (see table 1.3) [24,271]. Another common feature with hypokinetic basal circumference

and apical hyper-contractility (also known as the 'nutmeg' heart), and circumferential mid-ventricular hypo-kinesia with both basal and apical hyper-contractility (cardiac imaging resembling the ace of spades) [24,273–275]. The most common feature in the acute phase of TC is systolic failure due to the aberrant wall contraction kinetics, occurring in 12 – 45% of all cases [276–280]. LVEF usually recovers within 12 weeks, but other indicators, such as BNP levels and ECG changes, may take up to a year to normalise. In some cases, depending on severity of the initial episode, these can remain irregular, particularly if myocardial scarring occurs.

Table 1.4: In-hospital complications and long-term outcomes of TC. In-hospital complications and long-term outcomes of TC, as documented by Ponikowski et al [18]. Abbreviations: LV – left ventricle.

Complication/outcome	Frequency
Acute complications	
Right ventricular involvement	18 – 34%
Acute heart failure	12 – 45%
LV outflow tract obstruction	10 – 25%
Mitral regurgitation	14 – 25%
Cardiogenic shock	6 – 20%
Arrhythmias	
Atrial fibrillation	5 – 15%
Ventricular arrhythmias	4 – 9%
Bradycardia, asystole	2 – 5%
Thrombus formation	2 – 8%
Pericardial tamponade	<1%
Ventricular wall rupture	<1%
In-hospital mortality	1 – 4.5%
Recurrence	5 – 22%
5-year mortality	3 – 17%

TC has previously been described as a condition with a prompt and spontaneous recovery, but it is not always the case as a variety of complications have since been described in 52% of cases (see table 1.4), most common of which are subsequent AHF, formation of a thrombus, LV tract

obstruction, mitral regurgitation, ventricular tachycardia and cardiogenic shock [24,29,270,279–281]. There is increasing evidence that contractile abnormalities persist despite unobstructed ventricular function, with some patients having cardiac symptoms after the acute episode, including palpitations, angina, breathlessness on exertion, and an exacerbated anxiety state [24,282].

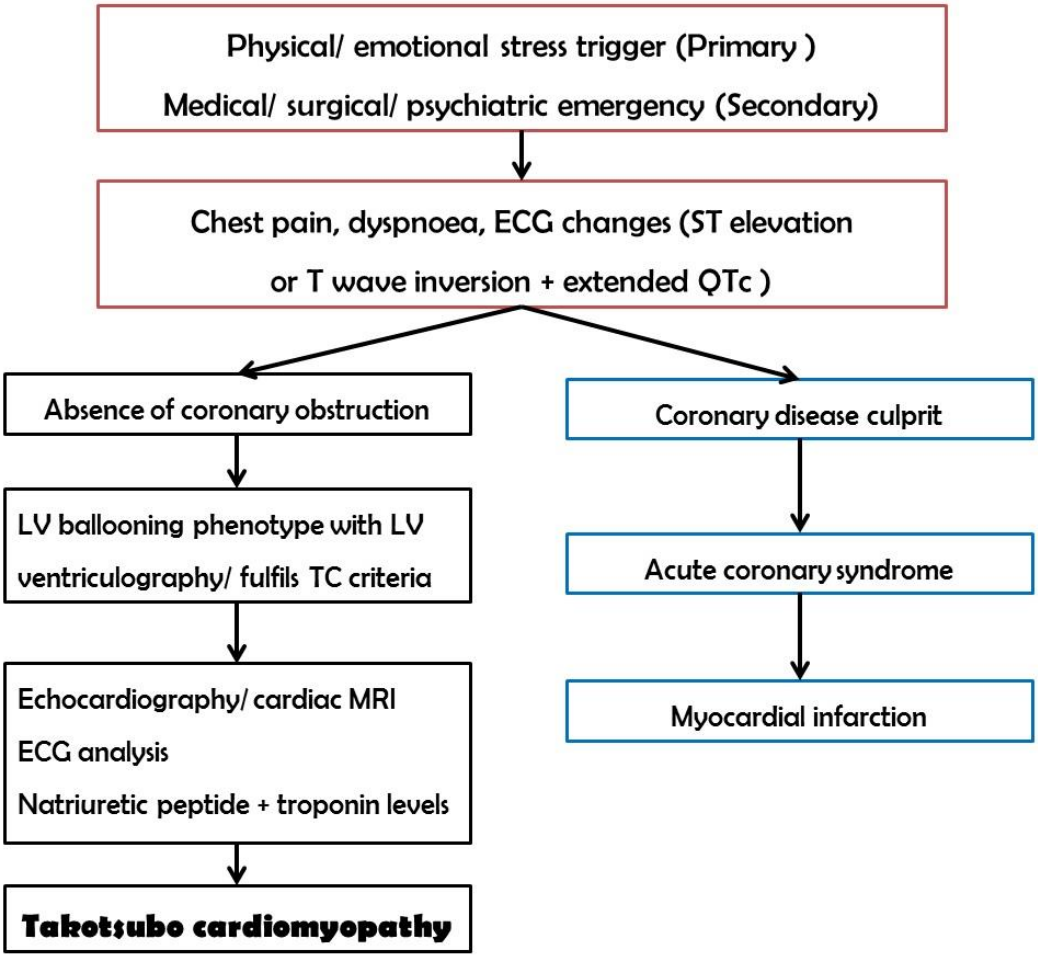

Figure 1.13: Takotsubo Cardiomyopathy Diagnostic Criteria. as per the Heart Failure Association of the European Society of Cardiology, 2015. Image adapted from Lyon et al [24]. Abbreviations: ACS – acute coronary syndrome; ECG - electrocardiogram; LV – left ventricle; MRI – magnetic resonance imaging; QTc – corrected QT interval; TC – Takotsubo cardiomyopathy.

Diagnosis of TC relies greatly on clinical judgement and awareness, as no single clinical characteristic is specific solely to TC. The phenotype of TC closely resembles that of acute myocardial infarction in terms of biomarkers and ECG abnormalities [269]. Four diagnostic criteria

have been proposed: (i) newly diagnosed ECG abnormalities together with (ii) transient apical dyskinesia or akinesia by colour Doppler imaging, beyond a single coronary artery distribution, (iii) non-obstructive coronary artery disease (stenosis < 50%) with angiography, and (iv) in the absence of hypertrophic cardiomyopathy, myocarditis, pheochromocytoma, head trauma and intracranial haemorrhage (summarised in Figure 1.13) [29,271,283].

3.2 Epidemiology

Incidences of TC appear to be more prevalent by gender and age group, with higher prevalence in women than men (9:1 in some reports), and also with older age [270]. Patient most often present with chest pain, dyspnoea, syncope and low ejection fraction typical of HF as their main symptoms [29,270]. While both physical and emotional stress serve as primary triggers, they are approximately equally represented, and in some cases even overlap as triggers [270]. There are also similar proportions of patients who present with spontaneous TC. Emotional triggers are typically more prevalent in women as an underlying cause, while physical triggers were more prevalent in men [270]. Risk factors include alcohol abuse, smoking, hyperlipidaemia, age and heightened anxiety [284,285].

It's estimated that there are 50k – 100k cases of TC in Europe and the USA annually, accounting for 0.02% of all acute hospitalisation [284]. Age and gender observations indicated that the majority of patients were women and/or older than 65 years of age – mainly, but not exclusively post-menopausal women. Other cohorts have echoed these observations, reporting similar age and gender patterns [278,286]. These studies indicated that the emotional stress and the absence of identifiable triggers was more common in women, while triggers due to physical stress, resuscitation or shock were more common in men – corresponding with higher levels of the cardiac biomarker of dysfunction such as troponin [270]. Mortality due to TC was higher in men, which reflected the severity of underlying causes [287]. Men who experience TC are also at a higher risk for cerebrovascular and cardiac events than women [270]. Older patients have poorer prognosis

following cases of TC, running a greater risk of developing hypertension and cerebrovascular disease, a lower glomerular filtration rate, and a lower LVEF at discharge, as well as higher in-hospital complications and mortality in comparison to younger patients [24,288].

In large-scale TC studies and registries, the in-hospital mortality rate due to TC is reported to be 2 – 5%, mainly due to ventricular fibrillation or cardiogenic shock [272,279–281]. Cardiogenic shock plays a significant role in mortality due to TC – with a mortality rate of 17 – 30% overall [24,277,279–281,289]. Data on the long-term prognosis of TC is limited. It can recur – second incidences have been reported from 3 months to 10 years after the initial one, with reported 5-year recurrence rates of 5–22% [276,277,289,290].

3.3 Distinction of Takotsubo cardiomyopathy from acute coronary syndrome

Patients with TC and ACS present with similar symptoms of chest pain and/ or dyspnoea [272]. Templin et al evaluated patients who presented with TC and ACS to identify clinical features present in each and distinguishing TC from ACS (summarised in table 1.5). They found divergence in terms of the natriuretic peptide levels, with higher BNP in TC patients. ECG analysis on admission showed sinus rhythm in most of their TC patients, but a significantly higher heart rate than patients with ACS [270]. TC patients display elevated troponin levels on admission to hospital– similar to patients with ACS [270]. Most TC patients displayed a reduced LV ejection fraction, while only approximately half of ACS patients had this. Notably, TC patients showed increased LV end diastolic pressure. Furthermore, one third of (TC and ACS) patients were on β-blockers, two fifths on ACEi or angiotensin receptor blockers on admission, usage rates which were almost doubled at discharge [270]. They found that more than half of the patients who presented with TC had a history or an acute episode of psychiatric or neurological disorders.

Table 1.5: Summary of characteristics in TC and ACS patients compared to controls. Table adapted from from Templin et al [270]. Abbreviations: ACS – acute coronary syndrome; BNP – Brain natriuretic peptide; IQR – inter-quartile range; LV – left ventricular, mmHg – millimetres of mercury; no. – number; TC – Takotsubo cardiomyopathy; ULN – upper limit of the normal range; yr – years.

Characteristic	Takotsubo cardiomyopathy		Acute coronary syndrome	p-value
	Total cohort (n=1750)	Matched cohort (n=455)	Matched cohort (n=455)	
Female n (%)	1571 (89.8)	411 (90.3)	411 (90.3)	1.00
Age years	66.4±13.1	67.7±12.5	68.7±12.3	0.19
Chest pain n/total n (%)	1229/1619 (75.9)	322/438 (73.5)	361/403 (86.9)	<0.001
Dyspnoea n/total n (%)	760/1620 (46.9)	208/439 (47.4)	128/363 (35.3)	0.001
Median Troponin (IQR) – factor x ULN	7.70 (2.22 – 24.00)	7.68 (2.38-24.21)	8.30 (1.80-36.40)	0.62
Median creatine (IQR) – factor x ULN	0.85 (0.52-1.48)	0.87 (0.55-1.42)	1.12 (0.60-2.97)	<0.001
Median BNP (IQR) – factor x ULN	6.12 (2.12-15.70)	5.89 (1.68-13.92	2.91 (0.88-8.26)	<0.001
Heart rate BPM	87.5±21.8	87.3±21.8	76.1±18.3	<0.001
Systolic blood pressure mmHg	130.6±28.8	131.6±31.4	131.5±28.2	0.96
LV ejection fraction %	41.1±11.8	40.7±11.2	51.5±12.3	<0.001
LV end diastolic pressure mmHg	21.3±8.0	22.1±7.7	20.1±7.8	0.001
Coexisting medical conditions				
Neurological or psychiatric disorder n /total n (%)	714/1525 (15.3)	252/452 (55.8)	115/448 (25.7)	<0.001
In-hospital outcomes				
Cardiogenic shock n /total n (%)	170/1716 (9.9)	55/445 (12.4)	48/455 (10.5)	0.39
Death n /total n (%)	72/1750 (4.1)	17/455 (1.7)	24/455 (1.7)	0.26

3.4 Pathophysiology

The pathophysiology of TC is complex, which reflects the nature of the physiological response to heightened, acute stress and the response by the cardiac chamber to catecholamine surges [23,291–294]. The ultimate underlying cause of AHF and specifically TC is uncertain, but there is strong evidence to suggest myocardial stunning – i.e. the reduction in cardiac function - as seen in TC is as a result of excessive sympathetic activation with catecholamine agents in response to physical or emotional stress,

3.4.1 Sympathetic nervous activation

Extreme sympathetic activation, often due to unexpected stress, appears to play a central role in the pathophysiology of TC. Catecholamines are released during stress, in response to sympathetic activation, including epinephrine, norepinephrine, and dopamine, levels of which are significantly higher in TC compared to patients at rest, or with AHF due to acute myocardial infarction (which also have raised catecholamine levels) [24,283]. These catecholamines stimulate cognitive courses of the brain, such as the fight or flight responses, and dilation of cardiovascular elements [24]. Different regions of the heart have been shown to express 2 different β adrenergic receptors (see figure 1.14) [23]. The interaction between the receptors and the catecholamines released cause differential contractile responses by region – this may underlie the Takotsubo shape of the LV seen in TC. Figure 1.14 illustrates the expression patterns of the β-adrenergic receptors and their location in the left ventricle of the heart. The interaction between these receptors and the catecholamines released under stressful conditions induce an abnormal contractile state which underlies apical ballooning seen in TC.

It is still not well understood as to why there are differences in wall motion abnormalities (see figure 1.14), but it has been suggested that the variance in regional wall motion occurs as a result of individual differences in anatomical location of adrenergic receptors, or adrenergic receptor polymorphisms which alter the response to excess sympathetic activity [272,295].

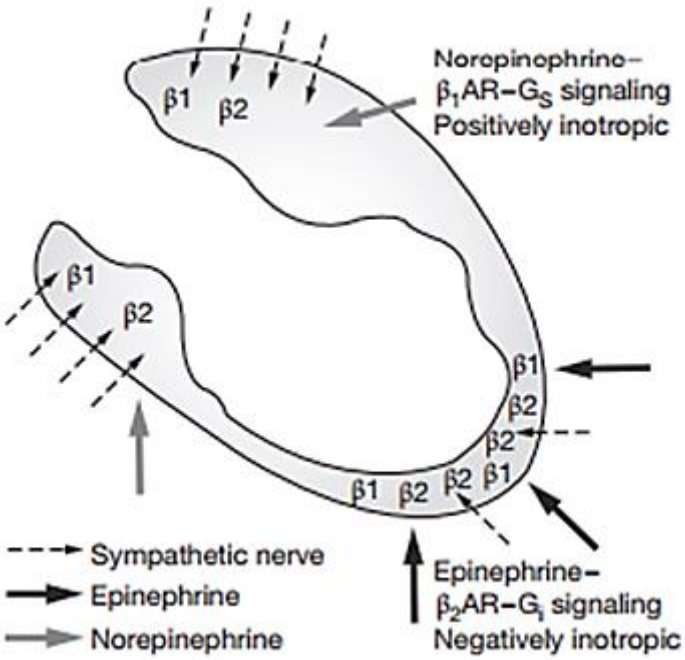

Figure 1.14: Schematic representation of the different β-adrenergic receptors in response to high catecholamine levels. Positive inotropic activity at the base of the heart causes constriction, while negatively inotropic activity at the apex causes dilatation. Together these responses cause the apical ballooning underlying Takotsubo cardiomyopathy. Image taken from Lyon et al [23]. Abbreviations: β_2AR-G_i – β2-adrenoceptors AR coupled to Gi-protein.

3.4.2 Arrhythmias in Takotsubo cardiomyopathy

TC patients commonly present with arrhythmias which worsens cardiac output, often associated with the new onset of HF [277,280,296,297]. Ventricular arrhythmias often result in cardiac arrest during the acute phase of presentation [24,277,280,296–298]. More than 95% of TC patients present with ECG abnormalities during the acute phase [285,299–302]. Patients also present with abnormal QT dynamics, with possible ST-segment elevation or T-wave inversion (see figure 1.15) [283,290].

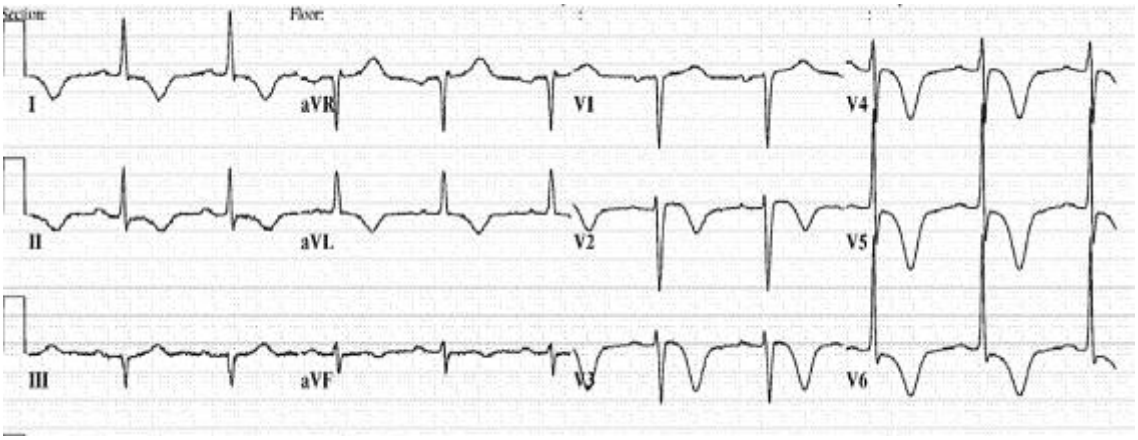

Figure 1.15: ECG traces of TC patients showing T-wave inversion (following v4 and v5) and ST-segment elevation (following aVR). It also demonstrates QT anomalies and arrhythmias seen with apical ballooning in Takotsubo Cardiomyopathy. Image taken from Prasad et al [290]. Abbreviations: ECG – electrocardiogram.

3.4.3 Echocardiographic evaluation of Takotsubo cardiomyopathy

TC can sometimes occur without symptoms [271]. The first point of reference is the movement of the left ventricle, assessed by echocardiography or cardiac MRI – transient akinesis, dyskinesis or hypokinesis of the LV mid-section and / or the apex occurs [290]. Trans-thoracic echocardiography assess ventricular dysfunction which is characterised by transient alterations of the contractile apparatus extended beyond a single vessel territory [29,290].

3.4.4 Markers for diagnosis of Takotsubo cardiomyopathy

Myocardial markers of necrosis, such as cardiac troponin-T, will be at least modestly elevated in TC [29,271,290]. Initial troponin levels which exceed 10 times the upper normal limit has been shown to predict a higher incidence of the combined end points described in section 3.1 [270].

Serum levels of natriuretic peptide (BNP and pro-BNP) are almost always elevated, often to extremely high levels that correlate closely with the degree of contractile abnormality [303–306]. One study found 82.9% of TC patients to have an elevated level of BNP upon admission, up to 5.9 times as much as the highest normal value in combination with EGC and/ or echocardiography

abnormalities (see table 1.6) – this makes it a good candidate to aid diagnosis, and it is thought to be a more useful diagnostic biomarker that troponin [24,270]. Lower levels of pro-BNP on admission indicate a more favourable prognosis for patients [24]. Serum catecholamine levels are not usually measured in clinical practice, but when measured, the catecholamine levels in this syndrome are elevated significantly – up to 34 times as high as normal physiological levels [271,283]. Plasma levels of creatinine kinase are not significantly elevated in TC [270].

Table 1.6: Serum catecholamine levels in patients with TC and MI. catecholamine levels in TC and myocardial infarction patients from 1 – 9 days after an initial incident. Table adapted from Wittstein et al [283]. Abbreviations: MI - Killip class III myocardial infarction; ml – millilitres; pg – picograms; TC – Takotsubo cardiomyopathy.

	Day 1 or 2		Day 3, 4 or 5		Day 7, 8 or 9		Normal values
	TC	MI	TC	MI	TC	MI	
Epinephrine (pg/ml)	1264 (916-1374)	376 (275-476)	1044 (733-1118)	330 (220-385)	348 (180-550)	275 (220-311)	37
Norepinephrine (pg/ml)	228 (1709-2910)	1100 (914-1320)	1573 (1235-2589)	289 (727-914)	1142 (525-1252)	541 (516-660)	169
BNP (pg/ml)	1033 (805-1783)	264 (192-483)	450 (205-684)	268 (249-684)	142 (72-236)	297 (142-419)	10 – 93

3.5 Animal models used to study acute heart failure and Takotsubo cardiomyopathy

3.5.1 Acute, catecholaminergic heart failure

Several animal models which simulate TC have been developed in vivo. One such model in rats makes use of a mode of 'social defeat' in which animals are stressed by a resident-intruder method – i.e. confined placement (behind a wire mesh) in an environment with strange rats [307]. Rats exposed to this method had elevated levels of corticosterone and troponin I, similar to that seen in TC (see section 3.5.4). This transient exposure caused an increase in heart weight/body weight and left ventricle/body weight ratios, as well as elongation of the heart itself.

A second model makes use of immobilization stress, in which rats are taped upside-down in a confined space to induce α and β-adrenoreceptor activation, similar to that seen in TC [308] [309]. Forced immobilization triggers release of epinephrine up to 40 times higher than normal, unstressed animals [308]. This method reproduces the ECG and left ventriculography changes seen in TC, which can be partially attenuated by increased serum oestrogen [309]. Observed changes with this immobilization method included activation of p44/42 mitogen-activated protein kinase, induction of heat shock protein 70, and upregulation of natriuretic peptides in the myocardium [309].

A third method induces a TC model by injection of a bolus dose of epinephrine [310]. This model showed increased cardiac contraction, and treatment with β2AR antagonist or a p38 MAPK inhibitor increased mortality, with all animals treated dying within 45 min, meaning that this particular method of cardiac heart rate reduction was counterproductive. This method showed similar contractile alterations to those seen in TC/ apical ballooning syndrome – with greater contractility in the apex, restricted contractility in the mid-LV, and reduced contractility at the base. Injection of epinephrine induced a hypertensive state with an approximate doubling of systolic blood pressure (SBP) for the first 4 minutes (min), followed by a steady decrease in SBP, with a maintained elevated diastolic blood pressure (DBP). Thereafter, left ventricular failure ensues, characterised by a drop in both SBP and DBP. The heart rate rapidly increases after administration, and drops after onset of failure, and partially recovers with time [310].

A fourth method induces a TC model by injection of isoproterenol in rats [311]. This model used female rats between the ages of 4-5 months injected with a single dose of isoproterenol (5mg/kg), which produces a 33% mortality rate within 2 hours of administration. Echocardiographic analysis of the LV in these after 2 hours showed a variable degree of hypokinesis, with an increased LV apical wall thickness, and a 15% increase in HR – resulting in a significantly reduced ejection fraction. Rats in this model were used for histology relating to the TC phenotype after 24 hours of

TC induction, analysis of which revealed hearts were still akinetic. As this was done within 24 hours of the initial injection, no recovery data was available in this study [311].

3.5.2 Hypotensive acute heart failure

An ex-vivo animal model has been developed in our laboratory to study a hypotensive model of AHF in rodents [312]. This model simulates low-pressure systems, as would be observed with major blood-loss in hypovolemic and haemorrhagic shock [313,314]. It also takes into account metabolic switches from free fatty-acids (FFAs) as a primary fuel in a healthy adult heart to glucose, due to poor oxygen availability and perfusion (see figure 1.16) [315,316].

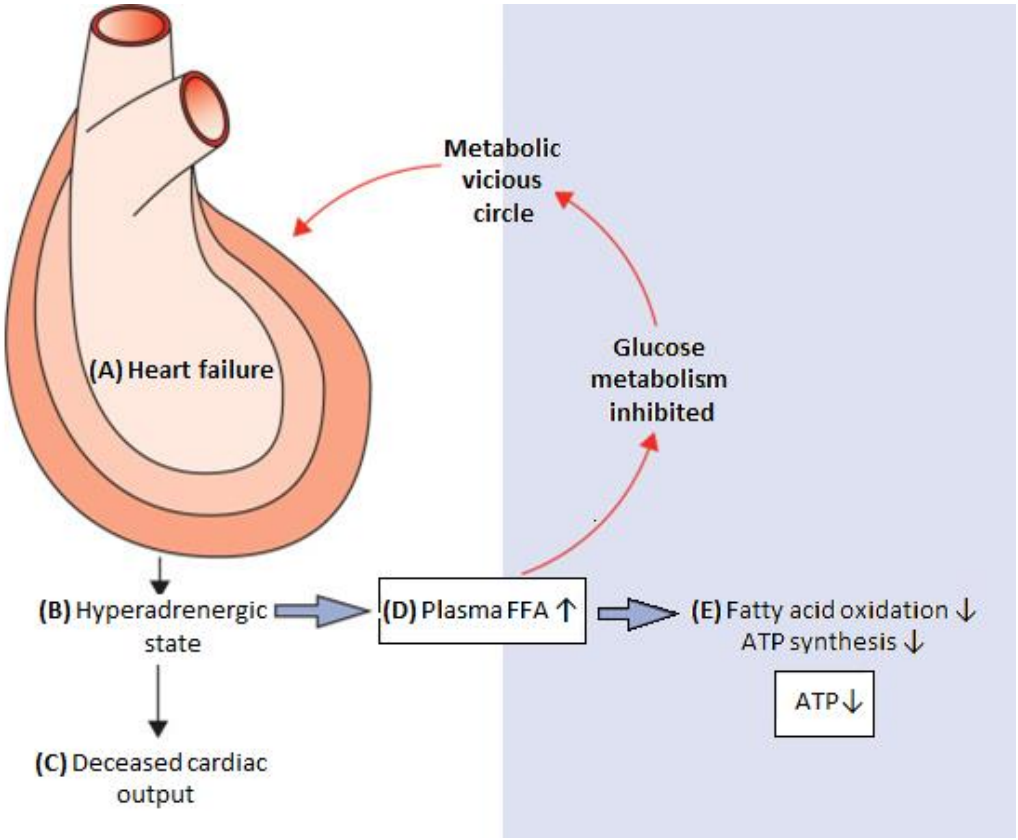

Figure 1.16: Metabolic changes in heart failure. Heart failure (A) induces a hyperadrenergic response (B) to encourage contractility. This stimulus in this state decreases cardiac output (C), while increasing plasma levels of FFA in an attempt to provide energy. Scarcity of oxygen, due to poor circulation, inhibits fatty acid oxidation, thereby reducing levels of ATP. With an increase in FFA, glucose metabolism is inhibited, and the metabolic combination exacerbates the heart failure state by a positive feedback loop. Image adapted from Heusch et al [320]. Abbreviations: ATP – adenosine triphosphate; FFA – free-fatty acids.

The addition of FFAs in this model as a fuel in the buffer exacerbates the heart failure-like metabolic state and contractile irregularities [317]. Epinephrine is also added during the low-pressure phase of this model to simulate the increase the heart rate as is observed initially in patients with AHF [318,319].

This model could be adapted to mimic TC by removing the hypotensive stimulus, and instead increasing adrenaline, while maintaining a normal pressure. Thus far, no ex-vivo models for TC exist, and it would be an ideal candidate for controlled simulation of TC.

3.6 Current therapies

Interventions for AHF at presentation in many cases require mechanical ventilation, intar-aortic balloon pumping, ionotropic support [24,321]. Treatment in the acute phase, during presentation, is mainly symptomatic, making use of intra-aortic balloon pump equipment for haemodynamically unstable patients together with cardiopulmonary circulatory support and veno-venous haemofiltration [24,322]. In severe cases with progressive circulatory failure and cardiogenic shock, mechanical support serves as a bridge to restoration and recovery [24]. Despite excessive catecholamine levels in most (but not all) TC cases, cardiac stimulants are still used in 20 – 40% of patients with TC [24,322].

3.7 Caveats in the treatment of acute heart failure and Takotsubo cardiomyopathy

AHF is a condition with severe medical consequences, and dire outcomes in terms of survival. Little research has been conducted to explore methods and treatments to improve the outcome of AHF sufferers. Very few innovative treatment strategies have been developed, despite greater focus in recent decades on the treatment of long-term HF. The current treatment of AHF could use a streamlined focus with consideration of targets other than those in targetted in the standard treatment of long-term HF.

TC is a recently recognised condition, as the imaging technology required to identify it are recent developments. It may have been present previously for a long time without identification. In the last decade research has expanded our knowledge from thinking that it is a reversible response to an emotional reaction, to identifying it as a secondary outcome following surgery and shock which can futher lead to cardiac dysfunction (see section 3.4). There is a lack of knowledge from which to draw when it comes to understanding TC, as it is not well known and there are presently very few simple models to help us understand the condition and its triggers.

4. Modulating heart rate to maximize the performance of the heart

The billion-beat hypothesis is a postulation in popular science culture that every animal has a limited number of heartbeats or breaths in their lifetime. It is based on the observation that smaller animals have faster heart rates but live shorter lives, while larger animals have slower heart rates and live longer [323]. On average, most animals have approximately one billion total heartbeats in a lifetime [323,324]. Present-day humans are an exception – we have, on average, 2.24 billion heartbeats in a lifetime, possibly as a result of medical interventions and disease management [324]. By the premise of the billion beat hypothesis, one could potentially lengthen their lifespan by slowing down their heart and breathing rates [323]. This is an interesting idea which complements observations in cardiac research – the outcome of cardiac events, morbidity and mortality are often preceded by high resting heart rates [324]. The higher the heart rate and more severe the arrhythmic pulse, the worse the overall outcome will be [323].

4.1 Physiological aspects of heart rate

The heartbeat and heart rate are controlled by both intrinsic and extrinsic factors. The intrinsic factors are those which mechanistically cause the heart to beat by means of an electrical impulse. Rhythmic control of the cardiac cycle relies on the regulation of impulses generated in the heart and conducted through its network to cause contraction. Extrinsic factors are those which can influence the autonomic nervous system by either sympathetic or parasympathetic activation. Response of receptors in the heart to these biochemical signals alters the activity of the conduction mechanism, thereby changing the heartbeat and heart rate.

4.1.1 Electrophysiological apparatus

The sinoatrial (SA) node, also known as the pacemaker of the heart, is comprised of a cluster of specialised cells located in the right atrium (see figure 1.17) [325]. These cells have a mixture of

muscle and neural properties and form part of a network known as the subendocardial plexus which includes all of the electrochemical components responsible for cardiac contraction [325,326]. The SA node cluster is the primary source of the electrical impulse which travels through the heart to cause contractions [327]. It first causes contraction of the atria, forcing blood into the ventricles which are still relaxed. It sets the heart rate and rhythm of the heartbeat. Normal sinus rhythm occurs when the SA node fires impulses regularly.

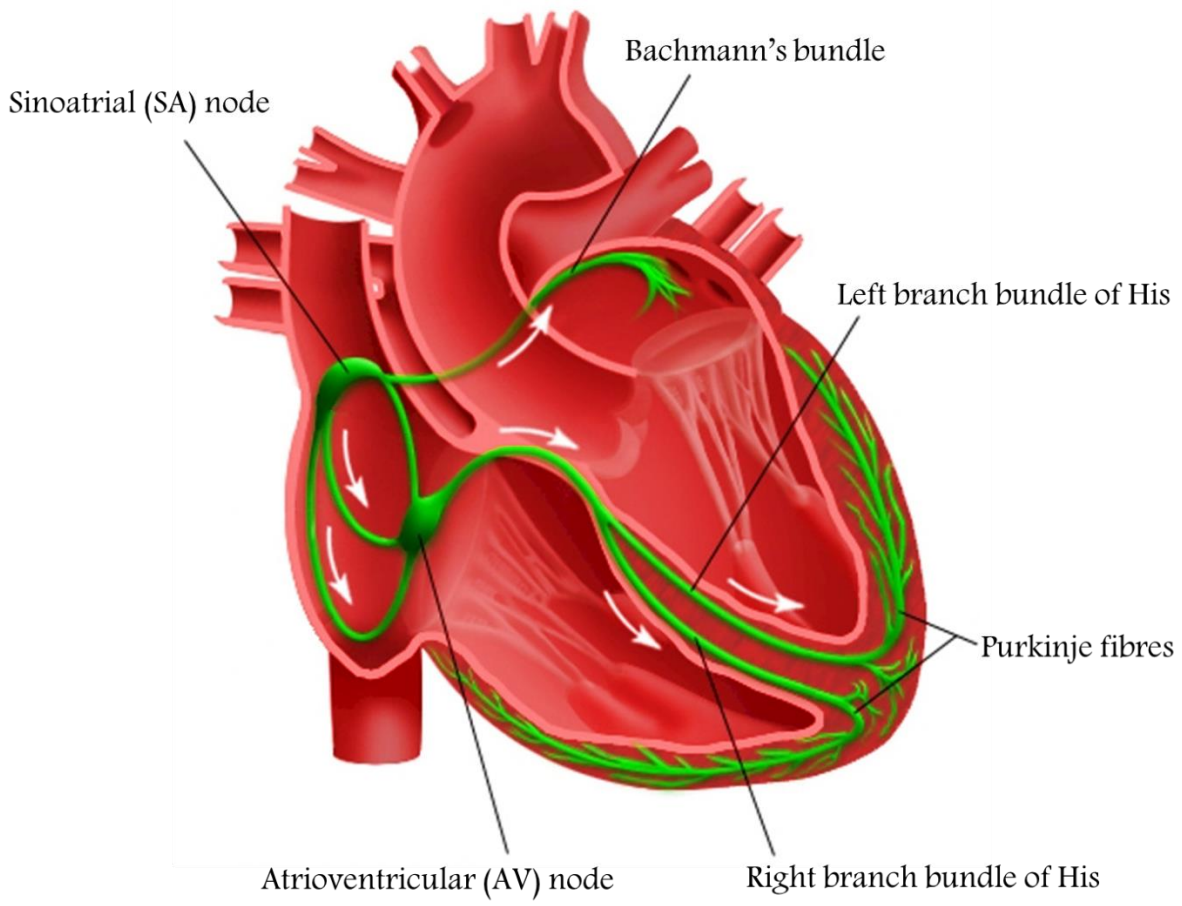

Figure 1.17: The electrical conduction apparatus in the heart. Electrical impulses start at the SA node, passing to Bachmann's bundle, causing the atria to contract. It then passes through the AV node which slows the impulse, allowing a pause between contraction of the atria and ventricles. The impulse continues from the AV node to the HIS-purkinje fibres in the walls of the ventricles stimulating contraction. Image adapted from heart-valve-surgery.com [328]. Abbreviations: AV – atrioventricular; SA – sinoatrial.

The atrioventricular (AV) node is a second cluster of specialised cells through which the impulse of the SA node passes (see Chapter 5, Opie, 2004) [327]. It is a secondary source of electrical impulse

located between the 2 ventricles. It acts as a gate to slow the impulse before it enters the ventricles, allowing the atria to fully contract before contraction of the ventricles [329].

The Purkinje fibres are the third point for propagation of the impulse (see Chapter 5, Opie, 2004) [327]. Purkinje cells are a specialised type of neuro-muscular cell which form a network of fibres in the ventricular muscle walls (see Chapter 5, Opie, 2004) [327]. These fibres conduct the impulse from the AV node through to the muscular walls of the ventricles, causing them to contract, forcing blood out [327]. The full electrical conduction pathway in the heart, extending from the SA node, to the AV node, and the Purkinje fibres is known at the His-Purkinje network.

Bachmann's bundle is the 4th neuromuscular impulse centre in the heart, also forming part of the His-Purkinje network. Bachmann's bundle is the band of conductive tissue stretching from SA node to the base of the left atrial appendage [330]. It serves as the pathway of inter-atrial conduction [330,331].

This impulse propagation is rhythmic and cyclic, starting again at the SA node once a contraction has been completed. The heartbeat itself can be divided into 2 phases – the systolic phase which is when contraction occurs, forcing blood out of the chambers, and the diastolic phase when the muscle relaxes and the chambers refill with blood (see Chapter 12, Opie, 2004) [327]. Each conductive centre/ cluster is capable of independent signal induction, but the most powerful, timely contractions occur with initiation by the SA node and cooperation of all of the conductive elements.

4.1.2 Pacemaker "funny" current

Pacemaking in the SA and AV node are controlled by an interplay of ionic currents, the most prominent of which is the "funny" current (I_f), an inward current activated on hyperpolarization during diastole [332]. Hyperpolarization-activated cyclic nucleotide–gated (HCN) channel proteins come in different isoforms, HCN4 is predominantly expressed in the heart, correlating with presence of funny channels, and is responsible for the rhythmic pacemaking activity [333]. These

channels generate impulses which conduct muscular contractions which regulate the heartbeat, and they are capable of generating spontaneous repetitive activity which is faster in the SA node, and slower in the AV node due to the proportion of funny channels in each [329] . The I_f is regulated by intracellular cyclic adenosine monophosphate (cAMP) (see figure 1.18) and is activated by β-adrenergic and inhibited by muscarinic M2 receptor stimulation and plays a role as a basic physiological apparatus which responds to autonomic regulation [334–337].

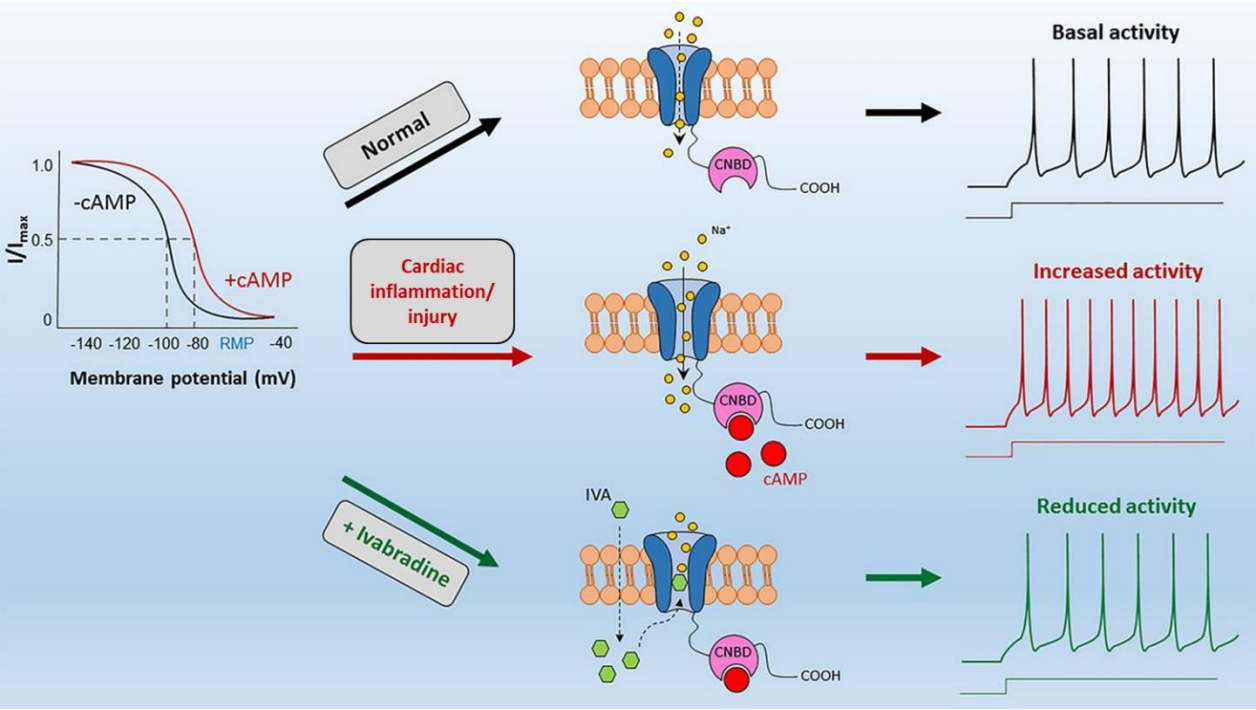

Figure 1.18: Ivabradine activity reduces heart rate by blocking funny channels in the sinoatrial node. Under normal physiological conditions, cAMP binds to its CNBD receptor, eliciting a conformational change in the HCN (blue) channel which allows current to pass through which facilitate heart beats. With adaptations in response to cardiac inflammation and injury (among other causes), heart rate is increased as there is more current passing through the channel. Ivabradine competitively blocks the HCN channels to delay depolarisation of the SA node, thus reducing heart rate. Image adapted from Tsantoulas et al [338] Abbreviations: CNBD -cyclic nucleotide-binding domain; cAMP – cyclic Adenosine monophosphate, IVA – ivabradine; HCN - Hyperpolarization-activated cyclic nucleotide–gated

Despite this response to autonomic activation, it is also capable of self-regulation and plays a major role in spontaneous activity generation and control of heart rate without innervation [339,340]. Diastolic depolarisation is responsible for the repetitive activity in pacemaking, as a new impulse

fires after voltage depolarises at the membrane surface [325,341,342]. Funny channels serve an exclusive role in pacemaking, and are as an ideal target for regulating heart rate by molecules which can specifically bind and block them with minimal adverse cardiovascular effects [339]. Regulating funny channels in the setting of HF, and related cardiovascular conditions where there are HR-linked irregularities (as described in previous chapters), could potentially serve as a strategy to improve these conditions.

4.1.3 Factors that affect heart rate and variability

Biological processes vary in complex, non-linear ways and are the result of continuous interactions between multiple neural, hormonal and mechanical control systems. The normal resting rhythm of the heart is highly variable when examining on a beat-to-beat basis, but too much variation, such as occurs with arrhythmias, is detrimental [343]. Conversely, too little variation indicates pathology, chronic stress or age-related system depletion [343]. Low heart rate variation is associated with sudden cardiac death [344,345]. Heart rate variability (HRV) is the change in time intervals between successive heartbeats and also reflects changes in response to physiological, environmental and psychological stresses [343]. Overall, the slower the heart rate, the higher the potential for HRV as there are longer gaps between individual heartbeats [343]. At rest, a normal heart can beat between 50 – 90 times per minute, though healthy individuals should have a heart rate below 75 beats per minute (BPM) [22]. Exercise, stress, fever, medication and emotions can increase the heart rate, sometimes to greater than 100 BPM [346].

- Temperature and dehydration

Temperature relates closely to vasodilation and constriction, but also blood pressure, as a rise in body temperature causes vasodilation, thus increasing heart rate [347]. Conversely, a drop in body temperature lowers heart rate and induces vasoconstriction [348,349].

- **Altitude**

Higher altitudes have less available atmospheric oxygen and constitute a hypoxic environment. As such, the heart beats faster to transport the requisite oxygen to organs and muscles. Despite the lower oxygen content at higher altitudes, the body can adapt to this, with a normal heart rate [350].

- **Respiration**

Inspiration and expiration cause what is known as respiratory sinus arrhythmia (RSA), a physiological phenomenon which causes heart rate variability in synchrony with respiration (see figure 1.19) [351]. SA node activity varies with respiration, activating the parasympathetic system during exhalation (thereby reducing heart rate), with only partial activation during inhalation (thereby increasing heart rate) [352]..

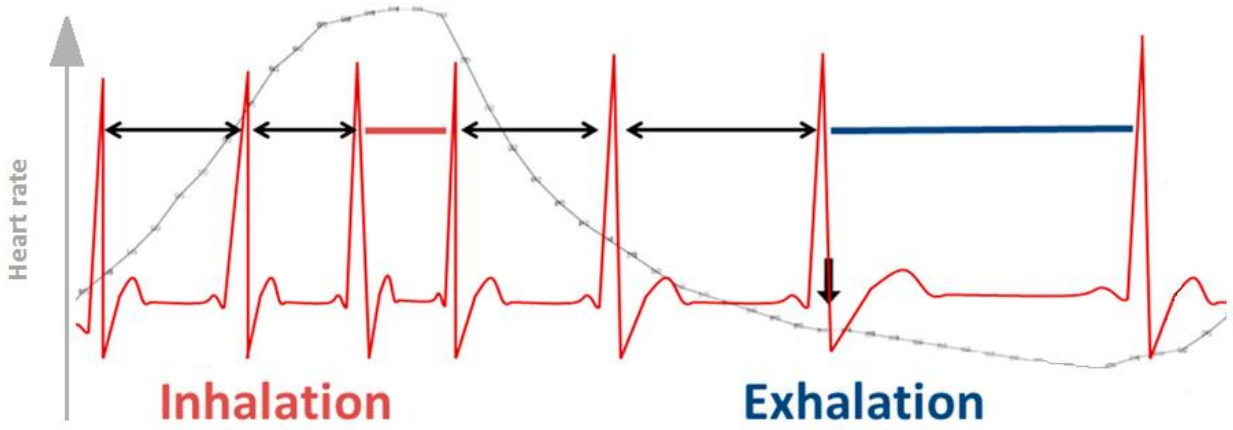

Figure 1.19: Heart rate variability with respiration. Heart rate increases during inhalation, and lowers during exhalation. Image adapted from Nederend et al [353]

- **Stimulant & inhibitory drugs**

Stimulant drugs, such as caffeine and cocaine, activate the central nervous system and release adrenaline, causing an increase in heart rate [354]. Inhibitory drugs such as β blockers are used to lower the heart rate when it is in excess of the norm for extended periods of time [22]. Many of these

work on the principle of blocking receptors that respond to, or activate the central nervous system [355].

- Thyroid hormones

Thyroid hormones affect all process in the body as it regulates intrinsic metabolism, cardiac function and mental state [356,357]. Interaction between the thyroid and pituitary glands regulate thyroid hormone release in the bloodstream, which in turn affects mitochondrial activity in liver, kidneys, myocardium and skeletal muscle, as observed in rats [358]. Hyperthyroidism accelerates cardiac processes, increasing heart rate, systolic and diastolic function, and increased atrial fibrillation while lowering systemic vascular resistance [357,359,360]. The opposite effect is seen with hypothyroidism.

- Stress hormones

Stress hormones form part of the autonomic nervous system (ANS), stimulation of which causes release of adrenaline, increasing heart rate [361–363]. These are the fight, flight and fright response systems which work by means of sympathetic activation and binding of adrenaline to its receptors in target organs and systems [362]. Hormonal release in responses to emotions can affect the patterns of coherence of the heartbeat (see figure 1.20) [364]. Coherence refers to the symmetry in the cyclic pattern of variability in heart rate – the more similar and repetitive the pattern, the better the coherence.

Various hormones can participate in the cardiac cycle, levels of which will affect cellular and psychological systems [364]. Many neurotransmitters, hormones and biochemical messengers are known to be released in a temporal fashion, such as melatonin, insulin, glucagon, aldosterone, renin, cortisol, vasopressin, adrenocortitropic hormone, growth hormone, luteinising hormone, follicular stimulating hormone, thyroid stimulating hormone, progesterone and testosterone among

others [364–366]. Chemical messengers and hormones affecting the cardiac cycle are released in a pulsatile fashion too, rhythmically, in synchrony with contractions [364].

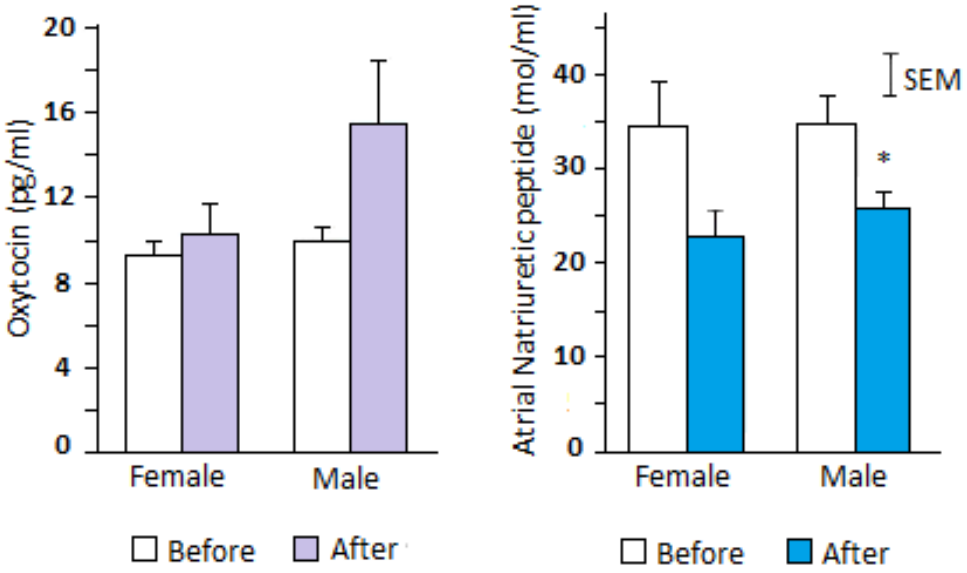

Figure 1.20: Oxytocin and ANP changes with heart rhythm coherence. Changes in ANP and oxytocin levels observed in males and females before and after maintaining coherence for 10 minutes are illustrated in the above graphs. Adapted from McCraty et al [364].Abbreviations: ANP – atrial natriuretic peptide; ml – millilitre; mol – moles; pg – picogram; SEM – standard error of the mean.

- **Emotions**

Emotions influence the nervous system and can cause sympathetic responses or parasympathetic responses depending on the emotion experienced [327]. Love, happiness, sadness and depression lower the heart rate and reflect a coherent rhythm, while anger, anxiety and fear cause an increase in heart rate (see Figure 1.21) [364]. These emotional states manifest as cardiovascular changes by means of autonomic nervous activity [327]. Among other sources, the anterior hypothalamus is noted for involvement in parasympathetic responses, while sympathetic responses emanate from the anterior, posterior and lateral hypothalamus, but predominantly the lateral region [367]. The two cerebral hemispheres are associated with separate aspects of autonomic control – the left hemisphere is predominantly parasympathetic, while the right hemisphere is predominantly

sympathetic [368]. As such, dominance with cerebral hemispheres may contribute to variable ANS activation from person to person in response to emotions [369,370]

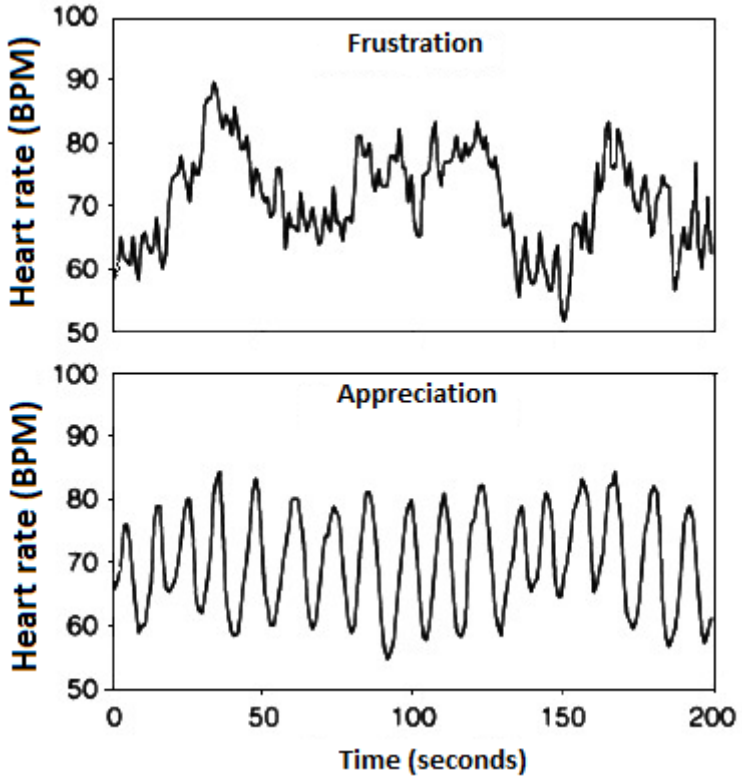

Figure 1.21: Emotions affect heart rhythm patterns. Erratic heart rhythm patterns (incoherence) are typical of negative emotions such as frustration or anger as illustrated in the top graph. Regular heart rhythm patterns (coherence) are observed with sustained positive emotions such as appreciation, as illustrated in the bottom graph. Image adapted from McCraty et al [364]. Abbreviations: BPM – beats per minute.

- **Autonomic nervous system regulation of heart rate**

The autonomic nervous system (ANS), regulated by the medulla oblongata and specific hormones, can alter conductive and contractile properties of the heart. Sympathetic activation by the ANS via the cervical sympathetic chain ganglia acts to increase the heart rate, and force of contraction, as well as the speed of the electrical impulse [343]. Conversely, parasympathetic activation via the vagal nerve slows the heart rate and lowers the power of contraction of the cardiac muscles by slowing impulse conduction (see figure 1.22) [327].

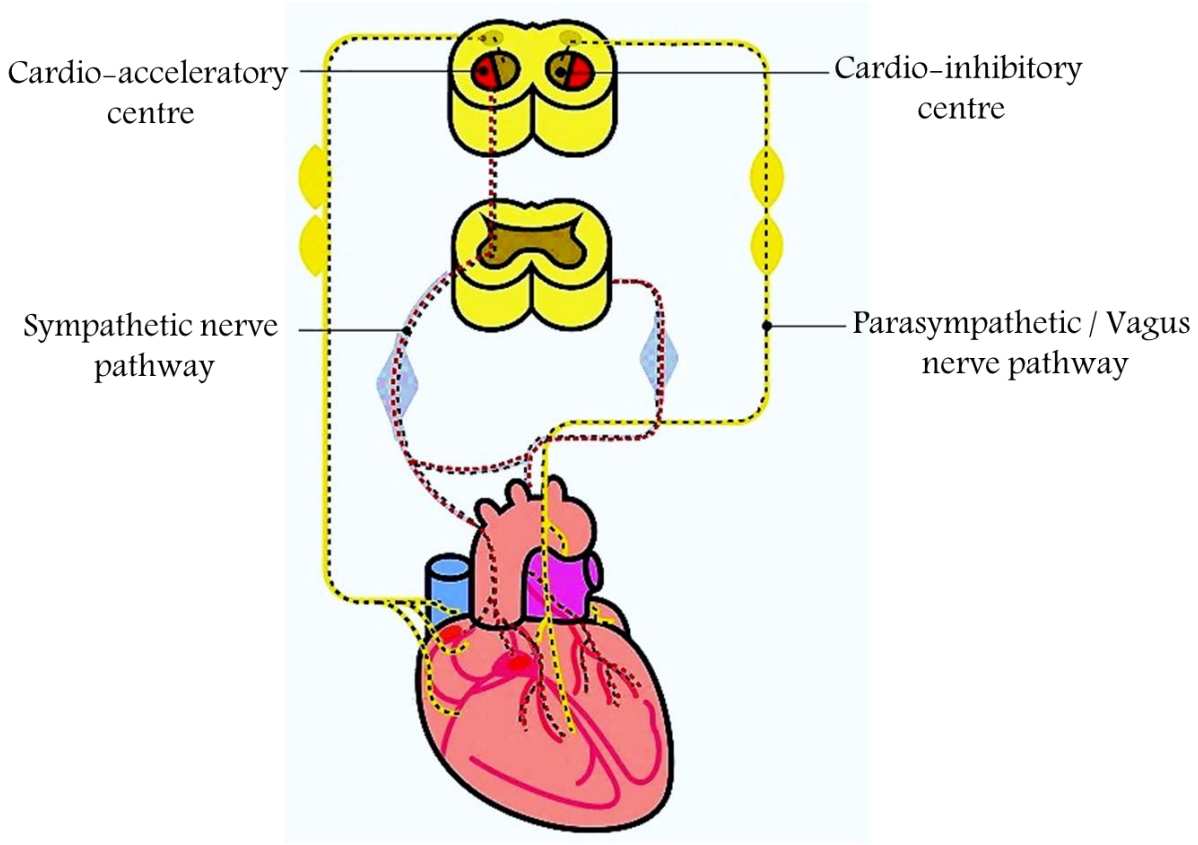

Figure 1.22: Adrenergic activation of the heart. The sympathetic nervous pathway targets the sinoatrial node directly, as well as the myocardium via the spinal cord, to accelerate heart rate. The parasympathetic / Vagus nerve pathway targets the myocardium to slow the heart rate, without affecting conductivity in the sinoatrial or atrioventricular nodes. Image adapted from perigen.com [371]

Sympathetic activation occurs when epinephrine and norepinephrine are released from the adrenal glands (see review by McCraty et al) [343]. Parasympathetic activation makes use of acetylcholine, a neurotransmitter that slows transmission of impulses by changing membrane permeability to potassium ions, causing hypo-polarisation of cells to slow down activity [343,351,372]. In addition to the release of hormones with ANS activation, there are also direct vagal and sympathetic nerves connecting to the sinoatrial and atrioventricular nodes, which allow for the direct mediation of ANS responses from the brain [373–377].

The electrical conduction patters associated with the cardiac cycle are measure by means of ECG (see section 1.2.5.2) and disruption in conduction patterns result in arrhythmias. Aberrant conduction can be dangerous and is associated with cardiac dysfunction.

Under normal circumstances the function of the heart is determined solely by the sinoatrial node. Under stress conditions, sympathetic and parasympathetic activation will modify function (see figure 1.22). Though both sympathetic and parasympathetic activation affects the function of the heart, they do not oppose each other equally – vagal effects have a shorter window to activation than sympathetic effects, due to the faster rate of metabolism of acetylcholine compared to that of noradrenaline [343,351,378,379].

These factors, among others such as age and circadian rhythms, play key roles in the regulation of HR.

4.2 Heart rate variability and pathological modification

Heart rate variability (HRV) had been recognised in some settings as a prognostic tool for cardiac health, and all-cause mortality [380]. HRV refers to the changes in time that occur between consecutive heart beats – lower heart rate variability means there is a regular rhythm.

An increased heart rate, together with low heart rate variability, has shown an association with increased, sub-clinical inflammation in apparently healthy individuals [381,382]. An increased resting heart rate and decreased heart rate variability were strongly associated in these studies with elevated levels of the inflammatory markers C-reactive protein, interleukin-6 and fibrinogen [381–384]. This can occur as a result of vagal depression, as the release of acetylcholine through the vagus nerve blocks cytokine production associated with inflammation (see figure 1.22) [385,386]. Thus, a lower resting heart rate resulting from vagal activation protects against inflammation, while a higher resting heart rate is strongly associated with low-grade inflammation.

Though in the long term a lower heart rate is favoured, increase and decrease in heart rate are necessary and physiologically important as they dynamically change when required in a healthy system. Inability to adjust heart rate correlates with disease and mortality, because of a reduced

capacity to respond to physiological challenges [387,388]. Reduction in the ability to self-regulate occurs with age and is more prominent in males than females [389]. This appears to be a result of lowered parasympathetic activity.

Many epidemiological studies associated a higher HR with development of cardiovascular diseases including atherosclerosis, hypertension and coronary heart disease leading to cardiovascular morbidity and mortality [388,390]. There have been data indicating a 3-fold increase in mortality in patients with HR of 90 – 100 BPM compared to patients with HR below 60 BPM [390]. HR could be considered an indicator of cardiovascular health, particularly in patients with cardiovascular risk factors such as hypertension, where a higher HR can be associated with a deteriorated cardiovascular system [324,391,392]. Higher HR correlates with increased incidences of coronary heart disease, cardiovascular disease, and all-cause mortality [391,393,394].

Animal models with 2 – 3 weeks of pacing showed development of congestive HF, and it was found that plasma levels of renin, angiotensin II, aldosterone, noradrenaline and adrenaline gradually increased with paced tachycardia, but returned to normal once pacing ceased [395–397].

Studies in human patients support the idea of remodelling with heart rate irregularity preventing maintenance of sinus rhythm [398,399]. The negative inotropic agent, verapamil, which acts as a calcium channel blocker served as a means to return atrial contraction to normal control values, reducing the time for remodelling [400,401]. These highlight the role of the regulation of heart rate in cardiac remodelling.

4.3 Therapeutic modulation of heart rate with ivabradine

Certain agents like inotropes target calcium channels and muscle contraction, while other target HR itself. Therapeutic modulation of HR has served as a useful tool for intervention in many settings of cardiac dysfunction. Modification of HR can be done by means of therapeutic

intervention, by targeting the apparatus involved in adrenergic responses in the heart. The most commonly used interventions for HR are β-blockers, which competitively inhibit binding of adrenaline to β-adrenergic cell surface receptors (see section 2.3), thereby decreasing the impact of sympathetic response, and decreasing HR.

4.3.1 Mode of action

Ivabradine is a specific inhibitor of the SA node and has no negative inotropic and lusitropic effects, and does not alter electrophysiological parameters unrelated to heart rate. It competitively inhibits the electrical pacemaker activity in the sinoatrial (SA) node controlled by the I*f* current, preventing current conduction (see section 4.1.2). HR is reduced, as contractility is left to the control of the Purkinje fibres (see section 4.1.1) [402].

4.3.2 Clinical use

Ivabradine is most mainly used as a treatment for chronic angina [403–405]. By reducing heart rate, it helps to lower the oxygen demand, lowering resistance and improving coronary flow [402]. It serves as a beneficial aide in cardiac conditions which have a high resting heart rate – including hypertension, coronary artery disease, and after cases of acute myocardial infarction [402,406]. It is used, in some cases of angina pectoris, together with β-blockers to improve overall contractile outcomes and heart rate [407]. It does not bind adrenergic receptors nor does it work via hormonal pathways, so it also has the potential to serve as a great agent in patients with intolerance to β-blockade [22,195].

4.3.3 Experimental findings with chronic use of ivabradine

Ivabradine has peripheral effects, aside from those seen by direct reduction of HR. It also has an effect on diastolic dysfunction and cardiac fibrosis. It improved overall cardiac performance and reduced both atrial and ventricular fibrosis in rabbits with long-term use [408]. It also reduced both

Ang II and aldosterone levels in blood plasma [408]. In rodent models, it inhibited the migration of inflammatory cells to the vascular system, preventing the formation of atherosclerotic lesions [409]. At a molecular level, it reduced the activity of NADPH oxidase and prevented eNOS uncoupling – factors which would underlie endothelial dysfunction involved in cardiovascular diseases and HF (see section 1.5.2) [410].

Ivabradine appears to have multi-factoral effect with long-term use. Direct – by inhibition of the SA node, and reduction of heart rate – and indirect – by preventing oxygen radical damage at a molecular level, preventing migration of inflammatory cells in the vascular system, and by reducing Ang II and aldosterone levels. These effects could stand to greatly benefit individuals suffering with cardiac dysfunction and failure, as its effects are applicable to multiple systems involved in dysfunction and failure.

4.4 Heart rate and heart failure

Considering the increased incidences of heart failure with an aging population, and as the end result of other complications, it would be a worthwhile venture to investigate the role of heart rate, in addition to other symptoms discussed in chapter 1, and the potential it holds as a therapeutic target to improve the outcome of patients who develop both acute/reversible and chronic HF.

Funny channels are expressed differentially in foetal and adult tissue, with greater abundance and sensitivity to voltage range during the foetal stages [411–413]. Under specific pathological conditions, membrane expression of funny channels can increase – as observed in spontaneously hypertensive rats which are characterised by development of cardiac hypertrophy [413]. Modification of I_f is also seen in humans, in explanted hearts with dilated cardiomyopathy, similar to that seen in hypertrophied rats, suggesting it could be an agent playing a role in mechanisms of heart failure [414–416]. Higher expression of funny current channels can increase electrical instability especially

with hyper-activated β-adrenergic responses, thereby contributing to the development of arrhythmias with heart failure [411].

Considering the observations linked to an increased HR (as discussed above), modification to slow HR could hold great promise in further improving the outcomes of HF.

4.4.1 Heart rate in peripartum cardiomyopathy

With the current approach to treating heart failure, increased HR does not take priority as a sign (or palpitation as a symptom). Little has been done to document patterns of HR in HF states, such as PPCM, and follow how this changes as patients' other symptoms improve. The role of the SA node in cardiac dysfunction as discussed here supports the idea that targeting HR directly in PPCM, without involving the sympathetic nervous system or blood pressure mechanisms, may be beneficial in a clinical setting. Early experimental studies suggest that reducing HR by means of the funny channels, may be of benefit in the recovery of heart failure [417].

Recently, a small study was conducted where HR was investigated as a target to improve the overall condition in PPCM patients [418]. It was observed that there was a reduction in HR which correlated with a significant improvement of cardiac function. This preliminary finding encourages further investigation of reducing HR as a potential treatment for PPCM patients.

An interesting consideration to take into account when reviewing PPCM is the potential for reversibility in less severe cases of cardiomyopathy. The same holds true for TC as well. In the cases that are secondary and/ or more severe, both of them have sudden onset and rapid (irreversible) decline in cardiac function and share many similarities in their pathological behaviour and outcomes. Both of these conditions have aberrances in HR.

4.4.2 Heart rate in Takotsubo cardiomyopathy

Modification of HR in a long-term setting shows promise. The SHIFT trial which followed the treatment of chronic heart failure showed improvement critical outcomes when using Ivabradine as a complementary therapy to standard recommended therapy simply by its action on heart rate [417]. Modification of HF in an acute setting has not been investigated, but may potentially improve the overall, long-term outcome of patients with conditions such as Takotsubo cardiomyopathy, acute heart failure and PPCM.

TC, of the acute HF states in particular, holds promise for modification with Ivabradine – the mechanistic means by which it occurs is the result of adrenergic activation (see section 3.5.1), and is meant to be a transient measure to compensate for environmental stimulus. By nature of the sympathetic activity, a high HR is a key identifier in TC. Ivabradine could potentially damped the HF state in this setting, as its activity to slow heart rate is independent of adrenergic pathways. This could serve as a critical intervention, as a slower HR is associated with better outcomes (as discussed above).

Chapter 2

Aims, hypothesis and objectives

1. Study rationale

Standard therapy for HF targets water retention, contractile strength, and neurohormonal activation (as discussed in previous chapters). These show benefit, but additional strategies are needed to address more severe, and acute-onset HF, both of which have causes and outcomes that are difficult to manage and result in high mortality rates.

A number of pathologies, myocardial infarction, uncontrolled hypertension, hypotension due to haemorrhagic shock and Takotsubo cardiomyopathy (TC) can lead to acute heart failure (AHF).

PPCM is the onset of HF shortly before, or up to 5 months after delivery. It is reversible in many patients treated with standard recommended HF therapy, and bromocriptine (see chapter 2). However, some patients with a more severe phenotype do not respond to current optimal therapy and there are high rates of morbidity. With these patients, it may be beneficial to investigate complementary targets, such as heart rate which elevates during pregnancy, and may exacerbate HF-like symptoms.

Hypotensive AHF most often results from a loss in blood volume and/ or pressure, that can occur due to incidents such as physical injury, and blood loss at childbirth. It has poor prognosis overall, and a high mortality rate. The immediate compensatory response is adrenergic activation to increase heart rate and strength of contractility – this has been proposed to link to the activity of the intrinsic pace-maker in the heart. Given this theory, modification of heart rate may play a crucial role if it is done via the pace-making centre, and could potentially improve the outcome in AHF.

Similarly, TC is an acute case of HF characterised by changes in contractility along the axis of the heart, due to a severe spike in adrenergic activity. TC has been referred to previously as a reversible cardiomyopathy. More recent evidence, shows that there are irreversible cases, which can be the outcome of complications of a variety of cardiovascular causes. It shows a sudden spike in heart rate, followed by HF, with a drop in HR. With the change in heart rate in TC, a strategy to target pace-making activity may hold potential to improve outcomes, but the timing of modification will be crucial.

Variability of HR is a recurring feature in these cardiomyopathies, and it has been under-utilised as a means for improving the outcomes of HF. HR has been largely overlooked in the treatment of HF and may hold the potential of improving the outcomes in patients by targeting the sinoatrial node as an additive therapy (see figure 2.1).

2. Hypothesis

We hypothesise that inhibition of the sinoatrial node to modulate the heart rate may benefit acute heart failure conditions, such as PPCM, hypotensive AHF and TC.

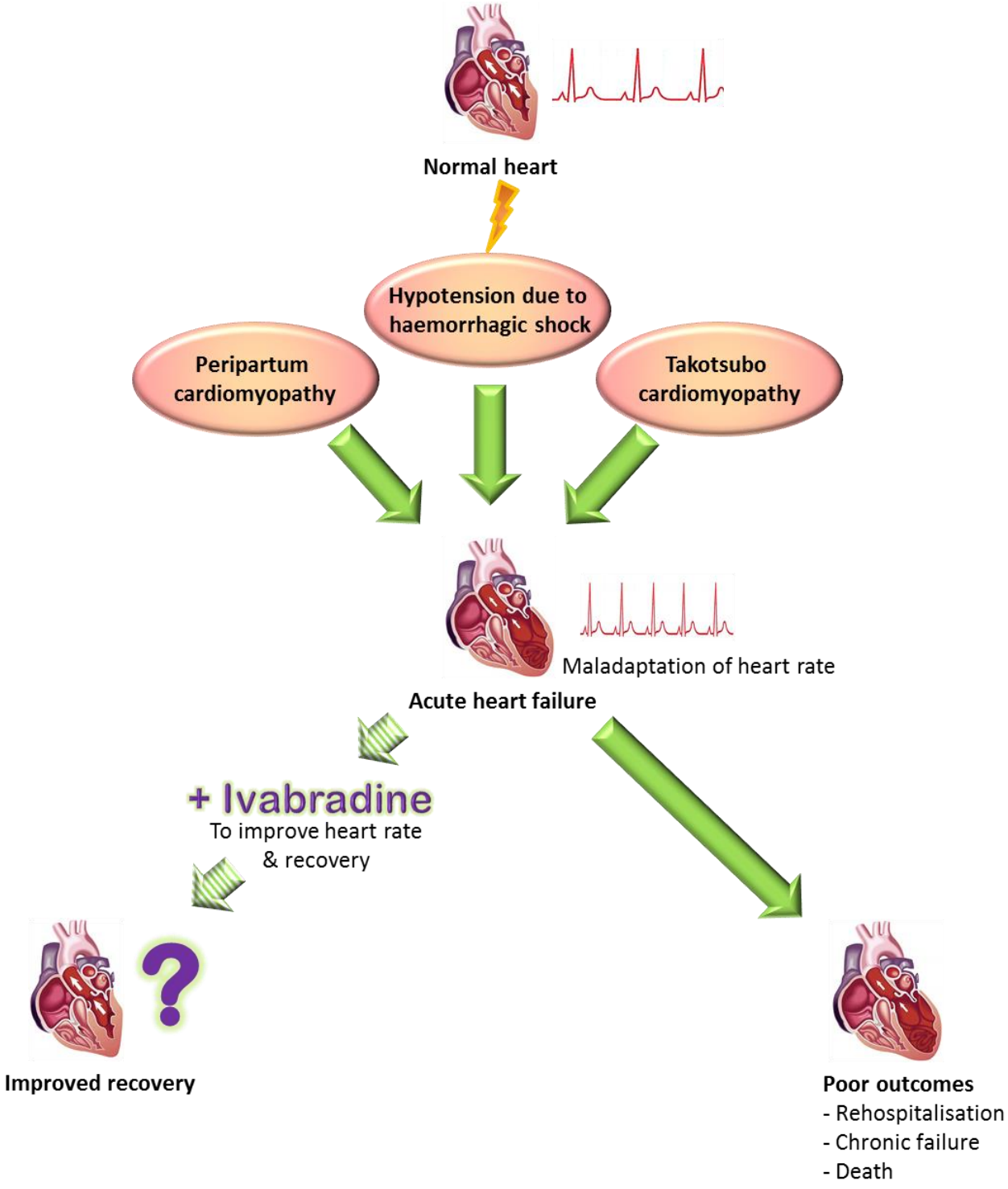

Figure 2.1: Experimental hypothesis. Hearts of patients who suffer from peripartum cardiomyopathy, Takotsubo cardiomyopathy, or hypotension due to haemorrhagic shock may rapidly develop acute heart failure. These events are characterised by a variation of heart rate which may exacerbate the condition. Many patients have poor recovery, despite optimal therapy. We propose that modulation of the heart rate during the acute incident by means of the sinoatrial node inhibitor, ivabradine, may improve these outcomes.

5. Aims

- In a retrospective study, we aim to evaluate the evolution of HR in a cohort of South African women suffering from PPCM and treated with standard therapy (chapter 3)
- In an established in-vivo mouse model of PPCM, we aim to evaluate the effect of a chronic treatment with ivabradine, an SA node inhibitor, on cardiac function and fibrosis observed with the disease (chapters 4 & 5)
- in an ex-vivo mouse model of hypotensive AHF and a newly developed ex-vivo model of TC, we aim to explore the possible cardioprotective effects of HR modulation with ivabradine (chapter 6)

6. Objectives

The first objective is to investigate heart rate in clinical PPCM cases by retrospective analysis of case files. Observations will be noted for change in heart rate and NYHA status from presentation to 6 months, and further to 1 year after diagnosis.

The second objective is to investigate the effect that a long-term treatment with ivabradine, an SA node inhibitor which reduces HR, will have on the outcome of an in-vivo animal model of PPCM. This will be done using a genetically modified STAT3 knockout (STAT3 KO) mouse model in which female mice develop cardiac hypertrophy during the third and subsequent pregnancies. A long-term (30 day) treatment with ivabradine will be given. Echocardiography will be used to measure hemodynamic parameters of the heart for chamber dimensions in ventricle diameter and wall thickness, ejection fraction, fractional shortening and ventricular weight prior to and post-treatment. Histological staining for collagen deposition will be used to evaluate the development of fibrosis. Furthermore, mRNA analysis of associated proteins will be done using qPCR. We will also evaluate miscellaneous markers of immune activation associated with heart failure using histological techniques.

The third objective is to investigate the effect of a short-term intervention with ivabradine on the measurable haemodynamic cardiac outcomes in the setting of simulated acute heart failure. This will be done using a Langendorff retrograde perfusion system, changing substrate and/or pressure to mimic clinical incidence of hypotensive acute heart failure (AHF) observed in haemorrhagic shock and TC. Parameters to be observed will include heart rate, left-ventricular developed pressure (LVDP), and rate-pressure product by means of a pressure-sensing balloon which will be inserted into the left ventricle.

Chapter 3

Retrospective evaluation of heart rate in peripartum cardiomyopathy patients

1. Study rationale

Peripartum cardiomyopathy (PPCM) is heart failure condition associated with pregnancy – developing during the last month of pregnancy or within the first 5 months postpartum [206,419]. A standard treatment program is recommended for patients, with use of diuretics, angiotensin-converting enzyme inhibitors (ACEi) and β-blockers [18]. However, use of β-blockers is not always possible as it can produce bradycardia, hypotension and acute decompensation in patients with sensitivity to the drug [420]. Bromocriptine, a drug which prevents the release of prolactin from the pituitary gland, thereby preventing cleavage of prolactin from its 23kD to a pathological 16kD form in PPCM, has recently been identified as a useful therapy [196]. These therapeutic strategies improve the overall HF phenotype, as indicated by the improvement in the NYHA classification [246]. However, the mortality rate remains high and additional therapies are required [226,227].

The design of the treatment strategies for PPCM (and other HF-like conditions) focuses largely on reducing volume load and improving strength of cardiac contractility. In normal pregnant women, there is a greater circulatory load which increases heart rate, but they recover (to below 75 beats per min) within a month of delivery [93,94]. There are many investigations which explore the progression of the HF phenotype in PPCM [219,226,421]. Despite this, there is little information on the recovery of heart rate over time, and its role in the pathophysiology of the disease.

Modulation of HR has shown benefit in other cardiac pathologies, such as chronic HF [407], but it has been under-explored in patients with PPCM. A single case study by Demir et al made use of ivabradine – an agent used to inhibit the sinoatrial node thereby reducing HR – to supplement

standard treatment of PPCM, the outcomes of which alluded to additional benefits with the use of ivabradine [422]. The patient treated was experiencing sinus tachycardia related to HF and was unable to tolerate β-blockade. After administration of ivabradine, HR decreased from 103 to 80 BPM, and had the added benefit of the patient being able to increase physical activity, without any side-effect. This case study is one of very few which examine HR in PPCM, and supports the idea that reducing HR in PPCM may further improve outcomes in patients.

In this retrospective clinical study, we therefore aimed to evaluate the evolution of HR in a cohort of women suffering from PPCM who were treated with standard therapy.

2. Methods

2.1 Human ethics and patient data collection

This retrospective study was approved by the Human Research Ethics Committee at the University of Cape Town (Human research ethics council project reference number: 848/2014), South Africa and complies with the Declaration of Helsinki 2013 [423]. All study participants gave written informed consent before study entry. The clinical data of 42 consenting patients diagnosed with PPCM and fulfilling the inclusion criteria were retrospectively gathered in this study, conducted at the Cardiac Maternity Clinic, at Groote Schuur hospital, Cape Town, South Africa. Patients were referred from local related clinics, secondary hospitals, and the department of obstetrics at Groote Schuur hospital.

Baseline data documenting symptoms of PPCM were recorded as part of the hospital assessment during first presentation at the cardiac maternity clinic. Clinical assessment and echocardiography data were further collected and recorded at 6 months and 1-year follow-up appointments. All patients with data points included at 1-year follow-up were present for 6 months follow-up, and all patients included for 6 months follow-up were present for baseline assessment. Inclusion

criteria at baseline were as follows: 1) Age 20 - 45 years; 2) displaying symptoms of congestive heart failure (HF) during the last month of pregnancy or the first 5 months postpartum; 3) no other identifiable causes of HF-like symptoms; 4) left ventricular ejection fraction (LVEF) ≤45% transthoracic echocardiographic assessment; and 5) sinus rhythm.

Exclusion criteria were as follows: 1) Significant organic valvular heart disease; 2) systolic blood pressure exceeding 160mmHg 3) diastolic blood pressure exceeding 100mmHg; and 5) any clinical condition warranting exclusion from the study as determined by the investigators. All aspects of the clinical examination as well as treatment-drug prescription were handled by the team at the Cardiac Maternity clinic, headed by Professor Karen Sliwa, the methods of which have been previously published by Sliwa et al [226]. For this investigation, data were retrospectively analysed for 42 PPCM patients.

2.2 Statistical analysis

Results are expressed as means ± standard error of mean (SEM) or median (interquartile range (IQR)). Statistical analyses were performed using Statistica v.13 software. Significant differences ($p < 0.05$) were determined for comparison of mean values of normally distributed data at baseline, 6 months and 1 year, and were performed using 2-way Anova with Fisher correction.

3. Results

3.1 Peripartum cardiomyopathy patient characteristics and maternal history

We collected data for 42 individuals at presentation, 25 at 6 months follow-up and 12 at 1-year follow-up. Physical characteristics and delivery information are summarised in table 3.1.

The median parity was 2 births. Of the 42 women, 17 had most recently had their first child, 12 their second child, 5 their third child, 5 their fourth child (1 of which was a twin pregnancy), 2 their fifth child (one of which was a twin pregnancy), and 1 their sixth child.

Table 3.1: Physical characteristics and delivery information of patients enrolled (n=42).

Physical Characteristics				
	Age (years)	Height (cm)	Weight (kg)	BMI
Range	21 - 44	148 - 170	37 – 150	17 – 52
Mean ± SEM	30±1	160±1	68±3	26±1
Maternal history				
Gravida	1st	2nd	3rd	>3rd
	29%	30%	17%	24%
Parity	1st	2nd	3rd	>3rd
	40%	29%	12%	19%
Delivery method	Vaginal birth		Caesarean section	
	64%		36%	

Abbreviations: BMI -body mass index; cm – centimetres; kg – kilograms; SEM – standard error of the mean.

3.2 Therapeutic interventions

All patients enrolled in the study were prescribed standard therapy comprised of diuretics, ACE inhibitors and β-blockers as detailed in table 3.2. At the 6-month follow-up, partial information was available for 25 patients (2 of which were not NYHA classified). All patients were treated with diuretics: 19 were treated with furosemide, 4 with HCTZ, and 3 with spironolactone – some patients were given more than 1 diuretic treatment. Twenty-two patients were treated with RAAS inhibitors: 20 received treatment with Elanapril, 1 with Perindopril (ACEi) and 1 with Losartan (ARB). Twenty-three of the patients were treated with β-blockers: all patients received treatment with carvedilol. Treatment strategy and doses separated by NYHA class are indicated in table 3.2.

Table 3.2: Treatment strategy at 6 months follow-up. There were no patients reported to be NYHA IV. IQR = 3rd – 1st quartile. Tribuss (trade name) contains efavirenz, tenofovir disoproxil fumarate, and emtricitabine.

	NYHA I		NYHA II		NYHA III	
	Median dose (mg) (IQR)	n	Median dose (mg) (IQR)	n	Median dose (mg) (IQR)	n
Diuretics						
Furosemide	80(40)	9	80(80)	8	120(40)	2
HCTZ	25	1	25(0)	3	-	0
Spironolactone	20	1	25(0)	2	-	0
ACEi						
Elanapril	10(0)	10	10(5)	8	7.5(2.5)	2
Perindopril	-	0	8	1	-	0
Losartan	-	0	50	1	-	0
B-blockers						
Carvedilol	18.75(12.5)	10	25(7.25)	11	6.25(0)	2
Other						
Bromocriptine	5(0)	8	5(0)	5	-	0
Warfarin	5	1	5(0)	4	-	0
Tribuss	-	0	1 dose	1	1 dose	1

Abbreviations: ACEi – Angiotensin-converting enzyme inhibitor; HCTZ - hydrochlorothiazide; IQR – inter-quartile range; mg – milligrams; NYHA – New York Heart Association class.

3.3 Cardiovascular function of patients with peripartum cardiomyopathy

Of the patients enrolled, 12% had a known history of hypertension, 2% had history of tuberculosis and 31% had HIV. Ten percent of the patients had a family history of cardiovascular disease, but none reported a family history of PPCM. In all of these patients, PPCM was presented as the diagnosis, when all other possible were excluded as the cause of HF.

Of the 42 patients enrolled, 24% had experienced PPCM symptoms in previous pregnancies. Physical symptoms were reported and recorded for patients as follows: 32% had dizziness, 37% had palpitations, 5% had angina, 61% had elevated jugular venous pressure, 59% had crepitations, and 5% had pulmonary thromboembolisms. Fifteen percent had right heart failure, and 15% had recorded systolic murmurs. Twenty-one percent of patients were reported to experience onset of PPCM symptoms pre-partum. Twenty-two percent of patients presented with gestational hypertension which persisted for 19% of them post-partum. Fifteen percent of patients presented with pre-partum heart failure while the remaining 85% presented with heart failure post-partum.

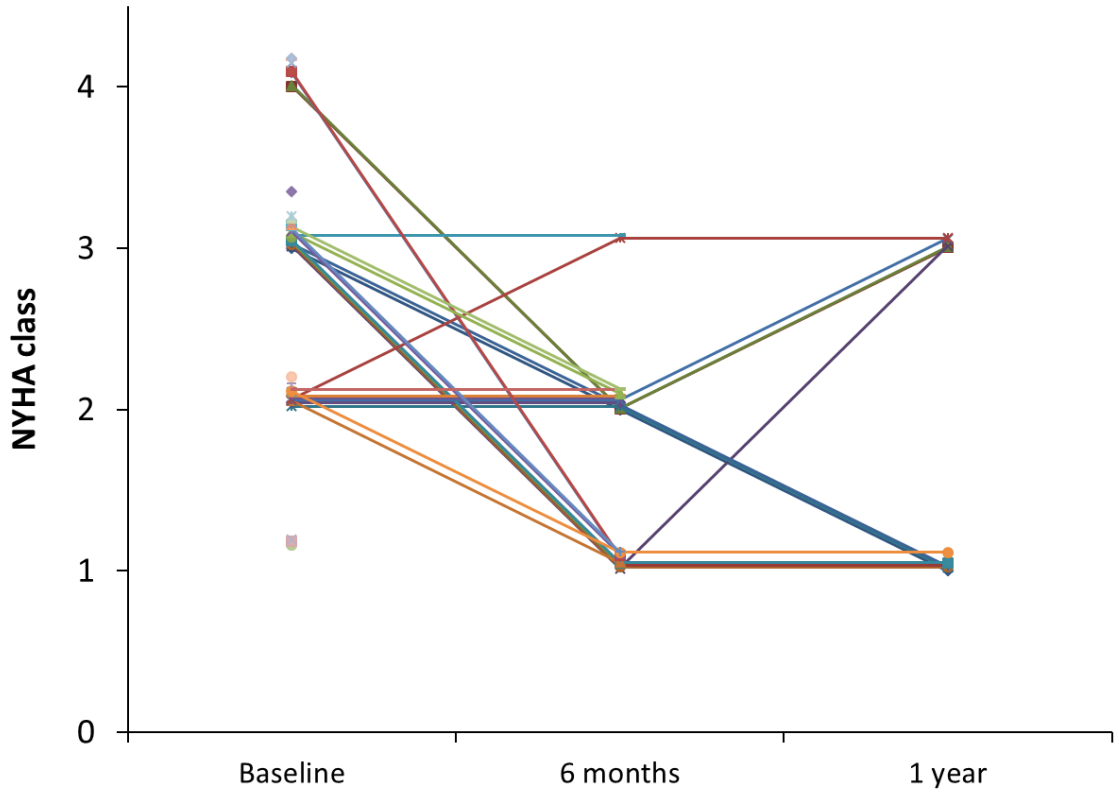

Figure 3.1: Patient NYHA classification. NYHA classification and changes of patients from baseline (n=42) to 6-month follow up (n=25) and further to 1 year (n=12). Most patients showed an improvement in NYHA classification after 6 months on standard recommended therapy. However, there were some who did not change classification at 6 months compared to baseline, most of whom were in NYHA II. Outcomes after 1 year on standard therapy were mixed – patients in NYHA I at 6 months continued in NYHA I, while a few patients in other classes improved, and some worsened. Abbreviations: NYHA – New York Heart Association class.

With treatment, most patients showed an improvement in NYHA class after 6 months (see figure 3.1), with only 1 of 25 patients showing a worsening in NYHA class. At 1 year, outcomes were mixed with 4 of 12 patients showing a worsening of NYHA class while the remaining 8 were stable or improved. These treatment strategies were very slow in improving HR, as only 3 of 25 patients at 6 months had improved to obtain a resting HR of less than 75 BPM (see figure 3.2), despite the length of treatment. At 1 year, there was further improvement in terms of HR in 3 of 12 patients to obtain a resting HR of less than 75 BPM.

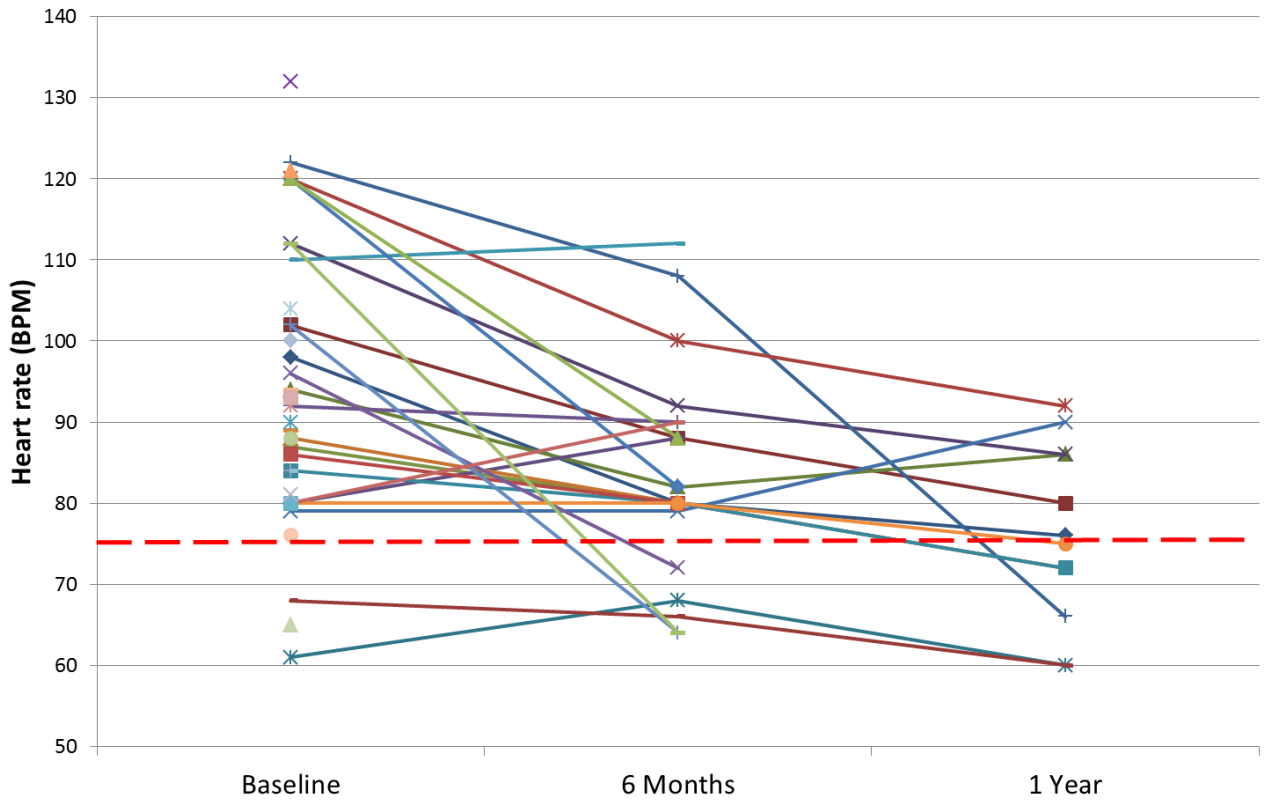

Figure 3.2: Individual heart rates of patients at baseline, after 6 months and 1 year on standard, recommended therapy. Only 3 of the 42 patients observed had a healthy heart rate of <75 BPM (indicated by the red dotted line) at baseline. This improved to 5 of 25 patients who had recovered their resting heart rate to normal values after 6 months and 6 of 12 after 1 year on standard recommended therapy. Abbreviations: BPM – beats per minute; PPCM – peripartum cardiomyopathy.

The initial grouping of patients according to the New York Heart Association (NYHA) scale (see table 3.3) produced the following clusters: 9% patients were classified as NYHA I, 31% as NYHA II,

43% as NYHA III, and 17% as NYHA IV. At 6 months follow-up, patients were assessed and reclassified as follows: 44% of patients were classified as NYHA I, 48% as NYHA II (3 re-hospitalised), 8% as NYHA III (2 re-hospitalised), and 0% as NYHA IV. At 1-year follow-up, patients were assessed and reclassified as follows: 58% of patients were classified as NYHA I, 0% as NYHA II, 42% as NYHA III, and 0% as NYHA IV.

Table 3.3: Cardiovascular function data as categorised by NYHA class. HR, SBP, DBP and EF values as recorded, distinguished by NYHA class at baseline, after 6 months, and after 1 year on standard recommended therapy. Values are expressed as mean ± SEM, and number of data points are indicated.

Baseline	NYHA I	NYHA II	NYHA III	NYHA IV	p-values
n (total n = 42)	4 (9%)	13 (31%)	18 (43%)	7 (17%)	
HR (BPM)	87 ± 3	85 ± 4	99 ± 4•	104 ± 6* #	*0.036 vs NYHA I; •0.005 vs NYHA II #0.002 vs NYHA II
SBP (mmHg)	111 ± 4	121 ± 4	119 ± 6	105 ± 7	NS
DBP (mmHg)	66 ± 5	76 ± 3	78 ± 4	70 ± 3	NS
EF (%)	39 ± 8	34 ± 2	31 ± 2	24 ± 4*	*0.030 vs NYHA I
6 Months					
n (total n = 25)	11 (44%)	12 (48%)	2 (8%)	0 (0%)	
HR (BPM)	78 ± 2	84 ± 4	106 ± 6*	-	*0.007 vs NYHA I
SBP (mmHg)	120 ± 4	111 ± 2	123 ± 23	-	NS
DBP (mmHg)	75 ± 2	66 ± 6	80 ± 20	-	NS
EF (%)	50 ± 3	37 ± 3*	36 ± 2	-	*0.008 vs NYHA I
1 Year					
n (total n = 12)	7 (58%)	0 (0%)	5 (42%)	0 (0%)	
HR (BPM)	69 ± 3	-	87 ± 2*	-	0.028 vs NYHA I
SBP (mmHg)	116 ± 8	-	105 ± 3	-	NS
DBP (mmHg)	70 ± 4	-	70 ± 2	-	NS
EF (%)	58 ± 3	-	36 ± 11*	-	*0.002 vs NYHA I

Abbreviations: BPM – beats per minute; DBP – diastolic blood pressure; EF – ejection fraction; HR - heart rate; mmHg – millimetres of mercury; NS – not significant; NYHA – New York Heart Association; SEM – standard error of the mean; SBP – systolic blood pressure.

Systolic blood pressure (SBP), diastolic blood pressure (DBP) and ejection fraction were recorded and are clustered by NYHA group in table 3.3. Patients in NYHA I had increased SBP and DBP at 6 months when compared to baseline. Patients in NYHA II had decreased SBP and DBP at 6 months (compared to baseline). Patients in NYHA III had comparable SBP and DBP at 6 months (compared to baseline) which decreased at 1-year follow-up.

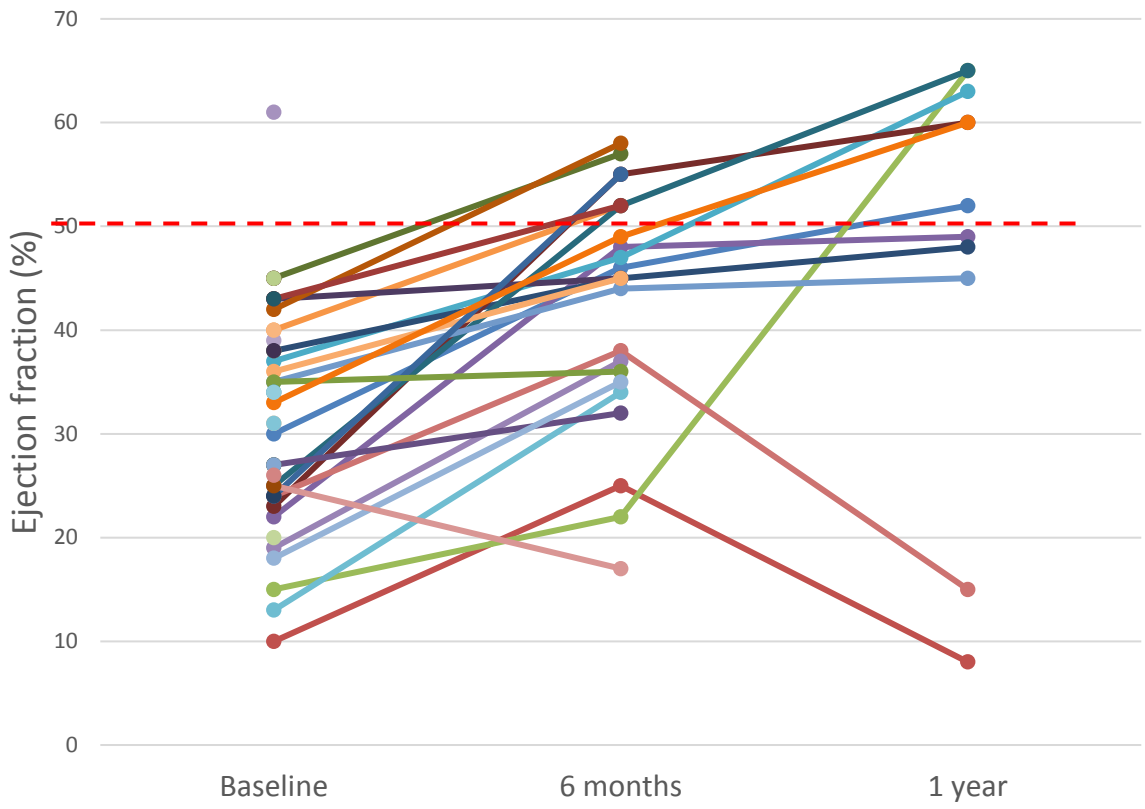

Figure 3.3: Individual ejection fractions of patients at baseline, after 6 months and 1 year on standard, recommended therapy. Only one of the 29 patients observed had a healthy ejection fraction of <50% (indicated by the red dotted line) at baseline. This increased to 6 of 25 patients with normal values after 6 months and 6 of 12 after 1 year on standard recommended therapy.

Echocardiography results were processed and ejection fraction (EF) was recorded and are clustered by NYHA group in table 3.3. Patients in NYHA I had increased EF at 6 months (compared to baseline) which further increased at 1-year follow-up. Patients in NYHA II had unchanged EF at 6 months (compared to baseline). Patients in NYHA III had slightly increased EF at 6 months (compared to baseline) which was unchanged at 1-year follow-up. There was a general trend

toward an increase in EF with time (see figure 3.3), with deterioration in only 1 of 25 patients at 6 months and 2 of 12 at 1-year follow-up. In terms of recovery of EF, 6 of 25 had normal EF (i.e. EF > 50%) at 6 months, while 6 of 12 had normal EF after 1 year.

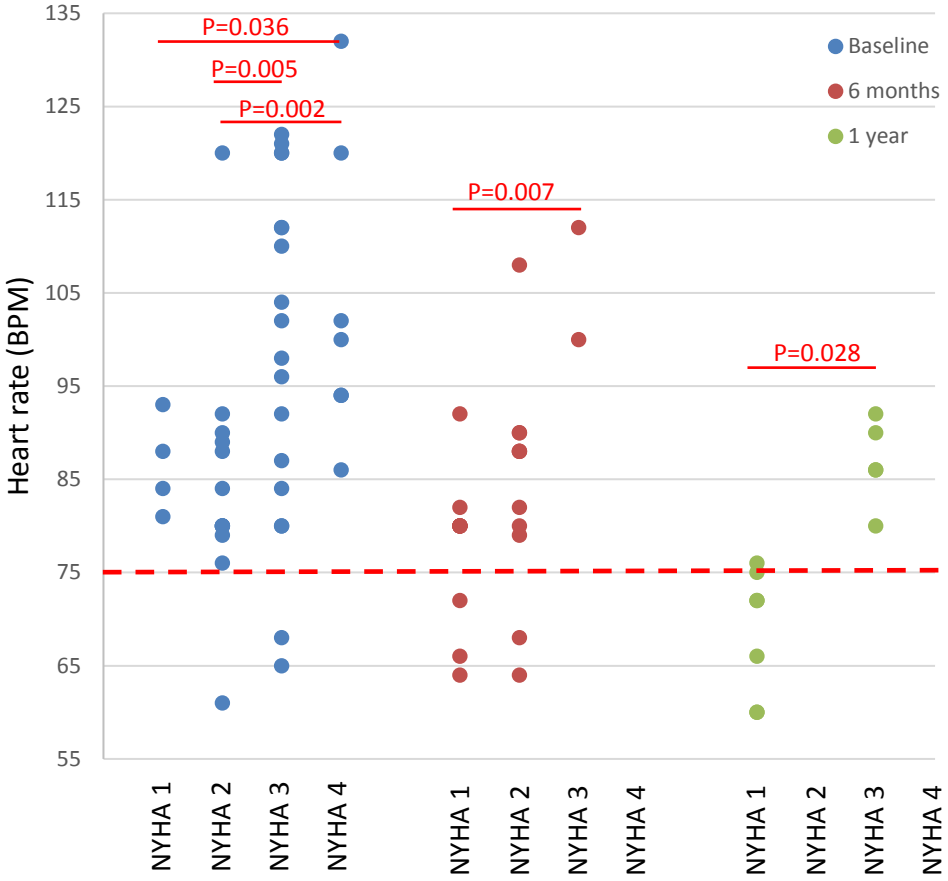

Figure 3.4: Heart rate of individual patients clustered by NYHA class at baseline (n=29), 6-month follow-up (n=25) and 1-year follow-up (n=9). The trend of a higher heart rate associated with NYHA class shows more prominently at 6 months, and further at 1-year follow-up. Red dotted line indicates the upper limit of a physiological resting heart rate of 75BPM. Abbreviations: BPM – beats per minute; NYHA – New York Heart Association class

Electrocardiogram (ECG) results at baseline indicated sinus tachycardia for 3 patients (7%). Resting heart rate (HR) was recorded for patients in NYHA I as follows: 87±3 beats per minute (BPM) at baseline, which decreased to78±2 BPM at 6 months follow-up and further deceased to 69±3 BPM at 1-year follow-up (see table 3.3). HR was recorded for patients in NYHA II as follows: 85±4 BPM at presentation, and remained constant at 84±4 BPM at 6 months follow-up. HR was recorded for

patients in NYHA III as follows: 99±4 BPM at presentation, which increased to 106±6 BPM at 6 months follow-up, and decreased to 87±2 BPM at 1-year follow-up. HR was recorded for patients in NYHA IV as follows: 104±6 BPM at presentation. Scattered illustration of the data obtained, as well as differences between groups can be found in figure 3.4.

There is a trend toward correlation of heart rate with severity of the NYHA class and HF-like phenotype, as illustrated in figure 3.4. Heart rate could perhaps serve as a useful predictive tool for the severity of the outcome of PPCM. Observations in figure 3.2 show more stability with a lower baseline HR, while the highest third of baseline HR points improved to varying degrees, but steadily over time.

4. Discussion

The aim of this study was to explore the recovery of HR, together with other HF-like symptoms, in South African PPCM women who were prescribed standard recommended therapy. Our data reported here show that most patients had partially improved in terms of HR after 6 months of standard recommended therapy, and further after 1 year, but still fell short of a healthy HR for most patients.

Our main findings were as follows:

- The majority of the PPCM patients enrolled in this study had an elevated HR (≥75BPM) at baseline (93%).
- This trend persisted after 6 months on standard, recommended treatment, as 80% of patients had an elevated HR.
- There was an improvement after 1 year on standard, recommended treatment, but 42% of patients still had an elevated HR.

- Higher HR was associated with higher NYHA classification, particularly after 6 months and 1 year on standard, recommended treatment.

In this population, we observed that of those delivering subsequent to their first child, 11 of the 26 had experienced PPCM symptoms in a previous pregnancy.

At the time of analysis of our data, Libhaber et al published a similar PPCM study, conducted in South Africa, in which they observed poor outcomes (i.e. mortality) in patients with HR above 100 BPM (see figure 3.5) [246]. A higher HR was more strongly correlated with mortality - this observation held true despite variation in SBP. This outcome echoes our findings – a single patient who had an initial heart rate of 100 BPM had died in our study – a higher heart rate corresponds with poorer cardiac outcomes in the setting of PPCM.

Furthermore, Haghikia et al also published a study during the time of our analysis which documented the use of Ivabradine in 20 German PPCM patients over a period of 6 months [418]. They reported significantly lower HR in patients after just 1 week of treatment, and better outcomes in LV function with Ivabradine in their cohort compared to those reported by previous registries. They showed that initial HR correlated with serum pro-BNP levels – an indicator that HR links to dysfunction. They also reported that ivabradine was well tolerated – as no patients suffered adverse reactions to treatment.

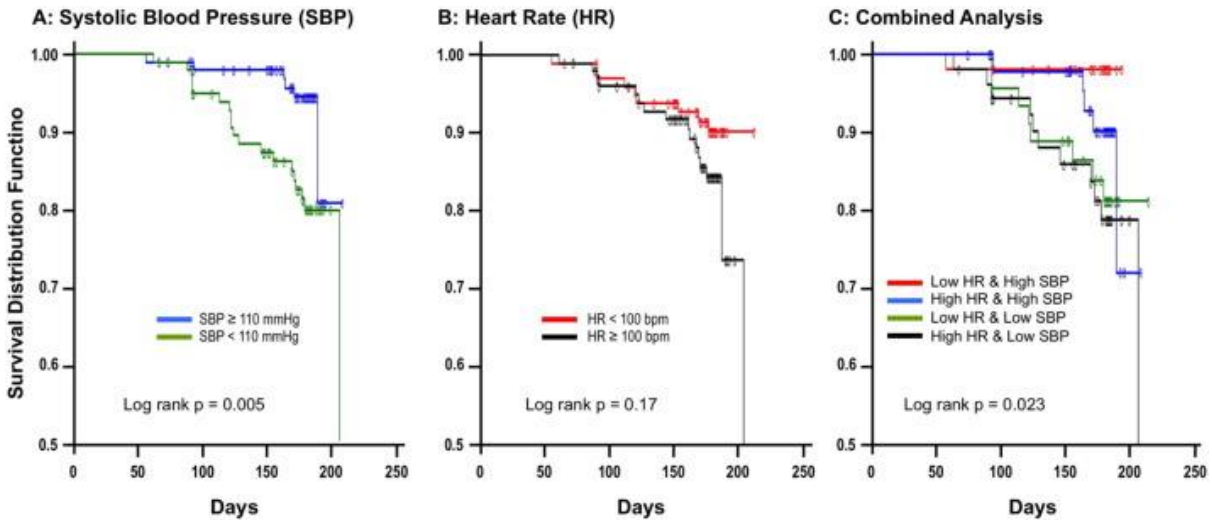

Figure 3.5: Cardiac parameters and outcomes in terms of survival as reported by Libhaber et al [246]. Heart rate above 100 BPM correlated with greater mortality after 200 days. When HR and systolic blood pressure measures were combined and analysed, the combination of higher heart rate with higher blood pressure proved to be most detrimental after 200 days, followed by the combination of higher heart rate and low systolic blood pressure. Abbreviations: DBP – diastolic blood pressure; HR – heart rate; mmHg – millimetres of mercury; SBP – systolic blood pressure.

Our study cohort had a smaller proportion of patients in NYHA III & IV cluster groups at baseline compared to that of Libhaber et al [246]. Although our groups showed comparable SBP, DBP, HR and EF at baseline, there were slight differences in treatment, as they were prescribed digoxin as part of their treatment strategy. Interestingly, they observed that patients with poorer outcomes in their study were on lower doses of β-blockers. This resonates with the findings of Haghikia et al who found that PPCM patients who did not improve had a lesser degree of β-blockade than those who recovered fully [205].

Our findings, in terms of HR and EF, were consistent with those of Haghikia et al [205] – their patients showed elevated HR at baseline together with reduced EF. However, their EF values were lower than those seen in our group. Treatment strategies were consistent (including the use of Bromocriptine), but again, they prescribed digoxin as part of their treatment strategy, while we did not. Differences in race and social status may possibly explain the variation seen between the German study and our study.

The treatment that was prescribed to our patients maintained systolic and diastolic blood pressure below 120/80mmHg (as observed in table 3.3). These treatment strategies, together with the use of bromocriptine, improved the overall HF phenotype, as indicated by the improvement in the NYHA classification and ejection fraction measures from baseline to 6 months and further, in most cases, to a year. The groups studied by Haghikia et al and Libhaber et al followed a similar treatment strategy, with use of diuretics, ACEi, beta-blockers and bromocriptine.

Libhaber et al observed that 57% of the patients who had poor outcomes in their study had HR greater than 100 BPM at baseline, which was significantly higher than patients who did not have poor outcomes (101+19 BPM vs 95+19 BPM, p=0.017) [246]. In their study, 75% of patients who died had SBP below 110mmHg and were on a lower dose of β-blockers, but their treatment was the same in all other aspects. There was no distinction in terms of EF (25% vs 27% respectively) when it came to survival, but they found HR and SBP to be the distinguishing factors which correlated with survival outcome – a higher HR correlated with poorer outcomes.

A lower HR correlates with lower NYHA class. These observations, particularly in terms of HR support the idea that modification of HR may serve as a useful tool to improve the outcome of HF. Thus, we propose that the use of the sinoatrial node inhibitor, ivabradine, to slow HR in patients with higher risk, particularly those with adverse reactions to β-blockers, may benefit outcome and NYHA classification in PPCM.

5. Limitations

One patient suffered a fatal cardiovascular-related event before the 6-month follow up, and information was thus only available for her baseline assessment. A second factor that limited the availability of data was that few patients reported for 6-month, and 1-year follow-ups. This restricted the statistical power and provided fewer comparative data points to work with. This may be a result of these patients deeming themselves recovered, and those who chose to attend did so

out of concern for a lack of improvement in their cardiac health status. The small sample size also served as a limitation in terms of statistical power.

6. Conclusion

The data we have presented here show that most PPCM patients had partially improved in terms of HR after 6 months of standard recommended therapy, and further after 1 year, but still fell short of a healthy HR. Patients improved HF-like symptoms with treatment – each patient improved by at least one NYHA class within the first 6 months of standard recommended therapy. However, we observed that patients who returned after 1 year were either stable or had deteriorated symptomatically. Further to this, patients with higher NYHA classification had higher HRs at all time points observed. These data, together with the findings by Haghikia et al [418] and Libhaber et al [246] support the idea of targeting HR by a means other than β-blockade to further improve the treatment of PPCM.

Ivabradine, an inhibitor of the sinoatrial node, has been shown to reduced HR in PPCM patients and could therefore be considered as a potential therapy in the setting of PPCM.

Chapter 4

Exploring the effect of reducing heart rate in an in-vivo mouse model of PPCM

1. Study rationale

PPCM is associated with reduced cardiac function (ejection fraction, fractional shortening), increased markers of cardiac stress (ANP, BNP), cardiac remodelling with dilatation and fibrosis [42–46]. Improvement in the PPCM phenotype is associated with an improvement of cardiac function, a drop in stress markers, limiting remodelling, thus preventing dilatation and chronic failure – but there is still a need for additional therapies, as the mortality rate remains high [226,227].

In South African PPCM women with optimum standard treatment, we have observed that HR remains elevated in most patients after 6 months, an effect which was still observed after a year (see chapter 3). Libhaber et al have recently observed that an elevated HR at baseline is associated with poorer outcomes [246].

The drug, ivabradine, reduces HR by slowing action-potentials without adrenergic involvement and is used to treat stable angina pectoralis and symptomatic chronic heart failure [417,424]. It exerts secondary effects – such as reducing Ang II and aldosterone levels, and reducing reactive oxygen species [410]- which may theoretically improve the outcomes of HF in addition to the slowing of HR [408].

Animal models used to study PPCM display similar features to those seen in humans. Cardiac-specific signal transducer and activator of transcription 3 knockout (STAT3 KO) mice have been established as an animal model of PPCM, the phenotype of which develops after 3 consecutive pregnancies [196]. The cardiac-specific STAT3 knockout mouse model of PPCM has been previously described as having reduced fractional shortening, increased heart weight to body weight ratio,

dilatation, cleavage of prolactin to its 16kD form and remarkable fibrosis when compared to healthy and nulliparous controls [196]. This model has, for example, been used to validate the efficacy of bromocriptine – the drug used to prevent the release of prolactin by the pituitary gland – in the treatment of PPCM, which is now commonly used in clinical settings [196,226]. However, HR modulation in this model has never been studied.

In the present study, we therefore aimed to evaluate the effect of a chronic treatment with ivabradine on the cardiac performance and remodelling in a STAT3 KO mouse model of PPCM.

2. Methods

2.1 Animal ethics

All animal-based experiments were conducted in female mice (9 – 38 weeks old). All procedures were approved by the Faculty of Health Sciences Animal Ethics Committee of the University of Cape Town (project reference number 015/045). All experiments were conducted, in accordance with the Guiding Principles in the Care and Use of Animals and National Institute of Health Guidelines (NIH publication No. 85-22, revised 1996) [425]. Cardiomyocyte-specific STAT3 KO and wildtype (WT) mice were bred at the animal unit at the University of Cape Town and were housed in a facility with 12-hour day/ night light cycles, with ad libitum access to food and water.

2.2 Cardiac-specific STAT3 knockout mouse model

Cardiac-specific STAT3-knockout mice (STAT3 KO) were created by crossing C57BL6 mice heterozygous for a Myosin Light Chain 2V (MLC2V) -driven Cre-recombinase [120] with C57BL6 mice homozygous for flox-surrounded section of STAT3 as previously described [426]. Mice characterised as homozygous for the deleted 1.4-kilobase fragment of STAT3 (containing exon 1, intron 1, exon 2 and part of intron 2) and MLC2V Cre-recombinase by means of polymerase chain reaction (PCR) analysis of tail biopsies [426,427] were used as STAT3 KO, and their littermates

characterised as lacking Cre-recombinase by PCR analysis were used as wildtype littermate controls, as previously described and published by our laboratory [426,428].

2.3 Establishment of a peripartum cardiomyopathy model in STAT3 KO mice

Hilfiker-Kleiner et al noted that cardiomyocyte-specific STAT3 KO mice developed PPCM, with heterozygote KO having a milder form than the homozygotes [196]. They also reported that, after 3 pregnancies, heterozygous STAT3 KO mice presented signs of HF, such as laboured breathing and generalised oedema. Echocardiography revealed left ventricular dilatation and depressed fractional shortening in STAT3 KO compared to control female mice, mimicking the setting of PPCM[196].

For experiments, STAT3 KO females and control littermates were age-matched and mated thrice, with weaning, before a baseline transthoracic echocardiography (TTE) was performed. A weaning period of 3 weeks was essential as lactation is believed to contribute to the development of PPCM[196].

2.4 Experimental protocol

Twenty-two days after the 3rd delivery, STAT3 KO mice and their littermate control were examined by means of TTE – this was considered as the baseline time point. Immediately thereafter, the treatment with ivabradine was started at a dose of 10mg/kg/day body weight dissolved in the drinking water [429]. The control mice did not receive any treatment in their drinking water. Drinking water containing ivabradine was continually available to mice and was changed every 3rd day. After 30 days of treatment [430], a second TTE was taken and hearts were harvested for histology and mRNA (messenger ribonucleic acid) analysis (see figure 4.1.). Genotyping was performed on tail biopsies obtained at birth and repeated after hearts were harvested.

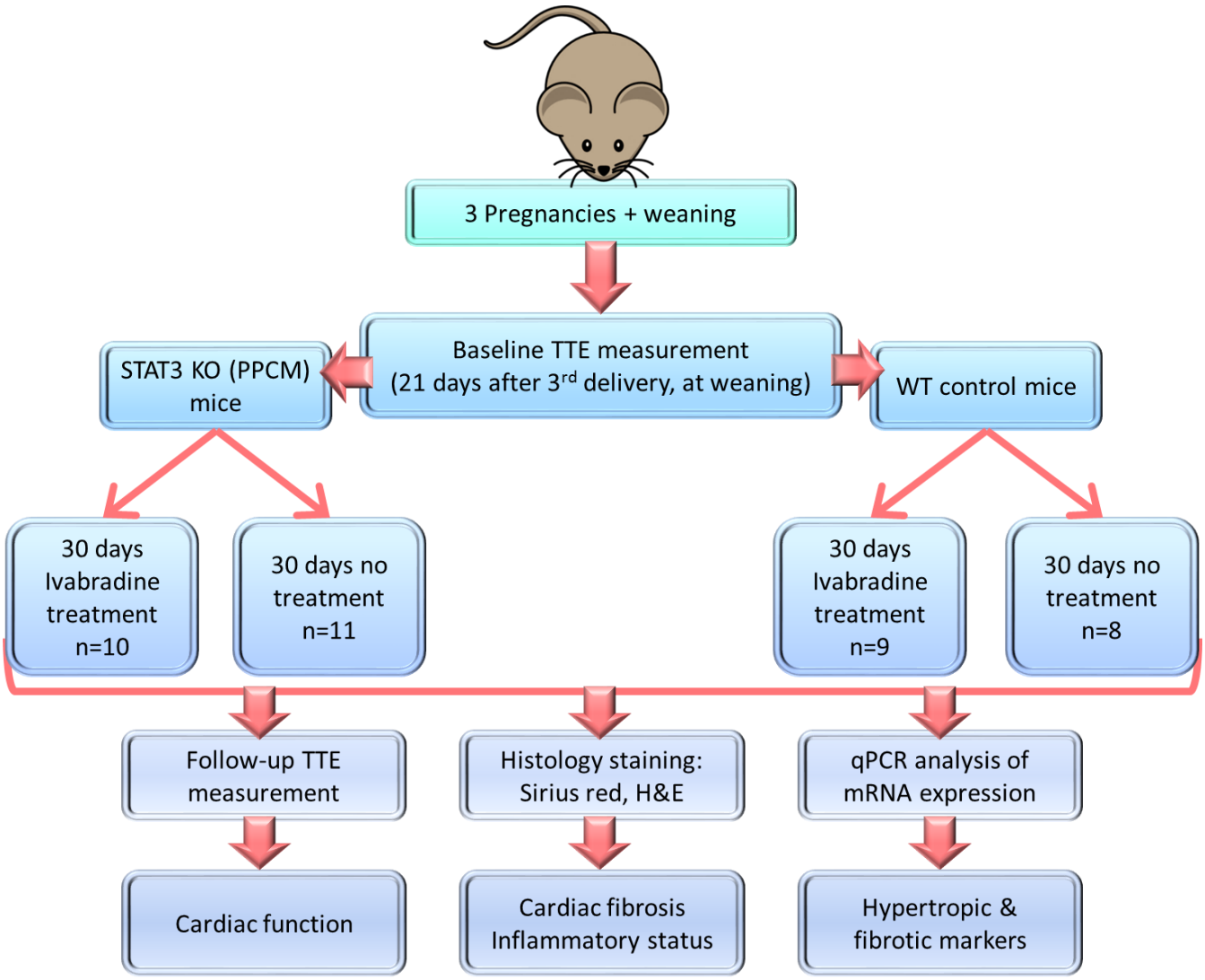

Figure 4.1: Experimental protocol to study the effect of ivabradine in a PPCM model. Mice had 3 consecutive pregnancies, with weaning, before a baseline TTE measurement. They were then treated with Ivabradine (10 mg/kg orally, in drinking water) for 30 days before a follow-up TTE was taken, and hearts were excised for histological staining and mRNA transcript analysis. Abbreviations: H&E – Haematoxylin and Eosin; mRNA – messenger RNA; qPCR – quantitative polymerase chain reaction; STAT3 KO – signal transducer and activator of transcription 3 knockout; PPCM –peripartum cardiomyopathy; TTE – transthoracic echocardiography; WT – wildtype

2.5 Mouse echocardiography

Mice were anaesthetised with inhalant anaesthetic (4% isoflurane in medical oxygen at a flow rate of 1 ml/min) until loss of the righting reflex. Mice were transferred to a heating pad and anaesthesia was maintained with 2% isoflurane in medical oxygen (1 ml/min) fed by means of a nose cone for the TTE procedure. A rectal thermometer was inserted to monitor body temperature,

which was maintained at 37°C. Mice were placed in the supine position on a warming pad, and fur was removed from the thoracic region. TTE gel was warmed and placed on the exposed chest. The mouse heart was assessed using a 550 MHz linear transducer using VisualSonics® Vevo® 2100 V.1.6.0 imaging software. The imaging probe was placed in contact with the gel only. The probe was positioned to obtain the left ventricular short-axis view of the heart without papillary muscle interference. The position along the axis of the heart was tracked using the M-mode function, and once the position was deemed central along the axis and satisfactory, the B-mode function was activated, and Doppler waveforms were recorded for measurements and analysis. TTE images were downloaded and blindly analysed, post-capture.

TTEs were done using B-mode and targeted M-mode echocardiography. Systolic and diastolic LV dimensions were measured.

Left ventricular (LV) anterior wall thickness (LVAW), LV internal diameter (LVID) and LV posterior wall thicknesses (LVPW) in systole and diastole (LVAWs, LWAVd, LVIDs, LVIDd, LVPWs & LVPWd respectively, see figure 4.2), as well as HR were measured from M-mode images at the level of the base just above the papillary muscles. Imaging software calculated approximate values for LV mass. LV ejection fraction (EF) and LV fractional shortening (FS) are measured for evaluation of LV global systolic function, and were calculated in this investigation by using the monoplane volume and ejection fraction.

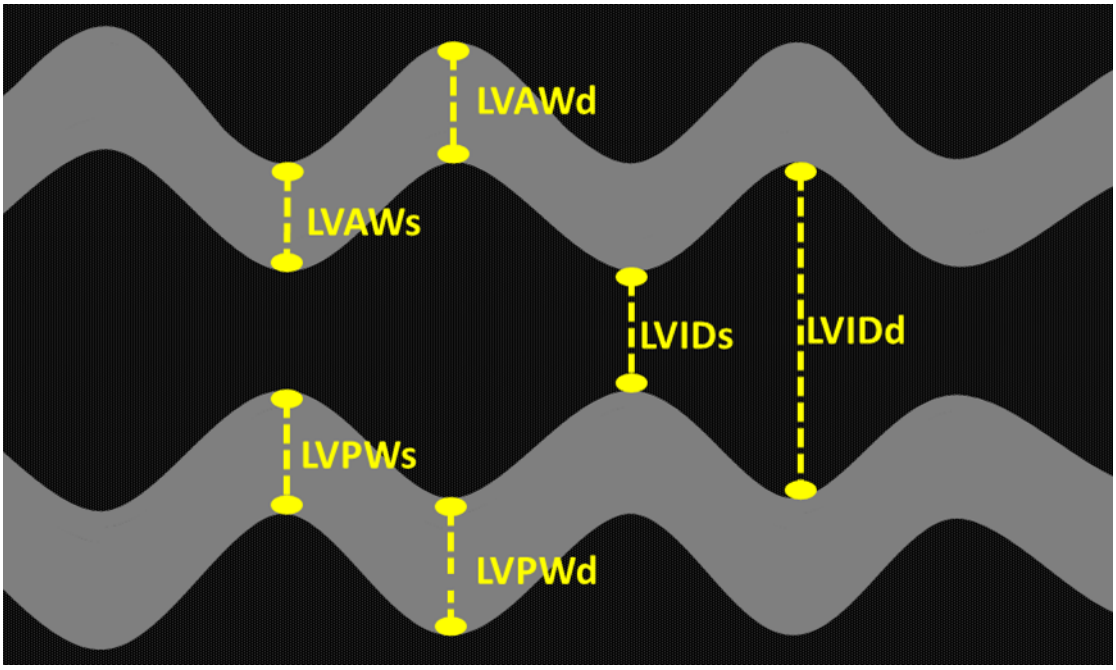

Figure 4.2: Cardiac dimensions measured in M-mode across the widest diameter of the left ventricle. Left ventricular (LV) anterior wall thickness (LVAW), LV internal diameter (LVID) and LV posterior wall thicknesses (LVPW) in systole and diastole (LVAWs, LWAVd, LVIDs, LVIDd, LVPWs & LVPWd respectively) were measured as indicated. Lighter grey sections indicate the chamber walls,

2.6 Histology

2.6.1 Sacrifice and histological fixing of hearts

Mice were anesthetized by intraperitoneal injection of sodium pentobarbitone (200mg/kg body mass) (Kyron Laboratories (PTY) LTD, Benrose, South Africa). Once a sufficient degree of anaesthesia had been obtained, indicated by absence of the pedal reflex, the chest was cut open, and saturated potassium chloride (50% potassium chloride, see appendix A) solution was injected into the left ventricular chamber until the heart arrested in diastole. It was then excised, and excess connective tissue trimmed before flushing with sterilized saline (9% sodium chloride, see appendix A). Body weight, heart weight, lung weight and tibia length were recorded.

The bottom third section of the heart, closest to the apex, was cut off and flash-frozen in liquid nitrogen for quantitative PCR (qPCR) analysis (see chapter 4, section 2.7). The remainder of the

heart was submerged in paraformaldehyde (4% in phosphate-buffered saline (PBS), see appendix A) for a minimum of 2 days and transferred to 70% ethanol until sectioning for histological staining.

The heart was then cut in transverse sections and set in paraffin wax in a histology cassette. Samples were dehydrated with 3 times 1-hour incubations in alcohol (70% - 90%), before 3 times 100% ethanol. This was followed by 3 times 1-hour incubations in iso-octane, 2 times paraffin wax (at 60°C), followed by 2 hours in 1 change of paraffin. Samples were then embedded gently with hot wax and set for 5 – 10 min on a cold plate. Sections were then sliced from the apex to the basal part of the left ventricle using a cryostat at 3-4µm thickness for Haematoxylin and Eosin (H&E) and Sirius red staining, and 7-9µm thickness for immunostaining. H&E staining was done to visualise immune cell infiltration in cardiac tissue, and Sirius red staining was done to visualise collagen fibres which underlie fibrosis. All sections were mounted on glass slides for staining and analysis.

2.6.2 De-waxing of paraffin-embedded tissue sections

Paraffin sections were de-waxed and hydrated using two 10-minute incubations in xylene and sequential incubations in ethanol solutions, 95% to 70%, and distilled water. Slides were stored in phosphate-buffered saline (PBS - see appendix A) until staining was performed.

2.6.3 Haematoxylin and Eosin staining

Separate slides were stained using the H&E method [431]. Each slide was submerged in haematoxylin stain for 5 min and then into running tap water for 5 min to stain nuclei blue. They were then submerged in the eosin stain for 30 seconds before dipping in distilled water. Samples were dehydrated once more (see above) before placing a drop of entellan on which to place the cover slip over.

2.6.4 Sirius Red collagen staining

Additional slides were stained with picrosirius red solution (1g Sirius red F3B per litre saturated aqueous solution of picric acid) for an hour. Sections were washed twice in acidified water (5 ml acetic acid per litre water) and drained before dehydrating in 3 changes of 100% ethanol. Sections were then cleared in xylene and mounted in a resinous medium for analysis.

2.6.5 Examination of stained histological sections

Picrosirius and H&E stained histological sections were examined, by a blinded researcher, with a Nikon Eclipse 90i microscope. Images were captured with the use of NIS-Elements Basic Research software [Nikon Instech Co. Ltd, Japan]. The amount of fibrosis for each heart was semi-quantitatively (visually) determined using a scale from 1 to 5, with a score of 1 having no visible signs of fibrosis, and 5 having complete tissue fibrosis with Sirius Red staining for collagen. The amount of immune cell infiltration was semi-quantitatively determined using a scale from 1 to 5, with a score of 1 having no signs of infiltration, and 5 having complete infiltration with H&E. Assessment of the tissue was performed in a blinded manner during the investigation. Visiopharm 6.9.2.3050 software was used to quantitatively verify measurements for fibrotic areas. Five images were taken at random across the section of the heart, and software was used to detect pixel quantities of red fibrotic fibres and normal muscle.

2.7 Quantitative PCR

2.7.1 Messenger RNA extraction

The apex of the heart was snap-frozen in liquid nitrogen and stored until mRNA extraction. All homogenization steps were carried out on ice using the Qiagen mRNA extraction mini kit (see figure 4.3). Beta-Mercaptoethanol was added at a ratio of 1:100 to the RLT lysis buffer provided in the kit. Approximately 30mg of each tissue sample was thawed in 300µL of this lysis buffer. Tissue

was disrupted using a 7mm probe rotor-stator in 10 second bursts for 30 – 80 seconds, depending on the size and toughness of the sample. Once uniformly homogenised, samples were incubated with 600µL of 0.33mg/mL proteinase K for 10 min at 55°C. They were centrifuged for 3 min at full speed to sediment cell debris. The supernatant was transferred to a clean Eppendorf tube and mixed 1:1 with 70% ethanol. The solution was then added 700µL at a time to an RNeasy spin column and centrifuged for 15 seconds at 8000g (10000 rpm) for the RNA to bind to the column. DNAse I enzyme solution was mixed 1:7 with the RDD buffer supplied in the kit. Eighty µL of this was added to the column and centrifuged for 15 seconds at 8000g. The column membrane was then washed by addition of 700µL of the RW1 buffer supplied in the kit and centrifugation for 15 seconds at 8000g. The spin column membrane was washed twice with 500µL of RPE buffer mixed 1:4 with 100% ethanol, first for 15 seconds then for 2 min at 8000g. The RNeasy spin column was then transferred to a 1.5mL collection tube before addition of 40µL of RNAse-free water. The column and collection tube were then centrifuged for 1 min at 8 000g to elute mRNA. mRNA was stored at -80°C.

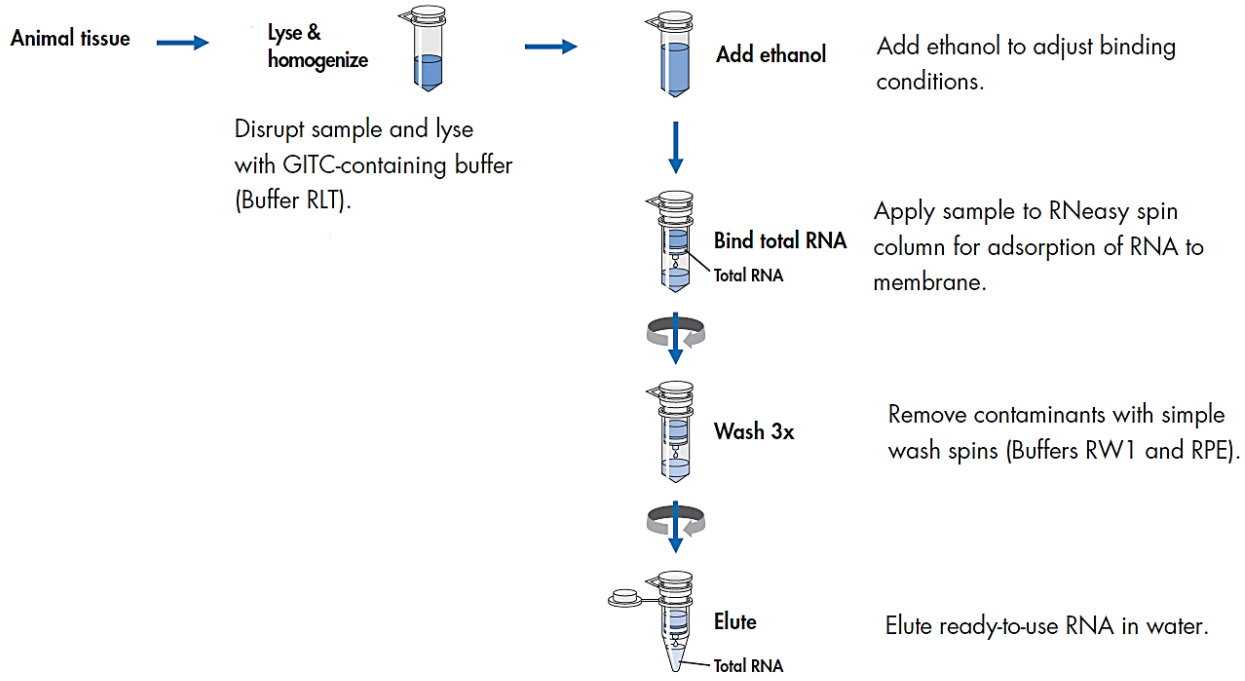

Figure 4.3: Protocol for extraction of mRNA from heart tissue as per Qiagen mRNA extraction mini kit. Adapted from RNeasy Mini Handbook [432]

2.7.2 Complementary DNA synthesis of isolated RNA

Complementary DNA (cDNA) synthesis was done using a high capacity reverse transcription kit (Applied Biosystems by Thermofisher Scientific, Life Technologies, Foster City, CA 94404, USA). The method was, briefly, as follows. Reagents for the reverse transcription kit were thawed and gently mixed on ice, per reaction, as follows: 2µL 10x reverse transcription (RT) buffer, 0.8µL 25x deoxynucleotide (dNTP) mix, 2µL 10x primers, 1µL multiscribe reverse transcriptase, and 4.2µL nuclease-free water. Ten µL of this master mix was added into a PCR tube on ice before addition of 10µL of the mRNA sample. This was pipetted up and down gently to mix. The plate with was then put through heat cycles as follows: 10 min at 25°C, 120 min at 37°C, and 5 min at 5°C. Samples were kept at 4°C before transfer to long-term storage of cDNA was at -20°C.

2.7.3 Complementary DNA quantification

Complementary DNA (cDNA) was quantified using the Qubit fluorometer 2.0. Briefly, the Qubit RNA HS agent was diluted 1 in 200 using the Qubit RNA HS buffer. 199µL of this was incubated with 1µL of cDNA in a PCR tube for 5 min. Two controls were used for standardisation; 10uL of each of the standard solutions was incubated with 190µL of the aforementioned mix for 5 min. The controls were used to calibrate the fluorometer, after which each sample was read in triplicate. Sample concentrations were adjusted to 10 ng/µL with nuclease-free water.

2.7.4 Quantitative analysis of cDNA with qPCR

Reverse transcription of cDNA was done using target primers to quantify expression of transcripts related to cardiac dysfunction (see appendix B, table 1, for primer sequences). Atrial natriuretic peptide (ANP), Angiotensin-converting enzyme (ACE), and mineralocorticoid receptor transcripts levels were examined as an indicator of blood-volume regulation. Cluster of differentiation 68 (CD68) transcript levels were examined as an indicator of inflammation. Brain natriuretic peptide (BNP), and bone morphogenic protein 4 (BMP4) transcript levels were examined as indicators of

anti-fibrotic activity. Galectin 3, and transforming growth factor β1 (TGFβ1) transcript levels were examined as indicators of pro-fibrotic activity. α-cardiac actin and α-skeletal actin transcript levels were examined as indicators of muscle contractility for reversion to the foetal gene program. Collagen 1, collagen 3, fibronectin, and tissue inhibitor of metalloproteinase 1 (TIMP1) transcript levels were examined as indicators of remodelling. α-myosin heavy chain (α-MHC) and β-myosin heavy chain (β-MHC) transcript levels were examined as indicators of reversion to the foetal gene program. Glyceraldehyde-3-phosphate dehydrogenase (GAPDH) served as a loading control.

Primers were diluted to 100μM with nuclease-free water. Each reaction was performed by combining 10ng cDNA, 0.1uL of each 100mM primer (forward and reverse, Integrated DNA Technologies, Leuven, Belgium) with 6.25uL RT SYBR green (ThermoFisher Scientific, Waltham, MA USA 02451) and nuclease-free water to make up a final volume of 12.5uL, on ice, in a capillary reaction tube. Samples were loaded and cycled at 95°C for 15 seconds followed by 60°C for 60 seconds for 50 cycles, using a Corbett RG-6000 thermocycler (NSW, 2137, Australia) with Rotor-Gene V,1.7.75 software. Reactions were done in duplicate with GAPDH as a loading control for each sample in each run.

2.8 Chemicals

Unless otherwise specified, all chemicals were obtained from Merck/ Sigma-Aldrich Inc., and all antibodies from Thermofisher Scientific Inc.

2.9 Statistical analysis

Results are expressed as means ± standard error of mean (SEM). Statistical analyses were performed using Statistica v.13 software. Significant differences ($p < 0.05$) were determined for normally distributed data using multi-factoral Anova, with Fisher correction, with $n \geq 6$.

3. Results

3.1 Echocardiographic and physical measurements

Echocardiographic measurements for STAT3 knockout mice (KO) and wildtype mice (WT) reflecting cardiac dimensions, calculated ejection fraction, fractional shortening and ventricular volumes at baseline and after 30 days of treatment, as well as HR, body weight, heart weight, lung weight/tibia length after 30 days of treatment are summarised in table 4.1, Echocardiographic measures are reported in both systole (s) and diastole (d).

The WT groups at baseline (postpartum) were consistent with each other, no differences were found in functional parameters between these groups. Fractional shortening was lower than values seen in WT mice postpartum from a previously published STAT3 KO model of PPCM, but there was also an increase in HR in our mice compared to their findings [196]. To our surprise, our WT mice seem to have thicker posterior walls compared to previous findings reported in the literature [196].

Comparison of the WT and KO groups at baseline (postpartum) showed no significant differences in any functional parameters. However, 1 month later, with no specific treatment, the KO group had significantly increased LVIDd ($p=0.01$), LVIDs ($p=0.04$), LV vol;d ($p=0.01$), and LV vol;s ($p=0.04$) compared to the WT untreated group.

Treatment with ivabradine in the WT group significantly increased LVIDd ($p=0.03$), calculated LV mass ($p=0.01$), LV vol;d ($p=0.03$), and body weight ($p=0.03$) compared to the untreated WT group, while significantly decreasing the heart weight/ body weight ratio ($p=0.03$).

Treatment with ivabradine in the KO group significantly decreased LVIDs ($p=0.01$), LV vol;d ($p=0.01$), and LV vol;s ($p=0.01$) compared to the untreated KO group.

Table 4.1: Physical and echocardiographic measures as obtained for wildtype and STAT3 KO mice after 3 pregnancies with weaning (postpartum) and after 30 days with, or without treatment.

	Wildtype				STAT3 KO			
	Untreated		Ivabradine-treated		Untreated		Ivabradine-treated	
	Postpartum (n=6)	1 month (n=8)	Postpartum (n=8)	1 month (n=9)	Postpartum (n=10)	1 month (n=9)	Postpartum (n=11)	1 month (n=11)
Body weight (g)	33±2	31±1	35±2	33±1*	35±1	35±1	33±1	34±1
Lung weight/tibia length (mg/mm)		15.90±1.20		16.10±1.61		19.39±1.03		18.21±1.19
Heart weight/tibia length (mg/mm)		13.04±0.67		9.69±1.72		11.84±1.46		11.94±0.44
Heart weight / body weight (mg/g)		6.88±0.36		6.15±0.22*		5.82±0.70		5.84±0.22
Heart rate (BPM)	462±41	485±34	487±12	422±23	487±20	503±26	475±21	433±15
LVAWd (mm)	1.00±0.03	0.93±0.06	0.89±0.05	0.89±0.03	0.87±0.05	0.83±0.07	0.92±0.06	0.86±0.06
LVAWs (mm)	1.33±0.02	1.31±0.08	1.21±0.10	1.27±0.07	1.25±0.04	1.20±0.06	1.30±0.08	1.25±0.06
LVIDd (mm)	4.91±0.19	4.58±0.20	4.68±0.10	4.87±0.07 *	4.80±0.12$	4.82±0.12*	4.59±0.10¤	4.68±0.11# # #
LVID;s (mm)	3.77±0.26	3.26±0.41	3.48±0.14	3.64±0.10	3.71±0.18	3.74±0.21*	3.38±0.11	3.46±0.14 **
LVPWd (mm)	0.92±0.06	0.76±0.06	0.84±0.04	0.81±0.08	0.76±0.06	0.85±0.06	0.85±0.04	0.80±0.04
LVPWs (mm)	1.22±0.10	0.98±0.09	1.18±0.04	1.04±0.08	1.05±0.08	1.10±0.05	1.11±0.06	1.10±0.05
Ejection Fraction (%)	47±4	54±8	51±3	49±3	46±3	45±4	52±2	52±2
Fractional Shortening (%)	24±3	30±7	26±2	25±2	23±2	23±3	27±2	26±2
Calculated LV mass (mg)	169±9	127±10	134±8	143±12*	130±9	139±12	136±6	124±6
LV vol; d (µL)	114±10	98±10	101±6	111±3*	108±7	109±6*	95±5 ¤	97±6 # **
LV vol; s (µL)	63±11	50±12	50±5	56±4	61±7	62±8*	47±4	45±4**

Abbreviations: d – diastole; LV – left ventricle; LVAW- left ventricular anterior wall thickness; LVID – left ventricular internal diameter, LVPW – left ventricular posterior wall thickness; s – systole; vol – volume *p<0.05 compared to WT 1 month untreated; # p<0.05 vs WT 1-month ivabradine-treated; ** p<0.05 compared to KO 1 month untreated; ## p<0.05 vs KO postpartum ivabradine group, ¤ p<0.05 vs KO postpartum untreated

After 1 month of ivabradine treatment, the KO group had significantly decreased LVID;d compared to the WT group(p=0.004 vs WT 1 month ivabradine).

No changes were observed between genetic or treatment groups for lung weight/tibia length (see table 4.1).

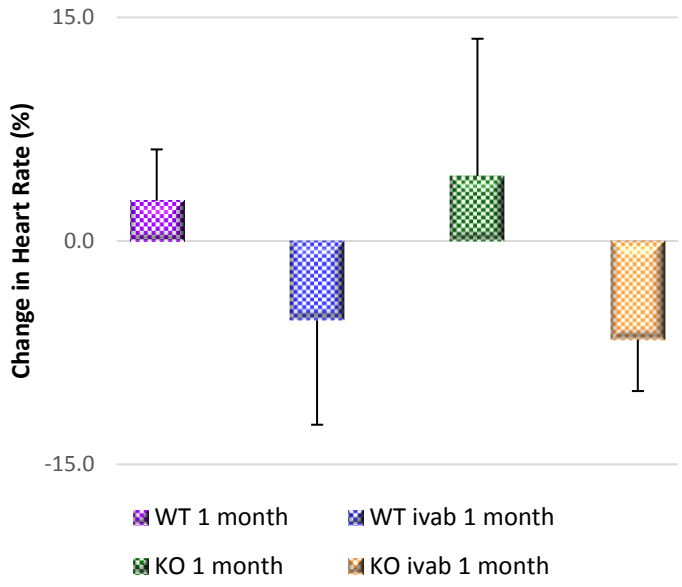

Figure 4.4: Percentage change in heart rate (HR) after 1 month (30 days) of ivabradine treatment. Percentage change was taken for each mouse individually, and data was pooled. Both wildtype (WT) and STAT3 knockout (KO) mice showed a trend toward decrease in HR with ivabradine treatment (10mg/kg orally in drinking water), albeit non-significant. WT untreated n=6, WT treated n=8, STAT3 KO untreated n=9, STAT3 KO n= 11.

Average HR did not show a marked decrease in groups treated with ivabradine. However, a trend toward a decrease in HR can be better observed in both KO and WT mice when looking at the average percentage change in HR for each mouse after 30 days, when compared to baseline (see figure 4.4).

3.2 Quantitative PCR

Cycle threshold (CT) scores obtained for qPCR analysis are represented in figures 4.5 – 4.11 which follow.

3.2.1 Markers of blood volume regulation

Results for the qPCR analysis of 3 markers of blood-volume regulation, ACE and mineralocorticoid receptor, did not differ significantly between WT and KO untreated groups (see figure 4.5)

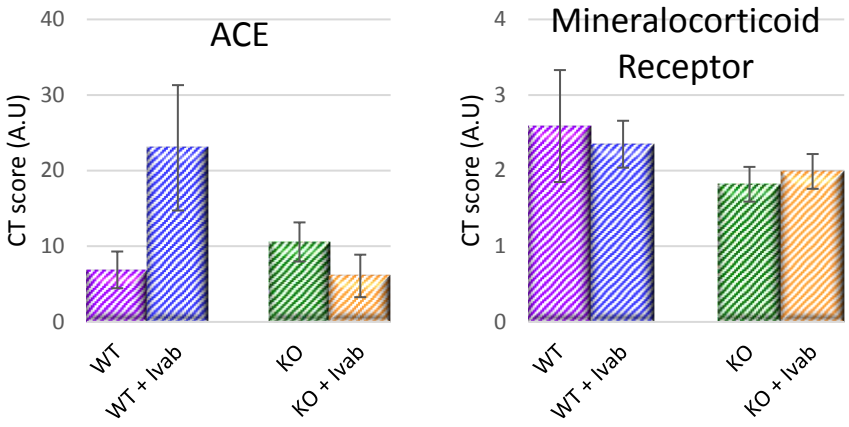

Figure 4.5: CT scores obtained for markers of blood volume regulation in heart tissue after 1 month of Ivabradine treatment. Values represented are mean ± SEM. Abbreviations: ACE – angiotensin-converting enzyme; A.U. – arbitrary units; CT – cycle threshold; Ivab – ivabradine; KO – cardiac-specific signal transducer and activator of transcription 3 knockout mice; SEM – standard error of the mean; WT – wildtype mice. WT n=6, WT + ivab n=8, KO n=7, KO + ivab n=6.

3.2.2 Marker of inflammation

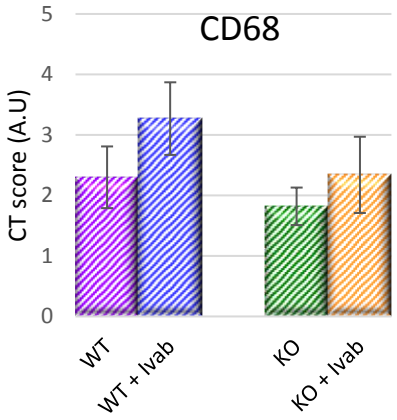

Figure 4.6: CT scores obtained for CD68, a marker of inflammation, in heart tissue after 1 month of Ivabradine treatment. Values represented are mean ± SEM. Abbreviations: A.U. – arbitrary units; CD68 - Cluster of differentiation 68; CT – cycle threshold; Ivab – ivabradine; KO – cardiac-specific signal transducer and activator of transcription 3 knockout mice; SEM – standard error of the mean; WT – wildtype mice. WT n=6, WT + ivab n=8, KO n=7, KO + ivab n=6.

Results for the qPCR analysis of CD68 as a marker of inflammation did not differ significantly between WT and KO untreated groups (see figure 4.6). Treatment with ivabradine did not alter levels of mRNA transcripts.

3.2.3 Markers of anti-fibrotic activity

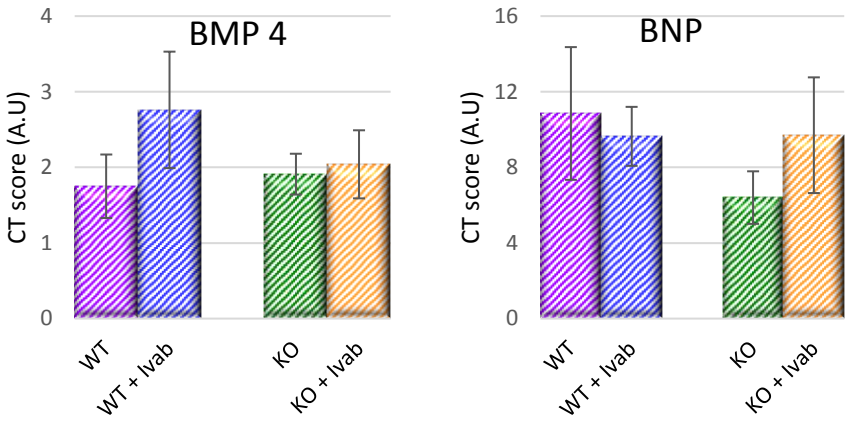

Figure 4.7: CT scores obtained for anti-fibrotic markers in heart tissue after 1 month of Ivabradine treatment. Values represented are mean ± SEM. Abbreviations: A.U. – arbitrary units; BMP4 – bone morphogenic protein 4; BNP –brain natriuretic peptide; CT – cycle threshold; Ivab – ivabradine; KO – cardiac-specific signal transducer and activator of transcription 3 knockout mice; SEM – standard error of the mean; WT – wildtype WT n=6, WT + ivab n=8, KO n=7, KO + ivab n=6.

Results for the qPCR analysis of markers of anti-fibrotic activity, BNP and BMP4, did not differ significantly between WT and KO untreated groups (see figure 4.7). Treatment with ivabradine made no change to levels of mRNA transcripts.

3.2.4 Markers of pro-fibrotic activity

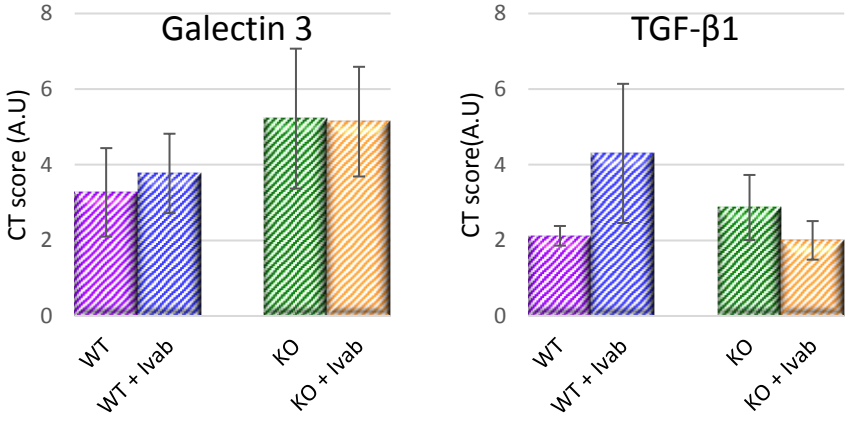

Figure 4.8: CT scores obtained for pro-fibrotic markers in heart tissue after 1 month of Ivabradine treatment. Values represented are mean ± SEM. Abbreviations: A.U. – arbitrary units; CT – cycle threshold; Ivab – ivabradine; KO – cardiac-specific signal transducer and activator of transcription 3 knockout mice; SEM – standard error of the mean; TGF-β1 – transcription growth factor -β1; WT – wildtype mice. WT n=6, WT + ivab n=8, KO n=7, KO + ivab n=6.

Results for the qPCR analysis of markers of pro-fibrotic activity, galectin 3 and TGFβ1, did not differ significantly between WT and KO untreated groups (see figure 4.8). Treatment with ivabradine did not alter levels of mRNA transcripts.

3.2.5 Markers of change in muscle contractility

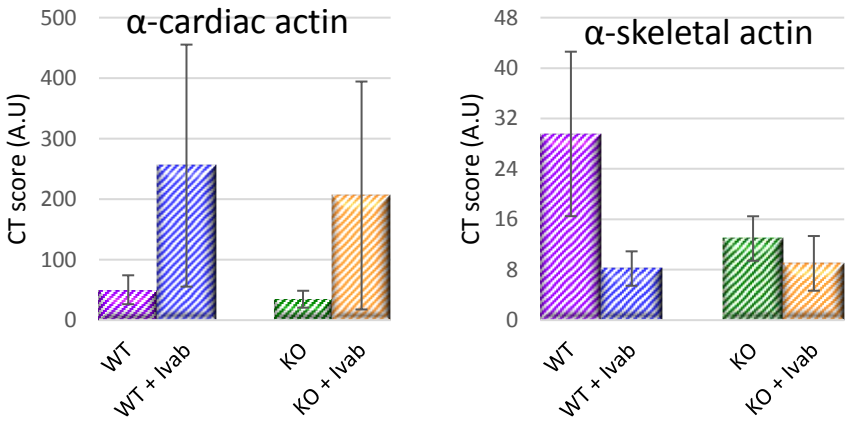

Figure 4.9: CT scores obtained for markers of muscle contractility in heart tissue after 1 month of Ivabradine treatment. Values represented are mean ± SEM. Abbreviations: A.U. – arbitrary units; CT – cycle threshold; Ivab – ivabradine; KO – cardiac-specific signal transducer and activator of transcription 3 knockout mice; SEM – standard error of the mean; WT – wildtype mice. WT n=6, WT + ivab n=8, KO n=7, KO + ivab n=6.

Results for the qPCR analysis of markers of muscle contractility, α-cardiac actin and α-skeletal actin, did not differ significantly between WT and KO untreated groups (see figure 4.9). Treatment with ivabradine did not alter levels of mRNA transcripts.

3.2.6 Markers of remodelling

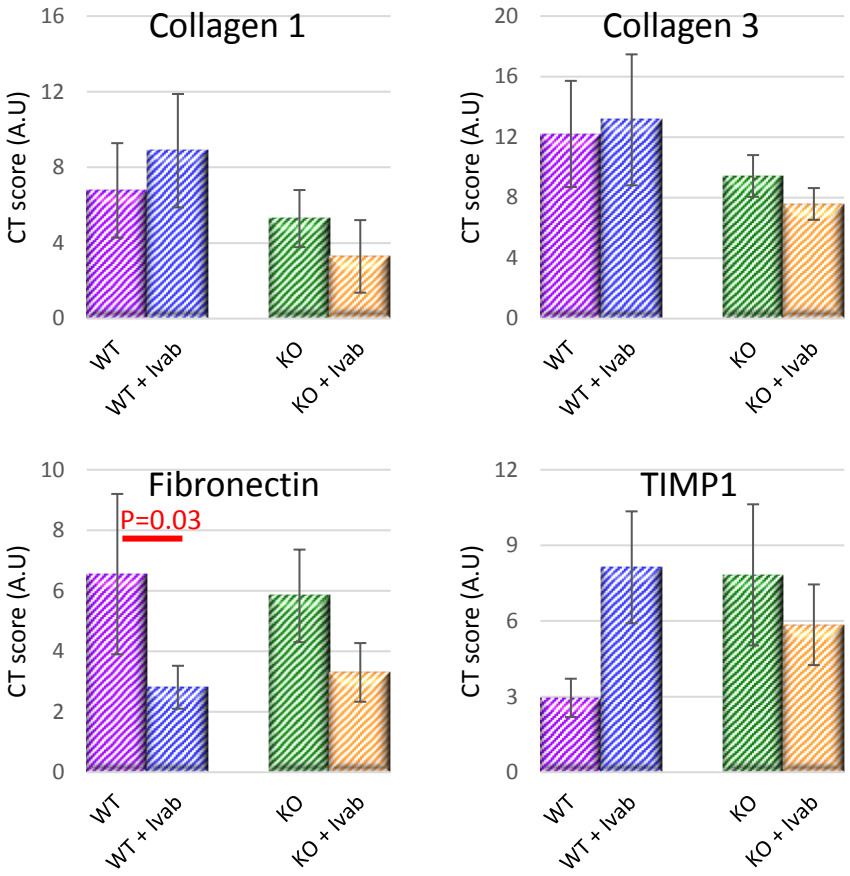

Figure 4.10: CT scores obtained for markers of remodelling in heart tissue after 1 month of Ivabradine treatment. Values represented are mean ± SEM. Abbreviations: A.U. – arbitrary units; Ivab – ivabradine; CT – cycle threshold; KO – cardiac-specific signal transducer and activator of transcription 3 knockout mice; SEM – standard error of the mean; TIMP1 – tissue inhibitor of metalloproteinases 1; WT – wildtype mice. WT n=6, WT + ivab n=8, KO n=7, KO + ivab n=6.

Results for the qPCR analysis of 4 markers of cardiac remodelling, collagen 1, collagen 3, fibronectin and TIMP1, did not differ significantly between WT and KO untreated groups (see figure 4.10). Ivabradine significantly decreased RNA transcript levels of fibronectin in WT mice (p=0.03), but this effect was absent in KO mice.

3.2.7 Markers of reversion to the foetal gene program

Results for the qPCR analysis of markers of reversion to the foetal gene program, α-MHC, β-MHC and ANP, did not differ significantly between WT and KO untreated groups (see figure 4.11). Ivabradine significantly increased RNA transcript levels of ANP in WT mice (p=0.02), but this effect was absent in KO mice.

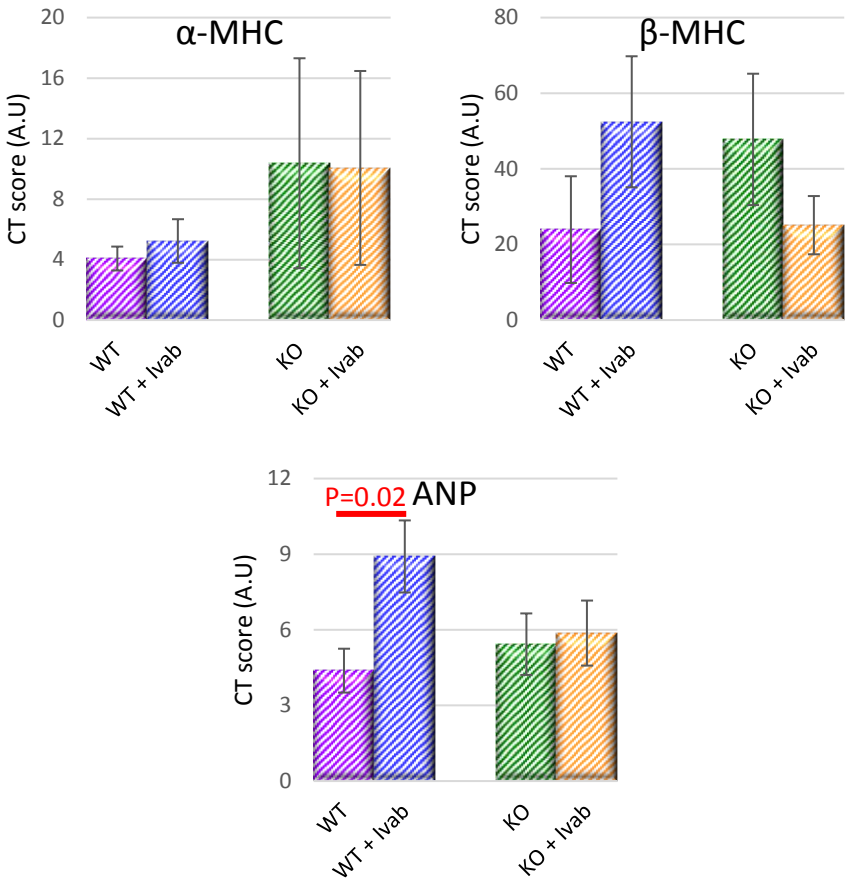

Figure 4.11: CT scores obtained for markers of reversion to the foetal gene program in heart tissue after 1 month of Ivabradine treatment. Values represented are mean ± SEM. Abbreviations: A.U. – arbitrary units; ANP – atrial natriuretic peptide; CT – cycle threshold; Ivab – ivabradine; KO – cardiac-specific signal transducer and activator of transcription 3 knockout mice; MHC – myosin heavy chain; SEM – standard error of the mean; WT – wildtype mice. WT n=6, WT + ivab n=8, KO n=7, KO + ivab n=6.

In summary, quantification of mRNA showed minimal differences in the chosen transcripts linked to cardiac remodelling between KO and WT groups, indicating a similar cellular state in both groups.

Treatment with ivabradine resulted in 2 significant changes in the WT group – increases in mRNA levels of ANP and fibronectin (see figures 4.10 & 4.11). ANP is an anti-hypertrophic factor which is involved in reducing cardiac load, and also suggesting reversion to the foetal gene program (see chapter 1, section 1.5). It was elevated in the WT group with treatment compared to the WT untreated group, without significant changes in ACE, mineralocorticoid receptor, TGF-β1, α-MHC, and β-MHC – the other transcripts examined which would indicate increased load stress or reversal to the foetal gene program.

3.3 Histological examination

3.3.1 Sirius red staining

Semi-quantitative analysis of Sirius red staining for collagen (a precursor of fibrosis) was consistent with quantitative analysis performed. Both semi-quantitative and quantitative analyses revealed no change in fibrosis (represented by collagen) between untreated WT and KO groups. Treatment with ivabradine tended to decrease fibrosis in WT mice, and significantly decreased fibrosis in KO mice ($p=0.017$). Illustrative images of each group with Sirius red staining are indicated in figure 4.12, For tabulated results of quantitation, see appendix B, table 2,

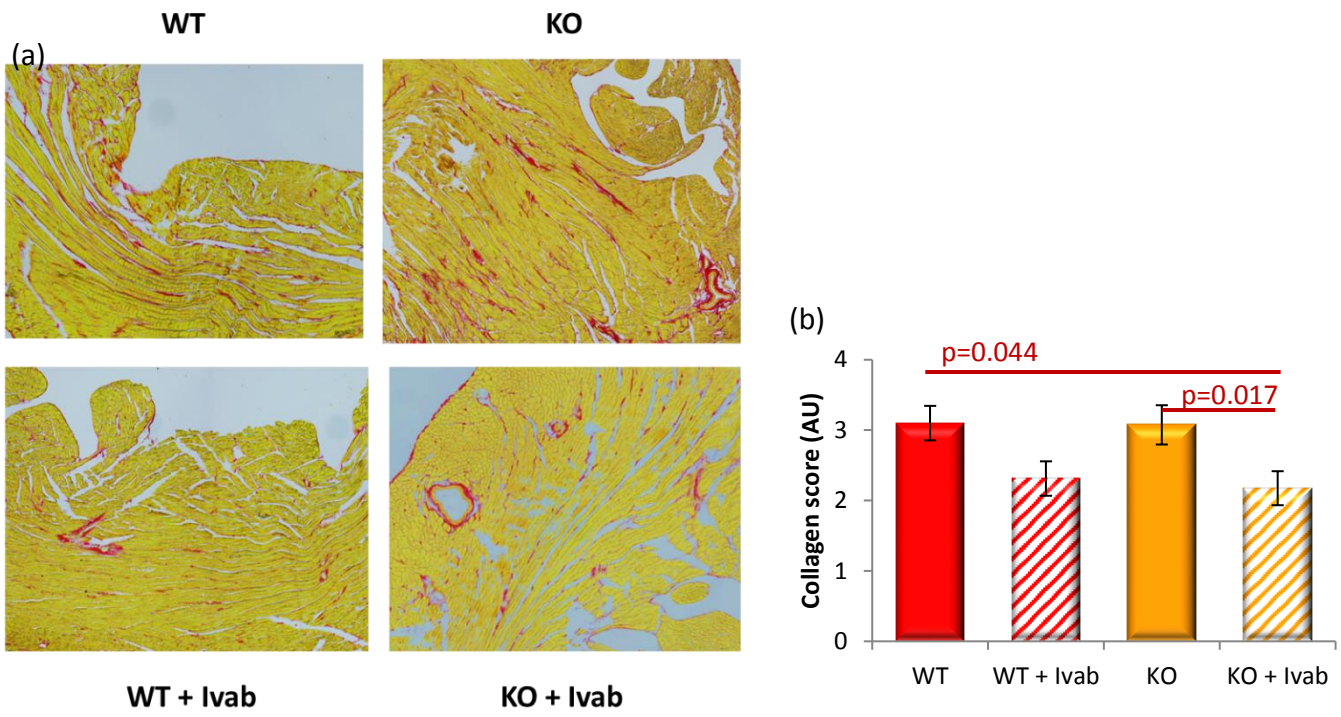

Figure 4.12: Histological staining with Sirius red for collagen. (a) Greater collagen deposition (red striations) in untreated hearts (top row) compared to hearts from mice treated with ivabradine (bottom row) was observed at 10 x magnification. (b) Ivabradine treatment decreased the amount of collagen (and thus fibrosis, as determined by semi-quantitative analysis) in both WT and KO mice. WT n=14, WT + ivab n=8, KO n=11, KO + ivab n=11.

Interestingly, WT mice showed more perivascular fibrosis, while KO mice showed more interstitial fibrosis. These results, together with the *q*PCR results for fibronectin (see chapter 4, section 3.2), suggest a propensity toward a decrease in fibrosis with ivabradine treatment.

3.3.2 Haematoxylin and Eosin staining

Semi-quantitative analysis of H&E staining for the presence of immune cells yielded no significant differences in immune cell infiltration between WT and KO groups. Treatment with ivabradine did not affect the level of infiltration (see figure 4.13, see appendix B, table 2, for tabulated results).

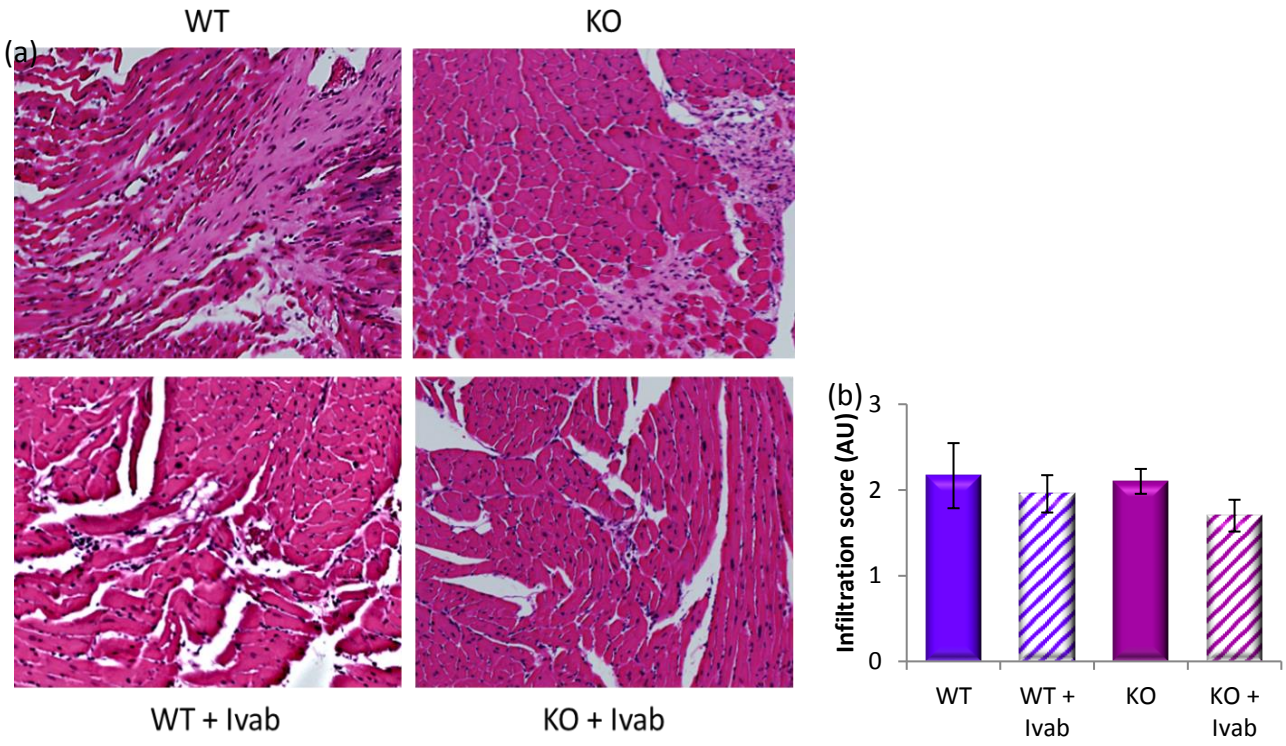

Figure 4.13: Histological staining with H&E to visualise immune cell infiltration in cardiac tissue. (a)Ivabradine very slightly reduced infiltration (lighter pink patches) in both wildtype and PPCM mice as observed at 10 x magnification, (b) but this was not significant. WT n=14, WT + ivab n=8, KO n=11, KO + ivab n=11.

4. Discussion

In this study, the aim was to evaluate the cardiac function and remodelling in a STAT3 KO mouse model of PPCM chronically treated with ivabradine. Although our data reported here show no cardiac alterations between WT littermate control and PPCM mice after 3 pregnancies – which is likely due to WT littermate control mice presenting with cardiac dysfunction – a chronic treatment with ivabradine reduced fibrosis in both healthy and PPCM mice.

Our main findings were as follows:

- Both WT littermate control and PPCM mice presented with low EF and FS when examined after 3 pregnancies with weaning

- No significant differences were seen for EF and FS for either WT littermate control or PPCM mice with ivabradine treatment, compared to untreated groups

- No significant differences were observed for HR between WT littermate control and PPCM mice

- Ivabradine did not significantly reduce HR, although there was a tendency toward a reduction in HR when observing each mouse individually

- Changes in qPCR CT scores were seen for ANP (increase in WT group with ivabradine treatment) and fibronectin (decrease in WT group with ivabradine treatment, trend seen in KO group too)

- Fibrosis was decreased in both groups with use of ivabradine (trend in WT, significant in KO)

When comparing our STAT3 KO mice to their corresponding wildtype littermate controls after 3 pregnancies, at the end of weaning (i.e. postpartum), we were surprised to find that physical and echocardiographic measurements were comparable between the 2 groups (see table 4.1). Both groups had low ejection fraction (<50%) and fractional shortening (<30%) at this time point compared to the literature with measurements on mice of the same background (C57BL6) [196,433].

Our observations here in terms of the differences in ejection fraction and fibrosis in KO and WT groups were not as marked as that seen by Hilfiker-Kleiner et al [196]. Previous experiments with mice in our laboratory have indicated that differences between C57BL6 floxed and non-floxed STAT3 mice can be observed (i.e non-littermates vs littermates) [434]. The model used by Hilfiker-Kleiner et al states that they use mice from the same background as that on which the STAT3 KO model was developed, but does not clearly define whether the corresponding littermates were used

as WT controls [196,435]. This may underlie our inconsistent findings when compared to their model and account for the lack of significance between the WT and KO groups in our setting.

The cardiac state in both control and STAT3 KO mice may also have been affected by the timing of pregnancies – 3 consecutive pregnancies initiated directly after weaning may have meant that there was insufficient time to recover between each pregnancy, and before treatment and analysis had begun. In order to determine whether the stress of consecutive pregnancies masks the contrast that has been described in the literature between WT mice and STAT3 KO mice [196], it would be necessary to compare these mice to nulliparous mice from the same strain (see additional experiments performed in section 7 of this chapter).

Echocardiographic outcomes in experimental mice did not indicate any notable differences in cardiac function between WT and KO mice regardless of ivabradine treatment. Measurements were taken in a blinded fashion and separated by genotype after the treatment period (as described in the methods section) in time for data analysis. Evaluation of cardiac function at baseline showed no differences between the WT and KO groups.

The natural progression in both groups after 1 month without treatment showed some degree of change when compared to their postpartum echocardiographic measures, though these were not statistically significant. There was, however, a trend toward better ejection fraction and fractional shortening in the WT group compared to their postpartum selves, while the STAT3 KO group remained low. It was also at this time point that physical measures associated with HF, such as increased body weight and lung weight to tibia length ratios, were more evident in the STAT3 KO group, though still not statistically significant.

Another unexpected result in our study was that treatment with ivabradine did not show a significant reduction of HR pre- and post-treatment when data were pooled (see table 4.1). Again,

this may have been due to the use of the anaesthetic used when HR measurements were taken - isoflurane, is well known for modulation of HR in animals [436]. We had used the same dosage of ivabradine as that reported by Custodis et al, for our long-term treatment, but the method of recording heart rate was different – they used a tail cuff system on conscious mice to measure HR, while we recorded HR in mice under anaesthesia [437]. The use of anaesthetic may therefore have masked the reduction of HR observed in the literature with a chronic treatment of ivabradine [437].

After 1 month of ivabradine, the WT group had comparable fibrosis (see figure 4.12) and immune cell infiltration to the STAT3 KO group (see figure 4.13), suggesting that after 3 successive pregnancies, both groups were in a similar state of function. After 1 month without treatment, the WT group showed some improvement in cardiac function, while the STAT3 KO group did not improve.

Fibronectin is an extracellular matrix protein which binds collagen (see chapter 1, section 1.5.7), an increase of which indicates the early stages of fibrosis. Reduction of fibrosis (significant in KO, and trend in WT) with ivabradine treatment in this model echoes the findings of Custodis et al, who found that a long-term (6 weeks) treatment with ivabradine prevented deposition of cardiac collagen and thus fibrotic remodelling [437]. This was also supported by the reduction we saw with ivabradine treatment in the collagen-anchoring element, fibronectin, which would help to reduce fibrosis. Custodis et al attributed their findings with ivabradine to downregulation of RAAS transcripts, an effect which was not supported by our findings, as we did not find any changes in mRNA levels of ACE and mineralocorticoid receptors [437]. They also reported that ivabradine modulated the migration of immune cells which play a key role in inflammation – we observed differences in the deposition of collagen, but we did not observe differences in inflammatory cell infiltration [437]. The differences seen in their model that could not be seen in ours may have been

explained by the duration of treatment (6 weeks vs 4 weeks in our model). Alternatively, it may be due to the stress involved in pregnancy in our model that was absent in their model.

It is also important to bear in mind that results for qPCR show a snapshot in time and may not necessarily correspond with larger scale events in the cell, such as protein concentrations or structural changes. This is evident in the qPCR results for collagens 1 and 3 when compared to the results for presence of collagen in the myocardium with Sirius red staining (see figure 4.10).

5. Limitations

As mentioned in the discussion, one limitation was the choice of anaesthetic in anaesthesia for echocardiography. Isoflurane, which was our anaesthetic of choice has been reported to have different effects on cardiac measures in comparison to other anaesthetic agents. In particular, measurements taken for FS, HR, and aortic ejection time have been reported to be lower with the use of isoflurane than with other agents such as tribromethanol, ketamine-midazolam and ketamine-xylazine – these differences intensify with time [438]. This may explain, at least in part, why our reported TTE values were lower than those seen by Hilfiker-Kleiner et al who used Ketamine-Xylazine as their anaesthetic[196]. Different genetic backgrounds of mice (e.g. C57BL6/6N vs C57BL6/JN mice) also have different reactions to anaesthetic, a factor which may contribute to differences seen by other groups [438].

6. Conclusion

In this study, we found that the STAT3 KO model did not produce a similar PPCM model to that previously reported in the literature [196], as both WT and STAT3 KO mice had unusually poor cardiac function. This may be as a result of the physiological stress caused by 3 successive pregnancies in our model, which may nullify the contribution of genotype as a factor in this study. Regardless, long-term treatment of both groups of mice with ivabradine elicited an effect on remodelling, as it reduced the formation of fibrotic scars in the heart.

In order to determine whether the poor cardiac function observed in both STAT3 KO and WT groups, are due to the physiological stress of 3 successive pregnancies on the heart, or due to a loss of genetic function, it would be necessary to compare the findings here with those of non-pregnant WT and STAT3 KO mice.

Chapter 5

Sub-study with comparison of naïve STAT3 knockout mice

1. Study rationale

In the above study, the STAT3 KO 'PPCM' mice did not show a difference in cardiac function or fibrosis when compared to wildtype littermates. Instead, both groups appeared to be in the same state with reduced cardiac function (poor fractional shortening and ejection fraction), as well as similar inflammation, immune infiltration, and fibrosis.

The previously described STAT3 KO model of PPCM was characterised by severe diastolic dysfunction, reduced fractional shortening, and the development of severe fibrosis compared to their wildtype controls after 3 pregnancies with weaning [196]. Their nulliparous STAT3 KO and WT mice showed similar function to WT mice after 3 pregnancies, but better function in comparison to the PPCM group. In order to determine whether the unusual findings in the main component of this study were due to genotype, or due to successive pregnancies, it would be necessary to compare the mice postpartum to their genotype-matched nulliparous (naïve) counterparts.

The aim of this sub-study therefore to determine whether the unusual findings in in the main study were influenced by genotype or pregnancy.

2. Methods

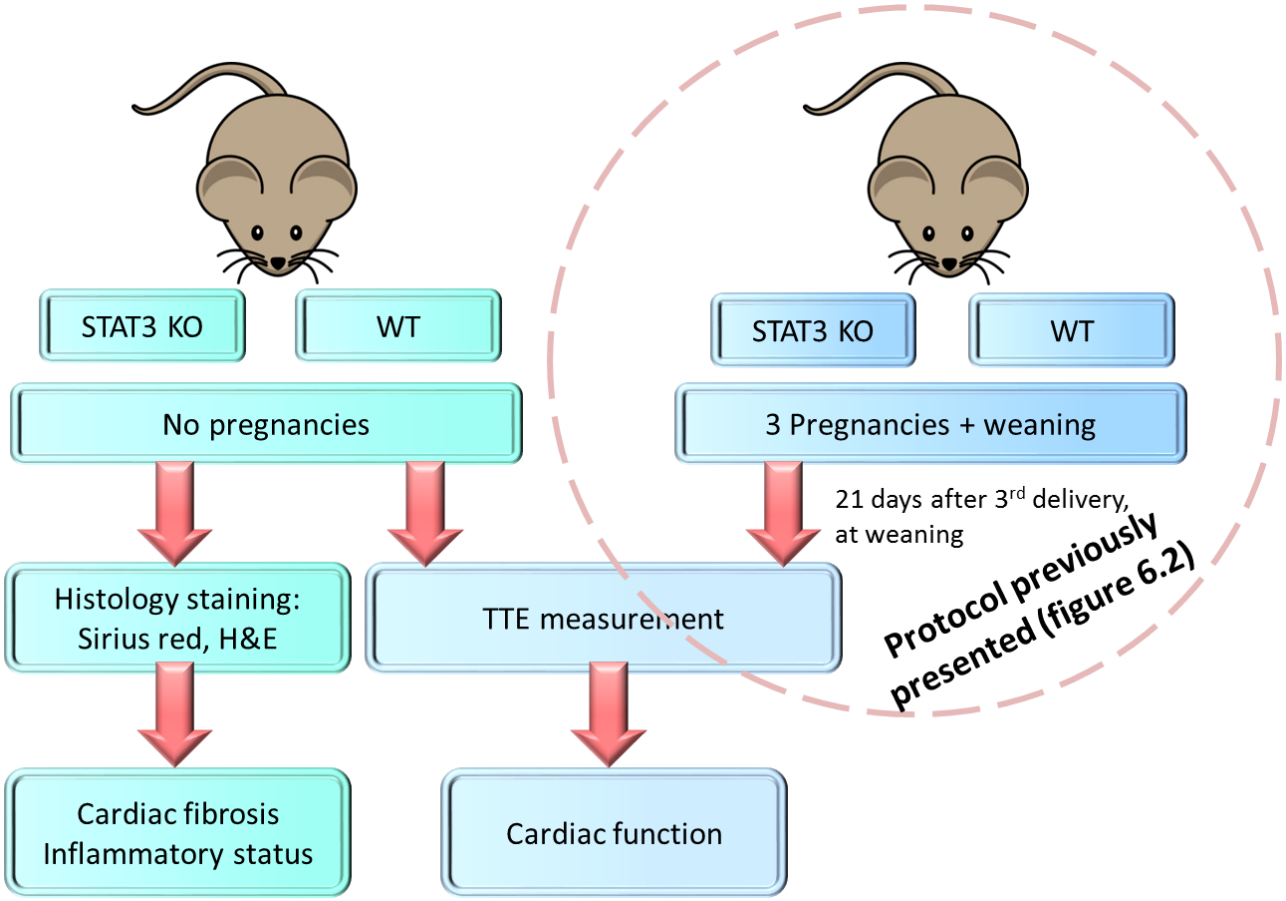

Figure 5.1: Experimental protocol to study the influence of genotype and pregnancy on cardiac outcomes in a PPCM model. TTE measurements were taken after 3 consecutive pregnancies, with weaning for both WT and STAT3 KO groups for comparative analysis. These were compared to TTEs taken in age-matched nulliparous (naïve) female mice from the same genetic background to evaluate changes with pregnancy. Hearts were excised, and Sirius red and H&E staining were done for nulliparous females to evaluate contributions of genotype without pregnancy. Abbreviations: H&E – Haematoxylin and Eosin; STAT3 KO – signal transducer and activator of transcription 3 knockout; PPCM –peripartum cardiomyopathy; TTE – transthoracic echocardiography; WT – wildtype.

Twelve-week old nulliparous (naïve) female mice with the same genetic background as described in chapter 4, section 2.3 were used for these experiments. Transthoracic echocardiography (TTE) as described in chapter 4, sections 2.5 was performed on these mice, as well as histology with Sirius red staining and haematoxylin and eosin staining as described in chapter 4, section 2.6 (see figure 4.1). Statistical analysis of results was performed as described in chapter 4, section 2.9, and included data obtained from the experimental protocol involving pregnancy for comparison.

3. Results

3.1 Echocardiographic measurements

Echocardiographic measurements for nulliparous knockout mice (KO), and naïve wildtype mice (WT) and experimental mice (who have had 3 successive pregnancies) reflecting cardiac dimensions, calculated ejection fraction, fractional shortening and ventricular volumes at 12 weeks of age, as well as HR, body weight, heart weight, lung weight/tibia length after are graphically represented in figures 5.2 – 5.4 (see appendix B, table 3 for detailed tabulated data).

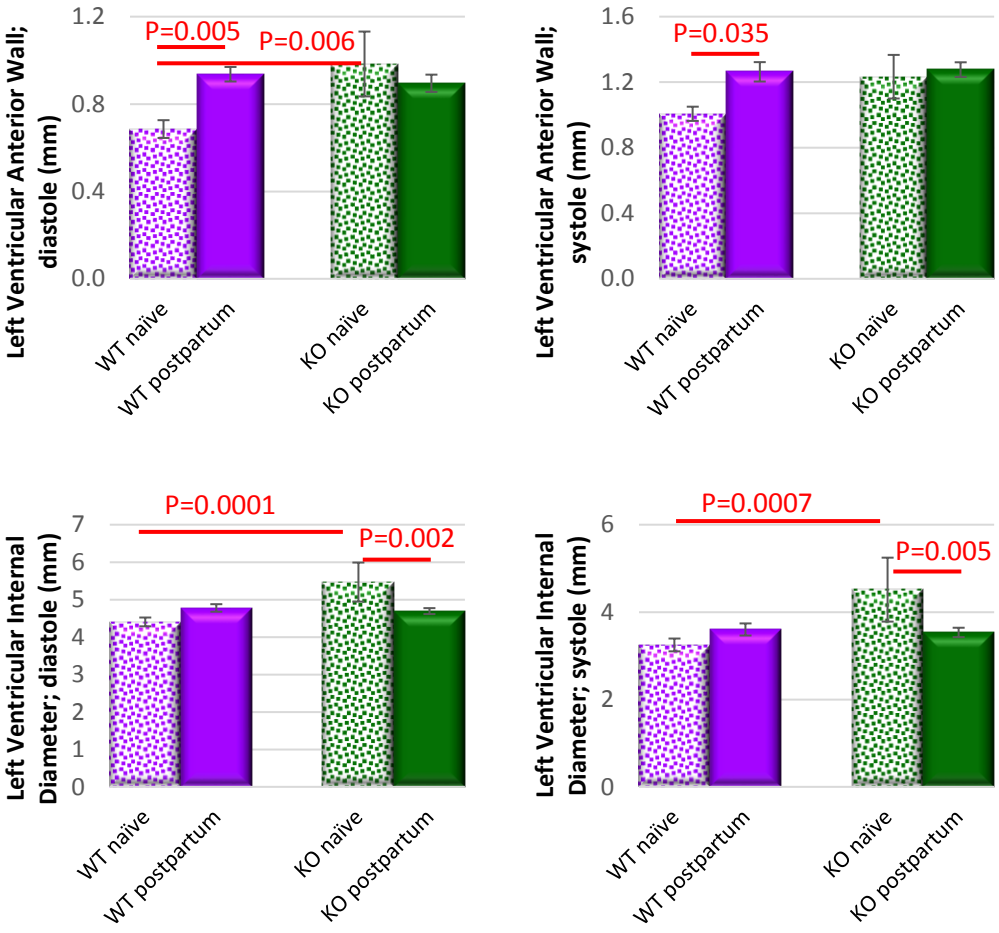

Figure 5.2: Left ventricular dimensions in nulliparous mice and after 3 pregnancies. Values (mean ± SEM) as obtained for nulliparous (naïve) as well as wildtype and STAT3 KO mice after 3 pregnancies with weaning (postpartum) from the main study. The postpartum groups reflect combined data for WT groups prior to treatment, as well as combined data for KO groups prior to treatment. Abbreviations: KO – signal transducer and activator of transcription genetic knockout mice; WT – wildtype mice; SEM – standard error of the mean. WT postpartum n=6, WT naïve n =10, KO postpartum=10, KO naïve n=3.

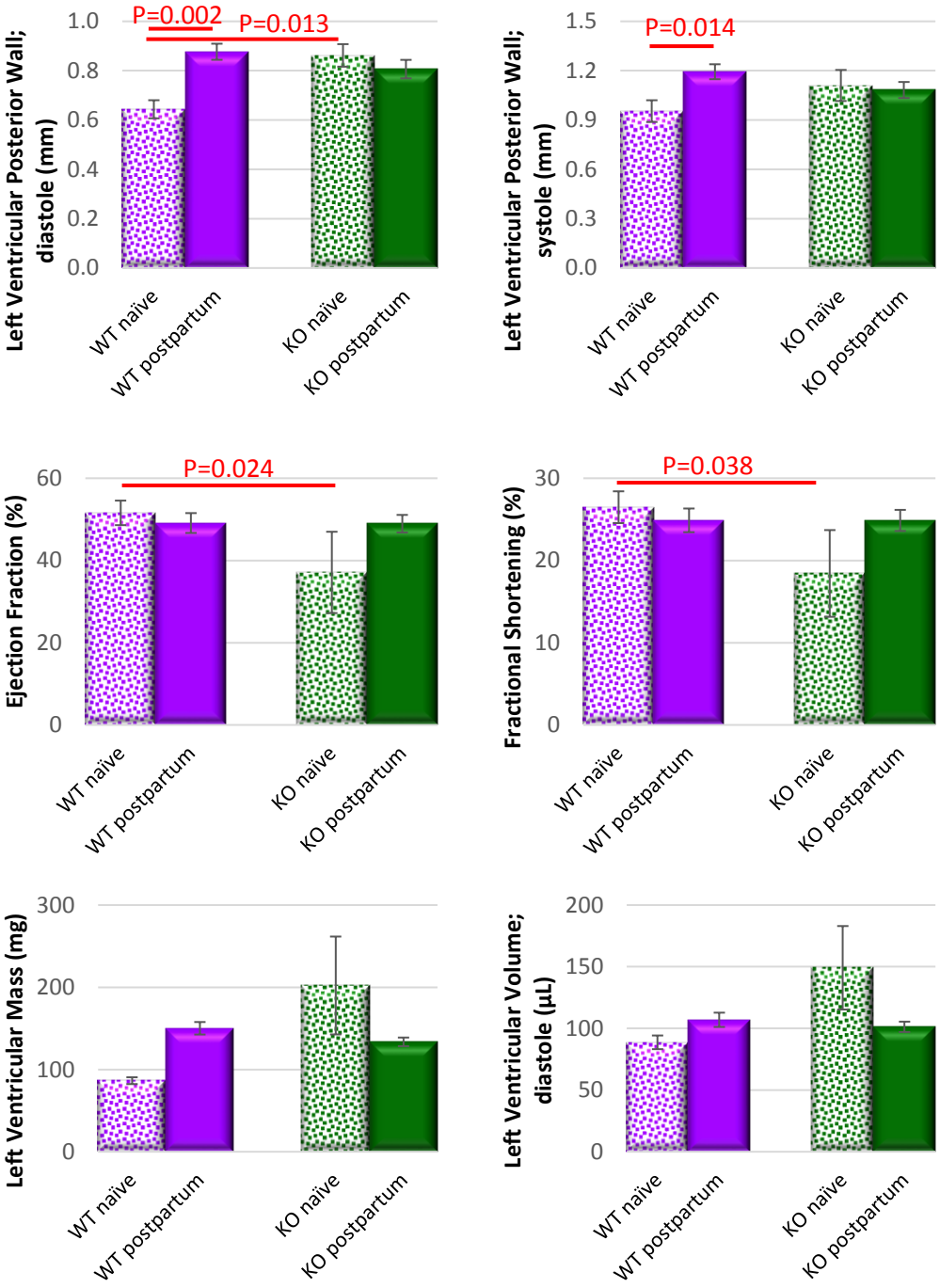

Figure 5.3: Left ventricular dimensions and functional measures in nulliparous mice and after 3 pregnancies. Values (mean ± SEM) as obtained for nulliparous (naïve) as well as wildtype and STAT3 KO mice after 3 pregnancies with weaning (postpartum) from the main study. The postpartum groups reflect combined data for WT groups prior to treatment, as well as combined data for KO groups prior to treatment. Abbreviations: KO – signal transducer and activator of transcription genetic knockout mice; WT – wildtype mice; SEM – standard error of the mean. WT postpartum n=6, WT naïve n =10, KO postpartum=10, KO naïve n=3.

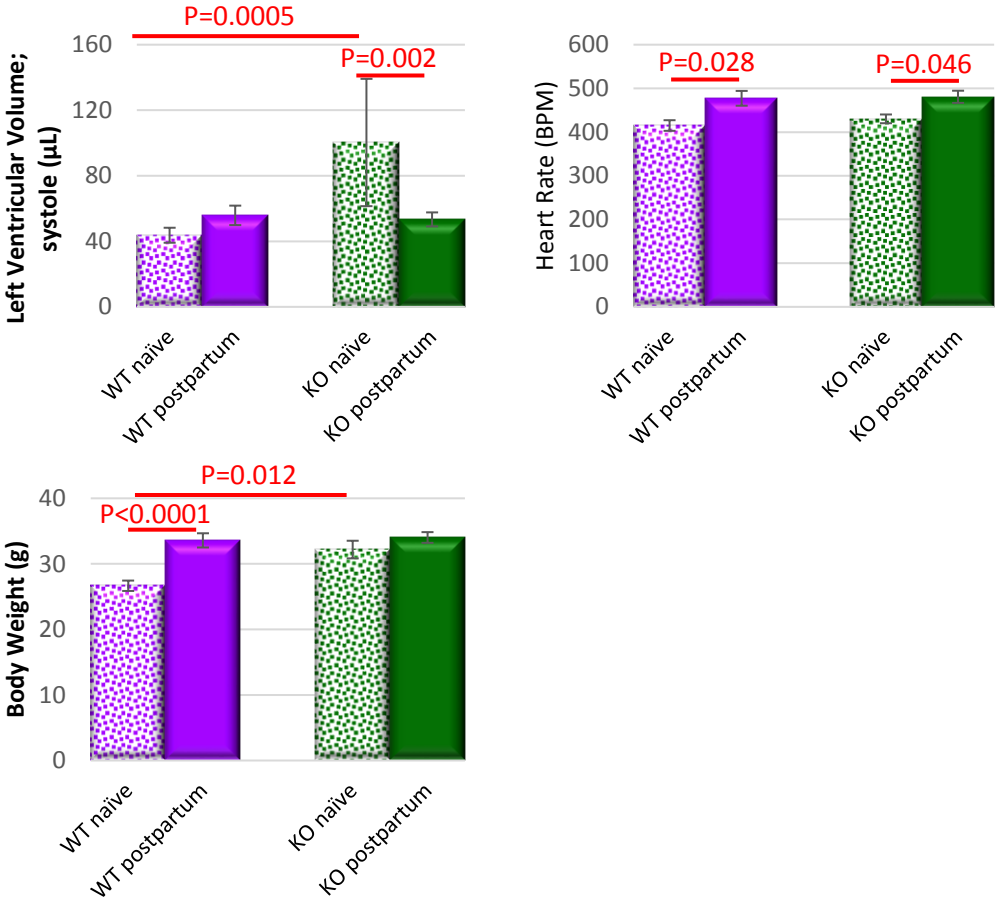

Figure 5.4: Left ventricular volume, and physical measures in nulliparous mice and after 3 pregnancies. Values (mean ± SEM) as obtained for nulliparous (naïve) as well as wildtype and STAT3 KO mice after 3 pregnancies with weaning (postpartum) from the main study. The postpartum groups reflect combined data for WT groups prior to treatment, as well as combined data for KO groups prior to treatment. Abbreviations: KO – signal transducer and activator of transcription genetic knockout mice; WT – wildtype mice; SEM – standard error of the mean. WT postpartum n=6, WT naïve n =10, KO postpartum=10, KO naïve n=3.

The WT naïve group had smaller LVAWd, LVIDd, LVIDs, LVPWd, lower weight, LV mass and volume (in both systole and diastole) higher EF and FS compared to the KO naïve group (see figure 5.2 – 5.4). These indicate that the nulliparous WT mice were in a state of better cardiac health, had less hypertrophy, and better function compared to the naïve KO mice.

The WT naïve group had lower values for LVAWd, LVAWs, LVPWd, LVPWs, LV mass, HR and body weight compared to the WT postpartum group (see figure 5.2 – 5.4). These data indicate that pregnancy in these WT mice induced the expected physiological changes (weight and HR – see chapter 1, section 2), as well as hypertrophy.

The KO naïve group had greater LVIDd, LVIDs, LV mass and volume, with a lower HR compared to the KO postpartum group (see figure 5.2 – 5.4). These data suggest that 3 consecutive pregnancies altered cardiac function in KO mice.

3.2 Histological examination

3.2.1 Sirius red staining

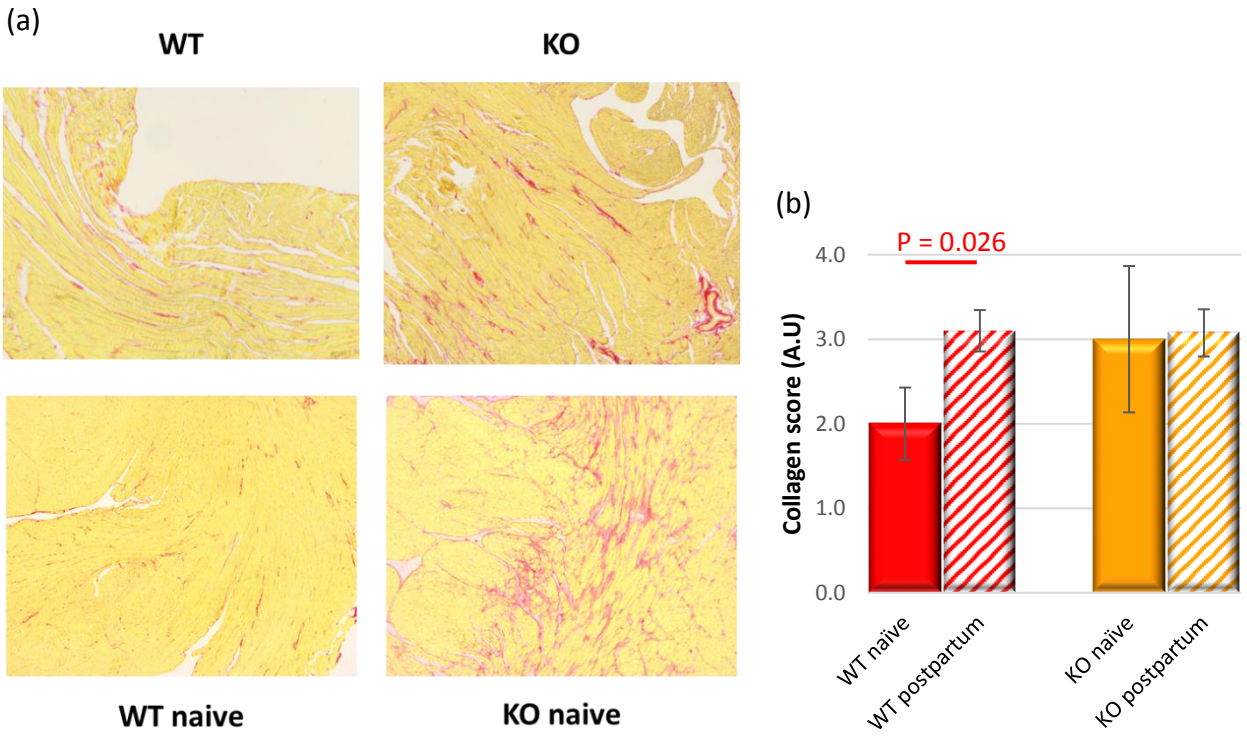

Figure 5.5: Histological staining with Sirius red for collagen. (a) Greater collagen deposition (red striations) was observed in naïve WT mice compared to their pregnant counterparts at 10 x magnification (p=0.026). Similar trends were seen for the naïve WT group compared to the naïve KO mice, but (b) this was not significant when analysed with semi-quantitatively. WT postpartum n=6, WT naive n=6, KO postpartum n=10, KO naïve n=3.

Semi-quantitative analysis of Sirius red staining for the detection of collagen (indicating fibrosis) showed a significant increase in collagen in WT mice after going through 3 pregnancies, compared to the naïve mice, therefore suggesting an increase in fibrosis associated with successive pregnancies and weaning (p=0.026, see figure 5.5, see appendix B, table 4, for tabulated results).

There was also a trend toward an increase in collagen deposition in KO naïve mice compared to WT naïve mice, but this was not significant.

3.2.2 Haematoxylin & Eosin staining

H&E staining for the presence of immune cells yielded results depicted in figure 5.6. Semi-quantitative analysis showed no significant differences between groups ($p>0.05$, see figure 5.6).

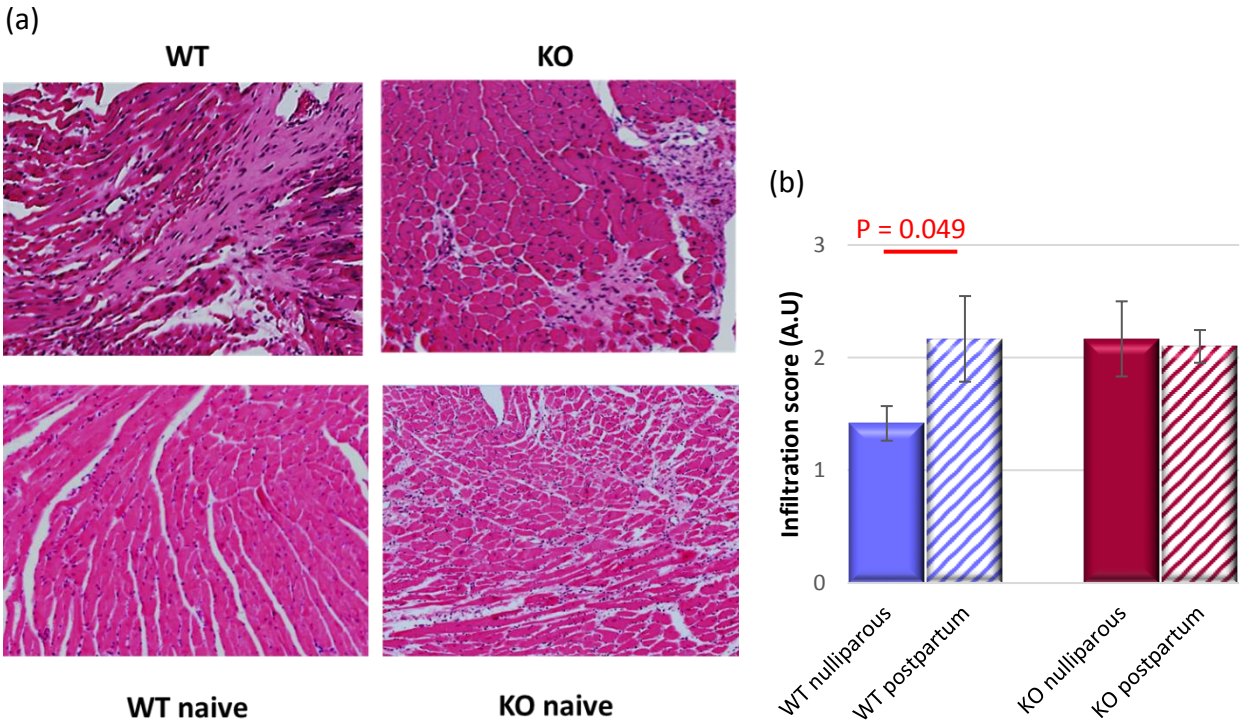

Figure 5.6: Histological staining with H&E for immune cell infiltration. (a) Greater immune cell infiltration (lighter pink patches) was observed in naïve WT mice compared to their pregnant counterparts at 10 x magnification ($p=0.049$). (b) Similar trends were seen for the naïve WT group compared to the naïve KO mice, but this was not significant. Abbreviations: H&E - Haematoxylin & Eosin; KO – signal transducer and activator of transcription 3 genetic knockout mice, WT – wildtype mice. WT postpartum n=6, WT naive n=6, KO postpartum n=10, KO naïve n=3.

Semi-quantitative analysis of H&E staining for the presence of immune cell infiltration showed a significant increase in immune cell infiltration in WT mice after going through 3 pregnancies, compared to naïve mice, therefore suggesting an increased inflammatory state associated with successive pregnancies and weaning ($p=0.049$, see figure 5.6, see appendix B, table 4, for tabulated

results). There was also a trend toward an increase in KO naïve mice compared to WT naïve mice, but this was not significant.

4. Discussion

In this sub-study, the aim was to determine whether the loss of function found in the 'healthy' WT littermate mice who had gone through 3 pregnancies was due to genotype, or due to the physiological stress of having 3 successive pregnancies (with weaning). We therefore compared cardiac function and fibrosis in nulliparous (naïve) WT and STAT3 KO mice with mice who were subjected to 3 consecutive pregnancies.

Our main findings were as follows:

- KO naïve mice showed wider ventricular dimensions in diastole, and had lower EF and FS than WT naïve mice
- Pregnancy in WT mice caused anterior and posterior wall expansion, and an increase in LV mass compared to naïve WT mice, while pregnancy in KO mice contracted internal LV diameter
- Fibrosis was increased in the KO naïve group, as well as the WT group postpartum compared to the WT naïve group
- Immune cell infiltration was increased in the KO naïve group, as well as the WT group postpartum compared to the WT naïve group

Our findings in the WT groups, when comparing naïve (non-pregnant) mice to mice who have gone through 3 consecutive pregnancies, indicate that there is increased hypertrophy (indicated by wider LV wall dimensions, see figures 5.2 – 5.3), as well as onset of fibrosis (indicated by increased collagen deposition, see figure 5.5) with 3 consecutive pregnancies. These findings suggest that

there is a degree of cardiac dysfunction associated with pregnancy in this model. It is possible that this occurred as a result of there being no recovery time between pregnancies, thus compounding cardiac symptoms, resulting in dysfunction and the onset of hypertrophy and fibrosis.

When comparing the WT naïve and KO naïve groups, there were clear differences between the 2 groups with dampening of cardiac function in nulliparous KO mice compared to WT controls (indicated by reduced EF and FS, see figure 5.3). The results, in terms of wall dimensions, also appear to indicate that the pathology associated with knocking out of the STAT3 gene in cardiomyocytes is consecutive to diastolic dysfunction (see figures 5.2 – 5.3). Further to this, we found tendencies toward reduced fibrosis and immune cell infiltration between the 2 groups, but this was not significant. These results indicate that there is cardiac (diastolic) dysfunction associated with KO mice even without pregnancy. It is necessary to note that STAT3 KO mice have been shown to develop dilated cardiomyopathies as they age [105] – an outcome which may be variable in terms of timing of onset, possibly depending on the genetic background of mice.

There were few differences found between the KO naïve and postpartum groups – overall cardiac function, fibrosis, and immune cell infiltration were consistent – both groups were in a similar state of dysfunction. The only differences were compensatory changes in HR and contractility which maintained stable cardiac output between the 2 groups. This works on a similar principle to that seen by Kulandavelu et al who found compensatory changes in HR and stroke volume pre- and post-pregnancy in eNOS deficient mice, which maintained stable cardiac output [439]. Our findings here do differ from those published by Hilfiker-Kleiner et al, as they found their nulliparous STAT3 KO mice to have normal function, while mice who were put through 3 pregnancies had notably decreased function, with hypertrophic thickening of walls, and severe fibrosis [196]. It appears that our knockout model has an earlier onset of cardiac dysfunction than that of Hilfiker-Kleiner et al [196]. This difference may be due to the method of inactivation of STAT3

in each model – the model we have used removes the entire STAT3 gene, producing no protein in cardiomyocytes [426], while the model used by Hilfiker-Kleiner et al removes only part of the gene [103], producing an aberrant protein which may possibly still have some cardioprotective effect prior to pregnancy.

These observations help to explain the results seen in chapter 4, section 3, in the main study – timing of pregnancies appears to be an important factor, as consecutive pregnancies are associated with cardiac dysfunction in our model, irrespective of the genetic background. Pregnancy in itself is a cardiac stress, and three consecutive pregnancies, without sufficient recovery time, may have masked the differences that would be expected in a STAT3 KO model of PPCM, due to WT mice suffering cardiac alterations with pregnancy.

It would have been useful to try a longer period after each weaning to see whether the dysfunctional state we have reported here could have been reversible in WT mice.

5. Conclusion

Our main finding in this study was that WT mice who are subjected to 3 consecutive pregnancies show abnormal function, similar to that of their PPCM littermates.

The STAT3 knockout / PPCM model we have used here behaves differently to those previously published by other groups – we did not observe a marked change in function between the WT and KO groups following 3 consecutive pregnancies, thus failing to mimic a PPCM model. This outcome appears to be linked to the timing of onset of dysfunction in the genetically modified mice, as our genetic knockout model shows marked functional changes prior to the onset of pregnancy, indicating early onset of cardiac dysfunction. It also appears to be linked to the timing of pregnancies, as 3 consecutive pregnancies in WT mice showed remodelling usually linked to long-

term cardiac dysfunction, thus masking the effects which would otherwise be seen between WT and a STAT3 KO model supposed to mimic PPCM.

Despite this limitation, we found that long-term use of ivabradine in a setting associated with cardiac stress and dysfunction helps to reduce fibrotic remodelling. This is consistent with findings in the literature [437], although our quantitation of transcripts suggests that the anti-fibrotic activity of ivabradine is facilitated by an alternate pathway to RAAS regulation. Our data here suggest that this effect of ivabradine is independent of the SA node (and HR) or STAT3. A candidate pathway facilitating the anti-fibrotic effect of ivabradine may possibly involve suppression of the phospho-inositol 3 kinase/ protein kinase B (PI3K/Akt), as a study by Yu et al in mice showed a decrease in PI3K activity with ivabradine treatment, together with reduced hypertrophy, fibrosis and cardiomyocyte apoptosis [440].

Chapter 6

Exploring the beneficial effect of reducing heart rate in ex-vivo mouse models of acute heart failure

1. Study rationale

AHF is the sudden onset of HF-like symptoms, with varying causes and manifestations. A switch in preference for energy substrate from glucose to free-fatty acids, higher circulating levels of catecholamines and changes in pressure and cardiac contractility are observed. AHF has high mortality rates, and one of the main problems with studying AHF is the lack of basic, pre-clinical models which mimic the condition [441–443]. Most data obtained in clinical studies are only able to record observations after interventions begin which make it difficult to study the pathophysiology of the disease and putative novel therapies for it.

One notable observation in clinical studies of AHF is the change in HR – in pathologies like haemorrhagic shock it is very low; in Takotsubo cardiomyopathy (TC), it is differentially modulated. In these pathologies, it is suggested that the change in HR is modulated by adrenergic activity, and compensatory mechanisms following changes in blood pressure [444,445].

A previously validated ex-vivo animal model which mimics hypotensive AHF as observed in haemorrhagic shock – with an increase in adrenergic activation, a switch in availability of metabolic substrates and a drop in pressure – shows poor recovery as would be associated with high mortality rates [312,446]. This model displays a great HR variability during the recovery phase, therefore suggesting that the sinoatrial node might be involved and may play a vital role in the outcomes. This ex-vivo model, which is un-paced and makes use of adrenaline to exacerbate the

HF-like insult, could also potentially be adapted to mimic TC, characterised by absence of severe hypotension at the onset of the pathology, but further increased adrenergic stimulation.

Observations in both clinical and experimental settings allude to the idea that the ability to regulate heart rate – without involvement of the adrenergic pathways – could modify the outcomes in HF conditions (see chapter 1, section 3) [310,417]. The sinoatrial node inhibitor, ivabradine, is a prime candidate to test this idea, and would provide a better mechanistic understanding of the role that the sinoatrial node may play in AHF.

In this study, we therefore aimed to evaluate the cardiac function recovery in ex-vivo models of hypotensive AHF, mimicking haemorrhagic shock, and a reductionist model of TC, in the presence of ivabradine, a modulator of HR.

2. Methods

2.1 Animal ethics

All procedures were approved by the Faculty of Health Sciences Animal Ethics Committee of the University of Cape Town (project reference number 014/029). All experiments were conducted, in accordance with the Guiding Principles in the Care and Use of Animals and National Institute of Health Guidelines (NIH publication No. 85-22, revised 1996). C57BL6 mice were bred at the faculty's breeding unit and housed in a facility with 12-hour day/ night light cycles, with ad libitum access to food and water. Only male mice (11 weeks – 15 weeks of age) were used, as oestrogen levels vary through the reproductive cycle and may misrepresent the outcomes attributed to drug treatments [446].

2.2 Langendorff isolated mouse heart perfusion system

The chemical composition of buffers used in the following protocols are given in appendix A. C57BL6 male mice between 13 – 15 weeks of age were used for the hypotensive AHF model and 11 – 14 weeks for the TC model.

2.2.1 Anaesthesia and heart excision

Mice were anaesthetized by intraperitoneal injection of sodium pentobarbitone (200mg/kg body weight) and heparin (80IU/kg body weight). A sufficient degree of anaesthesia was determined by absence of the pedal reflex, after which an incision was made to expose the thoracic cavity. This was cut open at the surface of the sternum, and the ribs and intercostal muscles were incised to access the heart. The heart was gently cupped and lifted slightly before cutting the connection with the aorta, vena cava and pulmonary vessels. The heart was rapidly immersed in ice cold Krebs buffer (see appendix A) and immediately cannulated. Cannulation was done by inserting a blunt-ended 21-gauge needle filled with Krebs buffer into the aorta and fastening it at the base of the needle by means of a silk suture thread. The cannulated heart was then connected to the Langendorff retrograde perfusion system to conduct the simulation protocols.

2.2.2 Measurement of left ventricular pressure

Balloons were constructed using a 2.5 x 2.5cm square of polyvinyl chloride film (clingfilm) which was carefully stretched over the end of a size 13 knitting needle to create an inelastic pocket protrusion (approximately 1cm in length) which would contour the inside of left ventricle. This pocket was filled with deionised water and carefully fastened to a length of fine polythene tubing attached to the blunt end of a 21-gauge needle. The balloon, once bound, was approximately 0.5cm in length. Extreme care was taken to remove any air bubbles present in the balloon and connected tubing as presence of air in any part of the recording system would cause dampening of the pressure signal. Balloons were stored in deionised water.

The balloon was connected to a pressure transducer, which was connected to a PowerLab signal-recording device (ADInstruments, Sydney, NSW, Australia). After the initiation of perfusion, the left atrial appendage was removed, and the balloon was deflated and inserted through the mitral valve into the left ventricle. Once in the ventricle, the balloon was secured using a clamp. The balloon was filled with water until a diastolic pressure of between 4 and 10mmHg was obtained during stabilisation. The mechanical beating of the heart was converted to an electrical trace which was digitally recorded and could be used for the continuous monitoring of the HR, left ventricular systolic and diastolic pressures and resultant left ventricular developed pressure (LVDP) [447].

2.3 Experimental protocol for ex-vivo hypotensive acute heart failure model

The perfusion model used to simulate hypotensive AHF, mimicking haemorrhagic shock, was validated by Deshpande et al in a rat model with administration of adrenaline during the low pressure phase [312]. The model used in the present study was adapted to mice, with the use of a pressure-sensing balloon, and administration of adrenaline during the low-pressure phase, as in the rat model.

Each heart included in the study had to meet the parameters listed in table 6.1 below:

Table 6.1: Baseline criteria for hearts used in the AHF experiments. Abbreviations: AHF – acute heart failure; BPM – beats per minute; min – minute; ml - millilitres; mmHg – millimetres of mercury

Parameter	Baseline
Heart rate	≥200 BPM
Left ventricular developed pressure	≥55mmHg [448,449]
Diastolic pressure	4-10mmHg
Coronary flow	≥1.5 ml/min
Temperature	~37°C

The perfusion apparatus consisted of 3 water-jacketed fluid reservoirs (see figure 6.1). All buffers were gassed with carbogen (95% O_2 + 5% CO_2) prior to and during perfusions.

The AHF protocol was split into three phases as follows - (1) stabilisation, (2) acute HF and (3) recovery. We switched between the three phases by means of a stopcock which allowed perfusion from separate reservoirs.

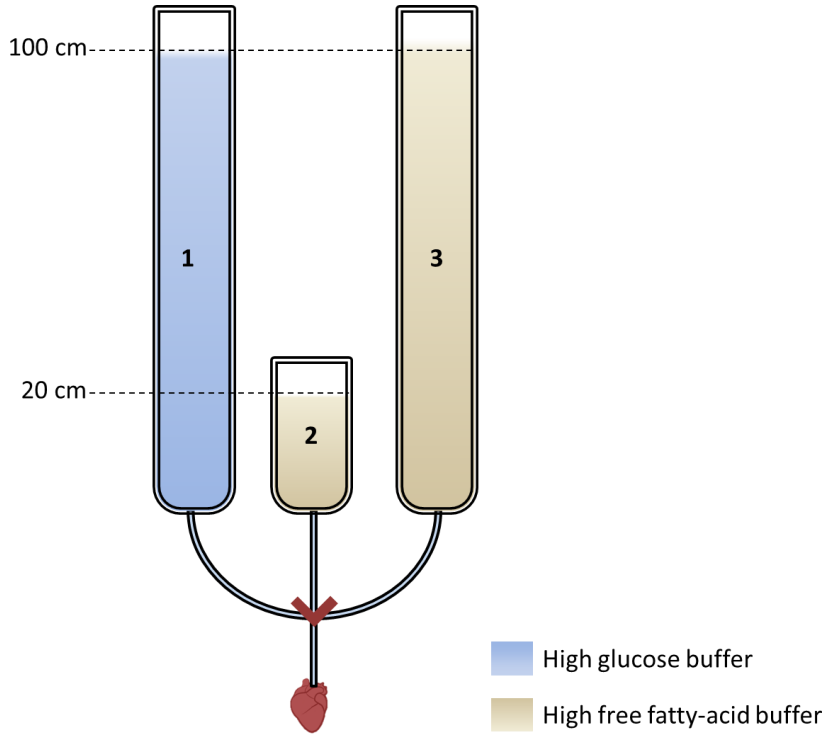

Figure 6.1: Perfusion setup as per AHF protocol. Phase 1, stabilisation, was perfusion with high glucose KHB at 100cm column height. Phases 2 and 3, AHF and recovery, were perfusion with high free fatty-acid KHB at 20cm and 100cm respectively. Abbreviations: AHF – acute heart failure; KHB - Krebs-Henseleit Buffer

Stabilisation phase

During the stabilisation phase, the fluid reservoir was filled to produce a pressure of 73mmHg (100cm) at the base of the cannula against which the heart pumped. The duration of this phase was 20 min with high glucose (11.1mM) as the sole substrate in Krebs buffer (see appendix A). The

basal functional parameters were recorded and hearts were continued only if functional values fell within the range indicated in the table 6.1. This phase served to flush the heart of blood and to achieve the necessary baseline functional data against which later measurements would be compared.

Acute heart failure phase

During the AHF phase, the fluid reservoir was filled to produce a pressure of 18mmHg (20cm) at the base of the cannula against which the heart pumped. The duration of this phase was 15 min with low glucose (2.5mM) and high free fatty-acids as substrates in Krebs buffer (see appendix A). Adrenaline ($1x10^{-8}$mM) was administered using a drug pump, via a side arm to further exacerbate the response as previously described by Deshpande et al [312]. These changes were made to mimic the metabolic state within the body at the onset of HF - the heart preferentially chooses FFA as a substrate, glucose is depleted, and the sympathetic nervous system is activated. Functional parameters were recorded at the end of the AHF period. This was the phase in which Ivabradine was administered to hearts in the treated groups (final concentration 3μM [450], delivered in buffer, see figure 6.2).

Recovery phase

During the recovery phase, the pressure was returned to 73mmHg (100cm) as in the stabilisation phase. The duration of this phase was 25 min with the same low glucose /high free fatty acid buffer as the AHF phase (see figure 6.1). These substrates together with an improved perfusion pressure mimic the recovery phase seen in patients with hypotensive de novo AHF.

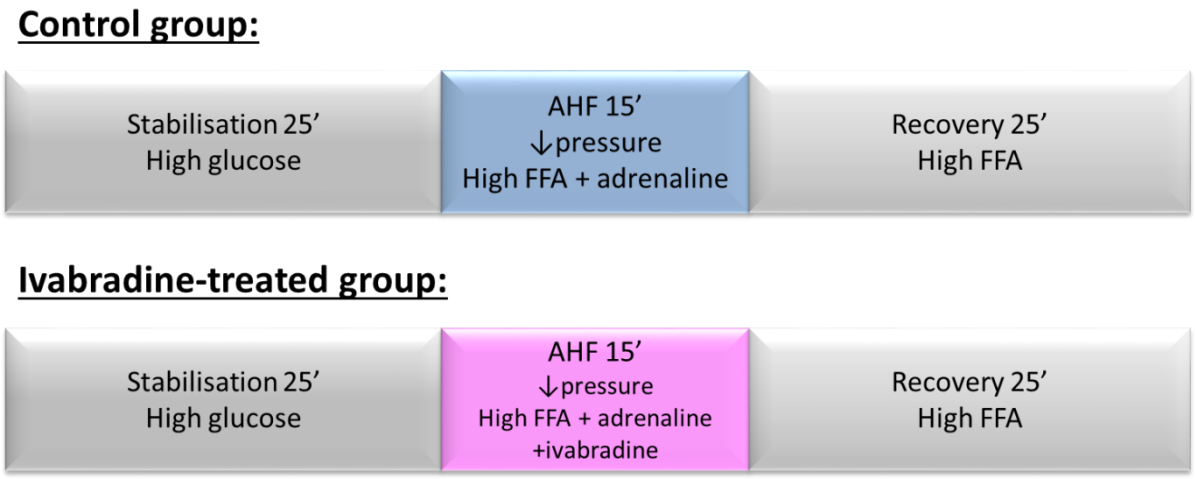

Figure 6.2: AHF perfusion protocol for control and ivabradine-treated groups. Treatment with ivabradine was administered during the low-pressure phase together with adrenaline in a high FFA buffer. Abbreviations: AHF – acute heart failure; FFA – free fatty acids.

2.4 Perfusion apparatus and setup for simulated Takotsubo cardiomyopathy

The perfusion apparatus was set up as indicated in figure 6.3, and inclusion criteria can be found in table 6.2 below. The TC protocol was split into three phases as follows - (1) stabilisation, (2) TC and (3) recovery.

Table 6.2: Baseline criteria for hearts used in TC experiments. Abbreviations: BPM – beats per minute; min – minute; ml - millilitres; mmHg – millimetres of mercury; TC – Takotsubo cardiomyopathy

Parameter	Baseline
Heart rate	≥200 BPM
Left ventricular developed pressure	≥70mmHg [109]
Diastolic pressure	4-10mmHg
Coronary flow	≥1.5 ml/min
Temperature	~37°C

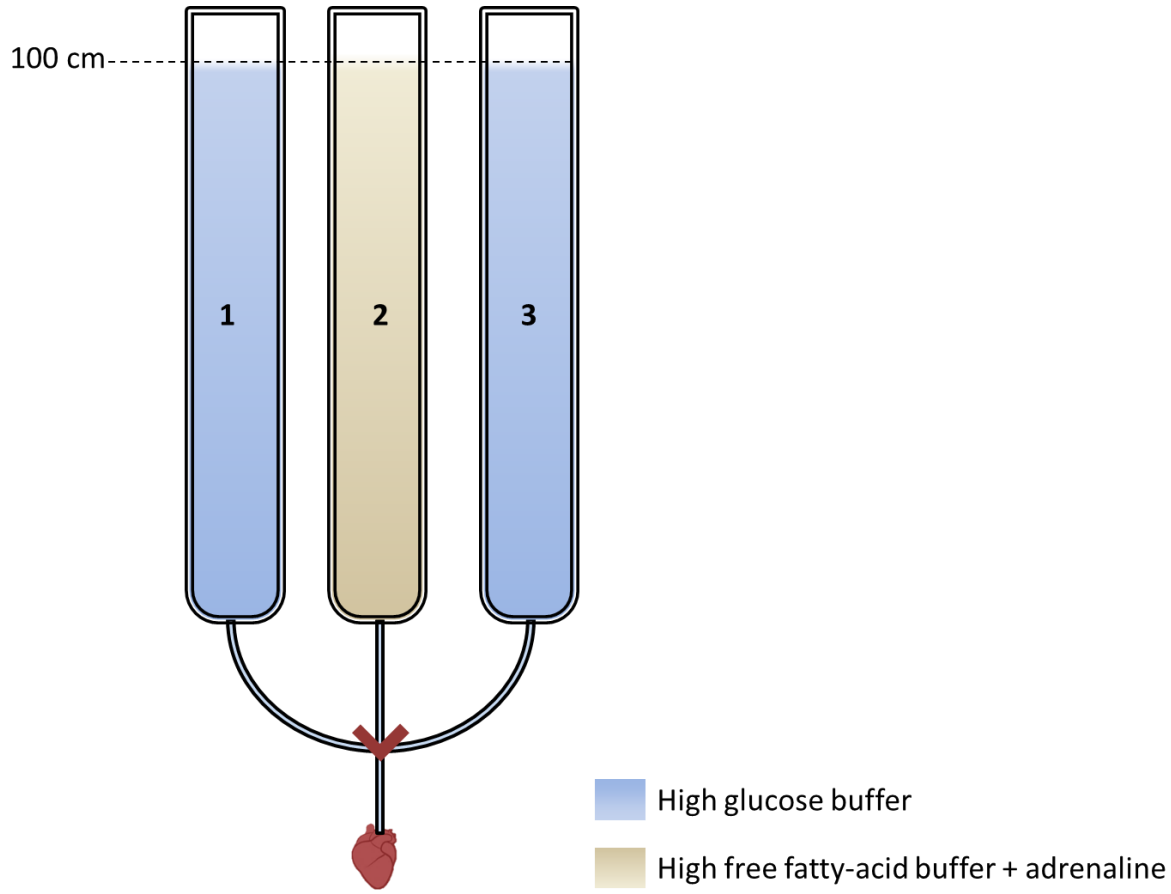

Figure 6.3: Perfusion setup as per AHF protocol. Phase 1, stabilisation, was perfusion with high glucose KHB at 100cm column height. Phases 2, TC stress simulation, was perfusion with high free fatty-acid KHB with adrenaline (10^{-7}M) at 100cm. Phase 3, TC recovery, was perfusion with high glucose KHB at 100cm. Abbreviations: KHB - Krebs-Henseleit Buffer; TC – Takotsubo cardiomyopathy

Stabilisation phase

Stabilisation was performed for 25 min, as described above, with inclusion criteria as per table 6.2.

Takotsubo cardiomyopathy phase

During the TC phase, the fluid reservoir was filled to produce a pressure of 73mmHg at the base of the cannula against which the heart pumped. The duration of this phase was 12 min with low glucose/ high free fatty-acids as substrates in Krebs buffer (see figure 6.4). Adrenaline ($1x10^{-7}$M) was administered in the buffer. These changes were made to mimic those described in TC (see chapter 1, section 3.5) with a sudden onset of adrenergic stimulation and spike in LVDP and HR.

The change in substrate in this phase was to preferentially favour the uptake of fatty acids as a substrate, so as to exacerbate the TC phenotype. This was the phase in which Ivabradine was administered to hearts in the treated groups (final concentration 3μM in high FFA Krebs buffer) [450]. Functional parameters were recorded at 3 min intervals through the TC phase.

Recovery phase

During the recovery phase, the fluid reservoir was a pressure of 73mmHg as in the stabilisation and TC phases. The duration of this phase was 25 min with high glucose Krebs buffer, as in the stabilisation phase. This substrate choice, together with a reduced adrenergic state theoretically simulates the recovery conditions in patients with TC (see chapter 1, section 3.5.4).

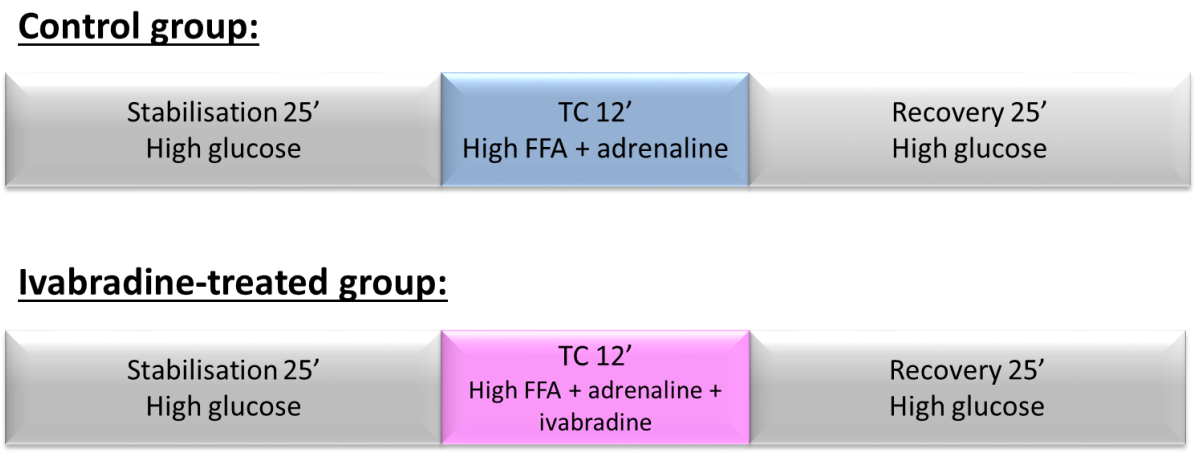

Figure 6.4: TC perfusion protocol for control and ivabradine-treated groups. Treatment with ivabradine was administered during the TC phase, together with 10 x the dose of adrenaline used in the AHF protocol, in a high FFA buffer. Abbreviations: AHF – acute heart failure; FFA – free fatty acids; TC – Takotsubo cardiomyopathy

2.5 Quantitative PCR

Quantitative PCR was performed as described in chapter 4 (see chapter 4, section 2.7) with primers for ANP and BNP.

2.6 Chemicals

Unless otherwise specified, all chemicals were obtained from Sigma-Aldrich Inc.

2.7 Statistical analysis of animal study data

Results are expressed as means ± standard error of mean (SEM). Statistical analyses were performed using Statistica v.13 software. Significant differences ($p < 0.05$) were determined, for normally distributed data, using multi-factoral Anova, with Fisher correction, with $n \geq 6$.

3. Results

3.1 Hypotensive acute heart failure simulation

Cardiac parameters were measured at the end of stabilisation, at the end of the AHF phase (1.e. after 15 min of hypotensive simulation) and 5, 15 and 25 min into recovery for both control (n=10) and ivabradine-treated (n=7) hearts. Parameters observed were HR, systolic and diastolic ventricular pressure, LVDP, rate pressure product and percentage functional recovery. Results produced are represented in figures 6.5 – 6.8 below (see appendix B, table 5 for tabulated results).

3.1.1 Heart rate

After 20 min of stabilisation, HR in the control group was 388±11 BPM, similar to the ivabradine-treated group (393±20 BPM) and to previously reported models of mouse heart perfusions [451]. At the end of the AHF phase, HR dropped to 94±28 BPM, and to 102±31 BPM in the control and ivabradine-treated groups respectively. In both groups, HR did not improve during the recovery phase compared to the AHF phase, and similar values were seen in the control and ivabradine-treated group (5 min recovery – 158±23 BPM control vs 216±23 BPM ivabradine; 15 min recovery – 120±22 BPM control vs 127±14 BPM ivabradine; 25 min recovery – 161±42 BPM control vs 105±13 BPM ivabradine).

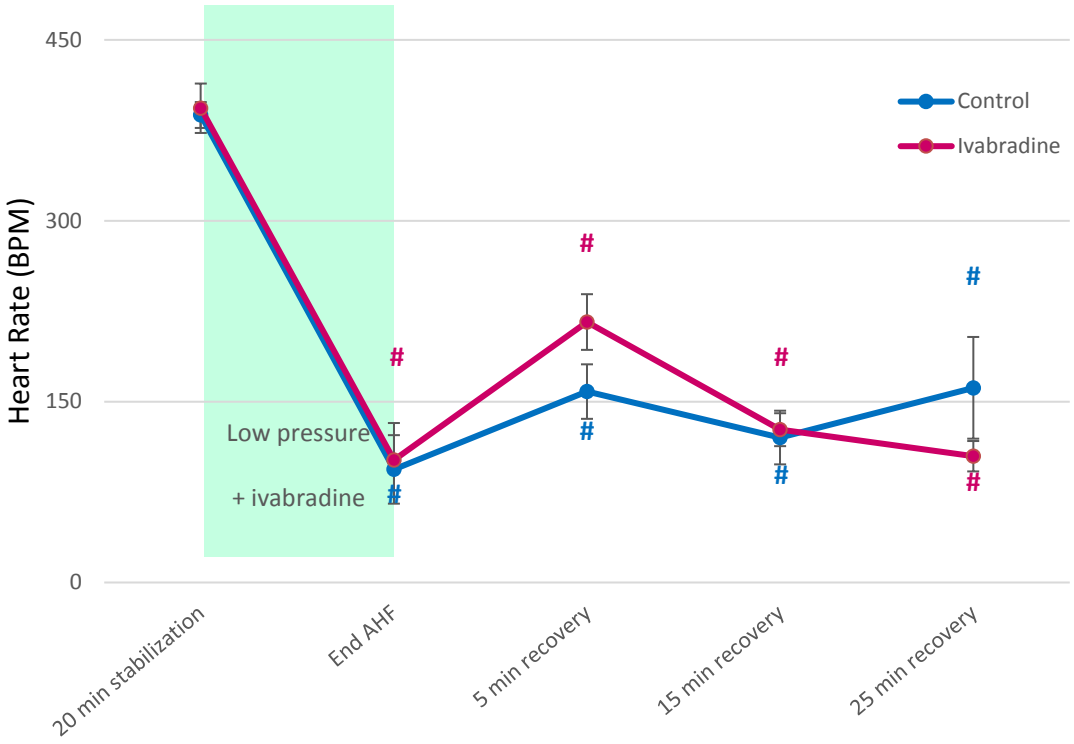

Figure 6.5: The effect of ivabradine on heart rate in an isolated heart model of hypotensive acute heart failure. Heart rate (HR) as recorded by pressure-sensing transducer. Abbreviation: AHF – acute heart failure; BPM – beats per minute; #p<0.05 vs respective stabilisation value. Control n =10, ivabradine n =7.

3.1.2 Systolic pressure

After 20 min of stabilisation, systolic pressure in the control group was 73±3mmHg, similar to the ivabradine-treated group (75±3mmHg) and to previously reported models of mouse heart perfusions [448,452]. At the end of the AHF phase, systolic pressure in the control group dropped to 54±14mmHg, and to 27±6mmHg in the ivabradine-treated group. Systolic pressure rose steadily in the control group during the recovery phase. A similar pattern was seen in the ivabradine-treated group but was significantly lower 5 min into recovery when compared to the control group – an effect which was lost with time (5 min recovery – 93±12mmHg control vs 61±8mmHg ivabradine; 15 min recovery – 105±14mmHg control vs 95±12mmHg ivabradine; 25 min recovery – 104±10mmHg control vs 103±8mmHg ivabradine).

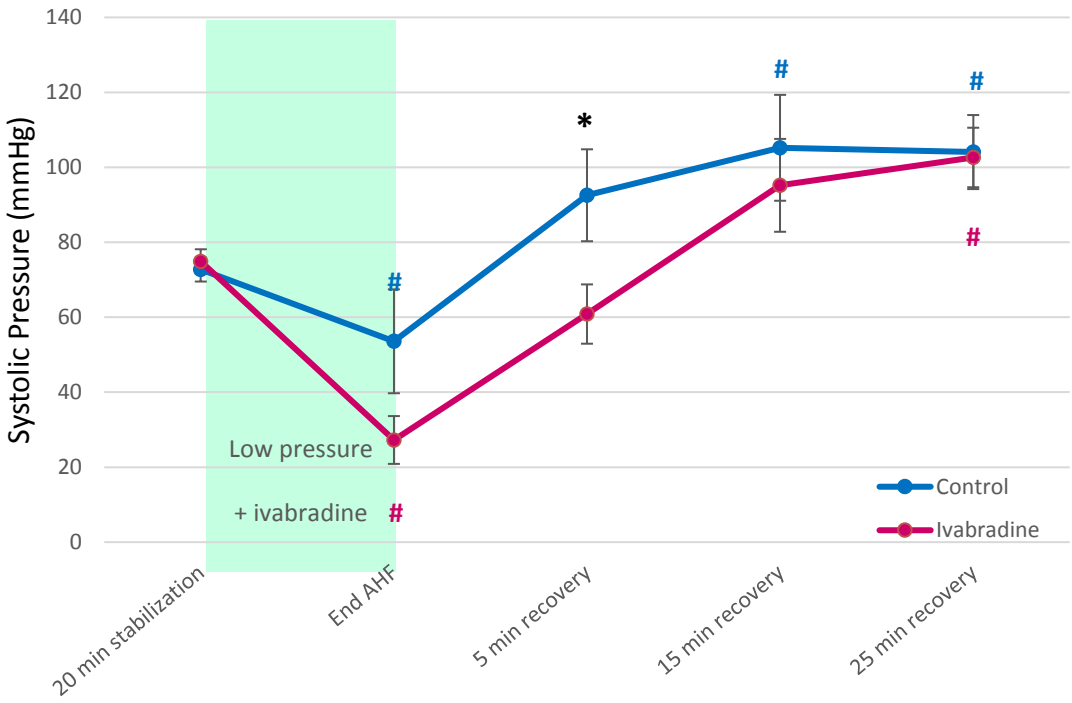

Figure 6.6: The effect of ivabradine on systolic pressure in an isolated heart model of hypotensive acute heart failure. Systolic pressure as recorded by pressure-sensing transducer. Abbreviation: AHF – acute heart failure; mmHg – millimetres of mercury. *p<0.05 control vs ivabradine at the same time point; #p<0.05 vs respective stabilisation value. Control n =10, ivabradine n =7.

3.1.3 Diastolic pressure

After 20 min of stabilisation, diastolic pressure in the control group was 6.4±0.6mmHg, similar to the ivabradine-treated group (6.5±0.5mmHg) and to previously reported models of mouse heart perfusions [447]. At the end of the AHF phase, diastolic pressure in the control group rose to 35.2±15.4mmHg, and to 15.4±0.6mmHg in the ivabradine-treated group. In both groups, diastolic pressure rose steadily during the recovery phase, similar values were seen in the control and ivabradine-treated group (5 min recovery – 46.0±12.6mmHg control vs 17.3±6.4mmHg ivabradine; 15 min recovery – 62.4±15.8mmHg control vs 31.9±8.4mmHg ivabradine; 25 min recovery – 65.0±12.1mmHg control vs 40.3±9.3mmHg ivabradine).

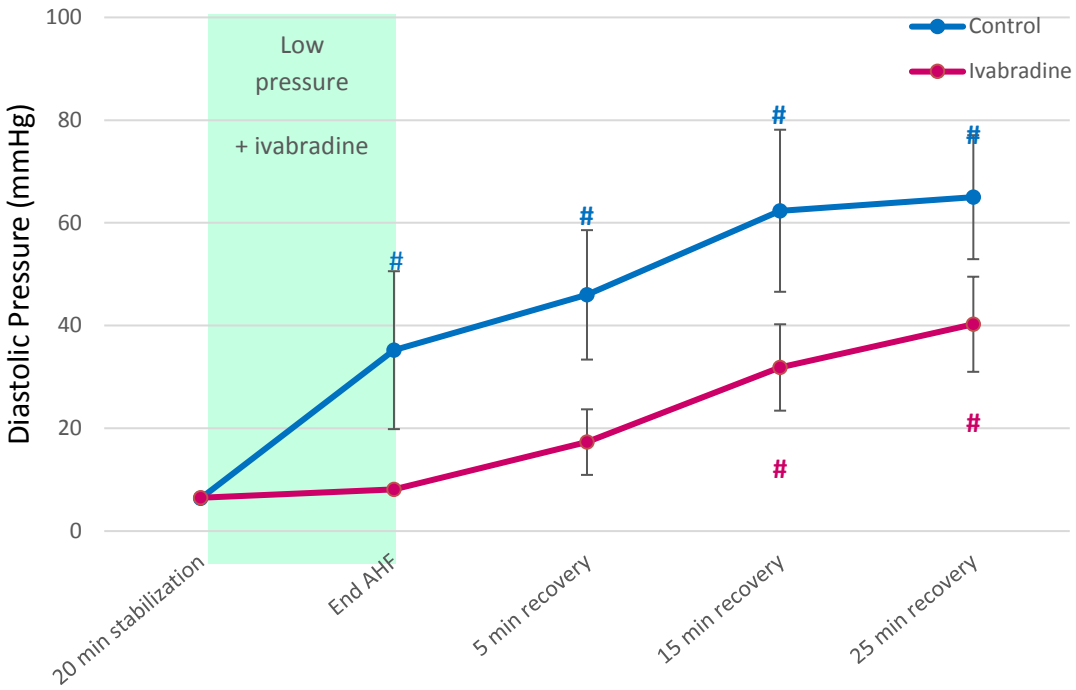

Figure 6.7: The effect of ivabradine on diastolic pressure in an isolated heart model of hypotensive acute heart failure. Diastolic pressure as recorded by pressure-sensing transducer. Abbreviation: AHF – acute heart failure; mmHg – millimetres of mercury. #p<0.05 vs respective stabilisation control. Control n =10, ivabradine n =7.

3.1.4 Left ventricular developed pressure

After 20 min of stabilisation, LVDP in the control group was 66±3mmHg, similar to the ivabradine-treated group (68±3mmHg) and to previously reported models of mouse heart perfusions [448,449]. At the end of the AHF phase, LVDP in the control group dropped to 18±4mmHg, and to 19±6mmHg in the ivabradine-treated group. In both groups, LVDP rose steadily in the control group for the first 5 min of recovery, stabilising thereafter. LVDP rose steadily in the ivabradine-treated group for the first 15 min of recovery, stabilising thereafter at a significantly higher level compared to the control group (5 min recovery – 47±7mmHg control vs 44±6mmHg ivabradine; 15 min recovery – 43±7mmHg control vs 63±8mmHg ivabradine; 25 min recovery – 39±6mmHg control vs 62±5mmHg ivabradine).

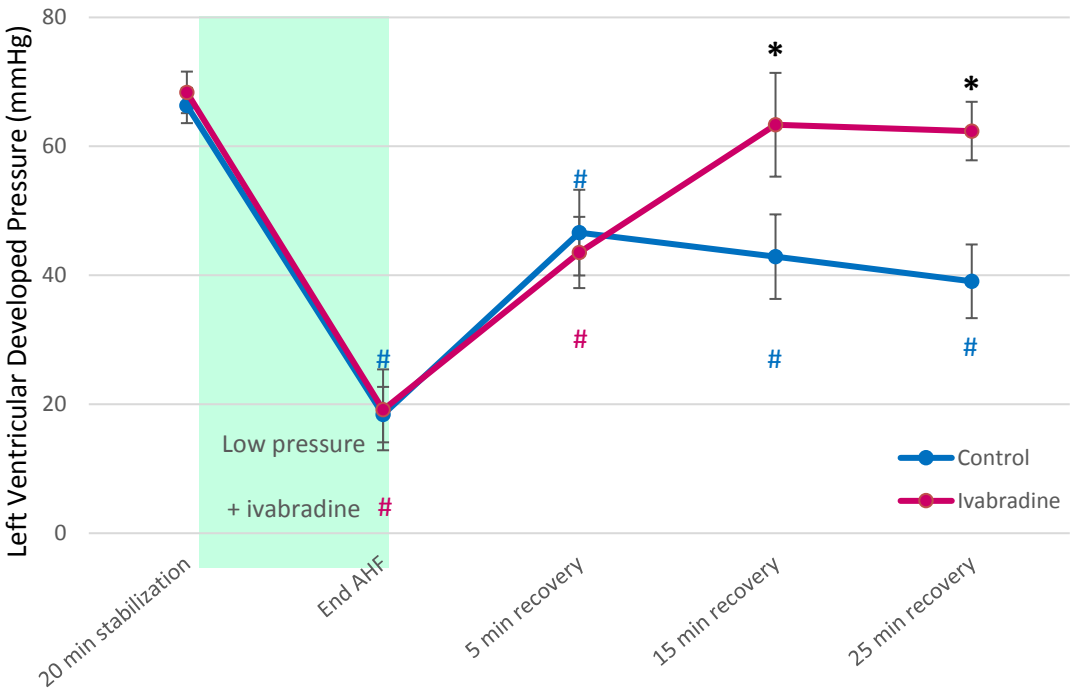

Figure 6.8: The effect of ivabradine on left ventricular developed pressure in an isolated heart model of hypotensive acute heart failure. Left ventricular developed pressure (LVDP) as recorded by pressure-sensing transducer. Abbreviation: AHF – acute heart failure; mmHg – millimetres of mercury. *p<0.05 control vs ivabradine at the same time point; #p<0.05 vs respective stabilisation value. Control n =10, ivabradine n =7.

The timing of the AHF protocol was protracted compared to the model used by Deshpande et al and Breedt et al, as the strain of mice and model we used displayed greater sensitivity to insults [312,446]. The 15 min duration we have used for AHF proved most suitable, as the outcomes would be able to indicate both improvement or detriment with treatment.

3.1.5 Atrial natriuretic peptide and B-type natriuretic peptide levels

CT scores obtained for qPCR analysis are summarised in figure 6.9 below (see appendix B, table 6 for tabulated results). Levels of ANP were variable and showed no significant change with ivabradine treatment. BNP levels were significantly higher in the ivabradine-treated group compared to the untreated group (p=0.01, n=5 per group).

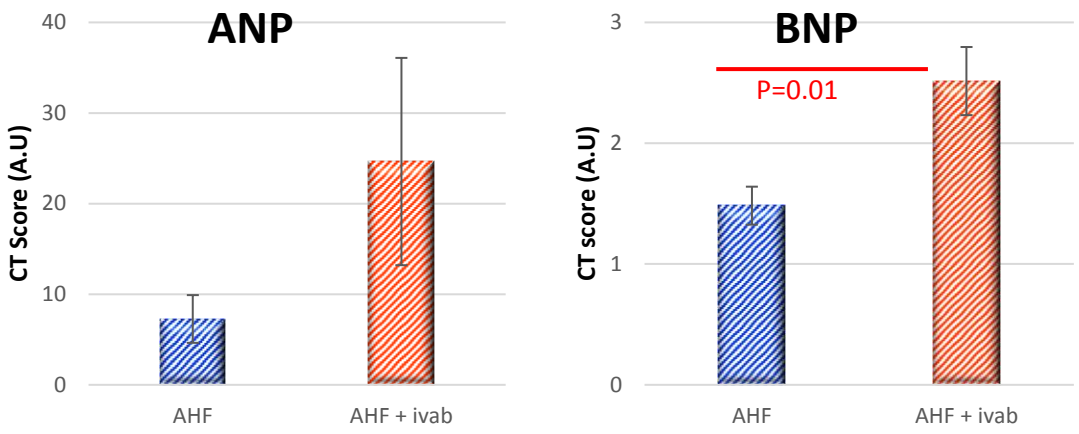

Figure 6.9: mRNA expression of ANP and BNP in mouse hearts subject to simulated AHF with ivabradine treatment. Administration of ivabradine significantly increased levels of BNP in a simulated model of hypotensive AHF. Abbreviations: AHF - acute heart failure; ANP – atrial natriuretic peptide; A.U – arbitrary units; BNP – brain natriuretic peptide; ivab – ivabradine; mRNA – messenger ribonucleic acid. Control n =10, ivabradine n =7.

3.2 TC protocol simulation

Cardiac parameters were measured at the end of stabilisation, 1, 3, 6, 9 and 12 min into TC phase, and 5, 10, 15, 20 and 25 min into recovery for both control (n=11) and ivabradine-treated (n=6) hearts. Parameters observed were HR, systolic and diastolic ventricular pressure, LVDP, rate pressure product and percentage functional recovery. Results produced are represented in figures 6.10 – 6.13 below (see appendix B, table 7 for tabulated results).

3.2.1 Heart rate

After 20 min of stabilisation, HR in the control group was 318±24 BPM, similar to the ivabradine-treated group (314±34 BPM) and to previously reported models of mouse heart perfusions [451]. HR in the control group remained steady for the first few min of the Takotsubo cardiomyopathy (TC) phase (simulated by addition of 10x adrenaline), dropping at the 6th min, and recovering at the end of the 12 min TC phase. The ivabradine-treated group had an immediate spike with administration of adrenaline and ivabradine together, at the start of the TC phase, and declined steadily (but not significantly until the end of the TC phase (1 min TC – 333±37 BPM control vs

431±17 BPM ivabradine; 3 min TC – 296±37 BPM control vs 318±67 BPM ivabradine; 6 min TC – 251±44 BPM control vs 273±44 BPM ivabradine; 9 min TC –250±35 BPM control vs 157±34 BPM ivabradine; 12 min TC –248±35 BPM control vs 149±32 BPM ivabradine). Treatment with ivabradine showed a tendency toward a decrease in HR after 9 and 12 min of administration during the TC phase, illustrating the action of ivabradine. HR was stable following the onset of recovery in the control group, and the same pattern was seen in the ivabradine-treated group (5 min recovery – 273±38 BPM control vs 188±36 BPM ivabradine; 10 min recovery – 259±28 BPM control vs 229±38 BPM ivabradine; 15 min recovery – 233±27 BPM control vs 249±45 BPM ivabradine; 20 min recovery – 230±27 BPM control vs 208±34 BPM ivabradine; 25 min recovery – 193±21 BPM control vs 184±29 BPM ivabradine).

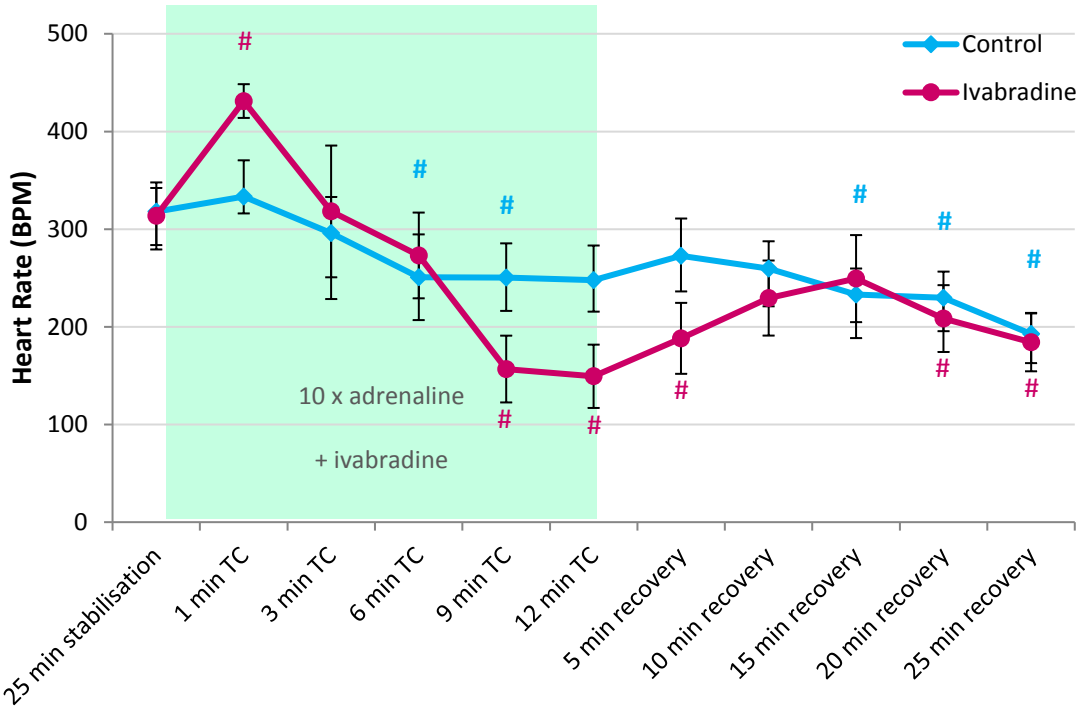

Figure 6.10: The effect of ivabradine on heart rate in an isolated heart model of Takotsubo cardiomyopathy. Heart rate (HR) as recorded by means of pressure-sensing transducer. Abbreviation: BPM – beats per minute, TC – Takotsubo Cardiomyopathy. #p<0.05 vs respective stabilisation value. Control n =11, ivabradine n =6.

3.2.2 Systolic pressure

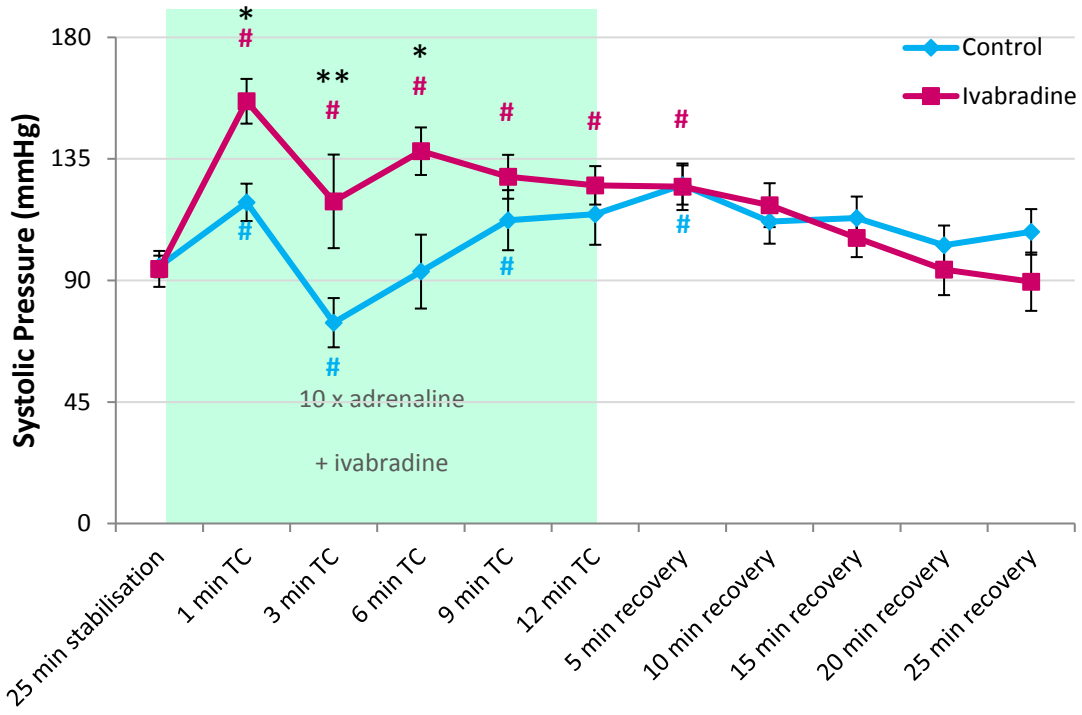

Figure 6.11: The effect of ivabradine on systolic pressure in an isolated heart model of Takotsubo cardiomyopathy. Systolic pressure as recorded by pressure-sensing transducer. Abbreviation: mmHg – millimetres of mercury; TC – Takotsubo Cardiomyopathy. *p<0.05 ivabradine-treated vs control; ** p<0.005 ivabradine-treated vs control; #p<0.05 vs respective stabilisation value. Control n =11, ivabradine n =6.

After 20 min of stabilisation, systolic pressure in the control group was 95±4mmHg, similar to the ivabradine-treated group (94±7mmHg) and to previously reported models of mouse heart perfusions [448,451]. Systolic pressure in the control group spiked suddenly at the onset of the TC phase, dropping rapidly thereafter, and rising again until the end of the phase. The ivabradine group also spiked at the onset of the TC phase, and maintained an elevated systolic pressure until the 6th min, declining slowly thereafter to match the control group (1 min TC – 119±7mmHg control vs 156±8mmHg ivabradine; 3 min TC – 74±9mmHg control vs 119±17mmHg ivabradine; 6 min TC – 93±14mmHg control vs 138±9mmHg ivabradine; 9 min TC – 112±11mmHg control vs 128±8mmHg ivabradine; 12 min TC – 115±11mmHg control vs 125±7mmHg ivabradine). The control group remained stable from the end of the TC phase, through the recovery phase. The

ivabradine-treated group declined steadily through the recovery phase to the similar levels as stabilisation (5 min recovery – 125±7mmHg control vs 125±9mmHg ivabradine; 10 min recovery – 112±8mmHg control vs 118±8mmHg ivabradine; 15 min recovery – 113±8mmHg control vs 106±7mmHg ivabradine; 20 min recovery – 103±7mmHg control vs 94±9mmHg ivabradine; 25 min recovery – 108±8mmHg control vs 90±11mmHg ivabradine).

3.2.3 Diastolic pressure

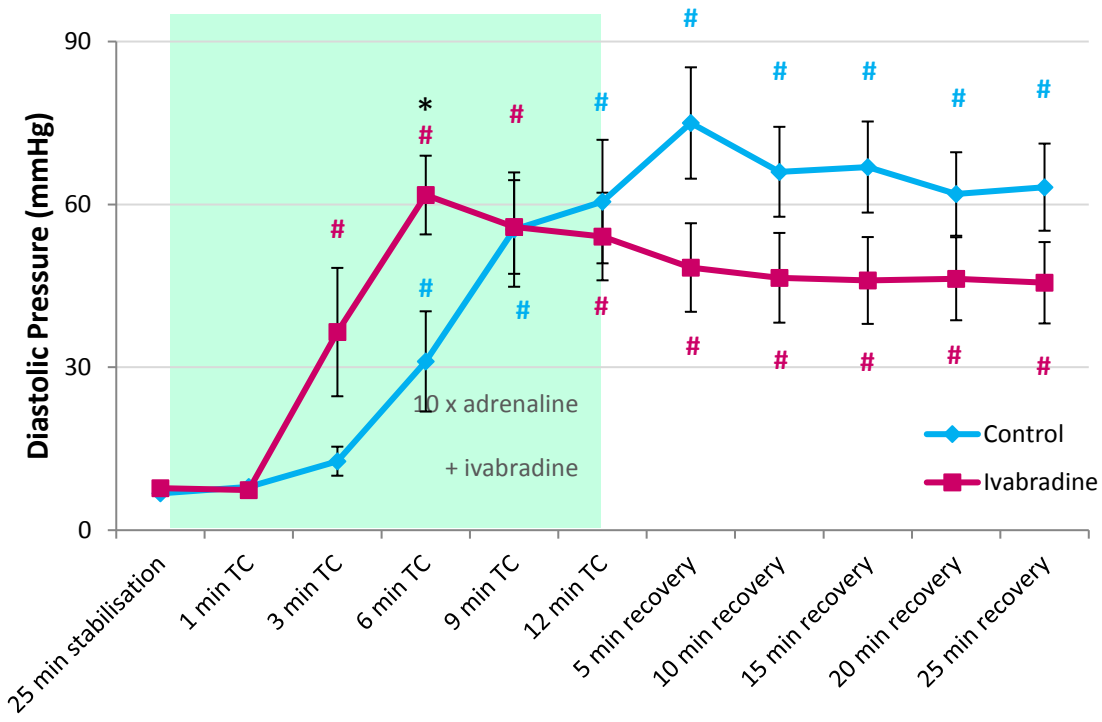

Figure 6.12. The effect of ivabradine on diastolic pressure in an isolated heart model of Takotsubo cardiomyopathy. Diastolic pressure as recorded by pressure-sensing transducer. Abbreviation: mmHg – millimetres of mercury; TC – Takotsubo Cardiomyopathy. #p<0.05 vs respective stabilisation value. Control n =11, ivabradine n =6.

After 20 min of stabilisation, diastolic pressure in the control group was 6.8±0.4mmHg, similar to the ivabradine-treated group (7.8±0.8mmHg) and to previously reported models of mouse heart perfusions [447]. Diastolic pressure in the control group rose steadily through the TC phase. Diastolic pressure in the ivabradine-treated group also increased steadily, but more rapidly through the TC phase, such that it was significantly higher 6 min compared to the control group, after which it

gradually decreased until the onset of recovery (1 min TC – 8.0±0.7mmHg control vs 7.4±1.0mmHg ivabradine; 3 min TC – 12.7±2.7mmHg control vs 36.5±11.8mmHg ivabradine; 6 min TC – 31.1±9.2mmHg control vs 61.7±7.3mmHg ivabradine; 9 min TC – 55.3±10.5mmHg control vs 55.8±8.6mmHg ivabradine; 12 min TC – 60.5±11.4mmHg control vs 54.1±8.1mmHg ivabradine). At the onset of recovery, diastolic pressure was raised, remaining stable through recovery in the control group, and the same pattern was seen in the ivabradine-treated group (5 min recovery – 75.0±10.3mmHg control vs 48.4±8.2mmHg ivabradine; 10 min recovery – 66.0±8.3mmHg control vs 46.0±8.0mmHg ivabradine; 15 min recovery – 66.9±8.4mmHg control vs 46.0±8.0mmHg ivabradine; 20 min recovery – 61.9±7.7mmHg control vs 46.3±7.6mmHg ivabradine; 25 min recovery – 63.2±8.0mmHg control vs 45.6±7.5mmHg ivabradine).

3.2.4 Left ventricular developed pressure

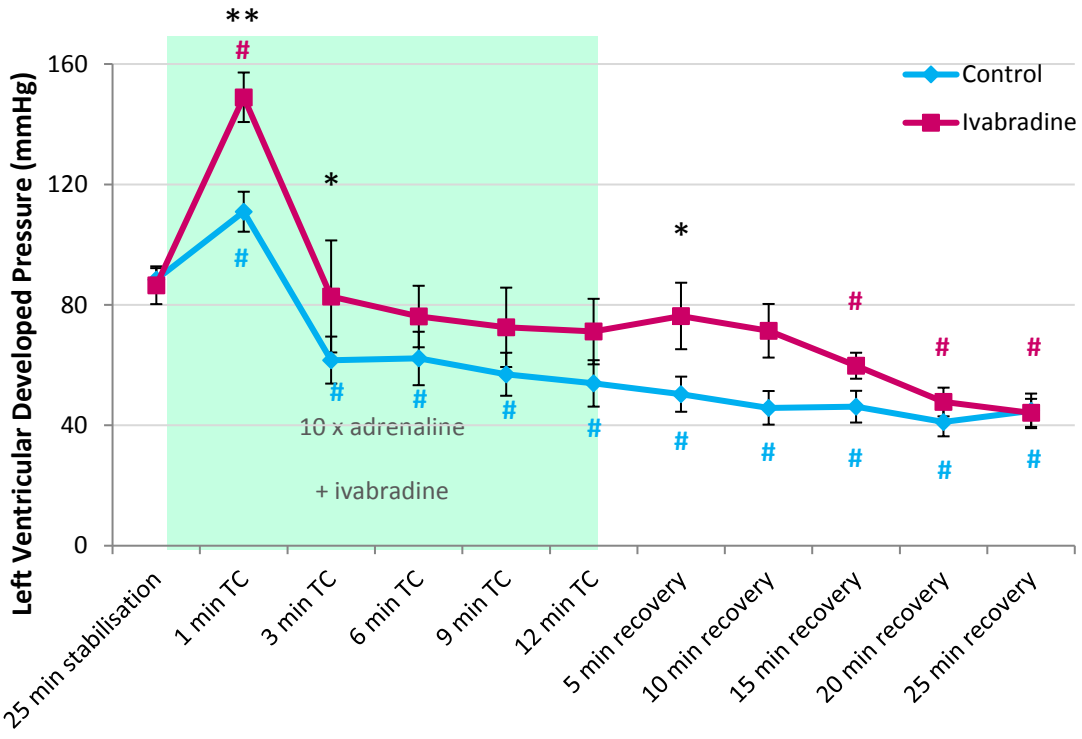

Figure 6.13: The effect of ivabradine on left ventricular developed pressure in an isolated heart model of Takotsubo cardiomyopathy. Left ventricular developed pressure (LVDP) as recorded by pressure-sensing transducer. Abbreviations: mmHg – millimetres of mercury; TC – Takotsubo Cardiomyopathy. *p<0.05 ivabradine-treated vs control; ** p<0.005 ivabradine-treated vs control; #p<0.05 vs respective stabilisation value. Control n =11, ivabradine n =6.

After 20 min of stabilisation, LVDP in the control group was 88±4mmHg, similar to the ivabradine-treated group (87±6mmHg) and to previously reported models of mouse heart perfusions [448,449]. LVDP in the control group spiked at the start of the TC phase, and rapidly dropped after 3 min, remaining stable thereafter. LVDP in the ivabradine treated group also spiked at the start of the TC phase, but much higher compared to the control group, dropping quickly to stabilisation levels, remaining stable thereafter (1 min TC – 111±7mmHg control vs 149±8mmHg ivabradine; 3 min TC – 62±8mmHg control vs 83±19mmHg ivabradine; 6 min TC – 62±9mmHg control vs 76±10mmHg ivabradine; 9 min TC –57±7mmHg control vs 73±13mmHg ivabradine; 12 min TC – 54±8mmHg control vs 71±11mmHg ivabradine). LVDP was stable following the onset of recovery in the control group. The ivabradine treated group had a slight increase at the onset of recovery compared to the control, an effect which was lost with time as LVDP continued to gradually decrease (5 min recovery – 5±6mmHg control vs 76±11mmHg ivabradine; 10 min recovery – 46±6mmHg control vs 71±9mmHg ivabradine; 15 min recovery – 46±5mmHg control vs 60±4mmHg ivabradine; 20 min recovery – 41±5mmHg control vs 48±5mmHg ivabradine; 25 min recovery – 45±5mmHg control vs 45±5mmHg ivabradine).

3.2.5 Atrial natriuretic peptide and B-type natriuretic peptide levels

CT scores obtained for qPCR analysis are summarised in figure 6.14 below (see appendix B, table 8 for tabulated results).

Levels of ANP were variable and showed no significant change with ivabradine treatment. BNP levels were significantly higher in the ivabradine-treated group compared to the untreated group ($p=0.001$, $n=4$ and $n=5$ in TC control and TC with ivabradine treated groups respectively).

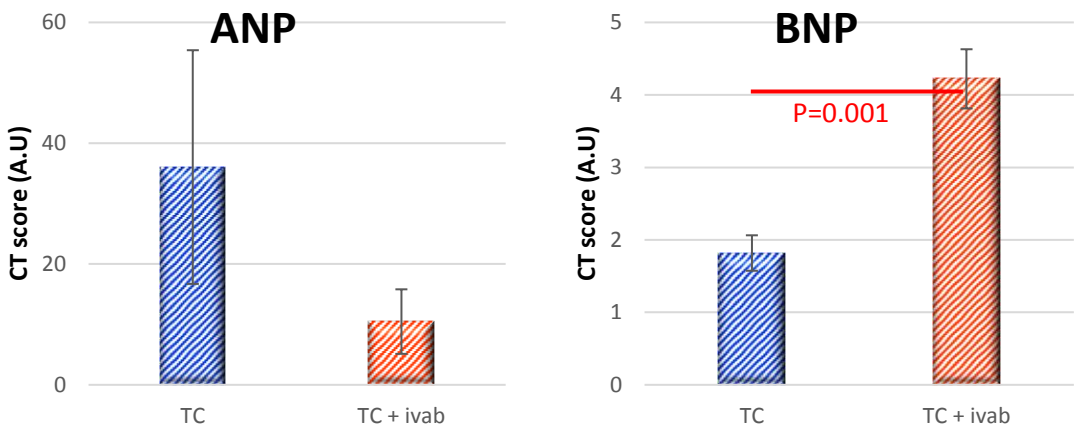

Figure 6.14: mRNA expression of ANP and BNP in mouse hearts subject to simulated TC, with ivabradine treatment. Administration of ivabradine significantly increased levels of BNP in a simulated model of Takotsubo cardiomyopathy. Abbreviations: ANP – atrial natriuretic peptide; A.U – arbitrary units; BNP – brain natriuretic peptide; ivab – ivabradine; mRNA – messenger ribonucleic acid; TC – Takotsubo cardiomyopathy. Control n =11, ivabradine n =6.

4. Discussion

4.1 Hypotensive acute heart failure

In this study, we aimed to evaluate the effect of HR modulation with ivabradine using an ex-vivo model of AHF. Modulation of HR with ivabradine during acute incidents (haemorrhagic shock) appears to improve cardiac function, as measures observed were closer to physiological levels with ivabradine treatment.

Our main findings were as follows:

- This model of simulated AHF is associated with a reduction in HR and LVDP, and an increase in systolic and diastolic pressures.
- Ivabradine administered during the acute phase of AHF improved LVDP compared to the control group.

Previous ex-vivo models on which we have based our design and experiments showed more severe outcomes following the AHF phase. The rat model described by Deshpande et al used a low

pressure insult with adrenaline (un-paced) for 35 min, followed by a 30 min recovery period – they reported a drop in function to ~3% during the acute phase, with overall functional recovery in their control group of ~15% [312]. The mouse model described by Breedt et al used a low pressure insult with pacing (no adrenaline) for 25 min, followed by a 25 min recovery period – they showed a drop in function to ~3% during the acute phase, with overall functional recovery in their control group of ~17% [446]. Our model showed a drop in function to ~8% during the acute phase, with overall functional recovery in the control group of 20 - 30%. We adjusted the timing of the low-pressure insult to give this approximate recovery, as it would allow scope to demonstrate benefit (increase in functional recovery) or detriment (decrease in functional recovery) with our intervention – either of which was possible. Additionally, the timing of 15 minutes used in the hypotensive model without pacing was chosen, as preliminary experiments with longer insults (18 min, 20 min, or 25min) caused hearts to die during the insult (data not shown).

As the experiments involved targeting the activity of the SA node, hearts were not paced. Without pacing, the intrinsic sensitivity of the heart is far more noticeable, and many factors that would otherwise be masked by pacing are evident. In the paced model used by Breedt et al, HR during the acute insult was well in excess of the stabilisation norm (>200%), and the same was true for recovery (~120%) [446], Our model did not show an increase, but rather a sustained decrease in HR both during and after the acute insult, similar to that demonstrated with the use of adrenaline in the model by Deshpande et al [312].

Our findings with the administration of ivabradine differ from previous publications – we showed a significant effect on lowering systolic pressure (at the onset of recovery) and a tendency to restore diastolic pressure, resulting in improvement of the LVDP with ivabradine, but no effect on HR [437,453]. This observation may be due to hearts being tested in isolation to the rest of the body, or perhaps it may be a secondary effect of the drug itself.

We were puzzled by the fact that we did not see any significant reduction of HR. However, similar findings have been reported in the context of ischaemia reperfusion (see Heusch et al)[454]. Our data suggest that the effect of ivabradine might be independent of its action on the sinoatrial node. Instead, the benefits derived from ivabradine in this ex-vivo model may be as a result of limiting cellular dysfunction due to ROS released into the myocardium. Ivabradine appears to oppose the activity of ROS, when the latter is released from mitochondria in response to cardiac stress – this anti-oxidant activity appears to be independent of HR reduction [454–456]. Ex-vivo experiments examining shear stress in aortic band demonstrated that acute administration of ivabradine linked to pathways involving activation of mammalian target of rapamycin complex (mTORC) 2 /Akt, and suppression of the pro-oxidative mTORC 1/ eNOS pathway [455]. It is therefore a possibility that regulation of these pathways by ivabradine (without significantly reducing HR) is the underlying mechanism involved in the cardioprotective effects in this acute setting.

The qPCR results for BNP tend to suggest that use of ivabradine in the setting of hypotensive AHF significantly increases transcription of the gene. This finding is counter-intuitive at first glance, but it must be taken into account that this method of quantification provides a snapshot in time, showing the transcription, but not necessarily translation of the BNP protein in these hearts. This snapshot is taken at the end of the recovery phase, and may be reflective of the greater loss of advantage seen with withdrawal of ivabradine over a shorter time, in the treated group.

BNP is a marker of adaptation, as it helps to maintain dimensions of the heart under stress, including hypertrophy and fibrosis. Levels of BNP, which are high in the setting of diabetes, have been shown to further increase with diastolic dysfunction [457]. Use of ivabradine in our model helped to maintain diastolic pressure, but withdrawal of ivabradine was followed by a rapid increase in diastolic pressure – considering the findings in the above-mentioned study, this may be a factor underlying the increase in BNP in the treated group.

In our model, ivabradine was only given during the acute phase of AHF. It would be of interest to check whether administration of ivabradine during the recovery phase (which would be more clinically relevant) could add further benefit.

In conclusion, our data suggest that administration of ivabradine during an acute, hypotensive HF phase results in an improvement of cardiac function during recovery and may benefit patients who suffer an acute episode of HF. Additionally, pre-clinical investigation in an in-vivo model of haemorrhagic shock which would take into account the possible role of sympathetic nervous activation would be required to confirm our novel findings.

4.2 Takotsubo cardiomyopathy

In this study, we aimed to 1) validate a model of TC using adrenaline and 2) evaluate the recovery in a novel ex-vivo model of TC with modification of HR by ivabradine. Our model, once established, showed that ivabradine, given during the acute TC incident, appears to improve cardiac function.

Our main findings were as follows:

- The model we have designed here mimics the adrenal action associated with TC, with reduced glucose and increased free-fatty acids as fuel as occurs in AHF (see chapter 1, section 1.5).

- In our isolated heart model, we observed patterns in response to adrenaline as described for TC – an initial increase in LVDP, followed by an exhaustive response where HR and LVDP drop.

- The model we have designed mimics a secondary incident of TC, as it does not reach full restoration of function. Even after the recovery phase starts, the events that occur only slightly improve, but mostly stabilise cardiac function, following the TC incident.

- Administration of ivabradine in this reductionist model of TC increased both systolic blood pressure and diastolic pressure, resulting in an increased LVDP during the insult,

This model of TC was adapted from the above model used for hypotensive AHF. The timing used in the TC model here was determined, in preliminary experiments, to be the most comparable to clinical description. Administration of 10 times the physiological dose of adrenaline (mimicking the clinical setting), together with change in the metabolic substrate produced a spike in LVDP as seen during the acute phase in patients. In preliminary experiments, heart exposed to longer TC insults (15 min, or 18 min) died during the recovery phase. Instead, we used a 12 min TC insult to mimic secondary TC – with incomplete recovery of cardiac function after restoration of metabolic compounds and withdrawal of adrenaline.

Surprisingly, our model did not show a spike in HR at the onset of the TC insult. It is possible that the excess of adrenaline perfused resulted in cellular absorption of the compound. A study conducted by Iversen et al clearly illustrated that higher concentrations of adrenaline in a perfusate buffer would have quicker uptake by cardiac tissue, and this might impair the expected activity of adrenaline [458], as it has to bind to the β1-adrenergic receptor at the cell surface in order to cause muscle contraction [458,459]. Once bound to β1-adrenergic receptors, adrenaline increases cardiac cell-membrane conductance to calcium ions (Ca^{2+}), allowing for more rapid, powerful heart muscle contractions [459]. With the addition of ivabradine to the perfusate, there may have been competitive binding at play which made the HR spike more apparent, as there may have been more adrenaline in the buffer available to bind to cell-surface β1-adrenergic receptors.

This model serves as a reductionist model. It is restrictive in some respects, as it is a model in an isolated heart and does not have full range of catecholaminergic responses elicited by the body in patients who experience TC. However, we are of the opinion that it shows sufficient similarity to the pathology, and can be used for proof of concept studies prior to in-vivo testing in small mammals.

Administration of ivabradine during the TC phase in this model improved LVDP, while better stabilising pressure during the latter part of the TC phase and early in recovery. These benefits were lost in the late phase of recovery during which ivabradine was not perfused. It is possible that ivabradine may benefit the heart if continued during the recovery phase as well.

Unfortunately, we were not able to evaluate the validity of maintained administration of ivabradine, as our experiments here were discontinued due to modification of the animal unit and breeding practices. There were changes in the strains, location and breeding of mice, each at a different time, and each factor of which would affect the reproducibility of our experiments. Housing and breeding locations of mice were scheduled to change internally at the University from a conventional breeding unit to an SPF unit – previous experience with animal experiments in which animals are housed in different places have shown us that they behave differently in response to cardiac insults, causing instability and inconsistency in function between groups based at each location. New mice were imported to start new strains which would be specifically bred in different unit at the University, thus, to continue tests with ivabradine during the recovery phases it would be necessary to restart experiments, as different strains react differently to cardiac insults [460]. This would have been a logical future direction, but would take far longer than the time allotted for a PhD, and as such it was not possible to test this idea. Nevertheless, we have established and validated a reductionist model of TC.

To our surprise, the qPCR results for BNP tend to suggest that use of ivabradine in the setting of TC significantly increases transcription of the gene, similar to our findings with hypotensive AHF. The same logic is applicable, as was discussed in chapter 6, section 4.1. Interestingly, a study which looked at circulating levels of BNP in patients with TC compared to those who had myocardial infarcts showed that between these pathologies, higher levels of BNP in TC did not correlate with greater cardiac haemodynamic failure [304].

As TC affects a greater proportion of women compared to that of men, it would have been useful to evaluate the model of TC we have developed here in female mouse hearts, (see chapter 1, section 3). However, we have used only male mice to evaluate this model of TC established here, as the study by Breedt et al examined a model similar to that of the AHF one used here, and found that the oestrous cycle in healthy females afforded healthy females an advantage in terms of recovery over healthy males [446]. In order to accurately evaluate the effect of the drug ivabradine, it was necessary to use males to avoid distortion of data due to oestrous cycles. Additionally, the age group for women who develop TC are mainly post-menopausal, and it was more beneficial to make use of male mice who do not experience the oestrous cycle, as they show similar patterns of susceptibility to cardiovascular insult as female mice who do not have healthy cycles [446].

5. Limitations

- One of the most notable limitations with the TC model was the limited catecholaminergic stimulation in our model compared to that found in the pathological setting in vitro. We administered adrenaline, while the human pathology would have adrenaline, noradrenaline, acetylcholine, and multiple other factors which are not enumerated here which would contribute to the phenotype in its entirety.
- Hearts were un-paced causing factors that would otherwise be masked – such as arrhythmias during stabilisation – to be more apparent.

6. Conclusion:

In this study, we have used an isolated heart model to validate 2 reductionist models of AHF: 1) a model of AHF mimicking haemorrhagic shock, and 2) a model of to excess adrenergic activation mimicking TC. In these models, we explored the effect of ivabradine, a well-known modulator of HR.

Administration of ivabradine during the acute phases of hypotension and TC, had effects on mechanical function which were most notable at the onset of recovery, and appeared to be independent of a reduction in heart rate.

Mechanisms of protection with ivabradine may involve activation of cardioprotective signalling pathways such as protein kinase B (Akt), and anti-oxidant pathways which ivabradine is known to activate [455]. Previous work that we have conducted in the laboratory has highlighted STAT3 activation as a possible target to protect in this model of AHF [461]. Further work will be required to delineate the possible cardioprotective mechanisms involved in the protective effect of ivabradine against AHF

Our findings here indicate that ivabradine could potentially improve the outcomes of acutely induced HF, an effect which might be further enhanced if ivabradine was also administered during the recovery phase. Further work using an in-vivo model of mimicking either haemorrhagic shock, or TC will be required to validate our findings.

Chapter 7
General conclusion and future work

Acute-onset heart failure is a burden disease with a high mortality rate. It has many aetiologies, and a standard set of agents which are recommended as a general treatment strategy to help with recovery after an acute event. During acute events themselves, there are very different approaches taken to try and stabilise patients and to limit damage. However, they still have poor outcomes as the mortality rate is very high. Modulation of HR with the sinoatrial node inhibitor, ivabradine, has successfully been shown to benefit patients suffering from chronic HF, but very little has been researched in patients suffering from AHF. Using different approaches, the main aim of this study was to explore the possible benefit of administering ivabradine in acute-onset HF.

1) A retrospective study was performed to evaluate the progression of HR in PPCM patients on standard recommended therapy at presentation, after 6 months, and 1 year of treatment (see Chapter 3).
2) A genetic mouse model of PPCM (STAT3 KO mice undergoing 3 pregnancies with weaning [196]) was used to explore the potential benefit of chronic treatment with ivabradine. (see Chapter 4).
3) An un-paced isolated heart model of AHF used to mimic clinical conditions of haemorrhagic shock and TC was adapted from rat hearts to mouse hearts, in order to test the potential benefit of ivabradine in these conditions. (see Chapter 6).

Our retrospective analysis highlighted an elevated HR in patients at presentation, with gradual improvement over the period of a year, but most patients still did not reach normal HR despite standard therapy. In this cohort, we observed a correlation between higher HR and poorer cardiac function – most prominently after 1 year of treatment. As an additive agent, ivabradine may help to modulate HR much earlier on and possibly assist in improving and maintaining cardiac function.

This is supported by a case study by Scadovi et al with a PPCM patient who manifested with cardiogenic shock had a HR of 180 BPM and severe hypotension. She did not respond to standard treatment interventions nor electrical cardioversion to restore sinus rhythm [462]. Her condition only began to improve when ivabradine was given, together with norepinephrine and inotropes, and continued to improve over the period of 18 months with ivabradine as part of her treatment program. Overall, these findings support the potential benefit of ivabradine as an additive agent in the setting of PPCM.

Following on from these findings, we explored the effect of sinoatrial node inhibition with ivabradine in a previously established mouse model of PPCM, where PPCM develops in mice with a cardiomyocyte-specific deletion of STAT3 after 3 pregnancies with weaning. Ivabradine showed its effect most prominently by reducing cardiac fibrosis, thus slowing ventricular remodelling (see figure 7.1). Surprisingly, we did not observe a significant reduction in HR with the use of ivabradine, as has been reported by other groups [437,463,464], suggesting that this effect on fibrosis may be independent of reducing HR. However, an important point to bear in mind is that mice have HR ranges approximately between 300 – 800 BPM [465], and there is great room for variability with such a large range. This variability may possibly have masked the HR-lowering effect of ivabradine when data are pooled from mice with cardiac dysfunction. When comparing our findings to those experiments conducted in-vivo by Custodis et al, from whence we had chosen our dosage, we did not find a clear reduction in HR with ivabradine as they did [437]. It must, however, be taken into account that they investigated signalling with ivabradine treatment in dyslipidemic mice, and had made use of tail-cuffs in conscious animals to record their data for HR, whereas our measurements were taken from TTEs when mice were under inhalant anaesthesia, which in itself alters HR [437,466].

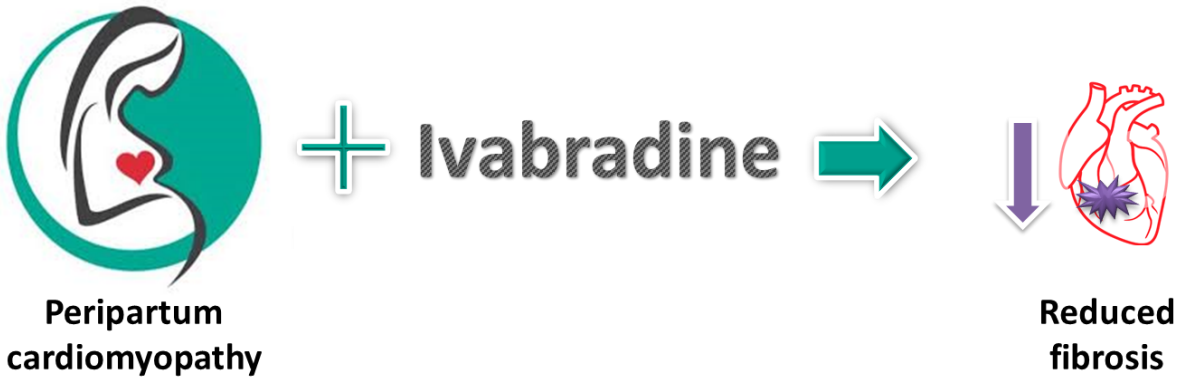

Figure 7.1: The potential use of ivabradine in the treatment of PPCM. Our findings in this study support the concept of using ivabradine in the setting of PPCM, for both the primary effect it has shown in clinical studies by others, in which it reduces HR of patients, but also because of the secondary effect we have illustrated here, where it assists in reducing fibrosis. Abbreviation: PPCM – peripartum cardiomyopathy

To our surprise, in our mouse model of PPCM, we found an unusual degree of cardiac dysfunction in the 'healthy' WT group – their functional parameters were similar to those of the PPCM mice. When comparing these mice to nulliparous mice from the same genetic backgrounds (both PPCM and 'healthy' WT), out findings strongly suggested that the stress of 3 consecutive pregnancies, without time to recover, induced cardiac dysfunction in healthy mice, which left their functional parameters recorded for TTE remarkably similar to those seen in PPCM mice. Future research involving this model may require that matings are timed with a recovery period for mice so as not to compound dysfunction in WT mice. This novel finding brings the question as to whether women who have multiple, consecutive pregnancies without significant recovery time in between pregnancies may have an increased risk of CVD.

In our ex-vivo experiments, we found that ivabradine administered during the acute phase showed beneficial effects on mechanical function at the onset of the recovery phase. These gain of advantage effects could potentially be magnified or sustained if ivabradine was to be given during the recovery phase. This echoes the report of cardiogenic shock in response to ivabradine as seen in the PPCM case reported by Scardovi et al (see above), whose poor mechanical function improved

with ivabradine as an agent, and was maintained as she continued to take ivabradine as part of her treatment following her acute incident [462].

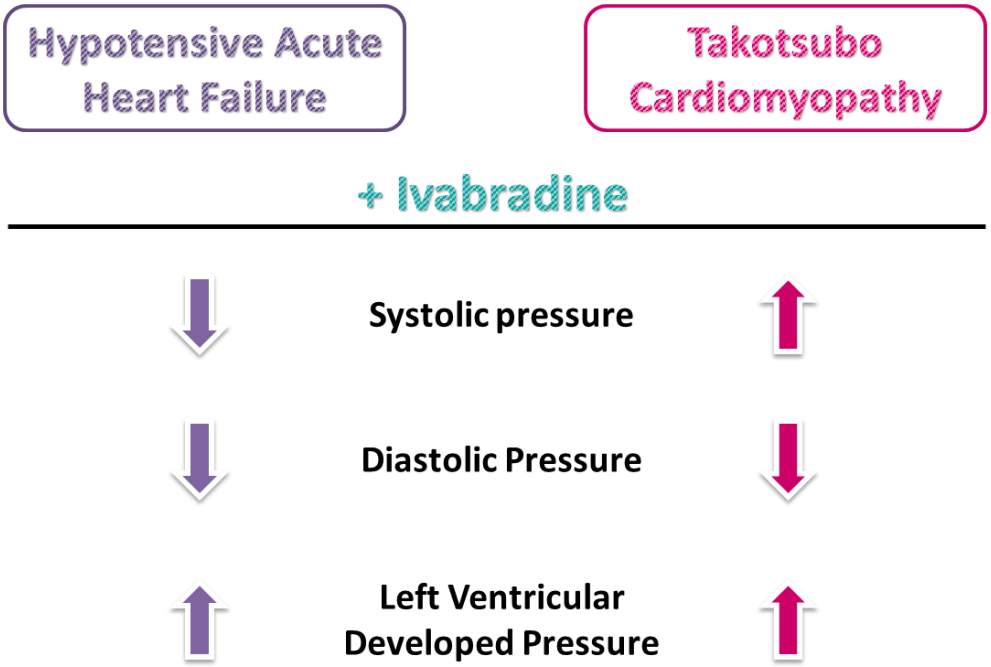

Figure 7.2: The effect of ivabradine in ex-vivo mouse models of hypotensive acute heart failure, and Takotsubo cardiomyopathy. Our findings in these studies show the effects of ivabradine on systolic and diastolic pressure, as well as left ventricular developed pressure.

In our ex-vivo studies, our findings with use of ivabradine during the acute phase – with low pressure for the hypotensive (haemorrhagic) heart failure model, and excess adrenaline for the TC model - support the notion that the sinoatrial node plays a distinct role in acutely-induced heart failure. Administration of ivabradine during these phases, to modulate the sinoatrial node, had effects on mechanical function which improved LVDP (see figure 7.2). The path forward on these models would be to administer ivabradine not just during the acute phase, but also during the recovery phase, to see whether it would sustain or improve function. Thereafter, the timing of ivabradine use would allow for the investigation of a mechanistic pathway of action.

The reduction in fibrosis associated with a chronic treatment of ivabradine did not correlate with levels of mRNA transcripts of pathways known to be involved in remodelling and long-term heart

failure. However, levels of mRNA transcripts are a reflection of gene transcription prior to translation into proteins in the cell, and there are many post-transcriptional modifications. Thus, the pathways involved in this anti-fibrotic activity of ivabradine are yet unclear. We propose that it is likely to work via a pathway independent of the sinoatrial node / heart rate, or STAT3 activity. Possibly, it exerts its effect on remodelling via suppression of the PI3K/Akt pathway in a chronic setting [440]. An additional pathway which may contribute to the effects of long-term treatment with ivabradine could involve micro-RNA's, miR-1 and miR-133, which modulate post-transcriptional expression of HCN2 and HCN4 genes. These micro-RNA's have been shown to be significantly increased in cardiomyocytes of rats with myocardial infarctions who were chronically treated with ivabradine [467].

Notably, in a short-term setting, ivabradine has also been shown to reduce ROS activity, thereby preventing oxidative stress and endothelial inflammation [455]. In animal models of ischemia-reperfusion, administration of ivabradine helped to reduce infarct size, even without HR reduction – an effect attributed to a reduction in ROS formation in mitochondria [454]. The mechanism of this antioxidant activity of ivabradine is proposed to work via activation of mTORC2 /Akt, together with suppression of the pro-oxidative mTORC 1/ eNOS pathway [455].

Mitochondrial dynamics and the pathways linked to mitochondrial function may also be linked to both short- and long-term effects of ivabradine. ROS often originates in the mitochondria [456], and long-term damage caused by ROS is known to be involved in the formation of fibrotic scars in the heart in certain contexts [468–471]. The mitochondria in particular would be an interesting point to investigate, as a study in dyslipidaemic mice illustrated an effect on glucose metabolism with the use of ivabradine which did not occur with the use of a beta-blocker, despite a similar reduction of HR in both cases [464].

In summary, our clinical study highlighted the correlation of high HR with worse outcomes in PPCM, and illustrated the potential place that ivabradine could fill to improve the current recommended treatment of HF. Our animal experiments, both in-vivo and ex-vivo, have shown that ivabradine has had beneficial effects in all of these models, diverse in nature as they are. The outcomes with ivabradine highlight the flexibility of use of the drug – it is already used in the management of angina, and it could potentially be used as an additive agent in acute cases of cardiac dysfunction to help stabilise patients, or in a more chronic setting to maintain or improve cardiac function, and also to prevent pathological remodelling. Much work is still required to take these ideas from rodent models through to clinical application, but these models are a first point of reference to direct future research with the use of ivabradine in AHF – the beneficial effects may be much more than just targeting HR.

Publications

1. Peer-reviewed journal articles

2018	Title	**Sphingosine-1-phosphate (S1P) activates STAT3 to protect against de novo acute heart failure (AHF)**
	Publication	*Life Sciences*. 2018. 196: p. 127 - 132
	Authors	Gaurang P Deshpande, Aqeela Imamdin, Sandrine Lecour, Lionel Opie
2017	Title	**Heart rate – a novel target for treatment of peripartum cardiomyopathy?**
	Publication	*Journal of the South African Heart Association*. 2017. 13(4): p. 304 - 307
	Authors	Aqeela Imamdin, Sandrine Lecour, Lionel Opie, Karen Sliwa and Feriel Azibani
2014	Title	**Cardiac preconditioning with sphingosine-1-phosphate requires activation of signal transducer and activator of transcription-3**
	Publication	*Cardiovascular Journal of Africa. 2014. 25(3): p. 118 - 123*
	Authors	Roisin F Kelly-Laubscher, Jonathan C King, Damian Hacking, Sarin Somers, Samantha Hastie, Tessa Stewart, Aqeela Imamdin, Gerald Maarman, Sarah Pedretti, Sandrine Lecour

2. Conference proceedings

2017	Title	**The potential effect of modulating heart rate on cardiac remodelling in peripartum cardiomyopathy**
	Conference proceeding	*The annual meeting of the ESC Working Group on Myocardial Function and the ESC Working Group on Cellular Biology of the Heart, Varenna, Italy, May 2017*
	Authors	Aqeela Imamdin, Feriel Azibani, Nkanyiso Hadebe, Lionel Opie, Karen Sliwa and Sandrine Lecour
2015	Title	**Heart rate as a novel target for peripartum cardiomyopathy**
	Conference proceeding	*43rd Annual conference of the Physiological Society of Southern Africa, Parys, South Africa, September 2015*
	Authors	Aqeela Imamdin, Sandrine Lecour, Lionel Opie, Karen Sliwa
2013	Title	**STAT3 - a position dependent gene knock-out model with age**
	Conference proceeding	*37th congress of the International Union of Physiological Sciences, Birmingham, United Kingdom, July 2013*
	Authors	Aqeela Imamdin, Joy McCarthy, Sandrine Lecour, Karen Sliwa, Neil Davies

2012	Title	**STAT3 and heart failure with age: A position-dependent gene knock-out model in mice**
	Conference proceeding	*6th international congress of the African Association of Physiological Sciences, Ismailia, Egypt, September 2012*
	Authors	Aqeela Imamdin, Joy McCarthy, Sandrine Lecour, Karen Sliwa, Neil Davies
2012	Title	**Glucose and insulin: emerging metabolic therapy against acute heart failure**
	Conference proceeding	*10th Annual Meeting of the Society for Heart and vascular Metabolism, United Kingdom, July 2012*
	Authors	Gaurang P Deshpande, Sandrine Lecour, Aqeela Imamdin and Lionel H Opie

References

1. Katz, A. M. Evolving concepts of heart failure: Cooling furnace, malfunctioning pump, enlarging muscle—Part I. *J. Card. Fail.* **3,** 319–334 (1997).
2. Ventura, H. O., Mehra, M. R. & Young, J. B. Bloodletting as a cure for dropsy: heart failure down the ages. *J. Card. Fail.* **11,** 247–52 (2005).
3. Wilkins, M. R., Kendall, M. J. & Wade, O. L. William Withering and digitalis, 1785 to 1985. *Br. Med. J. (Clin. Res. Ed).* **290,** 7–8 (1985).
4. Withering, W. *An Account of the Foxglove and some of its Medical Uses With Practical Remarks on Dropsy and Other Diseases*. (Cambridge University Press, 1785). at <http://www.gutenberg.org/files/24886/24886-h/24886-h.htm>
5. Dawber, T. R., Meadors, G. F. & Moore, F. E. Epidemiological Approaches to Heart Disease: The Framingham Study. *Am. J. Public Heal. Nations Heal.* **41,** 279–286 (1951).
6. Wolf, P. A., Abbott, R. D. & Kannel, W. B. Atrial fibrillation as an independent risk factor for stroke: the Framingham Study. *Stroke* **22,** 983–988 (1991).
7. WB, K. & DL, M. Diabetes and cardiovascular disease: The framingham study. *JAMA* **241,** 2035–2038 (1979).
8. Myers, R. H., Kiely, D. K., Cupples, L. A. & Kannel, W. B. Parental history is an independent risk factor for coronary artery disease: The Framingham Study. *Am. Heart J.* **120,** 963–969 (1990).
9. Sacco, R. L. *et al.* Subarachnoid and intracerebral hemorrhage: Natural history, prognosis, and precursive factors in the Framingham Study . *Neurol.* **34,** 847 (1984).
10. Kannel, W. B. & Feinleib, M. Natural history of angina pectoris in the Framingham study. *Am. J. Cardiol.* **29,** 154–163 (1972).
11. McKee, P. A., Castelli, W. P., McNamara, P. M. & Kannel, W. B. The Natural History of Congestive Heart Failure: The Framingham Study. *N. Engl. J. Med.* **285,** 1441–1446 (1971).
12. Story, C. & Cherney, K. The History of Heart Disease. *Healthline* (2016). at <http://www.healthline.com/health/heart-disease/history>
13. Shoja, M. M. *et al.* Leonardo da Vinci's studies of the heart. *Int. J. Cardiol.* **167,** 1126–1133 (2013).
14. Ribatti, D. William Harvey and the discovery of the circulation of the blood. *J. Angiogenes. Res.* **1,** 3 (2009).
15. Skalski, J. H. Myocardial infarction and angina pectoris in the history of Polish medicine. *Pol Arch Med Wewn* **118,** 243–247 (2008).
16. Davis, R. C., Hobbs, F. D. R. & Lip, G. Y. H. History and epidemiology. *BMJ Br. Med. J.* **320,** 39–42 (2000).
17. Cohn, J. N. The management of chronic heart failure. *N. Engl. J. Med.* **335,** 490–498 (1996).
18. Ponikowski, P. *et al.* ESC Guidelines for the diagnosis and treatment of acute and chronic heart failure 2008. *Eur. J. Heart Fail.* 933–989 (2016). doi:10.1016/j.ejheart.2008.08.005
19. Dickstein, K. *et al.* ESC Guidelines for the diagnosis and treatment of acute and chronic heart failure 2008. *Eur. J. Heart Fail.* 933–989 (2008). doi:10.1016/j.ejheart.2008.08.005
20. Damasceno, A., Mayosi, B., Sani, M. & Al, E. The causes, treatment, and outcome of acute heart failure in 1006 africans from 9 countries: Results of the sub-saharan africa survey of heart failure. *Arch. Intern. Med.* **172,** 1386–1394 (2012).
21. Ogah, O. S. & Falase, A. O. in (ed. Kirali, K. B. T.-C.-T. and T.) Ch. 16 (InTech, 2017). doi:10.5772/67023
22. Ponikowski, P. *et al.* ESC Guidelines for the diagnosis and treatment of acute and chronic heart failure 2008. *Eur. J. Heart Fail.* 933–989 (2016). doi:10.1016/j.ejheart.2008.08.005
23. Lyon, A. R., Rees, P. S. C., Prasad, S., Poole-Wilson, P. A. & Harding, S. E. Stress (Takotsubo) cardiomyopathy - a novel pathophysiological hypothesis to explain catecholamine-induced acute myocardial stunning. *Nat Clin Pr. Cardiovasc Med* **5,** 22–29 (2008).
24. Lyon, A. R. *et al.* Current state of knowledge on Takotsubo syndrome: a Position Statement from the Taskforce on Takotsubo Syndrome of the Heart Failure Association of the European Society of Cardiology. *Eur. J. Heart Fail.* **18,** 8–27 (2016).

25. De Luca, L. *et al.* Acute heart failure syndromes: clinical scenarios and pathophysiologic targets for therapy. *Heart Fail. Rev.* **12,** 97–104 (2007).
26. Kjekshus, J. *et al.* Rosuvastatin in older patients with systolic heart failure. *N. Engl. J. Med.* **357,** 2248–2261 (2007).
27. Nieminen, M. S. *et al.* EuroHeart Failure Survey II (EHFS II): a survey on hospitalized acute heart failure patients: description of population. *Eur. Heart J.* **27,** 2725–2736 (2006).
28. Mosterd, A. & Hoes, A. W. Clinical epidemiology of heart failure. *Heart* **93,** 1137 LP-1146 (2007).
29. Carita, P., Fazio, G. & Novo, G. Takotsubo cardiomyopathy. *E-journal Cardiol. Pract.* **8,** (2010).
30. Nohria, A. *et al.* Clinical assessment identifies hemodynamic profiles that predict outcomes in patients admitted with heart failure. *J. Am. Coll. Cardiol.* **41,** 1797–1804 (2003).
31. Stevenson, L. W. Design of therapy for advanced heart failure. *Eur. J. Heart Fail.* **7,** 323–331 (2005).
32. Ganiats, T. G., Browner, D. K. & Dittrich, H. C. Comparison of Quality of Well-Being scale and NYHA functional status classification in patients with atrial fibrillation. *Am. Heart J.* **135,** 819–824 (1998).
33. Butler, J. *et al.* Developing Therapies for Heart Failure With Preserved Ejection Fraction. *JACC Hear. Fail.* **2,** 97–112 (2014).
34. Abebe, T. B., Gebreyohannes, E. A., Tefera, Y. G. & Abegaz, T. M. Patients with HFpEF and HFrEF have different clinical characteristics but similar prognosis: a retrospective cohort study. *BMC Cardiovasc. Disord.* **16,** 232 (2016).
35. Redfield, M. *et al.* Burden of systolic and diastolic ventricular dysfunction in the community: Appreciating the scope of the heart failure epidemic. *JAMA* **289,** 194–202 (2003).
36. Philbin, E. F., Rocco, T. A., Lindenmuth, N. W., Ulrich, K. & Jenkins, P. L. Systolic versus diastolic heart failure in community practice: clinical features, outcomes, and the use of angiotensin-converting enzyme inhibitors. *Am. J. Med.* **109,** 605–613 (2000).
37. van Riet, E. E. S. *et al.* Prevalence of unrecognized heart failure in older persons with shortness of breath on exertion. *Eur. J. Heart Fail.* **16,** 772–777 (2014).
38. Thomas, J. T. *et al.* Utility of history, physical examination, electrocardiogram, and chest radiograph for differentiating normal from decreased systolic function in patients with heart failure. *Am. J. Med.* **112,** 437–445 (2002).
39. Davie, A. P. *et al.* Value of the electrocardiogram in identifying heart failure due to left ventricular systolic dysfunction. *BMJ Br. Med. J.* **312,** 222 (1996).
40. Kelder, J. C. *et al.* The Diagnostic Value of Physical Examination and Additional Testing in Primary Care Patients With Suspected Heart Failure. *Circulation* **124,** 2865 LP-2873 (2011).
41. Maisel, A. *et al.* State of the art: Using natriuretic peptide levels in clinical practice. *Eur. J. Heart Fail.* **10,** 824–839 (2008).
42. Hawkins, N. M. *et al.* Heart failure and chronic obstructive pulmonary disease: diagnostic pitfalls and epidemiology. *Eur. J. Heart Fail.* **11,** 130–139 (2009).
43. Zaphiriou, A. *et al.* The diagnostic accuracy of plasma BNP and NTproBNP in patients referred from primary care with suspected heart failure: Results of the UK natriuretic peptide study. *Eur. J. Heart Fail.* **7,** 537–541 (2005).
44. Berger, R. *et al.* B-Type Natriuretic Peptide Predicts Sudden Death in Patients With Chronic Heart Failure. *Circulation* **105,** 2392 LP-2397 (2002).
45. Clerico, A. *et al.* Circulating levels of cardiac natriuretic peptides (ANP and BNP) measured by highly sensitive and specific immunoradiometric assays in normal subjects and in patients with different degrees of heart failure. *J. Endocrinol. Invest.* **21,** 170–179 (1998).
46. Yoshimura, M. *et al.* Different secretion patterns of atrial natriuretic peptide and brain natriuretic peptide in patients with congestive heart failure. *Circulation* **87,** 464 LP-469 (1993).
47. Ojji, D. B. *et al.* The effect of left ventricular remodelling on soluble ST2 in a cohort of hypertensive subjects. *J. Hum. Hypertens.* **28,** 432 (2014).
48. Missov, E., Calzolari, C. & Pau, B. Circulating Cardiac Troponin I in Severe Congestive Heart Failure. *Circulation* **96,** 2953 LP-2958 (1997).
49. CR, deFilippi, JA, de L., RH, C. & al, et. Association of serial measures of cardiac troponin t using a

sensitive assay with incident heart failure and cardiovascular mortality in older adults. *JAMA* **304,** 2494–2502 (2010).
50. Redfield, M. M. *et al.* Plasma brain natriuretic peptide concentration: impact of age and gender. *J. Am. Coll. Cardiol.* **40,** 976–982 (2002).
51. Raymond, I. *et al.* The influence of age, sex and other variables on the plasma level of N-terminal pro brain natriuretic peptide in a large sample of the general population. *Heart* **89,** 745 LP-751 (2003).
52. Wang, T. J. *et al.* Impact of age and sex on plasma natriuretic peptide levels in healthy adults. *Am. J. Cardiol.* **90,** 254–258 (2002).
53. Krim, S. R. *et al.* Racial/Ethnic Differences in B-Type Natriuretic Peptide Levels and Their Association With Care and Outcomes Among Patients Hospitalized With Heart Failure: Findings From Get With The Guidelines–Heart Failure. *JACC Hear. Fail.* **1,** 345–352 (2013).
54. Benjamin, E. J. *et al.* Heart Disease and Stroke Statistics—2017 Update: A Report From the American Heart Association. *Circulation* **135,** e146 LP-e603 (2017).
55. Bleumink, G. S. *et al.* Quantifying the heart failure epidemic: prevalence, incidence rate, lifetime risk and prognosis of heart failureThe Rotterdam Study. *Eur. Heart J.* **25,** 1614–1619 (2004).
56. Ceia, F. *et al.* Prevalence of chronic heart failure in Southwestern Europe: the EPICA study. *Eur. J. Heart Fail.* **4,** 531–539 (2002).
57. Gerber, Y., Weston, S., Redfield, M. & Al, E. A contemporary appraisal of the heart failure epidemic in olmsted county, minnesota, 2000 to 2010. *JAMA Intern. Med.* **175,** 996–1004 (2015).
58. Owan, T. E. *et al.* Trends in Prevalence and Outcome of Heart Failure with Preserved Ejection Fraction. *N. Engl. J. Med.* **355,** 251–259 (2006).
59. Crespo-Leiro, M. G. *et al.* European Society of Cardiology Heart Failure Long-Term Registry (ESC-HF-LT): 1-year follow-up outcomes and differences across regions. *Eur. J. Heart Fail.* **18,** 613–625 (2016).
60. Kontogeorgos, S., Thunström, E., Johansson, M. C. & Fu, M. Heart failure with preserved ejection fraction has a better long-term prognosis than heart failure with reduced ejection fraction in old patients in a 5-year follow-up retrospective study. *Int. J. Cardiol.* **232,** 86–92 (2017).
61. Bonsu, K. O., Owusu, I. K., Buabeng, K. O., Reidpath, D. D. & Kadirvelu, A. Clinical characteristics and prognosis of patients admitted for heart failure: A 5-year retrospective study of African patients. *Int. J. Cardiol.* **238,** 128–135 (2017).
62. Ntusi, N. B. A. & Mayosi, B. M. Epidemiology of heart failure in sub-Saharan Africa. *Expert Rev. Cardiovasc. Ther.* **7,** 169–180 (2009).
63. Stewart, S., Karen, S., Mocumbi, A., Damasceno, A. & Ntsekhe, M. *The heart of Africa: clinical profile of an evolving burden of heart disease in Africa*. (John Wiley & Sons, 2016). doi:10.1002/9781119097136
64. Forouzanfar, M. H. *et al.* Prevalence of heart failure by cause in 21 regioins: Global burden of diseases, injuries and risk factors - 2010 study. *J. Am. Coll. Cardiol.* **61,** E786 (2013).
65. Cook, C., Cole, G., Asaria, P., Jabbour, R. & Francis, D. P. The annual global economic burden of heart failure. *Int. J. Cardiol.* **171,** 368–376 (2014).
66. Omran, A. R. The Epidemiologic Transition: A Theory of the Epidemiology of Population Change. *Milbank Q.* **83,** 731–757 (2005).
67. Dalal, S. *et al.* Non-communicable diseases in sub-Saharan Africa: what we know now. *Int. J. Epidemiol.* **40,** 885–901 (2011).
68. Cosnett, J. E. Heart disease in the Zulu: Especially cardiomyopathy and cardiac infarction. *Br. Heart J.* **24,** 76 LP-82 (1962).
69. Hellermann, J. P. *et al.* Heart failure after myocardial infarction: Prevalence of preserved left ventricular systolic function in the community. *Am. Heart J.* **145,** 742–748 (2003).
70. Maggioni, A. P. *et al.* EURObservational Research Programme: regional differences and 1-year follow-up results of the Heart Failure Pilot Survey (ESC-HF Pilot). *Eur. J. Heart Fail.* **15,** 808–17 (2013).
71. Mann, D. L., Felker, G. M., Sliwa, K. & Stewart, S. *Heart failure: a companion to Braunwald's heart disease*. (Elsevier Health Sciences, 2014).
72. Taegtmeyer, H., Sen, S. & Vela, D. Return to the fetal gene program. *Ann. N. Y. Acad. Sci.* **1188,** 191–

198 (2010).
73. Kurabayashi, M., Tsuchimochi, H., Komuro, I., Takaku, F. & Yazaki, Y. Molecular cloning and characterization of human cardiac alpha-and beta-form myosin heavy chain complementary DNA clones. Regulation of expression during development and pressure overload in human atrium. *J. Clin. Invest.* **82,** 524 (1988).
74. Everett, A. W. Isomyosin expression in human heart in early pre- and post-natal life. *J. Mol. Cell. Cardiol.* **18,** 607–615 (1986).
75. Reiser, P. J., Portman, M. A., Ning, X.-H. & Moravec, C. S. Human cardiac myosin heavy chain isoforms in fetal and failing adult atria and ventricles. *Am. J. Physiol. - Hear. Circ. Physiol.* **280,** H1814 LP-H1820 (2001).
76. Sack, M. N., Disch, D. L., Rockman, H. A. & Kelly, D. P. A role for Sp and nuclear receptor transcription factors in a cardiac hypertrophic growth program. *Proc. Natl. Acad. Sci.* **94,** 6438–6443 (1997).
77. van Rooij, E., Liu, N. & Olson, E. N. MicroRNAs flex their muscles. *Trends Genet.* **24,** 159–166 (2008).
78. Razeghi, P. *et al.* Metabolic Gene Expression in Fetal and Failing Human Heart. *Circulation* **104,** 2923 LP-2931 (2001).
79. Ørtenblad, N., Nielsen, J., Saltin, B. & Holmberg, H.-C. Role of glycogen availability in sarcoplasmic reticulum Ca(2+) kinetics in human skeletal muscle. *J. Physiol.* **589,** 711–725 (2011).
80. Heusch, G., Schulz, R. & Rahimtoola, S. H. Myocardial hibernation: a delicate balance. *Am. J. Physiol. - Hear. Circ. Physiol.* **288,** H984 LP-H999 (2005).
81. Matsui, T., Nagoshi, T. & Rosenzweig, A. Akt and PI 3-Kinase Signaling in Cardiomyocyte Hypertrophy and Survival. *Cell Cycle* **2,** 219–222 (2003).
82. Jonassen, A. K., Mjøs, O. D. & Sack, M. N. p70s6 kinase is a functional target of insulin activated Akt cell-survival signaling. *Biochem. Biophys. Res. Commun.* **315,** 160–165 (2004).
83. Sack, M. N. & Yellon, D. M. Insulin therapy as an adjunct to reperfusion after acute coronary ischemia: A proposed direct myocardial cell survival effect independent of metabolic modulation. *J. Am. Coll. Cardiol.* **41,** 1404–1407 (2003).
84. Whiteman, E. L., Cho, H. & Birnbaum, M. J. Role of Akt/protein kinase B in metabolism. *Trends Endocrinol. Metab.* **13,** 444–451 (2002).
85. Gottlob, K. *et al.* Inhibition of early apoptotic events by Akt/PKB is dependent on the first committed step of glycolysis and mitochondrial hexokinase. *Genes Dev.* **15,** 1406–1418 (2001).
86. Cook, S. A., Matsui, T., Li, L. & Rosenzweig, A. Transcriptional effects of chronic Akt activation in the heart. *J. Biol. Chem.* **277,** 22528–33 (2002).
87. M., V. P., H., S., M., F. & C., T. E. H. Endothelial dysfunction and vascular disease – a 30th anniversary update. *Acta Physiol.* **219,** 22–96 (2016).
88. Heitzer, T., Schlinzig, T., Krohn, K., Meinertz, T. & Münzel, T. Endothelial Dysfunction, Oxidative Stress, and Risk of Cardiovascular Events in Patients With Coronary Artery Disease. *Circulation* **104,** 2673 LP-2678 (2001).
89. Cai, H. & Harrison, D. G. Endothelial Dysfunction in Cardiovascular Diseases: The Role of Oxidant Stress. *Circ. Res.* **87,** 840 LP-844 (2000).
90. Landmesser, U. *et al.* Vascular Oxidative Stress and Endothelial Dysfunction in Patients With Chronic Heart Failure. *Circulation* **106,** 3073 LP-3078 (2002).
91. Suwaidi, J. Al *et al.* Long-Term Follow-Up of Patients With Mild Coronary Artery Disease and Endothelial Dysfunction. *Circulation* **101,** 948 LP-954 (2000).
92. Katz, S. D. *et al.* Vascular Endothelial Dysfunction and Mortality Risk in Patients With Chronic Heart Failure. *Circulation* **111,** 310 LP-314 (2005).
93. Eghbali, M., Wang, Y., Toro, L. & Stefani, E. Heart Hypertrophy During Pregnancy: A Better Functioning Heart? *Trends Cardiovasc. Med.* **16,** 285–291 (2006).
94. Schannwell, C. M. *et al.* Left Ventricular Hypertrophy and Diastolic Dysfunction in Healthy Pregnant Women. *Cardiology* **97,** 73–78 (2002).
95. Bueno, O. F. *et al.* The MEK1–ERK1/2 signaling pathway promotes compensated cardiac hypertrophy in transgenic mice. *EMBO J.* **19,** 6341–6350 (2000).

96. Modesti, P. A. *et al.* Release of preformed Ang II from myocytes mediates angiotensinogen and ET-1 gene overexpression in vivo via AT1 receptor. *J. Mol. Cell. Cardiol.* **34,** 1491–1500 (2002).
97. Matsui, T. & Rosenzweig, A. Convergent signal transduction pathways controlling cardiomyocyte survival and function: the role of PI 3-kinase and Akt. *J. Mol. Cell. Cardiol.* **38,** 63–71 (2005).
98. Kehat, I. & Molkentin, J. D. Molecular pathways underlying cardiac remodeling during pathophysiological stimulation. *Circulation* **122,** 2727–2735 (2010).
99. Kishimoto, I. *et al.* Natriuretic Peptide Signaling via Guanylyl Cyclase (GC)-A: An Endogenous Protective Mechanism of the Heart. *Curr. Cardiol. Rev.* **5,** 45–51 (2009).
100. Chen, Z. & Han, Z. C. STAT3: A critical transcription activator in angiogenesis. *Med. Res. Rev.* **28,** 185–200 (2008).
101. Niu, G. *et al.* Constitutive Stat3 activity up-regulates VEGF expression and tumor angiogenesis. *Oncogene* **21,** 2000 (2002).
102. Wei, D. *et al.* Stat3 activation regulates the expression of vascular endothelial growth factor and human pancreatic cancer angiogenesis and metastasis. *Oncogene* **22,** 319–329 (2002).
103. Hilfiker-Kleiner, D. *et al.* Signal Transducer and Activator of Transcription 3 Is Required for Myocardial Capillary Growth, Control of Interstitial Matrix Deposition, and Heart Protection From Ischemic Injury. *Circ. Res.* **95,** 187 LP-195 (2004).
104. Inoki, I. *et al.* Connective tissue growth factor binds vascular endothelial growth factor (VEGF) and inhibits VEGF-induced angiogenesis. *FASEB J.* **16,** 219–221 (2002).
105. Jacoby, J. J. *et al.* Cardiomyocyte-restricted knockout of STAT3 results in higher sensitivity to inflammation, cardiac fibrosis, and heart failure with advanced age. *Proc. Natl. Acad. Sci.* **100,** 12929–12934 (2003).
106. Bloomston, M., Shafii, A., Zervos, E. E. & Rosemurgy, A. S. TIMP-1 Overexpression in Pancreatic Cancer Attenuates Tumor Growth, Decreases Implantation and Metastasis, and Inhibits Angiogenesis. *J. Surg. Res.* **102,** 39–44 (2002).
107. Chua, C. C., Hamdy, R. C. & Chua, B. H. L. Regulation of thrombospondin-1 production by angiotensin II in rat heart endothelial cells. *Biochim. Biophys. Acta - Mol. Cell Res.* **1357,** 209–214 (1997).
108. Ohnishi, H. *et al.* Increased Expression of Connective Tissue Growth Factor in the Infarct Zone of Experimentally Induced Myocardial Infarction in Rats. *J. Mol. Cell. Cardiol.* **30,** 2411–2422 (1998).
109. Trueblood, N. A. *et al.* Exaggerated Left Ventricular Dilation and Reduced Collagen Deposition After Myocardial Infarction in Mice Lacking Osteopontin. *Circ. Res.* **88,** 1080 LP-1087 (2001).
110. Opie, L. H., Commerford, P. J., Gersh, B. J. & Pfeffer, M. A. Controversies in ventricular remodelling. *Lancet* **367,** 356–367 (2006).
111. Paterson, B. M. & Eldridge, J. D. Alpha-Cardiac actin is the major sarcomeric isoform expressed in embryonic avian skeletal muscle. *Science (80-.).* **224,** 1436–1439 (1984).
112. Hewett, T. E., Grupp, I. L., Grupp, G. & Robbins, J. Alpha-skeletal actin is associated with increased contractility in the mouse heart. *Circ. Res.* **74,** 740 LP-746 (1994).
113. Schwartz, K. *et al.* Alpha-skeletal muscle actin mRNA's accumulate in hypertrophied adult rat hearts. *Circ. Res.* **59,** 551 LP-555 (1986).
114. Hayward, L. J. & Schwartz, R. J. Sequential expression of chicken actin genes during myogenesis. *J. Cell Biol.* **102,** 1485–1493 (1986).
115. Ordahl, C. P. The skeletal and cardiac α-action genes are coexpressed in early embryonic striated muscle. *Dev. Biol.* **117,** 488–492 (1986).
116. Gunning, P., Ponte, P., Blau, H. & Kedes, L. alpha-skeletal and alpha-cardiac actin genes are coexpressed in adult human skeletal muscle and heart. *Mol. Cell. Biol.* **3,** 1985–1995 (1983).
117. Chaponnier, C. & Gabbiani, G. Monoclonal antibodies against muscle actin isoforms: epitope identification and analysis of isoform expression by immunoblot and immunostaining in normal and regenerating skeletal muscle. *F1000Research* **5,** 416 (2016).
118. Banfi, C. *et al.* Neurohormonal activation is associated with increased levels of plasma matrix metalloproteinase-2 in human heart failure. *Eur. Heart J.* **26,** 481–488 (2005).
119. Tamura, N. *et al.* Cardiac fibrosis in mice lacking brain natriuretic peptide. *Proc. Natl. Acad. Sci.* **97,**

4239–4244 (2000).
120. Depre, C. *et al.* Unloaded heart in vivo replicates fetal gene expression of cardiac hypertrophy. *Nat Med* **4,** 1269–1275 (1998).
121. Rajabi, M., Kassiotis, C., Razeghi, P. & Taegtmeyer, H. Return to the fetal gene program protects the stressed heart: a strong hypothesis. *Heart Fail. Rev.* **12,** 331–343 (2007).
122. van Berlo, J. H. *et al.* Signaling effectors underlying pathologic growth and remodeling of the heart. *J. Clin. Invest.* **123,** 37–45 (2013).
123. Ashrafian, H., Frenneaux, M. P. & Opie, L. H. Metabolic mechanisms in heart failure. *Circulation* **116,** 434–448 (2007).
124. Rundqvist, B., Elam, M., Bergmann-Sverrisdottir, Y., Eisenhofer, G. & Friberg, P. Increased Cardiac Adrenergic Drive Precedes Generalized Sympathetic Activation in Human Heart Failure. *Circulation* **95,** 169 LP-175 (1997).
125. Oka, T. *et al.* Genetic Manipulation of Periostin Expression Reveals a Role in Cardiac Hypertrophy and Ventricular Remodeling. *Circ. Res.* **101,** 313 LP-321 (2007).
126. Sassoon, D. A., Garner, I. & Buckingham, M. Transcripts of alpha-cardiac and alpha-skeletal actins are early markers for myogenesis in the mouse embryo. *Development* **104,** 155 LP-164 (1988).
127. Schwartz, K., Boheler, K. R., de la Bastie, D., Lompre, A. M. & Mercadier, J. J. Switches in cardiac muscle gene expression as a result of pressure and volume overload. *Am. J. Physiol. - Regul. Integr. Comp. Physiol.* **262,** R364 LP-R369 (1992).
128. Bogdarina, I., Welham, S., King, P. J., Burns, S. P. & Clark, A. J. L. Epigenetic Modification of the Renin-Angiotensin System in the Fetal Programming of Hypertension. *Circ. Res.* **100,** 520 LP-526 (2007).
129. Matsui, Y. *et al.* Role of Osteopontin in Cardiac Fibrosis and Remodeling in Angiotensin II-Induced Cardiac Hypertrophy. *Hypertension* **43,** 1195 LP-1201 (2004).
130. Wang, W. *et al.* Essential Role of Smad3 in Angiotensin II–Induced Vascular Fibrosis. *Circ. Res.* **98,** 1032 LP-1039 (2006).
131. Huentelman, M. J. *et al.* Protection from angiotensin II-induced cardiac hypertrophy and fibrosis by systemic lentiviral delivery of ACE2 in rats. *Exp. Physiol.* **90,** 783–790 (2005).
132. Johar, S., Cave, A. C., Narayanapanicker, A., Grieve, D. J. & Shah, A. M. Aldosterone mediates angiotensin II-induced interstitial cardiac fibrosis via a Nox2-containing NADPH oxidase. *FASEB J.* **20,** 1546–8 (2006).
133. Sussman, M. A. *et al.* Prevention of Cardiac Hypertrophy in Mice by Calcineurin Inhibition. *Science (80-.).* **281,** 1690 LP-1693 (1998).
134. Yang, Q. *et al.* A mouse model of myosin binding protein C human familial hypertrophic cardiomyopathy. *J. Clin. Invest.* **102,** 1292–1300 (1998).
135. Daehmlow, S. *et al.* Novel mutations in sarcomeric protein genes in dilated cardiomyopathy. *Biochem. Biophys. Res. Commun.* **298,** 116–120 (2002).
136. Olson, T. M., Michels, V. V, Thibodeau, S. N., Tai, Y.-S. & Keating, M. T. Actin Mutations in Dilated Cardiomyopathy, a Heritable Form of Heart Failure. *Science (80-.).* **280,** 750 LP-752 (1998).
137. Haudek, S. B. *et al.* Monocytic fibroblast precursors mediate fibrosis in angiotensin-II-induced cardiac hypertrophy. *J. Mol. Cell. Cardiol.* **49,** 499–507 (2010).
138. Ito, A. *et al.* Role of MAPK phosphatase-1 in the induction of monocyte chemoattractant protein-1 during the course of adipocyte hypertrophy. *J. Biol. Chem.* **282,** 25445–25452 (2007).
139. Suda, S., Williams, H., Medbury, H. J. & Holland, A. J. A. A Review of Monocytes and Monocyte-Derived Cells in Hypertrophic Scarring Post Burn. *J. Burn Care Res.* **37,** 265–272 (2016).
140. Shioi, T. *et al.* Increased Expression of Interleukin-1β and Monocyte Chemotactic and Activating Factor/Monocyte Chemoattractant Protein-1 in the Hypertrophied and Failing Heart With Pressure Overload. *Circ. Res.* **81,** 664 LP-671 (1997).
141. Yndestad, A. *et al.* Systemic inflammation in heart failure – The whys and wherefores. *Heart Fail. Rev.* **11,** 83–92 (2006).
142. Elenkov, I. J. Neurohormonal-cytokine interactions: Implications for inflammation, common human diseases and well-being. *Neurochem. Int.* **52,** 40–51 (2008).

143. Liu, Y. Renal fibrosis: New insights into the pathogenesis and therapeutics. *Kidney Int.* **69,** 213–217 (2006).
144. Bringardner, B. D., Baran, C. P., Eubank, T. D. & Marsh, C. B. The Role of Inflammation in the Pathogenesis of Idiopathic Pulmonary Fibrosis. *Antioxid. Redox Signal.* **10,** 287–301 (2008).
145. Letterio, J. J. & Roberts, A. B. Regulation of immune responses by TGF-β. *Annu. Rev. Immunol.* **16,** 137–161 (1998).
146. Leask, A. Potential Therapeutic Targets for Cardiac Fibrosis. *Circ. Res.* **106,** 1675 LP-1680 (2010).
147. Villarreal, F. J. & Dillmann, W. H. Cardiac hypertrophy-induced changes in mRNA levels for TGF-beta 1, fibronectin, and collagen. *Am. J. Physiol. - Hear. Circ. Physiol.* **262,** H1861 LP-H1866 (1992).
148. Mann, D. L. & Young, J. B. Basic mechanisms in congestive heart failure. Recognizing the role of proinflammatory cytokines. *CHEST J.* **105,** 897–904 (1994).
149. Edelmann, F. *et al.* Galectin-3 in patients with heart failure with preserved ejection fraction: results from the Aldo-DHF trial. *Eur. J. Heart Fail.* **17,** 214–223 (2015).
150. Suarez, G. & Meyerrose, G. Heart failure and galectin 3. *Ann. Transl. Med.* **2,** 86 (2014).
151. Bošnjak, I., Selthofer-Relatić, K. & Včev, A. Prognostic value of galectin-3 in patients with heart failure. *Dis. Markers* **2015,** (2015).
152. Sorescu, G. P. *et al.* Bone Morphogenic Protein 4 Produced in Endothelial Cells by Oscillatory Shear Stress Induces Monocyte Adhesion by Stimulating Reactive Oxygen Species Production From a Nox1-Based NADPH Oxidase. *Circ. Res.* **95,** 773 LP-779 (2004).
153. Sorescu, G. P. *et al.* Bone morphogenic protein 4 produced in endothelial cells by oscillatory shear stress stimulates an inflammatory response. *J. Biol. Chem.* **278,** 31128–31135 (2003).
154. Zhang, Y. *et al.* Inhibition of Bone Morphogenic Protein 4 Restores Endothelial Function in Diabetic Mice. *Arterioscler. Thromb. Vasc. Biol.* **34,** 152 LP-159 (2014).
155. Brock, M. *et al.* Interleukin-6 Modulates the Expression of the Bone Morphogenic Protein Receptor Type II Through a Novel STAT3–microRNA Cluster 17/92 Pathway. *Circ. Res.* **104,** 1184 LP-1191 (2009).
156. Lijnen, P. J., Petrov, V. V & Fagard, R. H. Induction of Cardiac Fibrosis by Transforming Growth Factor-β1. *Mol. Genet. Metab.* **71,** 418–435 (2000).
157. Pauschinger, M. *et al.* Dilated Cardiomyopathy Is Associated With Significant Changes in Collagen Type I/III ratio. *Circulation* **99,** 2750 LP-2756 (1999).
158. Carver, W., Nagpal, M. L., Nachtigal, M., Borg, T. K. & Terracio, L. Collagen expression in mechanically stimulated cardiac fibroblasts. *Circ. Res.* **69,** 116 LP-122 (1991).
159. Brown, L., Duce, B., Miric, G. & Sernia, C. Reversal of cardiac fibrosis in deoxycorticosterone acetate-salt hypertensive rats by inhibition of the renin-angiotensin system. *J. Am. Soc. Nephrol.* **10 Suppl 1,** S143-8 (1999).
160. Zeisberg, E. M. *et al.* Endothelial-to-mesenchymal transition contributes to cardiac fibrosis. *Nat Med* **13,** 952–961 (2007).
161. Barton, P. J. R. *et al.* Increased expression of extracellular matrix regulators TIMP1 and MMP1 in deteriorating heart failure. *J. Hear. Lung Transplant.* **22,** 738–744 (2003).
162. Li, Y. Y., McTiernan, C. F. & Feldman, A. M. Interplay of matrix metalloproteinases, tissue inhibitors of metalloproteinases and their regulators in cardiac matrix remodeling. *Cardiovasc. Res.* **46,** 214–224 (2000).
163. Li, Y. Y., Feldman, A. M., Sun, Y. & McTiernan, C. F. Differential Expression of Tissue Inhibitors of Metalloproteinases in the Failing Human Heart. *Circulation* **98,** 1728 LP-1734 (1998).
164. Rodger, M., Sheppard, D., Gándara, E. & Tinmouth, A. Haematological problems in obstetrics. *Best Pract. Res. Clin. Obstet. Gynaecol.* **29,** 671–684 (2015).
165. Soma-Pillay, P. *et al.* Physiological changes in pregnancy. *Cardiovasc. J. Afr.* **27,** 89–94 (2016).
166. Ramsay, M. Normal hematological changes during pregnancy and the puerperium. *Obstet. Hematol. Man.* 3 (2010).
167. Fischer, P. & Hilfiker-Kleiner, D. Survival pathways in hypertrophy and heart failure: the gp130-STAT axis. *Basic Res. Cardiol.* **102,** 279–297 (2007).

168. Walters, W. A. W. in *Reproductive Endocrinology and Biology* (eds. Edward Bittar, E. & Edward Bittar, N. B. T.-P. of M. B.) **12,** 183–209 (Elsevier, 1998).
169. Ueland, K., Novy, M. J., Peterson, E. N. & Metcalfe, J. Maternal cardiovascular dynamics. *Am. J. Obstet. Gynecol.* **104,** 856–864 (2018).
170. Sanghavi, M. & Rutherford, J. D. Cardiovascular physiology of pregnancy. *Circulation* **130,** 1003–1008 (2014).
171. Conrad, K. P. & Davison, J. M. The renal circulation in normal pregnancy and preeclampsia: is there a place for relaxin? *Am. J. Physiol. - Ren. Physiol.* **306,** F1121–F1135 (2014).
172. Conrad, K. P. Emerging Role of Relaxin in the Maternal Adaptations to Normal Pregnancy: Implications for Preeclampsia. *Semin. Nephrol.* **31,** 15–32 (2011).
173. Tkachenko, O., Shchekochikhin, D. & Schrier, R. W. Hormones and Hemodynamics in Pregnancy. *Int. J. Endocrinol. Metab.* **12,** e14098 (2014).
174. Dörr, H. G. *et al.* Longitudinal Study of Progestins, Mineralocorticoids, and Glucocorticoids throughout Human Pregnancy. *J. Clin. Endocrinol. Metab.* **68,** 863–868 (1989).
175. Elsheikh, A. *et al.* The renin-aldosterone system during normal and hypertensive pregnancy. *Arch. Gynecol. Obstet.* **264,** 182–185 (2001).
176. Krop, M. & Danser, A. H. J. Circulating versus tissue renin-angiotensin system: on the origin of (pro) renin. *Curr. Hypertens. Rep.* **10,** 112 (2008).
177. Gant, N. F., Worley, R. J., Everett, R. B. & MacDonald, P. C. Control of vascular responsiveness during human pregnancy. *Kidney Int.* **18,** 253–258 (1980).
178. Davison, J. M., Sheills, E. A., Barron, W. M., Robinson, A. G. & Lindheimer, M. D. Changes in the metabolic clearance of vasopressin and in plasma vasopressinase throughout human pregnancy. *J. Clin. Invest.* **83,** 1313–1318 (1989).
179. Castro, L. C., Hobel, C. J. & Gornbein, J. Plasma levels of atrial natriuretic peptide in normal and hyprtensive pregnancies: A meta-analysis. *Am. J. Obstet. Gynecol.* **171,** 1642–1651 (1994).
180. Resnik, J. L. *et al.* Evaluation of B-type natriuretic peptide (BNP) levels in normal and preeclamptic women. *Am. J. Obstet. Gynecol.* **193,** 450–454 (2005).
181. Hameed, A. B., Chan, K., Ghamsary, M. & Elkayam, U. Longitudinal Changes in the B-Type Natriuretic Peptide Levels in Normal Pregnancy and Postpartum. *Clin. Cardiol.* **32,** (2009).
182. Rigg, L. A., Lein, A. & Yen, S. S. C. Pattern of increase in circulating prolactin levels during human gestation. *Am. J. Obstet. Gynecol.* **129,** 454–456 (1977).
183. Kletzky, O. A., Rossman, F., Bertolli, S. I., Platt, L. D. & Mishell, D. R. Dynamics of human chorionic gonadotropin, prolactin, and growth hormone in serum and amniotic fluid throughout normal human pregnancy. *Am. J. Obstet. Gynecol.* **151,** 878–884 (1985).
184. Angueira, A. R. *et al.* New Insights Into Gestational Glucose Metabolism: Lessons Learned From 21st Century Approaches. *Diabetes* **64,** 327–334 (2015).
185. Butte, N. F. Carbohydrate and lipid metabolism in pregnancy: normal compared with gestational diabetes mellitus. *Am. J. Clin. Nutr.* **71,** 1256s–1261s (2000).
186. Newbern, D. & Freemark, M. Placental hormones and the control of maternal metabolism and fetal growth. *Curr. Opin. Endocrinol. Diabetes Obes.* **18,** 409–416 (2011).
187. Kalkhoff, R. K., Jacobson, M. & Lemper, D. Progesterone, Pregnancy and the Augmented Plasma Insulin Response1. *J. Clin. Endocrinol. Metab.* **31,** 24–28 (1970).
188. Mazaki-Tovi, S. *et al.* Insulin sensitivity in late gestation and early postpartum period: the role of circulating maternal adipokines. *Gynecol. Endocrinol.* **27,** 725–731 (2011).
189. Hilfiker-Kleiner, D., Sliwa, K. & Drexler, H. Peripartum Cardiomyopathy: Recent Insights in its Pathophysiology. *Trends Cardiovasc. Med.* **18,** 173–179 (2008).
190. Patten, R. D. *et al.* 17β-Estradiol Reduces Cardiomyocyte Apoptosis In Vivo and In Vitro via Activation of Phospho-Inositide-3 Kinase/Akt Signaling. *Circ. Res.* **95,** 692 LP-699 (2004).
191. Johansson, E. D. B. Plasma levels of progesterone in pregnancy measured by a rapid competitive protein binding technique. *Acta Endocrinol. (Copenh).* **61,** 607–617 (1969).
192. Turnbull, A. C. *et al.* Significant fall in progesterone and rise in oestradiol levels in human peripheral

plasma before onset of labour. *Lancet* **303,** 101–104 (1974).
193. Llauró, J., Runnebaum, B. & Zander, J. Progesterone in human peripheral blood before, during, and after labor. *Am. J. Obstet. Gynecol.* **101,** 867–873 (1968).
194. Sliwa, K. *et al.* Long-term prognosis, subsequent pregnancy, contraception and overall management of peripartum cardiomyopathy: practical guidance paper from the Heart Failure Association of the European Society of Cardiology Study Group on Peripartum Cardiomyopathy. *Eur. J. Heart Fail.* (2018).
195. Sliwa, K. *et al.* Current state of knowledge on aetiology, diagnosis, management, and therapy of peripartum cardiomyopathy: A position statement from the Heart Failure Association of the European Society of Cardiology Working Group on peripartum cardiomyopathy. *Eur. J. Heart Fail.* **12,** 767–778 (2010).
196. Hilfiker-Kleiner, D. *et al.* A cathepsin D-cleaved 16 kDa form of prolactin mediates postpartum cardiomyopathy. *Cell* **128,** 589–600 (2007).
197. Fett, J. D. *et al.* Unrecognized peripartum cardiomyopathy in Haitian women. *Int. J. Gynecol. Obstet.* **90,** 161–166 (2005).
198. Desai, D., Moodley, J. & Naidoo, D. Peripartum cardiomyopathy: experiences at King Edward VIII Hospital, Durban, South Africa and a review of the literature. *Trop. Doct.* **25,** 118–123 (1995).
199. Chapa, J. B. *et al.* Prognostic value of echocardiography in peripartum cardiomyopathy. *Obstet. Gynecol.* **105,** 1303–1308 (2005).
200. Brar, S. S. *et al.* Incidence, mortality, and racial differences in peripartum cardiomyopathy. *Am. J. Cardiol.* **100,** 302–304 (2007).
201. Modi, K. A., Illum, S., Jariatul, K., Caldito, G. & Reddy, P. C. Poor outcome of indigent patients with peripartum cardiomyopathy in the United States. *Am. J. Obstet. Gynecol.* **201,** 171-e1 (2009).
202. Goland, S., Modi, K., Hatamizadeh, P. & Elkayam, U. Differences in clinical profile of African-American women with peripartum cardiomyopathy in the United States. *J. Card. Fail.* **19,** 214–218 (2013).
203. Hilfiker-Kleiner, D. & Sliwa, K. Pathophysiology and epidemiology of peripartum cardiomyopathy. *Nat. Rev. Cardiol.* **11,** (2014).
204. Morales, A. *et al.* Rare variant mutations in pregnancy-associated or peripartum cardiomyopathy. *Circulation* **121,** 2176–2182 (2010).
205. Haghikia, A. *et al.* Phenotyping and outcome on contemporary management in a German cohort of patients with peripartum cardiomyopathy. *Basic Res. Cardiol.* **108,** 366 (2013).
206. Sliwa, K., Fett, J. & Elkayam, U. Peripartum cardiomyopathy. *Lancet* **368,** 687–693 (2006).
207. Sundstrom, J. B., Fett, J. D., Carraway, R. D. & Ansari, A. A. Is peripartum cardiomyopathy an organ-specific autoimmune disease? *Autoimmun. Rev.* **1,** 73–77 (2002).
208. Hibbard, J. U., Lindheimer, M. & Lang, R. M. A modified definition for peripartum cardiomyopathy and prognosis based on echocardiography. *Obstet. Gynecol.* **94,** 311–316 (1999).
209. Wallukat, G., Nissen, E., Morwinski, R. & Müller, J. Autoantibodies against the Beta- and Muscarinic Receptors in Cardiomyopathy. *Herz* **25,** 261–266 (2000).
210. de Leeuw, N. *et al.* Autoimmune markers are undetectable in end stage idiopathic dilated cardiomyopathy. *J. Clin. Pathol.* **52,** 739 LP-743 (1999).
211. Herskowitz, A., Neumann, D. A. & Ansari, A. A. Concepts of autoimmunity applied to idiopathic dilated cardiomyopathy. *J. Am. Coll. Cardiol.* **22,** 1385–1388 (1993).
212. Caforio, A. L. *et al.* Identification of alpha- and beta-cardiac myosin heavy chain isoforms as major autoantigens in dilated cardiomyopathy. *Circulation* **85,** 1734 LP-1742 (1992).
213. Gravanis, M. B. & Ansari, A. A. Idiopathic cardiomyopathies. A review of pathologic studies and mechanisms of pathogenesis. *Arch. Pathol. Lab. Med.* **111,** 915–929 (1987).
214. Ansari, A. A. *et al.* Autoimmune mechanisms as the basis for human peripartum cardiomyopathy. *Clin. Rev. Allergy Immunol.* **23,** 301 (2002).
215. Fett, J. D., Carraway, R. D., Dowell, D. L., King, M. E. & Pierre, R. Peripartum cardiomyopathy in the hospital Albert Schweitzer district of Haiti. *Am. J. Obstet. Gynecol.* **186,** 1005–1010 (2002).
216. Duran, N., Günes, H., Duran, I., Biteker, M. & Özkan, M. Predictors of prognosis in patients with

peripartum cardiomyopathy. *Int. J. Gynecol. Obstet.* **101,** 137–140 (2008).
217. Forster, O. *et al.* Reversal of IFN-gamma, oxLDL and prolactin serum levels correlate with clinical improvement in patients with peripartum cardiomyopathy. *Eur. J. Heart Fail.* **10,** 861–868 (2008).
218. Sliwa, K. *et al.* Peripartum cardiomyopathy: analysis of clinical outcome, left ventricular function, plasma levels of cytokines and Fas/APO-1. *J Am Coll Cardiol* **35,** 701–5 (2000).
219. Sliwa, K. *et al.* Peripartum cardiomyopathy: inflammatory markers as predictors of outcome in 100 prospectively studied patients. *Eur. Heart J.* **27,** 441–446 (2006).
220. Tabruyn, S. P. *et al.* The Antiangiogenic Factor 16K Human Prolactin Induces Caspase-Dependent Apoptosis by a Mechanism that Requires Activation of Nuclear Factor-κB. *Mol. Endocrinol.* **17,** 1815–1823 (2003).
221. Macotela, Y. *et al.* Matrix metalloproteases from chondrocytes generate an antiangiogenic 16 kDa prolactin. *J. Cell Sci.* **119,** 1790 LP-1800 (2006).
222. Corbacho, A. M., Martinez De La Escalera, G. & Clapp, C. Roles of prolactin and related members of the prolactin/growth hormone/placental lactogen family in angiogenesis. *J. Endocrinol.* **173,** 219–238 (2002).
223. Gonzalez, C. *et al.* 16K-prolactin inhibits activation of endothelial nitric oxide synthase, intracellular calcium mobilization, and endothelium-dependent vasorelaxation. *Endocrinology* **145,** 5714–5722 (2004).
224. Tabruyn, S. P. *et al.* The angiostatic 16K human prolactin overcomes endothelial cell anergy and promotes leukocyte infiltration via nuclear factor-κB activation. *Mol. Endocrinol.* **21,** 1422–1429 (2007).
225. Ellis, J. E. *et al.* Inhibition of Progenitor Dendritic Cell Maturation by Plasma from Patients with Peripartum Cardiomyopathy: Role in Pregnancy-associated Heart Disease. *Clin. Dev. Immunol.* **12,** 265–273 (2005).
226. Sliwa, K. *et al.* Evaluation of bromocriptine in the treatment of acute severe peripartum cardiomyopathy: a proof-of-concept pilot study. *Circulation* **121,** 1465–73 (2010).
227. Hilfiker-Kleiner, D. *et al.* Recovery From Postpartum Cardiomyopathy in 2 Patients by Blocking Prolactin Release With Bromocriptine. *J. Am. Coll. Cardiol.* **50,** 2354 LP-2355 (2007).
228. Patten, I. S. *et al.* Cardiac angiogenic imbalance leads to peripartum cardiomyopathy. *Nature* **485,** 333–338 (2012).
229. Adams, J. W. *et al.* Enhanced G q signaling: A common pathway mediates cardiac hypertrophy and apoptotic heart failure. *Proc. Natl. Acad. Sci.* **95,** 10140–10145 (1998).
230. Hayakawa, Y. *et al.* Inhibition of Cardiac Myocyte Apoptosis Improves Cardiac Function and Abolishes Mortality in the Peripartum Cardiomyopathy of Gαq Transgenic Mice. *Circ.* **108,** 3036–3041 (2003).
231. Cataldo, L. *et al.* Inhibition of oncogene STAT3 phosphorylation by a prolactin antagonist, hPRL-G129R, in T-47D human breast cancer cells. *Int. J. Oncol.* **17,** 1179–1186 (2000).
232. Bozkurt, B. *et al.* Intravenous immune globulin in the therapy of peripartum cardiomyopathy. *J. Am. Coll. Cardiol.* **34,** 177 LP-180 (1999).
233. Ricke-Hoch, M. *et al.* Opposing roles of Akt and STAT3 in the protection of the maternal heart from peripartum stress. *Cardiovasc. Res.* **101,** 587–596 (2014).
234. Sliwa, K. *et al.* The addition of pentoxifylline to conventional therapy improves outcome in patients with peripartum cardiomyopathy. *Eur. J. Heart Fail.* **4,** 305–309 (2002).
235. Nagafuchi, H., Suzuki, N., Kaneko, A., Asai, T. & Sakane, T. Prolactin locally produced by synovium infiltrating T lymphocytes induces excessive synovial cell functions in patients with rheumatoid arthritis. *J. Rheumatol.* **26,** 1890–1900 (1999).
236. Roberg, K. & Ollinger, K. Oxidative stress causes relocation of the lysosomal enzyme cathepsin D with ensuing apoptosis in neonatal rat cardiomyocytes. *Am. J. Pathol.* **152,** 1151–1156 (1998).
237. Schulz, R. Intracellular targets of matrix metalloproteinase-2 in cardiac disease: rationale and therapeutic approaches. *Annu. Rev. Pharmacol. Toxicol.* **47,** 211–242 (2007).
238. Halkein, J. *et al.* MicroRNA-146a is a therapeutic target and biomarker for peripartum cardiomyopathy. *J. Clin. Invest.* **123,** 2143–54 (2013).

239. Hilfiker-Kleiner, D., Struman, I., Hoch, M., Podewski, E. & Sliwa, K. 16-kDa prolactin and bromocriptine in postpartum cardiomyopathy. *Curr. Heart Fail. Rep.* **9,** 174–82 (2012).
240. Nishimura, H. *et al.* Autoimmune Dilated Cardiomyopathy in PD-1 Receptor-Deficient Mice. *Science (80-.).* **291,** 319 (2001).
241. Kubasiak, L. A., Hernandez, O. M., Bishopric, N. H. & Webster, K. A. Hypoxia and acidosis activate cardiac myocyte death through the Bcl-2 family protein BNIP3. *Proc. Natl. Acad. Sci.* **99,** 12825–12830 (2002).
242. Diwan, A. *et al.* Nix-Mediated Apoptosis Links Myocardial Fibrosis, Cardiac Remodeling, and Hypertrophy Decompensation. *Circulation* **117,** 396 LP-404 (2008).
243. Elsherif, L. *et al.* Combined deficiency of dystrophin and β1 integrin in the cardiac myocyte causes myocardial dysfunction, fibrosis and calcification. *Circ. Res.* **102,** 1109–1117 (2008).
244. Van Tintelen, J. P., Pieper, P. G., Van Spaendonck-Zwarts, K. Y. & Van Den Berg, M. P. Pregnancy, cardiomyopathies, and genetics. *Cardiovasc. Res.* **101,** 571–578 (2014).
245. Hernandez, A. F. *et al.* Clinical Effectiveness of Beta-Blockers in Heart Failure: Findings From the OPTIMIZE-HF (Organized Program to Initiate Lifesaving Treatment in Hospitalized Patients With Heart Failure) Registry. *J. Am. Coll. Cardiol.* **53,** 184–192 (2009).
246. Libhaber, E., Sliwa, K., Bachelier, K., Lamont, K. & Böhm, M. Low systolic blood pressure and high resting heart rate as predictors of outcome in patients with peripartum cardiomyopathy. *Int. J. Cardiol.* **190,** 376–82 (2015).
247. Opie, L. H. Cardiomyopathies and heart failure. *Hear. Metab* **46,** 17–24 (2010).
248. Ray, J. G., Vermeulen, M. J. & Koren, G. Taking ACE inhibitors during early pregnancy: Is it safe? *Can. Fam. Physician* **53,** 1439–1440 (2007).
249. Antranik.org. The Renin Angiotensin Aldosterone Reflex. (2012). at <http://antranik.org/the-renin-angiotensin-aldosterone-reflex/>
250. Domanski, M. *et al.* Diuretic use, progressive heart failure, and death in patients in the studies of left ventricular dysfunction (SOLVD). *J. Am. Coll. Cardiol.* **42,** 705 LP-708 (2003).
251. Brown, N. J. *et al.* Aldosterone modulates plasminogen activator inhibitor-1 and glomerulosclerosis in vivo. *Kidney Int.* **58,** 1219–1227 (2000).
252. Pitt, B. *et al.* The effect of spironolactone on morbidity and mortality in patients with severe heart failure. *N. Engl. J. Med.* **341,** 709–717 (1999).
253. Zannad, F., Alla, F., Dousset, B., Perez, A. & Pitt, B. Limitation of Excessive Extracellular Matrix Turnover May Contribute to Survival Benefit of Spironolactone Therapy in Patients With Congestive Heart Failure. *Circulation* **102,** 2700 LP-2706 (2000).
254. Campbell, T. J. & MacDonald, P. S. Digoxin in heart failure and cardiac arrhythmias. *Med. J. Aust.* **179,** 98–102 (2003).
255. Ma, H. *et al.* Correction of a pathogenic gene mutation in human embryos. *Nature* **548,** 413 (2017).
256. Kim, M.-J. & Shin, M.-S. Practical management of peripartum cardiomyopathy. *Korean J. Intern. Med.* **32,** 393–403 (2017).
257. Chow, M. S. S. Assessing the treatment of congestive heart failure: diuretics, vasodilators, and angiotensin-converting enzyme inhibitors. *Pharmacother. J. Hum. Pharmacol. Drug Ther.* **13,** 82S–87S (1993).
258. Jeremias, A. & Brown, D. L. *Cardiac Intensive Care*. (Saunders, 2010). doi:https://doi.org/10.1016/B978-1-4160-3773-6.X0001-8
259. Bauersachs, J. *et al.* Current management of patients with severe acute peripartum cardiomyopathy: practical guidance from the Heart Failure Association of the European Society of Cardiology Study Group on peripartum cardiomyopathy. *Eur. J. Heart Fail.* **18,** 1096–1105 (2016).
260. DeFronzo, R. A. Bromocriptine: A Sympatholytic, D2-Dopamine Agonist for the Treatment of Type 2 Diabetes. *Diabetes Care* **34,** 789–794 (2011).
261. Thorner, M. O., Besser, G. M., Jones, A., Dacie, J. & Jones, A. E. Bromocriptine treatment of female infertility: report of 13 pregnancies. *Br. Med. J.* **4,** 694 LP-697 (1975).
262. Lutterbeck, P. M., Pryor, J. S., Varga, L. & Wenner, R. Treatment of non-puerperal galactorrhoea with

an ergot alkaloid. *Br Med J* **3,** 228–229 (1971).
263. Karmali, R. A. & Horrobin, D. F. Letter: Prolactin, bromocriptine, and haemostasis. *Br. Med. J.* **3,** 307 (1975).
264. Osbourne, G. K. *et al.* THE EFFECTS OF QUINESTROL AND BROMOCRIPTINE ON BLOOD COAGULATION, SERUM PROLACTIN AND SERUM FSH LEVELS IN PUERPERAL WOMEN. *BJOG An Int. J. Obstet. Gynaecol.* **85,** 687–691 (1978).
265. Lu, C.-H. *et al.* Comparison of clinical outcomes in peripartum cardiomyopathy and age-matched dilated cardiomyopathy: A 15-year nationwide population-based study in Asia. *Medicine (Baltimore).* **96,** e6898 (2017).
266. Elliott, C., Sliwa, K. & Burton, R. Pregnancy and cardiac disease. *South African Med. Journal; Vol 104, No 9* (2014). at <http://www.samj.org.za/index.php/samj/article/view/8762/6270>
267. Sliwa, K. & Böhm, M. Incidence and prevalence of pregnancy-related heart disease. *Cardiovasc. Res.* **101,** 554–560 (2014).
268. Akashi, Y. J., Nef, H. M. & Lyon, A. R. Epidemiology and pathophysiology of Takotsubo syndrome. *Nat Rev Cardiol* **12,** 387–397 (2015).
269. Ghadri, J.-R. *et al.* International Expert Consensus Document on Takotsubo Syndrome (Part I): Clinical Characteristics, Diagnostic Criteria, and Pathophysiology. *Eur. Heart J.* **39,** 2032–2046 (2018).
270. Templin, C. *et al.* Clinical features and outcomes of takotsubo (stress) cardiomyopathy. *N. Engl. J. Med.* **373,** 929–938 (2015).
271. Kawai, S., Kitabatake, A., Tomoike, H. & Takotsubo Cardiomyopathy Study Group. Guidelines for Diagnosis of Takotsubo (Ampulla) Cardiomyopathy. *Circ. J.* **71,** 990–992 (2007).
272. Eitel, I. *et al.* Clinical characteristics and cardiovascular magnetic resonance findings in stress (takotsubo) cardiomyopathy. *JAMA* **306,** 277–286 (2011).
273. Maréchaux, S. *et al.* Pathology of inverted Takotsubo cardiomyopathy. *Cardiovasc Pathol* **17,** (2008).
274. Van de Walle, S. O. A., Gevaert, S. A., Gheeraert, P. J., De Pauw, M. & Gillebert, T. C. Transient Stress-Induced Cardiomyopathy With an "Inverted Takotsubo" Contractile Pattern. *Mayo Clin. Proc.* **81,** 1499–1502 (2006).
275. Cacciotti, L. *et al.* A new variant of Tako-tsubo cardiomyopathy: transient mid-ventricular ballooning. *J. Cardiovasc. Med.* **8,** 1052–1054 (2007).
276. Bybee, K., Kara, T., Prasad, A. & Al, E. Systematic review: Transient left ventricular apical ballooning: a syndrome that mimics st-segment elevation myocardial infarction. *Ann. Intern. Med.* **141,** 858–865 (2004).
277. Sharkey, S. W. *et al.* Acute and reversible cardiomyopathy provoked by stress in women from the United States. *Circulation* **111,** (2005).
278. Schneider, B. *et al.* Gender differences in the manifestation of tako-tsubo cardiomyopathy. *Int. J. Cardiol.* **166,** 584–588 (2013).
279. Citro, R. *et al.* Echocardiographic Correlates of Acute Heart Failure, Cardiogenic Shock, and In-Hospital Mortality in Tako-Tsubo Cardiomyopathy. *JACC Cardiovasc. Imaging* **7,** 119–129 (2014).
280. Schneider, B. *et al.* Complications in the clinical course of tako-tsubo cardiomyopathy. *Int. J. Cardiol.* **176,** 199–205 (2014).
281. Redfors, B. *et al.* Mortality in takotsubo syndrome is similar to mortality in myocardial infarction — A report from the SWEDEHEART1 registry. *Int. J. Cardiol.* **185,** 282–289 (2015).
282. Elesber, A. A. *et al.* Four-Year Recurrence Rate and Prognosis of the Apical Ballooning Syndrome. *J. Am. Coll. Cardiol.* **50,** 448–452 (2007).
283. Wittstein, I. S. *et al.* Neurohumoral features of myocardial stunning due to sudden emotional stress. *N Engl J Med* **352,** (2005).
284. Deshmukh, A. *et al.* Prevalence of Takotsubo cardiomyopathy in the United States. *Am. Heart J.* **164,** 66–71 (2012).
285. Pilgrim, T. M. & Wyss, T. R. Takotsubo cardiomyopathy or transient left ventricular apical ballooning syndrome: A systematic review. *Int. J. Cardiol.* **124,** 283–292 (2008).
286. Bowles, E. J. A. *et al.* Risk of Heart Failure in Breast Cancer Patients After Anthracycline and

Trastuzumab Treatment: A Retrospective Cohort Study. *JNCI J. Natl. Cancer Inst.* **104,** 1293–1305 (2012).
287. Brinjikji, W., El-Sayed, A. M. & Salka, S. In-hospital mortality among patients with takotsubo cardiomyopathy: A study of the National Inpatient Sample 2008 to 2009. *Am. Heart J.* **164,** 215–221 (2012).
288. Citro, R. *et al.* Differences in Clinical Features and In-Hospital Outcomes of Older Adults with Tako-Tsubo Cardiomyopathy. *J. Am. Geriatr. Soc.* **60,** 93–98 (2012).
289. Schultz, T. *et al.* Stress-Induced Cardiomyopathy in Sweden: Evidence for Different Ethnic Predisposition and Altered Cardio-Circulatory Status. *Cardiology* **122,** 180–186 (2012).
290. Prasad, A., Lerman, A. & Rihal, C. S. Apical ballooning syndrome (Tako-Tsubo or stress cardiomyopathy): a mimic of acute myocardial infarction. *Am Hear. J* **155,** (2008).
291. Merli, E., Sutcliffe, S., Gori, M. & Sutherland, G. G. R. Tako-Tsubo cardiomyopathy: New insights into the possible underlying pathophysiology. *Eur. J. Echocardiogr.* **7,** 53–61 (2006).
292. Tranter, M. H., Wright, P. T., Sikkel, M. B. & Lyon, A. R. Takotsubo Cardiomyopathy: The Pathophysiology. *Heart Fail. Clin.* **9,** 187–196 (2013).
293. Redfors, B., Shao, Y., Ali, A. & Omerovic, E. Are the different patterns of stress-induced (Takotsubo) cardiomyopathy explained by regional mechanical overload and demand: Supply mismatch in selected ventricular regions? *Med. Hypotheses* **81,** 954–960 (2013).
294. Nef, H. M., Mollmann, H., Akashi, Y. J. & Hamm, C. W. Mechanisms of stress (Takotsubo) cardiomyopathy. *Nat Rev Cardiol* **7,** 187–193 (2010).
295. Yoshida, T. *et al.* A rare case of tako-tsubo cardiomyopathy with variable forms of left ventricular dysfunction: A new entity. *Int. J. Cardiol.* **134,** e73–e75 (2009).
296. Syed, F. F., Asirvatham, S. J. & Francis, J. Arrhythmia occurrence with takotsubo cardiomyopathy: a literature review. *EP Eur.* **13,** 780–788 (2011).
297. Pant, S. *et al.* Burden of arrhythmias in patients with Takotsubo Cardiomyopathy (Apical Ballooning Syndrome). *Int. J. Cardiol.* **170,** 64–68 (2013).
298. Murakami, T. *et al.* Characterization of predictors of in-hospital cardiac complications of takotsubo cardiomyopathy: Multi-center registry from Tokyo CCU Network. *J. Cardiol.* **63,** 269–273 (2014).
299. Gianni, M. *et al.* Apical ballooning syndrome or takotsubo cardiomyopathy: a systematic review. *Eur Hear. J* **27,** (2006).
300. Ogura, R. *et al.* Specific Findings of the Standard 12-Lead ECG in Patients With `Takotsubo' Cardiomyopathy. *Circ. J.* **67,** 687–690 (2003).
301. Kurisu, S. *et al.* Time Course of Electrocardiographic Changes in Patients With Tako-Tsubo Syndrome. *Circ. J.* **68,** 77–81 (2004).
302. Sharkey, S. W. Electrocardiogram mimics of acute ST-segment elevation myocardial infarction: insights from cardiac magnetic resonance imaging in patients with tako-tsubo (stress) cardiomyopathy. *J. Electrocardiol.* **41,** 621–625 (2008).
303. Madhavan, M., Borlaug, B. A., Lerman, A., Rihal, C. S. & Prasad, A. Stress hormone and circulating biomarker profile of apical ballooning syndrome (Takotsubo cardiomyopathy): insights into the clinical significance of B-type natriuretic peptide and troponin levels. *Heart* **95,** 1436 LP-1441 (2009).
304. Ahmed, K. A., Madhavan, M. & Prasad, A. Brain natriuretic peptide in apical ballooning syndrome (Takotsubo/stress cardiomyopathy): comparison with acute myocardial infarction. *Coron. Artery Dis.* **23,** 259–264 (2012).
305. Fröhlich, G. M. *et al.* Takotsubo cardiomyopathy has a unique cardiac biomarker profile: NT-proBNP/myoglobin and NT-proBNP/troponin T ratios for the differential diagnosis of acute coronary syndromes and stress induced cardiomyopathy. *Int. J. Cardiol.* **154,** 328–332 (2012).
306. Nguyen, T. H. *et al.* N-Terminal Pro-Brain Natriuretic Protein Levels in Takotsubo Cardiomyopathy. *Am. J. Cardiol.* **108,** 1316–1321 (2011).
307. Wideman, C. H., Cierniak, K. H., Sweet, W. E., Moravec, C. S. & Murphy, H. M. An animal model of stress-induced cardiomyopathy utilizing the social defeat paradigm. *Physiol. Behav.* **120,** 220–227 (2013).

308. Kvetnansky, R. *et al.* Effect of Handling and Forced Immobilization on Rat Plasma Levels of Epinephrine, Norepinephrine, and Dopamine-β-Hydroxylase. *Endocrinology* **103,** 1868–1874 (1978).
309. Ueyama, T. Emotional Stress-Induced Tako-tsubo Cardiomyopathy: Animal Model and Molecular Mechanism. *Ann. N. Y. Acad. Sci.* **1018,** 437–444 (2004).
310. Paur, H. *et al.* High Levels of Circulating Epinephrine Trigger Apical Cardiodepression in a β2-Adrenoceptor/Gi-Dependent Manner: A New Model of Takotsubo Cardiomyopathy. *Circulation* **135,** (2012).
311. Surikow, S. Y. *et al.* Nitrosative Stress as a Modulator of Inflammatory Change in a Model of Takotsubo Syndrome. *JACC Basic to Transl. Sci.* **3,** 213 LP-226 (2018).
312. Deshpande, G. P., McCarthy, J., Mardikar, H., Lecour, S. & Opie, L. Effects of sphingosine-1-phosphate on acute contractile heart failure (ACHF). *Cardiovasc. Drugs Ther.* **24,** 459–460 (2010).
313. Itoh, M. & Guth, P. H. Role of Oxygen-Derived Free Radicals in Hemorrhagic Shock-Induced Gastric Lesions in the Rat. *Gastroenterology* **88,** 1162–1167 (1985).
314. Gutierrez, G., Reines, Hd. & Wulf-Gutierrez, M. E. Clinical review: Hemorrhagic shock. *Crit. Care* **8,** 373 (2004).
315. Sack, M. N. *et al.* Fatty Acid Oxidation Enzyme Gene Expression Is Downregulated in the Failing Heart. *Circulation* **94,** 2837 LP-2842 (1996).
316. Stanley, W. C., Recchia, F. A. & Lopaschuk, G. D. Myocardial Substrate Metabolism in the Normal and Failing Heart. *Physiol. Rev.* **85,** 1093 LP-1129 (2005).
317. Ventura-Clapier, R., Garnier, A. & Veksler, V. Energy metabolism in heart failure. *J. Physiol.* **555,** 1–13 (2004).
318. Gheorghiade, M., WT, A., NM, A. & al, et. Systolic blood pressure at admission, clinical characteristics, and outcomes in patients hospitalized with acute heart failure. *JAMA* **296,** 2217–2226 (2006).
319. Nieminen, M. S. *et al.* Executive summary of the guidelines on the diagnosis and treatment of acute heart failureThe Task Force on Acute Heart Failure of the European Society of Cardiology. *Eur. Heart J.* **26,** 384–416 (2005).
320. Heusch, G. *et al.* Cardiovascular remodelling in coronary artery disease and heart failure. *Lancet (London, England)* **383,** 1933–43 (2014).
321. Madhavan, M., Rihal, C. S., Lerman, A. & Prasad, A. Acute Heart Failure in Apical Ballooning Syndrome (TakoTsubo/Stress Cardiomyopathy): Clinical Correlates and Mayo Clinic Risk Score. *J. Am. Coll. Cardiol.* **57,** 1400–1401 (2011).
322. Komamura, K., Fukui, M., Iwasaku, T., Hirotani, S. & Masuyama, T. Takotsubo cardiomyopathy: Pathophysiology, diagnosis and treatment. *World J. Cardiol.* **6,** 602–609 (2014).
323. Levine, H. J. Rest heart rate and life expectancy. *J. Am. Coll. Cardiol.* **30,** 1104–1106 (1997).
324. Zhang, G. Q. & Zhang, W. Heart rate, lifespan, and mortality risk. *Ageing Res. Rev.* **8,** 52–60 (2009).
325. Boyett, M. R., Honjo, H. & Kodama, I. The sinoatrial node, a heterogeneous pacemaker structure. *Cardiovasc. Res.* **47,** 658–687 (2000).
326. Boyett, M. R. *et al.* Sophisticated Architecture is Required for the Sinoatrial Node to Perform Its Normal Pacemaker Function. *J. Cardiovasc. Electrophysiol.* **14,** 104–106 (2003).
327. Opie, L. H. *Heart physiology: from cell to circulation*. (Lippincott Williams & Wilkins, 2004).
328. Heart Valve Surgery. (2007). at <http://www.heart-valve-surgery.com/heart-surgery-blog/2007/08/23/diagram-of-cardiac-conduction-system/>
329. Liu, J. *et al.* Role of pacemaking current in cardiac nodes: Insights from a comparative study of sinoatrial node and atrioventricular node. *Prog. Biophys. Mol. Biol.* **96,** 294–304 (2008).
330. Lemery, R., Guiraudon, G. & Veinot, J. P. Anatomic description of Bachmann's Bundle and its relation to the atrial septum. *Am. J. Cardiol.* **91,** 1482–1485 (2003).
331. James, T. N. The connecting pathways between the sinus node and A-V node and between the right and the left atrium in the human heart. *Am. Heart J.* **66,** 498–508 (1963).
332. Boyett, M. R. *et al.* Sophisticated Architecture is Required for the Sinoatrial Node to Perform Its Normal Pacemaker Function. *J. Cardiovasc. Electrophysiol.* **14,** 104–106 (2003).

333. Fernández-Velasco, M. *et al.* Regional distribution of hyperpolarization-activated current (If) and hyperpolarization-activated cyclic nucleotide-gated channel mRNA expression in ventricular cells from control and hypertrophied rat hearts. *J. Physiol.* **553,** 395–405 (2003).
334. Brown, H. F., DiFrancesco, D. & Noble, S. J. How does adrenaline accelerate the heart? *Nature* **280,** 235–236 (1979).
335. Barbuti, A., Terragni, B., Brioschi, C. & DiFrancesco, D. Localization of f-channels to caveolae mediates specific β2-adrenergic receptor modulation of rate in sinoatrial myocytes. *J. Mol. Cell. Cardiol.* **42,** 71–78 (2007).
336. Rybin, V. O., Xu, X., Lisanti, M. P. & Steinberg, S. F. Differential targeting of beta -adrenergic receptor subtypes and adenylyl cyclase to cardiomyocyte caveolae. A mechanism to functionally regulate the cAMP signaling pathway. *J. Biol. Chem.* **275,** 41447–57 (2000).
337. DiFrancesco, D., Ducouret, P. & Robinson, R. B. Muscarinic modulation of cardiac rate at low acetylcholine concentrations. *Science (80-.).* **243,** 669–672 (1989).
338. Tsantoulas, C., Mooney, E. R. & McNaughton, P. A. HCN2 ion channels: basic science opens up possibilities for therapeutic intervention in neuropathic pain. *Biochem. J.* **473,** 2717 LP-2736 (2016).
339. DiFrancesco, D. The Role of the Funny Current in Pacemaker Activity. *Circ. Res.* **106,** 434–446 (2010).
340. DiFrancesco, D. The contribution of the 'pacemaker' current (if) to generation of spontaneous activity in rabbit sino-atrial node myocytes. *J. Physiol.* **434,** 23–40 (1991).
341. Noble, D. & Tsien, R. W. The kinetics and rectifier properties of the slow potassium current in cardiac Purkinje fibres. *J. Physiol.* **195,** 185–214 (1968).
342. DiFrancesco, D. A study of the ionic nature of the pace-maker current in calf Purkinje fibres. *J. Physiol.* **314,** 377–393 (1981).
343. McCraty, R. & Shaffer, F. Heart Rate Variability: New Perspectives on Physiological Mechanisms, Assessment of Self-regulatory Capacity, and Health risk. *Glob. Adv. Heal. Med.* **4,** 46–61 (2015).
344. Singer, D. H. *et al.* Low heart rate variability and sudden cardiac death. *J. Electrocardiol.* **21,** S46–S55 (1988).
345. Task Force of the European Society of Cardiology the North American Society of Pacing Electrophysiology. Heart Rate Variability. *Circulation* **93,** 1043–1065 (1996).
346. Achten, J. & Jeukendrup, A. E. Heart rate monitoring. *Sport. Med.* **33,** 517–538 (2003).
347. Fritzsche, R. G., Switzer, T. W., Hodgkinson, B. J. & Coyle, E. F. Stroke volume decline during prolonged exercise is influenced by the increase in heart rate. *J. Appl. Physiol.* **86,** 799–805 (1999).
348. José, G.-A., Mora-Rodríguez, R., Below, P. R. & Coyle, E. F. Dehydration markedly impairs cardiovascular function in hyperthermic endurance athletes during exercise. *J. Appl. Physiol.* **82,** 1229–1236 (1997).
349. Charkoudian, N. Skin Blood Flow in Adult Human Thermoregulation: How It Works, When It Does Not, and Why. *Mayo Clin. Proc.* **78,** 603–612 (2003).
350. Yamamoto, Y., Hoshikawa, Y. & Miyashita, M. Effects of acute exposure to simulated altitude on heart rate variability during exercise. *J. Appl. Physiol.* **81,** 1223–1229 (1996).
351. Draghici, A. E. & Taylor, J. A. The physiological basis and measurement of heart rate variability in humans. *J. Physiol. Anthropol.* **35,** 22 (2016).
352. Eckberg, D. L. Human sinus arrhythmia as an index of vagal cardiac outflow. *J. Appl. Physiol.* **54,** 961 LP-966 (1983).
353. Nederend, I., Jongbloed, M. R. M., de Geus, E. J. C., Blom, N. A. & ten Harkel, A. D. J. Postnatal Cardiac Autonomic Nervous Control in Pediatric Congenital Heart Disease. *J. Cardiovasc. Dev. Dis.* **3,** 16 (2016).
354. National Institute on Drug Abuse. *Testing for abuse liability of drugs in humans*. (National Institute on Drug Abuse, 1989). at <https://archives.drugabuse.gov/sites/default/files/monograph92.pdf>
355. Triposkiadis, F. *et al.* The Sympathetic Nervous System in Heart Failure. *J. Am. Coll. Cardiol.* **54,** 1747–1762 (2009).
356. Boas, M., Feldt-Rasmussen, U. & Main, K. M. Thyroid effects of endocrine disrupting chemicals. *Mol. Cell. Endocrinol.* **355,** 240–248 (2012).

357. Fazio, S., Palmieri, E. A., Lombardi, G. & Biondi, B. Effects of thyroid hormone on the cardiovascular system. *Recent Prog. Horm. Res.* **59,** 31–50 (2004).
358. Sterling, K., Milch, P. O., Brenner, M. A. & Lazarus, J. H. Thyroid hormone action: the mitochondrial pathway. *Science (80-.).* **197,** 996–999 (1977).
359. Voronych, S. M., Pavlykivs' ka, B. M. & Voronych-Semchenko, N. M. Physiological Aspects of Analysis of Heart Rate Variability Parameters in Adolescents with Latent Hypothyroidism. *Int. J. Physiol. Pathophysiol.* **3,** (2012).
360. Klein, I. & Ojamaa, K. Thyroid Hormone and the Cardiovascular System. *N. Engl. J. Med.* **344,** 501–509 (2001).
361. Chrousos, G. P. Stress and disorders of the stress system. *Nat Rev Endocrinol* **5,** 374–381 (2009).
362. Tsigos, C. & Chrousos, G. P. Hypothalamic–pituitary–adrenal axis, neuroendocrine factors and stress. *J. Psychosom. Res.* **53,** 865–871 (2002).
363. Black, P. H. Central nervous system-immune system interactions: psychoneuroendocrinology of stress and its immune consequences. *Antimicrob. Agents Chemother.* **38,** 1–6 (1994).
364. McCraty, R., Atkinson, M., Tomasino, D. & Bradley, R. T. The Coherent Heart Heart-Brain Interactions, Psychophysiological Coherence, and the Emergence of System-Wide Order. *Integr. Rev. A Transdiscipl. Transcult. J. New Thought, Res. Prax.* **5,** 10–115 (2009).
365. Brabant, G. Pulsatile und zirkadiane TSH-Sekretion Klinische Relevanz? *Internist (Berl).* **39,** 619–622 (1998).
366. Schaefer, M. *et al.* Mechanisms of arginine-vasopressin-induced Ca2+ oscillations in β-cells (HIT-T15): a role for oscillating protein kinase C. *Endocrinology* **145,** 4635–4644 (2004).
367. Melville, K. I., Blum, B., Shister, H. E. & Silver, M. D. Cardiac ischemic changes and arrhythmias induced by hypothalamic stimulation. *Am. J. Cardiol.* **12,** 781–791 (1963).
368. Oppenheimer, S. M., Gelb, A., Girvin, J. P. & Hachinski, V. C. Cardiovascular effects of human insular cortex stimulation. *Neurology* **42,** 1727–1732 (1992).
369. Samuels, M. A. The Brain–Heart Connection. *Circulation* **116,** 77–84 (2007).
370. Ahern, G. L. *et al.* Heart Rate and Heart Rate Variability Changes in the Intracarotid Sodium Amobarbital Test. *Epilepsia* **42,** 912–921 (2001).
371. Hamilton, E. & Warrick, P. Perinatal Software: A Primer on the Physiology of Fetal Heart Rate Control. *Understanding how the heart reacts to labor is essential knowledge for clinicians who are responsible for the interpretation of fetal heart rate tracings* (2018). at <http://perigen.com/fetal-heart-rate-physiology/>
372. Sakmann, B., Noma, A. & Trautwein, W. Acetylcholine activation of single muscarinic K+ channels in isolated pacemaker cells of the mammalian heart. *Nature* **303,** 250–253 (1983).
373. Ardell, J. L. & Randall, W. C. Selective vagal innervation of sinoatrial and atrioventricular nodes in canine heart. *Am. J. Physiol. - Hear. Circ. Physiol.* **251,** H764–H773 (1986).
374. Chiou, C.-W., Eble, J. N. & Zipes, D. P. Efferent Vagal Innervation of the Canine Atria and Sinus and Atrioventricular Nodes. *Circulation* **95,** 2573–2584 (1997).
375. Carlson, M. D. *et al.* Selective stimulation of parasympathetic nerve fibers to the human sinoatrial node. *Circulation* **85,** 1311–1317 (1992).
376. Dahlström, A., Fuxe, K., Mya-Tu, M. & Zetterström, B. E. M. Observations on adrenergic innervation of dog heart. *Am. J. Physiol. -- Leg. Content* **209,** 689–692 (1965).
377. Hou, Y. *et al.* Ganglionated Plexi Modulate Extrinsic Cardiac Autonomic Nerve Input. *J. Am. Coll. Cardiol.* **50,** 61–68 (2007).
378. Koizumi, K., Terui, N. & Kollai, M. Effect of cardiac vagal and sympathetic nerve activity on heart rate in rhythmic fluctuations. *J Aut. Nerv Syst* **12,** (1985).
379. Hedman, A. E., Tahvanainen, K. U., Hartikainen, J. E. & Hakumäki, M. O. Effect of sympathetic modulation and sympatho-vagal interaction on heart rate variability in anaesthetized dogs. *Acta Physiol Scand* **155,** (1995).
380. Tsuji, H. *et al.* Reduced heart rate variability and mortality risk in an elderly cohort. The Framingham Heart Study. *Circulation* **90,** 878–883 (1994).

381. Sajadieh, A. *et al.* Increased heart rate and reduced heart-rate variability are associated with subclinical inflammation in middle-aged and elderly subjects with no apparent heart disease. *Eur. Heart J.* **25,** 363–370 (2004).
382. Whelton, S. P. *et al.* Association Between Resting Heart Rate and Inflammatory Biomarkers (High-Sensitivity C-Reactive Protein, Interleukin-6, and Fibrinogen) (from the Multi-Ethnic Study of Atherosclerosis). *Am. J. Cardiol.* **113,** 644–649 (2014).
383. Lanza, G. A. *et al.* Relation of Heart Rate Variability to Serum Levels of C-Reactive Protein in Patients With Unstable Angina Pectoris. *Am. J. Cardiol.* **97,** 1702–1706 (2006).
384. Lampert, R. *et al.* Decreased heart rate variability is associated with higher levels of inflammation in middle-aged men. *Am. Heart J.* **156,** 759.e1-759.e7 (2008).
385. Huston, J. M. & Tracey, K. J. The Pulse of Inflammation: Heart Rate Variability, the Cholinergic Anti-Inflammatory Pathway, and Implications for Therapy. *J. Intern. Med.* **269,** 45–53 (2011).
386. Borovikova, L. V *et al.* Role of vagus nerve signaling in CNI-1493-mediated suppression of acute inflammation. *Auton. Neurosci.* **85,** 141–147 (2000).
387. Berntson, G. G., Norman, G. J., Hawkley, L. C. & Cacioppo, J. T. Cardiac Autonomic Balance vs. Cardiac Regulatory Capacity. *Psychophysiology* **45,** 643–652 (2008).
388. Palatini, P. Elevated heart rate as a predictor of increased cardiovascular morbidity. *J. Hypertens. Suppl.* **17,** 3–10 (1999).
389. Umetani, K., Singer, D. H., McCraty, R. & Atkinson, M. Twenty-Four Hour Time Domain Heart Rate Variability and Heart Rate: Relations to Age and Gender Over Nine Decades. *J. Am. Coll. Cardiol.* **31,** 593–601 (1998).
390. Wilhelmsen, L. *et al.* The multifactor primary prevention trial in Göteborg, Sweden. *Eur. Heart J.* **7,** 279–288 (1986).
391. Gillman, M. W., Kannel, W. B., Belanger, A. & D'Agostino, R. B. Influence of heart rate on mortality among persons with hypertension: The Framingham Study. *Am. Heart J.* **125,** 1148–1154 (1993).
392. Mancia, G. *et al.* Blood pressure and heart rate variabilities in normotensive and hypertensive human beings. *Circ Res* **53,** 96–104 (1983).
393. Palatini, P. *et al.* Predictive value of clinic and ambulatory heart rate for mortality in elderly subjects with systolic hypertension. *Arch. Intern. Med.* **162,** 2313–2321 (2002).
394. Diaz, A., Bourassa, M. G., Guertin, M.-C. & Tardif, J.-C. Long-term prognostic value of resting heart rate in patients with suspected or proven coronary artery disease. *Eur. Heart J.* **26,** 967–974 (2005).
395. Riegger, A. J. G. & Liebau, G. The Renin-Angiotensin-Aldosterone System, Antidiuretic Hormone and Sympathetic Nerve Activity in an Experimental Model of Congestive Heart Failure in the Dog. *Clin. Sci.* **62,** 465–469 (1982).
396. Armstrong, P. W., Stopps, T. P., Ford, S. E. & de Bold, A. J. Rapid ventricular pacing in the dog: pathophysiologic studies of heart failure. *Circulation* **74,** 1075–1084 (1986).
397. Chow, E., Woodard, J. C. & Farrar, D. J. Rapid ventricular pacing in pigs: an experimental model of congestive heart failure. *Am. J. Physiol. - Hear. Circ. Physiol.* **258,** H1603–H1605 (1990).
398. Olsson, S. B., Cotoi, S. & Varnauskas, E. Monophasic action potential and sinus rhythm stability after conversion of atrial fibrillation. *Acta Med. Scand.* **190,** 381–387 (2009).
399. Cotoi, S., Gavrilescu, S., Pop, T. & Vicas, E. The Prognostic Value of Right Atrium Monophasic Action Potential after Conversion of Atrial Fibrillation. *Eur. J. Clin. Invest.* **2,** 472–474 (1972).
400. Zipes, D. P. Electrophysiological Remodeling of the Heart Owing to Rate. *Circulation* **95,** 1745 LP-1748 (1997).
401. Tieleman, R. G. *et al.* Verapamil Reduces Tachycardia-Induced Electrical Remodeling of the Atria. *Circulation* **95,** 1945–1953 (1997).
402. Sulfi, S. & Timmis, A. D. Ivabradine–the first selective sinus node If channel inhibitor in the treatment of stable angina. *Int. J. Clin. Pract.* **60,** 222–228 (2006).
403. Fox, K. *et al.* Ivabradine in stable coronary artery disease without clinical heart failure. *N. Engl. J. Med.* **371,** 1091–1099 (2014).
404. Borer, J. S., Fox, K., Jaillon, P. & Lerebours, G. Antianginal and antiischemic effects of ivabradine, an I f

inhibitor, in stable angina. *Circulation* **107,** 817–823 (2003).
405. Tardif, J.-C., Ford, I., Tendera, M., Bourassa, M. G. & Fox, K. Efficacy of ivabradine, a new selective I f inhibitor, compared with atenolol in patients with chronic stable angina. *Eur. Heart J.* **26,** 2529–2536 (2005).
406. Kjekshus, J. K. Importance of heart rate in determining beta-blocker efficacy in acute and long-term acute myocardial infarction intervention trials. *Am. J. Cardiol.* **57,** F43–F49 (1986).
407. Tardif, J.-C., Ponikowski, P. & Kahan, T. Efficacy of the If current inhibitor ivabradine in patients with chronic stable angina receiving beta-blocker therapy: a 4-month, randomized, placebo-controlled trial. *Eur. Heart J.* **30,** 540–548 (2009).
408. Busseuil, D. *et al.* Heart Rate Reduction by Ivabradine Reduces Diastolic Dysfunction and Cardiac Fibrosis. *Cardiology* **117,** 234–242 (2010).
409. Walcher, T. *et al.* Ivabradine Reduces Chemokine-Induced CD4-Positive LymphocyteMigration. *Mediators Inflamm.* 751313 (2010).
410. Kröller-Schön, S. *et al.* Differential effects of heart rate reduction with ivabradine in two models of endothelial dysfunction and oxidative stress. *Basic Res. Cardiol.* **106,** 1147–1158 (2011).
411. Barbuti, A., Baruscotti, M. & Difrancesco, D. The pacemaker current: from basics to the clinics. *J. Cardiovasc. Electrophysiol.* **18,** 342–347 (2007).
412. Robinson, R. B., Yu, H., Chang, F. & Cohen, I. S. Developmental change in the voltage-dependence of the pacemaker current, if, in rat ventricle cells. *Pflügers Arch.* **433,** 533–535 (1997).
413. Cerbai, E., Pino, R., Sartiani, L. & Mugelli, A. Influence of postnatal-development on If occurrence and properties in neonatal rat ventricular myocytes. *Cardiovasc. Res.* **42,** 416–423 (1999).
414. Cerbai, E. *et al.* Characterization of the Hyperpolarization-Activated Current, I_f, in Ventricular Myocytes From Human Failing Heart. *Circulation* **95,** 568 LP-571 (1997).
415. Hoppe, U. C., Jansen, E., Südkamp, M. & Beuckelmann, D. J. Hyperpolarization-Activated Inward Current in Ventricular Myocytes From Normal and Failing Human Hearts. *Circulation* **97,** 55–65 (1998).
416. Cerbai, E. *et al.* The Properties of the Pacemaker Current IF in Human Ventricular Myocytes are Modulated by Cardiac Disease. *J. Mol. Cell. Cardiol.* **33,** 441–448 (2001).
417. Swedberg, K. *et al.* Ivabradine and outcomes in chronic heart failure (SHIFT): a randomised placebo-controlled study. *Lancet* **376,** 875–885 (2010).
418. Haghikia, A. *et al.* Early ivabradine treatment in patients with acute peripartum cardiomyopathy: Subanalysis of the German PPCM registry. *Int. J. Cardiol.* **216,** 165–167 (2018).
419. Demakis, J. G. & Rahimtoola, S. H. Peripartum cardiomyopathy. *Circulation* **44,** 964–968 (1971).
420. Hery, E. *et al.* Prédiction du risque d'intolérance du traitement bêtabloquant chez l'insuffisant cardiaque chronique par le dosage du BNP. *Ann. Cardiol. Angeiol. (Paris).* **53,** 298–304 (2004).
421. Sliwa, K. *et al.* Effects of pentoxifylline on cytokine profiles and left ventricular performance in patients with decompensated congestive heart failure secondary to idiopathic dilated cardiomyopathy. *Am. J. Cardiol.* **90,** 1118–1122 (2002).
422. Demir, S., Tufenk, M., Karakaya, Z., Akilli, R. & Kanadas, M. The Treatment of Heart Failure-Related Symptoms with Ivabradine in a Case with Peripartum Cardiomyopathy. *Int. Cardiovasc. Res. J.* **7,** 33–36 (2013).
423. World Medical Association. World Medical Association Declaration of Helsinki: Ethical Principles for Medical Research Involving Human Subjects. *Clin. Rev.* 2013–2016 (2013).
424. Zarifis, J., Grammatikou, V., Kallistratos, M., Katsivas, A. & on Behalf of the Investigators of the Prospective Observational Study of the Antianginal Efficacy of Ivabradine During a 4-Month Treatment of a Greek Population With Coronary Artery Disease, N. Treatment of Stable Angina Pectoris With Ivabradine in Everyday Practice: A Pan-Hellenic, Prospective, Noninterventional Study. *Clin. Cardiol.* **38,** 725–732 (2015).
425. Sumeray, M. S., Rees, D. D. & Yellon, D. M. Infarct size and nitric oxide synthase in murine myocardium. *J. Mol. Cell. Cardiol.* **32,** 35–42 (2000).

426. Suleman, N. The role of signal transducer and activator of transcription-3 (STAT-3) in ischaemic and pharmacological preconditioning. (2006).
427. Aznar, S. *et al.* Simultaneous Tyrosine and Serine Phosphorylation of STAT3 Transcription Factor Is Involved in Rho A GTPase Oncogenic Transformation. *Mol. Biol. Cell* **12,** 3282–3294 (2001).
428. Lacerda, L., Somers, S., Opie, L. H. & Lecour, S. Ischaemic postconditioning protects against reperfusion injury via the SAFE pathway. *Cardiovasc. Res.* **84,** 201–208 (2009).
429. Ceconi, C. *et al.* Heart rate reduction with ivabradine prevents the global phenotype of left ventricular remodeling. *Am. J. Physiol. - Hear. Circ. Physiol.* **300,** H366 LP-H373 (2011).
430. Halaas, J. L. *et al.* Physiological response to long-term peripheral and central leptin infusion in lean and obese mice. *Proc. Natl. Acad. Sci.* **94,** 8878–8883 (1997).
431. Fischer, A. H., Jacobson, K. A., Rose, J. & Zeller, R. Hematoxylin and Eosin Staining of Tissue and Cell Sections. *Cold Spring Harb. Protoc.* **2008,** pdb.prot4986 (2008).
432. Qiagen. RNeasy Mini Handbook. 9 (2012). at <http://www.bea.ki.se/documents/EN-RNeasy handbook.pdf>
433. Tanaka, N. *et al.* Transthoracic echocardiography in models of cardiac disease in the mouse. *Circulation* **94,** 1109–1117 (1996).
434. Somers, S. J., Lacerda, L., Opie, L. & Lecour, S. Age, genetic characteristics and number of cycles are critical factors to consider for successful protection of the murine heart with postconditioning. *Physiol. Res.* **60,** 971 (2011).
435. Fuchs, M. *et al.* Role of interleukin-6 for LV remodeling and survival after experimental myocardial infarction. *FASEB J.* **17,** 2118–2120 (2003).
436. Tramèr, M. R., Moore, R. A. & McQuay, H. J. Propofol and bradycardia: causation, frequency and severity. *Br. J. Anaesth.* **78,** 642–651 (1997).
437. Custodis, F. *et al.* Heart Rate Reduction by Ivabradine Reduces Oxidative Stress, Improves Endothelial Function, and Prevents Atherosclerosis in Apolipoprotein E–Deficient Mice. *Circ.* **117,** 2377–2387 (2008).
438. Roth, D. M., Swaney, J. S., Dalton, N. D., Gilpin, E. A. & Ross, J. Impact of anesthesia on cardiac function during echocardiography in mice. *Am J Physiol Hear. Circ Physiol* **282,** (2002).
439. Kulandavelu, S., Qu, D. & Adamson, S. L. Cardiovascular Function in Mice During Normal Pregnancy and in the Absence of Endothelial NO Synthase. *Hypertension* **47,** 1175 LP-1182 (2006).
440. Yu, Y., Hu, Z., Li, B., Wang, Z. & Chen, S. Ivabradine improved left ventricular function and pressure overload-induced cardiomyocyte apoptosis in a transverse aortic constriction mouse model. *Mol. Cell. Biochem.* 1–10 (2018).
441. Knight, M. *et al.* Trends in postpartum hemorrhage in high resource countries: a review and recommendations from the International Postpartum Hemorrhage Collaborative Group. *BMC Pregnancy Childbirth* **9,** 55 (2009).
442. Green, L. *et al.* The epidemiology and outcomes of women with postpartum haemorrhage requiring massive transfusion with eight or more units of red cells: a national cross-sectional study. *BJOG An Int. J. Obstet. Gynaecol.* **123,** 2164–2170 (2016).
443. Jacobsen, J. & Secher, N. H. Heart rate during haemorrhagic shock. *Clin. Physiol.* **12,** 659–666 (1992).
444. Scully, C. G., Kramer, G. C. & Strauss, D. G. Evaluation of heart rate and blood pressure variability as indicators of physiological compensation to hemorrhage before shock. *Shock* **43,** 463–469 (2015).
445. Yeh, R. W., Yu, P. B. & Drachman, D. E. Takotsubo Cardiomyopathy Complicated by Cardiac Tamponade. *Circulation* **122,** 1239 LP-1241 (2010).
446. Breedt, E., Lacerda, L. & Essop, M. F. Trimetazidine therapy for diabetic mouse hearts subjected to ex vivo acute heart failure. *PLoS One* **12,** e0179509 (2017).
447. Sutherland, F. J., Shattock, M. J., Baker, K. E. & Hearse, D. J. Mouse isolated perfused heart: Characteristics and cautions. *Clin. Exp. Pharmacol. Physiol.* **30,** 867–878 (2003).
448. Belke, D. D., Larsen, T. S., Gibbs, E. M. & Severson, D. L. Altered metabolism causes cardiac dysfunction in perfused hearts from diabetic (db/db) mice. *Am. J. Physiol. Metab.* **279,** E1104–E1113 (2000).

449. Bell, R. & Yellon, D. The contribution of endothelial nitric oxide synthase to early ischaemic preconditioning: the lowering of the preconditioning threshold. An investigation in eNOS. *Cardiovasc. Res.* **52,** 274–280 (2001).
450. Barbuti, A. *et al.* Molecular composition and functional properties of f-channels in murine embryonic stem cell-derived pacemaker cells. *J. Mol. Cell. Cardiol.* **46,** 343–51 (2009).
451. Bell, R. M., Mocanu, M. M. & Yellon, D. M. Retrograde heart perfusion: the Langendorff technique of isolated heart perfusion. *J. Mol. Cell. Cardiol.* **50,** 940–50 (2011).
452. Bell, R. M., Mocanu, M. M. & Yellon, D. M. Retrograde heart perfusion: The Langendorff technique of isolated heart perfusion. *J. Mol. Cell. Cardiol.* **50,** 940–950 (2018).
453. Simon, L., Ghaleh, B., Puybasset, L., F Giudicelli, J. & Berdeaux, A. *Coronary and hemodynamic effects of S 16257, a new bradycardic agent, in resting and exercising conscious dogs*. *The Journal of pharmacology and experimental therapeutics* **275,** (1995).
454. Heusch, G. & Kleinbongard, P. Ivabradine: cardioprotection by and beyond heart rate reduction. *Drugs* **76,** 733–740 (2016).
455. Li, B., Zhang, J., Wang, Z. & Chen, S. Ivabradine prevents low shear stress induced endothelial inflammation and oxidative stress via mTOR/eNOS pathway. *PLoS One* **11,** e0149694 (2016).
456. Chandel, N. S. *et al.* Mitochondrial reactive oxygen species trigger hypoxia-induced transcription. *Proc. Natl. Acad. Sci.* **95,** 11715 LP-11720 (1998).
457. van der Horst, I. C. C. *et al.* Neurohormonal profile of patients with heart failure and diabetes. *Netherlands Hear. J.* **18,** 190–196 (2010).
458. Iversen, L. The uptake of catecholamines at high perfusion concentrations in the rat isolated heart: a novel catecholamine uptake process. *Br. J. Pharmacol.* **120,** 267–282 (2011).
459. Pappano, A. J. Calcium-Dependent Action Potentials Produced by Catecholamines in Guinea Pig Atrial Muscle Fibers Depolarized by Potassium. *Circ. Res.* **27,** 379–390 (1970).
460. Reichelt, M. E., Willems, L., Hack, B. A., Peart, J. N. & Headrick, J. P. Cardiac and coronary function in the Langendorff-perfused mouse heart model. *Exp. Physiol.* **94,** 54–70 (2009).
461. Deshpande, G. P., Imamdin, A., Lecour, S. & Opie, L. H. Sphingosine-1-phosphate (S1P) activates STAT3 to protect against de novo acute heart failure (AHF). *Life Sci.* **196,** 127–132 (2018).
462. Scardovi, A. B., De Maria, R. & Ricci, R. Acute peripartum cardiomyopathy rapidly evolving in cardiogenic shock. *Int. J. Cardiol.* **189,** 255–6 (2015).
463. Du, X.-J. *et al.* I(f) channel inhibitor ivabradine lowers heart rate in mice with enhanced sympathoadrenergic activities. *Br. J. Pharmacol.* **142,** 107–112 (2004).
464. Vaillant, F. *et al.* Ivabradine and metoprolol differentially affect cardiac glucose metabolism despite similar heart rate reduction in a mouse model of dyslipidemia. *Am. J. Physiol. Circ. Physiol.* **311,** H991–H1003 (2016).
465. The John Hopkins University. Animal care and Use Committee. *The Mouse* at <http://web.jhu.edu/animalcare/procedures/mouse.html#normative>
466. Yang, C.-F., Yu-Chih Chen, M., Chen, T.-I. & Cheng, C.-F. Dose-dependent effects of isoflurane on cardiovascular function in rats. *Tzu Chi Med. J.* **26,** 119–122 (2014).
467. Suffredini, S. *et al.* Long-term treatment with ivabradine in post-myocardial infarcted rats counteracts f-channel overexpression. *Br. J. Pharmacol.* **165,** 1457–1466 (2012).
468. Forman, H. J. & Kennedy, J. A. Role of superoxide radical in mitochondrial dehydrogenase reactions. *Biochem. Biophys. Res. Commun.* **60,** 1044–1050 (1974).
469. Loschen, G., Azzi, A., Richter, C. & Flohé, L. Superoxide radicals as precursors of mitochondrial hydrogen peroxide. *FEBS Lett.* **42,** 68–72 (1974).
470. Oury, T. D. *et al.* Extracellular superoxide dismutase, nitric oxide, and central nervous system O2 toxicity. *Proc. Natl. Acad. Sci. U. S. A.* **89,** 9715–9 (1992).
471. Takuwa, N. *et al.* S1P3-mediated cardiac fibrosis in sphingosine kinase 1 transgenic mice involves reactive oxygen species. *Cardiovasc. Res.* **85,** 484–493 (2010).

Appendix A

High free-fatty acid Krebs buffer

NaCl 118.5mM; $NaHCO_3$ 25.0mM; KCl 4.7mM; $MgSO_4$ 1.2mM; KH_2PO_4 1.2mM; palmitic acid conjugated to BSA (FFA 1.2mM); glucose 2.5mM; $CaCl_2$ 1.4mM, pH 7.4

Potassium chloride (KCl) 50%

50g per 100ml dH_2O

Sodium chloride (NaCl) 9%

9g NaCl per 100ml dH_2O

Phosphate-Buffered Saline (PBS)

NaCl 137mM; KCl 2.7mM; Na_2HPO_4 10mM; KH_2PO_4 1.8mM; pH 7.4

Paraformaldehyde 4%

4 g paraformaldehyde per 100 ml PBS; pH 7 – 7.5

Stabilization Krebs-Henseleit buffer (KHB)

NaCl 118.5mM; $NaHCO_3$ 25.0mM; KCl 4.7mM; $MgSO_4$ 1.2mM; KH_2PO_4 1.2mM; glucose 11.0mM; $CaCl_2$ 1.4mM, pH 7.4

Appendix B

Table 1: RNA transcript sequences.

RNA transcript	Primer sequence (5' to 3')
Atrial Natriuretic Peptide (ANP)	CCT AAG CCC TTG TGG TGT GT (F)
	CAG AGT GGG AGA GGC AAG AC (R)
Angiotensin-converting enzyme (ACE)	CAG AAT CTA CTC CAC TGG CAA GGT (F)
	TCG TGA GGA AGC CAG GAT GT (R)
Mineralocorticoid receptor (MR)	TCA CAT TTT TAA CAT GTG ACG GC (F)
	CTT AGT CAG CTC AGG CTT GCC (R)
Cluster of differentiation 68(CD68)	TTC TGC TGT GGA AAT GCA AG (F)
	AGA GGG GCT GGT AGG TTG AT (R)
Brain Natriuretic Peptide (BNP)	AGA CCC AGG CAG AGT CAG AA (F)
	CAG CTC TTG AAG GAC CAA GG (R)
Bone morphogenic protein 4 (BMP4)	TGA GCC TTT CCA GCA AGT TT (F)
	CTT CCC GGT CTC AGG TAT CA (R)
Galectin 3	CAG TGC TCC TGG AGG CTA TC (F)
	ATT GAA GCG GGG GTT AAA GT (R)
Transforming Growth Factor (TGFβ1)	TGG AGC AAC ATG TGG AAC TC (F)
	GTC AGC CGG TTA CCA (R)
α cardiac actin	ACT CTT GCT TGC TGA TCC AC (F)
	GCC AAC AAT GTC CTA TCT GG (R)
α skeletal actin	GCA TGC AGA AGG AGA TCA CA (F)
	TTG TCG ATT GTC CTC AG (R)
Collagen 1	GCA GGT TCA CCT ACT CTG TCC T (F)
	CTT GCC CCA TTC ATT TGT CT(R)
Collagen 3	TCC CCT GGA ATC TGT GAA TC (F)
	TGA GTC GAA TTG GGG AGA AT (R)
Fibronectin	ACT GAC GAA GAG CCC TTA C (F)
	AGA TAA CCG CTC CCA TTC C (R)
Tissue Inhibitor of Metalloproteinase 1 (TIMP-1)	ATT CAA GGC TGT GGG AAA TG(F)
	CTC AGA GTA CGC CAG GGA AC (R)
α-Myosin Heavy Chain (α-MHC)	ACC GTC TGG ACG AGG AGA GCA GA(F)
	CGT GCA TCT TGG CAC CAA (R)
β-Myosin Heavy Chain (β-MHC)	TGC AAA GGC TCC AGG TCT GAG TCT (F)
	GCC AAC ACC AAC CTG TGC AAG TTC (R)
Glyceraldehyde-3-Phosphate Dehydrogenase (GAPDH)	ACA CAT TGG GGG TAG GAA CA (F)
	AAC TTT GGC ATT GTG GAA GG (R)

Primer sequences used to quantify expression of mRNA transcripts related to cardiac dysfunction. Abbreviations: F – forward; R – reverse.

Table 2: Histological results for Sirius red, and H&E staining.

	WT	WT + ivab	KO	KO + ivab	p
Immune cell infiltration score (A.U)	2.17+0.38	1.95+0.22	2.10+0.15	1.70+0.19	p>0.1
Sirius red scale score (A.U)	3.10+0.28	2.31+0.22	3.08+0.28	2.18+0.24	0.017 KO vs KO + ivab
Sirius red (% total area)	4.77+0.58	3.39+0.53	5.15+0.83	3.23+0.44	0.036 KO vs KO+ ivab

Semi-quantitative analysis of H&E staining was done using a rating scale with 1 being no immune cell infiltration, and 5 being complete immune cell infiltration. There were no significant changes between WT and KO groups either with or without treatment. Semi-quantitative analysis of collagen deposition with Sirius red was done using a rating scale with 1 being no collagen present, and 5 being complete collagen infiltration. Results obtained for quantitative Sirius red staining analysis were expressed as a percentage of the total area; these were consistent with that of the semi-quantitative analysis.

Table 3: Physical and echocardiographic measures as obtained for nulliparous (naïve) as well as wildtype and STAT3 KO mice after 3 pregnancies with weaning (postpartum) from the main study.

	Wildtype		STAT3 KO	
	Naïve (n=10)	Postpartum (n=14)	Naïve (n=3)	Postpartum (n=21)
LVAWd (mm)	0.68±0.05	0.94±0.03	0.98±0.15	0.89±0.04
LVAWs (mm)	1.03±0.07	1.26±0.06	1.23±0.13	1.28±0.04
LVIDd (mm)	4.35±0.18	4.78±0.10	5.47±0.52	4.69±0.08
LVIDs (mm)	3.18±0.19	3.60±0.14	4.51±0.73	3.53±0.11
LVPWd (mm)	0.65±0.04	0.88±0.03	0.86±0.05	0.81±0.04
LVPWs (mm)	1.02±0.12	1.19±0.05	1.11±0.09	1.08±0.05
Ejection Fraction (%)	53.10±2.54	49.11±2.42	37.10±9.89	48.95±2.14
Fractional Shortening (%)	27.18±1.56	24.88±1.44	18.42±5.28	24.87±1.28
LV vol; d (μL)	86±8	107±6	149±34	101±4
LV vol; s (μL)	41±5	56±6	100±39	53±4
Heart rate (BPM)	440±17	477±17	430±17	481±14
Body weight (g)	28.68±1.18	33.6 ±1.1	32.18±1.35	34.0±0.8
Lung weight/tibia length (mg/mm)	13.45±0.82		17.15±3.08	
Heart weight/tibia length (mg/mm)	10.00±0.42		17.24±5.44	

The postpartum groups reflect combined data for WT groups prior to treatment, as well as combined data for KO groups prior to treatment. Abbreviations: d – diastole; LV – left ventricle; LVAW- left ventricular anterior wall

thickness; LVID – left ventricular internal diameter, LVPW – left ventricular posterior wall thickness; s – systole; Vol – volume

Table 4: Histological results for H&E and Sirius red staining.

	WT naïve	WT postpartum	KO naïve	KO postpartum	p
Immune cell infiltration score	1.42+0.15	2.17+0.38	2.17+0.33	2.10+0.15	0.026 WT vs WT nulliparous
Sirius red scale score	2.00+0.43	3.10+0.28	3.00+0.87	3.08+0.28	0.049 WT vs WT nulliparous
Sirius red (% total area)		4.77+0.58		5.15+0.83	

Semi-quantitative analysis of H&E staining was done using a rating scale with 1 being no immune cell infiltration, and 5 being complete immune cell infiltration. Semi-quantitative analysis of collagen deposition with Sirius red was done using a rating scale with 1 being no collagen present, and 5 being complete collagen infiltration. Both immune cell infiltration and collagen deposition was significantly increased in WT mice who have had successive pregnancies. Abbreviations: KO – signal transducer and activator of transcription 3 genetic knockout mice, WT – wildtype mice

Table 5: Data obtained at the end of stabilisation, at the end of the AHF phase, and 5, 15 and 25 min into recovery

		Heart rate (BPM)	Systolic pressure (mmHg)	Diastolic pressure (mmHg)	LVDP (mmHg)	Rate Pressure product (mmHg.BPM)	Recovery (%)
20 min Stabilisation	**Control (n=10)**	388 ± 11	72.73 ± 3.20	6.39 ± 0.64	66.33 ± 2.73	25755 ± 1366	100
	Ivabradine (n=7)	393 ± 20	74.86 ± 3.28	6.49 ± 0.48	68.37 ± 3.23	26754 ± 1570	100
15 min AHF	**Control**	94 ± 28	53.59 ± 13.86	35.22 ± 15.37	18.40 ± 4.30	2053 ± 633	7 ± 2
	Ivabradine	102 ± 31	27.26 ± 6.38	8.12 ± 0.64	19.14 ± 6.27	1263 ± 295	5 ± 1
5 min recovery	**Control**	158 ± 23	92.55 ± 12.26	45.99 ± 12.60	46.62 ± 6.65	6604 ± 739	25 ± 3
	Ivabradine	216 ± 23	60.86 ± 7.91	17.32 ± 6.38	43.54 ± 5.52	9091 ± 981	36 ± 6
15 min recovery	**Control**	120 ± 22	105.21 ± 14.13	62.36 ± 15.77	42.89 ± 6.56	6141 ± 1272	23 ± 5
	Ivabradine	127 ± 14	95.20 ± 12.39	31.85 ± 8.41	63.35 ± 8.05	7550 ± 598	29 ± 3
25 min recovery	**Control**	161 ± 42	104.08 ± 9.88	65.00 ± 12.07	39.07 ± 5.71	6405 ± 1625	25 ± 6
	Ivabradine	105 ± 13	102.63 ± 7.94	40.26 ± 9.26	62.37 ± 4.54	5419 ± 1163	24 ± 2

Data are expressed for both control (n=10) and ivabradine-treated (n=7) hearts. Parameters observed were HR, systolic and diastolic ventricular pressure, rate pressure product and percentage functional recovery. Abbreviations: min – minute, AHF – acute (haemorrhagic) HF; BPM – beats per minute; LVDP – left ventricular developed pressure; mmHg – millimetres of mercury

Table 6: CT scores for mRNA transcript analysis

	AHF	AHF + ivab	p
ANP	7.27±2.63	24.64±11.44	>0.05
BNP	1.48±0.16	2.51±0.28	0.01

Values are expressed as mean ± SEM (A.U). No changes were observed in levels of ANP between the treated and untreated groups. BNP was significantly higher in the AHF group treated with ivabradine. Abbreviations: AHF – acute haemorrhagic heart failure; ANP – atrial natriuretic peptide; BNP – brain natriuretic peptide; ivab – ivabradine

Table 7: Data obtained at the end of stabilisation, at the end of the TC phase, and 5, 15 and 25 min after restoration to high glucose and low adrenergic state

		Heart rate (BPM)	Systolic pressure (mmHg)	Diastolic pressure (mmHg)	LVDP (mmHg)	Rate Pressure product (mmHg.BPM)	Recovery (%)
25 min Stabilisation	**Control**	318 ± 24	95.18 ± 4.02	6.78 ± 0.45	88.37 ± 3.82	28057 ± 2331	100
	Ivabradine	314 ± 34	94.27 ± 6.66	7.75 ± 0.85	86.52 ± 6.27	26801 ± 2838	100
1 min TC	**Control**	333 ± 37	118.91 ± 6.92	7.98 ± 0.75	110.93 ± 6.64	38598 ± 5947	143 ± 22
	Ivabradine	431 ± 17	156.34 ± 8.28	7.39 ± 0.98	148.95 ± 8.22	65862 ± 6150	247± 7
3 min TC	**Control**	296 ± 37	74.36 ± 9.11	12.70 ± 2.67	61.65 ± 7.80	18965 ± 3705	70 ± 14
	Ivabradine	318 ± 67	119.28 ± 17.33	36.48 ± 11.82	82.80 ± 18.60	20333 ± 4193	81 ± 18
6 min TC	**Control**	251 ± 44	93.27 ± 13.68	31.08 ± 9.23	62.19 ± 8.88	14974 ± 2682	56 ± 10
	Ivabradine	273 ± 44	137.85 ± 8.80	61.72 ± 7.25	76.13 ± 10.22	18621 ± 2775	73 ± 11
9 min TC	**Control**	250 ± 35	112.31 ± 11.12	55.36 ± 10.52	56.95 ± 7.14	13733 ± 2850	51 ± 9
	Ivabradine	157 ± 34	128.38 ± 8.13	55.84 ± 8.63	72.54 ± 13.81	13447 ± 3480	48 ± 13

12 min TC	**Control**	248 ± 35	114.53 ± 11.33	60.52 ± 11.38	53.91 ± 7.71	11636 ± 1486	44 ± 6
	Ivabradine	149 ± 32	125.21 ± 7.80	54.09 ± 8.07	71.12 ± 10.89	12263 ± 3010	44 ± 11
5 min recovery	**Control**	273 ± 38	125.33 ± 7.26	74.99 ± 10.26	50.33 ± 5.84	13194 ± 2502	48 ± 8
	Ivabradine	188 ± 36	124.68 ± 8.62	48.38 ± 8.16	76.31 ± 11.04	15637 ± 3721	56 ± 12
10 min recovery	**Control**	259 ± 28	111.81 ± 8.20	66.01 ± 8.28	45.80 ± 5.58	10981 ± 1518	42 ± 6
	Ivabradine	229 ± 38	117.88 ± 8.12	46.48 ± 8.26	71.39 ± 8.91	16989 ± 3706	61 ± 10
15 min recovery	**Control**	233 ± 27	113.16 ± 7.90	66.84 ± 8.39	46.18 ± 5.27	9954 ± 1162	39 ± 5
	Ivabradine	249 ± 45	105.77 ± 7.14	45.99 ± 8.00	59.78 ± 4.32	15242 ± 3018	56 ± 9
20 min recovery	**Control**	230 ± 27	103.02 ± 7.31	61.92 ± 7.69	41.11 ± 4.78	8401 ± 881	33 ± 5
	Ivabradine	208 ± 34	94.04 ± 9.49	46.31 ± 7.65	47.74 ± 4.76	9604 ± 1241	56 ± 4
25 min recovery	**Control**	193 ± 21	107.97 ± 8.45	63.18 ± 8.03	44.71 ± 5.75	7522 ± 875	29 ± 5
	Ivabradine	184 ± 30	89.53 ± 10.80	45.57 ± 7.49	44.12 ± 4.66	7927 ± 1316	30 ± 5

Data are expressed for both control (n=11) and ivabradine-treated (n=6) hearts. Parameters observed were HR, systolic and diastolic ventricular pressure, rate pressure product and percentage functional recovery. Abbreviations: min – minutes; LVDP – Left Ventricular Developed Pressure; BPM – beats per minute; mmHg – millimetres of mercury

Table 8: CT scores for mRNA transcript analysis

	TC	TC + ivab	p
ANP	36.05±19.34	10.47±5.34	>0.05
BNP	1.82±0.24	4.22±0.41	0.001

Values are expressed as mean ± SEM (A.U.). No changes were observed in levels of ANP between the treated and untreated groups. BNP was significantly higher in the TC group treated with ivabradine. Abbreviations: ANP – atrial natriuretic peptide; BNP – brain natriuretic peptide; TC – Takotsubo cardiomyopathy; ivab – ivabradine